YIELD CRITERIA FOR REINFORCED CONCRETE SLABS.

THESIS SUBMITTED FOR THE DEGREE OF

DOCTOR OF PHILOSOPHY

BY

CHRISTAKIS ARNAOUTI, B.Sc.(Eng.)

DEPARTMENT OF CIVIL ENGINEERING

THE UNIVERSITY OF ASTON IN BIRMINGHAM

SEPTEMBER 1972.

ACKNOWLEDGEMENTS

The author wishes to express his thanks to Professor M. Holmes, B.Sc., Ph.D., C.Eng., F.I.C.E., F.I.Struct.E., F.I.Mun.E., the head of the Department of Civil Engineering at the University of Aston in Birmingham, for his continual help, encouragement and very useful discussions throughout this research project.

Special thanks are due to Mr. W. Parsons, the Chief Technician in the Civil Engineering Department at the University of Aston and to his assistants for their technical advice for designing the testing rigs, and their willing assistance.

My thanks also to Mr. H. E. Walker, M.Eng., F.I.C.E., F.I.Mun.E., F.I.O.B., the Head of the Department of Civil Engineering and Building at the Lanchester Polytechnic for allowing the author to carry out this research project at the University of Aston in Birmingham.

Finally, acknowledgement is due to the author's family who received less attention than they deserve whilst this research was carried out.

SUMMARY

This thesis is primarily concerned with the yield behaviour and the prediction of normal moments at yield of underreinforced concrete slabs in which membrane and shear forces do not exist. A new expression for normal and twisting moments has been developed. Further, using these expressions and expressions for principal applied moments, a new yield criterion has been developed. For the first time a new yield criterion has been developed that incorporates the shear and bending stiffness of the reinforcing bars, the crushing strength of the concrete adjacent to the reinforcing bars and the effective crack width. A program of experimental work on Steel Analogue Slabs and Mono-steel bar Concrete strips is described in this thesis. This testing program was concerned with validating certain conditions and assumptions made in developing the theory. Another program of experimental work on underreinforced concrete slabs subjected to combined bending and torsion is also described in detail in this thesis. This series of experiments justify the overall validity of the theory. Experimental results of other researches were also used to test the theory. The experimental results are in good agreement with the results predicted by the theory.

In addition to the theoretical and experimental work, this thesis presents a critical review of the existing literature on the subject.

LIST OF CONTENTS

		Page
Acknowledgements		I
Summary		II
List of Contents		III
Notation		VII
CHAPTER 1	INTRODUCTION	1
1.1	Object	1
1.2	Outline of Mono-steel bar test series	1
1.3	Outline of General Moment Series	2
1.4	Outline of Analytical studies	2
CHAPTER 2	A REVIEW OF PREVIOUS WORK BY OTHER RESEARCHERS ON THE YIELD LINE THEORY	3
2.1	Historical Introduction of Yield Line Theory	3
2.2	Work by Johansen	4
2.2.1	Johansen's 'stepped' yield criterion	4
2.3	Work by Wood	7
2.4	Work by Kemp	8
2.5	Theoretical work by Kwiecinski	11
2.6	Tests by Kwiecinski	13
2.7	Theoretical work by Prince	13
2.8	Experimental work by Prince	18
2.9	Tests by Baus and Tolaccia	19
2.10	Work by Morley	22
2.11	Work by Downham	24
2.12	Discussion and Conclusions	28
	Tables to Chapter 2	30
	Figures to chapter 2	32

CHAPTER	3	A NEW CRITERION FOR THEORETICAL YIELD	45
	3.1	Introduction	45
	3.2	The Ideal and Perfect crack	45
	3.2.1	Normal and tangential stresses on a steel bar transversing Ideal crack	46
	3.3	The concrete crack transversed by a steel bar	50
	3.3.1	Normal and Tangential stresses on a steel bar transversing a concrete crack	51
	3.4	Development of Theoretical Normal and Twisting moments at yield	56
	3.5	The Yield Criterion	58
	3.5.1	The Yield Criterion in the Isotropic and Orthotropic case	59
	3.6	Discussion and Conclusions	63
		Figures to Chapter 3	67
		Plates to Chapter 3	81
CHAPTER	4	THE DEVELOPMENT OF EXPERIMENTAL TECHNIQUES	82
	4.1	Introduction	82
	4.2	Steel Analogue Series	83
	4.2.1	Description of Apparatus	83
	4.2.2	Testing Procedure	85
	4.2.3	Results	86
	4.3	Mono-Steel bar Concrete Strip Series	88
	4.3.1	Description of Slab Strips	88
	4.3.2	Testing Procedure	90
	4.3.3	Results	91
	4.4	Effects of the 'effective crack width'	93

	4.5	Conclusions on Results	94
		Tables to Chapter 4	96
		Figures to Chapter 4	99
		Plates to Chapter 4	107
CHAPTER	5	TESTS ON REINFORCED CONCRETE SLABS SUBJECTED TO BENDING AND TORSION	112
	5.1	Introduction	112
	5.2	Materials used for the test series	113
	5.2.1	Cement	113
	5.2.2	Aggregates	113
	5.2.3	Concrete Mixes	113
	5.2.4	Concrete Control Specimens	113
	5.2.5	Reinforcement	114
	5.3	Instrumentation	115
	5.3.1	Steel strains	115
	5.3.2	Concrete strains	116
	5.3.3	Mechanical dial gauges	117
	5.4	Description of specimens	117
	5.5	Test Set up	119
	5.5.1	Testing Rig	119
	5.5.2	Description of a typical test	121
		Tables to Chapter 5	124
		Figures to Chapter 5	128
		Plates to Chapter 5	134
CHAPTER	6	COMPARATIVE ANALYSIS OF RESULTS FROM THE COMBINED BENDING AND TORSION SERIES	142
	6.1	Introduction	142
	6.2	Effective crack length derived by Downham	143

	6.3	Effective crack length derived by the Author	143
	6.4	General formulae used in the proceeding analysis	147
	6.5	Comparison of results	149
	6.5.1	Introduction	149
	6.5.2	The effect of mesh orientation on the ultimate strength of the concrete slab elements	150
	6.5.3	The effect of mesh orientation on the stiffness of the concrete slab element	152
	6.5.4	Maximum principal compression strains on concrete surface	154
	6.5.5	Steel strain observations	156
	6.5.6	Formation of yield lines and comparison with principal directions	158
	6.6	Conclusions on results	162
		Tables to Chapter 6	164
		Figures to Chapter 6	174
		Plates to Chapter 6	230
CHAPTER 7		DISCUSSIONS AND CONCLUSIONS	232
	7.1	Introduction	232
	7.2	The Theoretical Yield Criterion	233
	7.3	Experimental Work	235
	7.4	Conclusions	238
	7.5	Future Work	238
List of References			240

NOTATION

A_{st}	Area of steel in bar direction per unit width of slab.
a-direction	Direction of main, lower layer of steel reinforcement.
b-direction	Direction of upper layer of steel reinforcement orthogonal to a-direction.
l_{eo}	Effective length of yield line based on Author's theory.
l_e, b^1	Effective length of yield line based on Downham's theory.
d_1	Depth of main steel layer below compressive upper slab surface.
K	Constant used to calculate ultimate moments in bar directions.
$m_a = m$	Ultimate moment of resistance in a-direction per unit width.
$m_b = \mu m$	Ultimate moment of resistance in b-direction per unit width.
m_n	Ultimate moment of resistance normal to crack direction at failure.
m_{nj}	Ultimate moment of resistance normal to crack direction at failure given by Johansen's theory.
m_{nt}	Twisting moment on crack at failure associated with m_n and m_{nj}.
M_x	Applied moment in span or X-direction per unit length.
M_y	Applied moment in the Y-direction per unit length.
M_{xy}	Twisting moment applied in X-Y co-ordinate system per unit length.
M_1	External principal moment per unit length in 1-direction.

M_2	External principal moment per unit length in 2-direction.
M_a	Total moment of resistance in a-direction due to a-bars crossing the yield line.
M_b	Total moment of resistance in b-direction due to b-bars crossing the yield line.
M_n	Applied moment per unit length normal to possible crack direction.
M_{nt}	Twisting moment per unit length to possible crack direction.
N	Normal tensile force per unit length along a yield line provided by the reinforcement.
T	Tangential force per unit length along a yield line provided by the reinforcement.
n_a	Number of a-bars crossing yield line at failure.
n_b	Number of b-bars crossing yield line at failure.
s_a	Spacing of bars in a-direction.
s_b	Spacing of bars in b-direction.
la	Lever arm used to produce M_x.
Ta	Lever arm used to produce M_{xy}.
e_a	Axial elongation of reinforcing bar.
lo	Half length of steel bar crossing the artificial crack in the steel analogue series.
E	Young's Modulus (for steel).
G	Shear modulus (for steel).
2L	Artificial crack width in the steel analogue series and effective crack width in the Mono-steel bar concrete strip series.
2Δ	Increase in artificial crack or effective crack width.

lp	Length of reinforcing bar required for equilibrium of shear force and concrete pressure acting on the reinforcing bar crossing a yield line.
q	Interaction force between concrete and reinforcing bar (force/unit length).
V, F	Shear force acting on the bar crossing a yield line at the point of antisymmetry.
U	Concrete compressive strength.
fu	Modulus of rupture.
fy	Yield stress in steel.
X-direction	Span direction in test series.
Y-direction	Direction transverse to span.
γ	Angle between X-direction and maximum principal concrete strain direction.
ω	Angle between X-direction and maximum principal curvature direction.
η	Angle between X-direction and yield line direction.
η_1	Angle between X-direction and maximum principal applied moment direction.
β	Angle between X-direction and direction of main reinforcement (a-bars).
θ	Angle between a yield line direction and the original direction of an a-bar.
ψ	Angle between normal to the crack and maximum principal applied moment direction.
ϕ	Angle between main reinforcement (a-bars) direction and maximum principal applied moment direction.
α	Angle between main reinforcement (a-bars) direction and normal to the crack.

τ Shear stress in a bar, crossing the yield line, at the point of antisymmetry.

σ Axial stress in a bar, crossing the yield line, at the point of antisymmetry.

D Diameter of reinforcing bar.

CHAPTER 1

INTRODUCTION

1.1 Object.

The over-all objective of this study was to develop an expression to predict the ultimate normal moment and twisting moment at yield in an under-reinforced concrete slab, incorporating the shear and axial stresses acting on the bars within the crack. Further, a yield criterion was developed relating external moments and internal moments of resistance for under-reinforced concrete slabs.

In addition to the analytical work, a detailed testing program was carried out. The first part of the program tested certain conditions of the theory and the second part of the program studied the general applicability of the new theory as well as past theories. The results confirmed the new theory and also showed that the Johansen criterion is conservative.

1.2 Outline of mono-steel bar test series.

This series consists of two parts:-

(a) The steel analogue series.

(b) Mono-steel bar concrete strip series.

The steel analogue test series is described in detail in section 4.2.1. The object of this series was to study the behaviour of a single bar crossing an ideal crack that cannot crush.

This series clearly showed the existence of shear stresses on the bar.

The mono-steel bar concrete strip series is also described in detail in section 4.3.1. The object of this series was to study the

effect of the plastic properties and crushing of concrete on the over-all strength of the concrete strip. This over-all reduction enables a crushing factor to be determined. The crushing factor was successfully determined for small angles of the steel bar to the normal of the crack.

For large angles the concrete adjacent to the bar fail in tension because of the small lateral concrete cover.

1.3 Outline of General Moment Series.

This series of experiments was carried out on slab elements with variable mesh orientation and degree of orthotropy under varying conditions of combined bending and torsion. Twenty-eight slab elements were tested in all, of which seven were isotropically reinforced, eleven had a degree of orthotropy of 0.5 (nominal) and ten had a degree of orthotropy of 0.25 (nominal). The results of this series of experiments have been presented in detail in Chapter 5.

1.4 Outline of Analytical studies.

As stated in section 1.1, the main object of this study was to develop an expression for the normal moment at yield and also the twisting moment. This has been achieved by considering the shear and axial forces acting on a single bar crossing the crack.

The second objective, to develop a yield criterion, was also achieved and presented in a graphical form. An expression for the effective crack length was developed, yielding results similar to those put forward by other researchers but, unlike other expressions, is not based on any formula for normal moments at yield.

CHAPTER 2

A REVIEW OF PREVIOUS WORK BY OTHER RESEARCHERS ON THE YIELD LINE THEORY

2.1 Historical Introduction of Yield Line Theory.

In 1922, at the Institution of Structural Engineers, Ewart S. Andrews described a paper by Ingerslev [1] entitled "The strength of rectangular slabs" as being "of paramount interest to the concrete branch of structural engineering". Ingerslav's method may be recognised as the alternative "equilibrium" approach to Johansen's yield line theory. Ingerslev assumed a constant normal moment to the yield line and zero twisting moment along the yield line.

Johansen [2] had derived his yield moments by imagining "steps" in yield lines. This was equivalent to considering the equilibrium of a tiny triangular portion of a slab. This provided the moments in the normal and tangential directions.

$$\text{Normal moment} = m_n = m(\cos^2\alpha + \mu \sin^2\alpha) \quad .. \quad .. \quad 2.1$$

$$\text{Twist} = m_{nt} = \frac{m}{2}(1-\mu)\sin 2\alpha \quad .. \quad .. \quad 2.2$$

$$\text{Tangential moment} = m_t = m(\sin^2\alpha + \mu \cos^2\alpha) \quad .. \quad .. \quad 2.3$$

The basic method used in yield line theory is the work equation. This method, however, uses equation 2.1 only, therefore as far as the yield line is concerned, equations 2.2 and 2.3 are irrelevant. Johansen [2] found that the normal moment on the yield line could not alone satisfy equilibrium of the elements of the slab bounded by yield lines.

To overcome this difficulty, Johansen [2] introduced a new concept of nodal forces. These forces act at the junctions of the yield

lines. Of course, these forces can be translated as twisting moments and shear forces on the yield lines. Johansen's equilibrium method in addition to equation 2.1 requires equation 2.2. The so called "equilibrium method" gives an upper bound solution because the nodal-force theory (equilibrium) only considers equilibrium across the yield line and not in the "rigid" area of the slab.

2.2 Work by Johansen.

The main object of structural analysis is to ensure that a structure shall have a suitable factor against failure. Obviously, to know the safety factor involved, it is necessary to know the load (moment) that will cause a structure to fail. A method was necessary which would predict ultimate loads and which was relatively easy to handle and understand. Johansen [2] in 1943 put forward this method in his Ph.D thesis which he named "yield line theory". He put forward two alternative methods to determine the failure load.

(a) The energy or 'work' method for calculating the failure load.

(b) An alternative 'Equilibrium' method involving the so-called nodal forces, which gives the same value of the failure load as the work method but which provides additional information.

It must be realized that in the yield line theory, failure of a slab is assumed to occur when lines along which the steel has yielded, have together formed a valid yield line mechanism. To be able to use method (a) to solve the structure, the normal moment on the yield line must be known. To be able to use method (b) both the normal and twisting moments on the yield line must be known.

2.2.1 Johansen's 'stepped' yield criterion

The basic assumptions made to derive the normal and twisting moments on the yield line are:-

(a) The normal and twisting moments on a yield line can be obtained by considering each band of reinforcement in turn, the total effect being the addition of the individual effects.

(b) For each band of reinforcement taken on its own, the yield line may be considered to be divided into small steps parallel to, and at right angles to the reinforcement, figure 2.1.

(c) All reinforcement is assumed to stay in its original straight line direction.

(d) The moments of resistance due to reinforcement, when considering the small steps are principal moments.

The normal and twisting moments on the yield line are of course due to the normal (principal) moments on the steps due to the reinforcement. By considering the equilibrium of one step, figure 2.1

$$m_n = m(\cos^2\alpha + \mu \sin^2\alpha) \qquad .. \quad .. \quad 2.4$$

$$m_{nt} = \frac{m}{2}(1-\mu)\sin 2\alpha \qquad .. \quad .. \quad 2.5$$

(a) Work method

The work method employs equation 2.4 only. A valid mechanism is postulated by which the slab can fail; it is given a hypothetical displacement at a convenient point. Using this hypothetical displacement, the energy lost by the external loads is found. Again using the hypothetical displacement, the rotation of the sections of the slab meeting at a yield line is found. Equation 2.4 gives the normal moment on the yield line, the product of rotation and normal moment gives the internal energy dissipated. By equating the energies a relationship between load and moment is found. Equation 2.5 is not used because the twisting moments do not do any work on the yield line.

(b) Equilibrium method.

Until recently the equilibrium method was considered as an alternative to the work method; in fact it is not. It is the same method presented in another form. The equilibrium of each rigid region is considered. To consider the equilibrium of a rigid region though, the forces acting on the yield line must be found. The distribution of the forces along a yield line is difficult to determine so it is assumed that the forces act on the joints of the yield lines. Using equations 2.4 and 2.5, the nodal forces can be determined. Considering the equilibrium of each region a relationship between load and moment is obtained. This method is rather more convenient than the work method because no differentiation is involved to determine the direction of yield lines.

The criterion developed by Johansen [2] is very easy to use and understand, but has some drawbacks. From the kinematic point of view, the stepped yield line assumed, from which the criterion is developed, is kinematically impermissible; in other words the mechanism of rotation of the two adjoining rigid parts of a slab is impossible. Also the moments predicted by the theory seem fairly conservative in relation to experimental results. The enhancement of the normal moments obtained by Downham [3] is as much as 42%, by Kwiencinski [4] 18.8%, and by the Building Research Station 16%. A more general theory is required to take into account the twist on the slab, shear forces as well as membrane forces. Of course the contribution of Johansen [2] in this field is of paramount importance, and it can be said that he set the cornerstone of the yield line theory.

2.3 Work by Wood.

Wood [6] of the Building Research Station has done an enormous amount of work, both theoretical and experimental, on the yield line criterion. His work springs from the original work done by Johansen. Wood noticed that the mechanism on which the "stepped" yield criterion is based is kinematically impossible. He suggested an alternative mechanism, by assuming that the reinforcement bars "kink" across the yield line, so that their new direction was normal to the yield line, figure 2.2. From this diagram, if moments normal and tangential to the cracks are resolved

$$m_n = m(\cos\alpha + \mu \sin\alpha) \qquad .. \quad .. \quad 2.6$$

$$m_{nt} = o \qquad .. \quad .. \quad 2.7$$

Equation 2.6 means that the directions of the yield moment vector produced by any given yield line coincides with the direction of the line itself; hence m_n is a principal moment. The twisting moment of course is always zero.

This criterion takes into account the full benefit attributed to the change of direction of bars. It must be emphasized that the mechanism is kinematically permissible. However, this mechanism is still rather far from reality because it implies that there is no crushing of the concrete caused by the pressure of bars which tend to straighten. Work produced by Downham [3], Morley [7] and Prince [8] showed that there is no kinking at all. Therefore, the suggested mechanism contradicts experimental evidence produced by a number of researchers. Also, this criterion overestimates the strength of the concrete slabs. Figure 2.3 shows the theoretical values of the normal moments for isotropic slabs derived from the three distinct

theories, namely Johansen's [2], Wood's [6] and Prince's [8].

2.4 Work by Kemp

The work done by Kemp [9] on the yield line criterion is of a theoretical nature although he directed experimental research work at University College, London. Most of his work is on upper and lower bound solutions in search of unique solutions for reinforced concrete plates; he also worked on the nodal forces theory, that is to evaluate the nodal forces. The evaluations of the nodal forces is of importance when solving slabs by means of the "equilibrium" method.

In the writer's opinion, the most important contribution to the development of the yield line criterion contributed by Kemp [9] is the yield criterion for orthotropically reinforced concrete slabs.

He started with the basic concept introduced by Johansen [2], that is

$$m_n = m(\cos^2\alpha + \mu\sin^2\alpha) \qquad .. \quad .. \quad 2.8$$

and

$$m_{nt} = \frac{m}{2}(1-\mu)\sin 2\alpha \qquad .. \quad .. \quad 2.9$$

Kemp assumed that the slab had top and bottom reinforcement of values $m, \mu m, -m^1, -\eta m^1$ perpendicular to x and y axes. He also assumed that the slab was subjected to principal bending moments of values M_1 and M_2 inclined at an angle ϕ measured clockwise from the y and x direction respectively. Kemp [9] stated that the moments of resistance must be compared with the applied moment in all directions in the xy plane. If the principal moments are such that yielding occurs in bending, the direction of the corresponding curvature rate will not in general coincide with the principal moments, but will be inclined at some angle ψ measured clockwise from the plane of M_1. This condition is illustrated graphically in figure 2.4, where the variation of the external normal bending moment M_n, with angular

orientation is shown superimposed on the corresponding variation in the yield normal bending moment m_n. Again Kemp stated that yielding will take place when curve M_n touches curve m_n. Mathematically, this means that:-

$$m_n = M_n \qquad .. \quad .. \quad 2.10$$

$$\frac{\partial m_n}{\partial \alpha} = \frac{\partial M_n}{\partial \psi} \qquad .. \quad .. \quad 2.11$$

The external normal moment is given by:-

$$M_n = M_1 \cos^2\psi + M_2 \sin^2\psi \qquad .. \quad .. \quad 2.12$$

and the twisting moment is given by:-

$$M_{nt} = \frac{M_1 - M_2}{2} \sin 2\psi \qquad .. \quad .. \quad 2.13$$

Equating equations 2.8 and 2.12 according to condition 2.10

$$M_1 \cos^2\psi + M_2 \sin^2\psi = m(\cos^2\alpha + \mu \sin^2\alpha)$$

Modifying the above equation

$$\frac{M_1+M_2}{2} + \frac{M_1-M_2}{2} \cos 2\psi = \frac{m}{2}(1+\mu) + \frac{m}{2}\cos 2(\phi+\psi) \qquad .. \quad .. \quad 2.14$$

where $\alpha = \phi + \psi$

Differentiating equations 2.9 and 2.13 and equating according to condition 2.11

$$\frac{M_1-M_2}{2} \sin 2\psi = \frac{m}{2}(1-\mu)\sin 2(\phi+\psi) \qquad .. \quad .. \quad 2.15$$

From equations 2.14 and 2.15 ψ was eliminated.

$$mM_1(\sin^2\phi + \mu\cos^2\phi) + mM_2(\cos^2\phi + \mu\sin^2\phi) - M_1M_2 - \mu m^2 = 0$$

$$.. \quad .. \quad 2.16$$

For isotropic slabs $\mu = 1$ and equation 2.16 reduces to

$$(m-M_1)(m-M_2) = 0$$

This equation yields the positive portion of the square yield criterion.

The yield criterion for negative yield is similar to that for positive yield.

The general equation for negative yield is

$$m^1M_1(\sin^2\phi+\eta\cos^2\phi) + m^1M_2(\cos^2\phi+\eta\sin^2\phi) + M_1M_2 + \eta m^{1(2)} = 0 \quad \ldots\ldots\ 2.17$$

for isotropic slabs $\eta=1$ and equation 2.17 reduces to

$$(m^1 + M_1)(m^1 + M_2) = 0.$$

This equation yields the negative portion of the square yield criterion. The yield loci corresponding to equations 2.16 and 2.17 are shown plotted in figure 2.5 for a range of values of ϕ for the particular case $\mu=\eta=\frac{1}{2}$ and $m = m^1$. When $\alpha = 0$ or $\frac{\pi}{2}$ the yield locus becomes the familiar rectangular criterion.

When $\frac{\pi}{2} > \phi > 0$, the yield locus is composed of two hyperbolas and is no longer symmetrical about the principal axes. Discontinuities in the loci are now restricted to the two points where simultaneous positive and negative yield takes place.

The theoretical criterion developed by Kemp is of great importance. Baus and Tolaccia [10] showed experimentally that for $\alpha=0$ the yield criterion is not square but of the shape shown in figure 2.16, i.e. the shape is concave.

If the experimental results produced by Baus and Tolaccia are accepted as correct, then obviously the criterion of Kemp is conservative. This is due to the conservativeness of the normal moments of resistance obtained from the Johansen expressions. Of course Kemp dealt with the idealized problem with no effects such as Poisson's ratio of membrane and shear forces.

2.5 Theoretical work by Kwiecinski

Kwiecinski [5] put forward a theory of the partial kinking of reinforcement. He took the kinematically permissible mechanism shown in figure 2.6 where the crushing of concrete due to overstressing in the vicinity of the kinks in the reinforcement results in a tendency to straighten out the reinforcement bars. By assuming the angles of kink were γ and δ and resolving moments, he found that

$$m_n = \cos\alpha\cos\gamma + \mu\sin\alpha\cos\delta \qquad .. \quad .. \quad 2.18$$

$$m_{nt} = \cos\alpha\sin\gamma - \mu\sin\alpha\sin\delta \qquad .. \quad .. \quad 2.19$$

In the case of full kinking, $\gamma=\delta=0$, hence the above equations are reduced to:-

$$m_n = \cos\alpha + \mu\sin\alpha$$

$$m_{nt} = 0$$

which are the equations put forward by Wood [6].

When there is no kinking, i.e. $\gamma=\alpha$, $\delta=\frac{\pi}{2}-\alpha$, equations 2.18 and 2.19 are reduced to:-

$$m_n = m(\cos^2\alpha + \mu\sin^2\alpha)$$

$$m_{nt} = \frac{m}{2}(1-\mu)\sin 2\alpha$$

which are the equations put forward by Johansen [2]. Kwiecinski persists that the kinking is not full, but he maintains that the twisting moment must vanish at all times along the yield line. From equation 2.19

$$\frac{\sin\gamma}{\sin\delta} = \mu\tan\alpha \qquad .. \quad .. \quad 2.20$$

Looking at equations 2.18 and 2.20, there are three unknowns, therefore a third equation is required.

He assumes a function of the type $g(\alpha, \gamma) = 0$ exists. To determine this function he fixed an experimental coefficient characteristic for the problem and then determined it according to the empirical requirements. The following parameter was introduced.

$$K = \frac{m_n}{m} \quad (\alpha = \text{constant}) \qquad .. \; .. \; 2.21$$

and since he was dealing with isotropically reinforced slabs, $\mu = 1$. If $\alpha = \frac{\pi}{4}$ in equation 2.21, the parameter K controls the yield criterion.

After a series of trials, he found that

$$\sin\gamma = A\sin\alpha \qquad .. \; .. \; 2.22$$

where A is a constant. For $\alpha = \frac{\pi}{4}$, by symmetry $\gamma = \delta$, and from equation 2.18 and 2.21 $\cos\gamma = \frac{k}{\sqrt{2}}$ and from equation 2.22 $A = \sqrt{2-k^2}$, hence

$$m_n = m\left[\sqrt{1-A^2\sin^2\alpha}.\cos\alpha + \sqrt{1-A^2\cos^2\alpha}.\sin\alpha\right] \qquad .. \; .. \; 2.23$$

where $1 \geqslant A = \sqrt{2-k^2} \geqslant 0$.

The left-hand side limiting value corresponds to stepped line theory and the right-hand one to full kinking theory. Graphically the criterion is shown in Figure 2.7. The main criticism of this theory is that it fails to explain how it is possible for the bars to kink at all while there is no twist at any part of the yield line at any instant during the yielding process. Also, this criterion is semi-empirical and contradictory to existing experimental results. If there were no twisting moments on the yield line, one would expect that the direction of the principal compressive concrete strain would always be perpendicular to the yield line. Of course, this is not the case as Downham [3] and the author have clearly shown in their experiments, thus implying the existence of concrete shearing stresses on

the yield line, and hence twisting moments on the steel.

2.6 Tests by Kwiecinski.

To justify his new theory, Kwiecinski [4] carried out a series of experiments, divided into four groups. The grouping of the tests was arranged according to the inclination of the orthogonal mesh to the side of the slabs. The degrees of inclination were 0°, 15°, 30°, 45°. Four models of each type of slab were made, 16 in all. The slab sizes were 32" x 20" x 1.5". All slabs were simply supported along each shorter side and subjected to bending by means of a concentrated line load across the centre. The values of ultimate load were then read by means of a concrete testing machine specially adapted for flexure tests. Loads were applied at a uniform, reasonably slow rate throughout the tests.

Figures 2.8 and 2.9 show how the moment strength is increased by rotating the mesh. A maximum increase of 18.8% when $\alpha = 45^{\circ}$ is obtained from his theory and also from his experiments. Kwiecinski's experimental moments seem to be in good agreement with his theory only after the test values have been modified. In reducing his results, he used the effective width technique, which takes into account the actual number of bars crossing the yield line; he also assumed that at least one bar slipped during each experiment, thus contributing no moment of resistance.

2.7 Theoretical work by Prince.

The work of Prince [8] is mainly of a theoretical nature. His main objective was to find the plastic moment of resistance normal to the yield line. His fundamental assumption was that the strain takes place normal to the yield line. By working in terms of steel forces

and taking into account shear and axial stresses developed in the reinforcement bars, he related these stresses to the yield stress by means of Von Mises criterion. This resulted in a criterion giving strengths between unkinked and fully kinked yield criteria predictions.

Prince [8] considered two cases:-

(a) No bending of reinforcement.

(b) Bending of reinforcement across the crack.

Case (a) pre-supposes that the crack width is small and the bending deformation negligible, and in case (b) the crack width is large and bending deformations considerable.

Case a

The bars are assumed to be subjected to axial and shear stresses as shown in figure 2.10 and straining to take place in the n-direction. Referring to figure 2.10, from the geometrical properties

$$\tau x = \frac{G}{E} \sigma x \tan\alpha$$

$$\tau y = \frac{G}{E} \sigma y \cot\alpha.$$

Resolving in the N-direction

$$N = A(\sigma x \cos^2\alpha + \tau x \cos\alpha \sin\alpha) + A(\sigma y \sin^2\alpha + \tau y \sin\alpha \cos\alpha).$$

Resolving in the T-direction

$$T = A(\sigma x \cos\alpha \sin\alpha - \tau x \cos^2\alpha) - A(\sigma y \sin\alpha \cos\alpha - \tau y \sin^2\alpha).$$

Substituting the first two equations in the last two equations

$$N = A\sigma x(\cos^2\alpha + \frac{G}{E} \sin^2\alpha) + A\sigma y\ (\sin^2\alpha + \frac{G}{E} \cos^2\alpha) \quad .. \quad .. \quad 2.24$$

$$T = A(\sigma x - \sigma y)(1 - \frac{G}{E})\ \sin\alpha\cos\alpha \quad .. \quad .. \quad 2.25$$

What remains is to express σx and σy in terms of fy (yield stress). Prince thought that three possible postulations existed..

(i) T = 0, this is an attempt to satisfy both strain compatibility and equilibrium for all values of α. i.e. $\frac{\sigma x}{\sigma y} = 1$.

(ii) Crack width remains constant for both sets of bars, from the strain diagram figure 2.10.

$$\frac{\sigma x}{E} \text{ d.sec}\alpha\cos\alpha + \frac{\tau x}{G} \text{ d.sec}\alpha\sin\alpha = \frac{\sigma y}{E} \text{ d.cosec}\alpha\sin\alpha + \frac{\tau y}{G} \text{ d.cosec}\alpha\cos\alpha$$

$$\text{i.e.} \quad \frac{\sigma x}{\sigma y} = \cot^2\alpha$$

(iii) Both sets of bars yield, if the Von-Mises criterion is used, the axial and shear stresses are related in the following way:-

$$\sigma x^2 + 3\tau x^2 = \sigma y^2 + 3\tau y^2 = fy^2$$

replacing τx and τy

$$\frac{\sigma x}{\sigma y} = \left[\frac{E^2 + 3G^2\cot^2\alpha}{E^2 + 3G^2\tan^2\alpha}\right]^{\frac{1}{2}} \qquad .. \quad .. \quad 2.26$$

However, it is clear that only one of these conditions may be satisfied at any time for a general angle α.

Prince argued that cases (i) and (ii) were not valid, although the tangential forces might be small, the width of crack might not be constant. Case (iii) is claimed to be valid, although both sets of bars do not yield simultaneously. If the shear and axial stresses after yield are assumed to remain uniformly distributed over the cross section, and the plastic deformation of the reinforcing bars are calculated using plastic potential theory, then the Von-Mises yield function, the ratio of the shear to axial stress necessary for compatibility deformation is given by $\frac{\tau x}{\sigma x} = \frac{G}{E}\tan\alpha = \frac{1}{3}\tan\alpha$ 2.27

Equation 2.26 is unrealistic at values of α close to 0° and 90° if bending deformations are ignored.

Using 2.26 and 2.27, and the Von Mises criterion

$$\sigma x = \frac{Efy}{(E^2+3G^2\tan^2\alpha)^{\frac{1}{2}}} \quad \text{and } \sigma y = \frac{Efy}{(E^2+3G^2\cot^2\alpha)^{\frac{1}{2}}}$$

then

$$N = Afy\left[\frac{E\cos^2\alpha+G\sin^2\alpha}{(E^2+3G^2\tan^2\alpha)^{\frac{1}{2}}} + \frac{E\sin^2\alpha+G\cos^2\alpha}{(E^2+3G^2\cot^2\alpha)^{\frac{1}{2}}}\right] \quad .. \quad .. \quad 2.28$$

and

$$T = Afy\,(E-G)\sin\alpha\cos\alpha\left[\frac{1}{(E^2+3G^2\tan^2\alpha)^{\frac{1}{2}}} - \frac{1}{(E^2+3G^2\cot^2\alpha)^{\frac{1}{2}}}\right] \quad .. \quad 2.29$$

Case b

Prince [8] to generalize his criterion and also to make a correction for the lack of continuity at values of α close to 0° and 90° had to allow bending deformation effects on the previously derived formulae. It is clear, Prince argues, that the shearing forces acting on a bar crossing a yield line at an oblique angle will set up bending moments in the unrestrained portion of the bar, and these will result in a bending deformation across the crack, the magnitude of which is a function of the crack width. The total bending deflection shown in Figure 2.11 is

$$\delta_b = 2\,\frac{S}{3EI}\,\frac{(d\sec\alpha)^3}{8} \quad \text{where } S = \tau\pi r^2,\ I = \frac{\pi r^4}{4}$$

i.e. $$\delta_b = \frac{\tau(d\sec\alpha)^3}{3Er^2} .$$

Using the condition that the resultant deformation direction must be normal to the crack direction

$$\tan\alpha = \frac{\tau x}{\sigma x}\left[\frac{E}{G} + k^2\frac{\sec^2\alpha}{3}\right] ;\ \cot\alpha = \frac{\tau y}{\sigma y}\left[\frac{E}{G} + k^2\frac{\operatorname{cosec}^2\alpha}{3}\right]$$

where $k = \frac{d}{r}$

Simplifying

$$\tau x = K_1 \sigma x \tan\alpha \quad \text{where } K_1 = \frac{3G}{3E+GK^2\sec^2\alpha} \qquad .. \quad .. \quad 2.30$$

$$\tau y = K_2 \sigma y \cot\alpha \quad \text{where } K_2 = \frac{3G}{3E+GK^2\operatorname{cosec}^2\alpha} \qquad .. \quad .. \quad 2.31$$

From equations 2.24, 2.25, 2.30 and 2.31, and Von Mises criterion

$$N = Afy\left[\frac{\cos^2\alpha + K_1\sin^2\alpha}{(1+3K_1{}^2\tan^2\alpha)^{\frac{1}{2}}} + \frac{\sin^2\alpha+K_2\cos^2\alpha}{(1+3K_2{}^2\cot^2\alpha)^{\frac{1}{2}}}\right] \qquad .. \quad .. \quad 2.32$$

$$T = Afy\sin\alpha\cos\alpha\left[\frac{1-K_1}{(1+3K_1{}^2\tan^2\alpha)^{\frac{1}{2}}} + \frac{1-K_2}{(1+3K_2{}^2\cot^2\alpha)^{\frac{1}{2}}}\right] \qquad .. \quad 2.33$$

It should be noted that σx and σy are not effected by bending. Prince claims that this is justified for small values of K. A plot of $\frac{N\alpha}{No}$ and $\frac{T\alpha}{No}$ against α is shown in figure 2.12. The apparent discontinuity which existed in the curve of normal force at $\alpha=0$, and 90° when bending was ignored has now been corrected. This theory is based on elastic analysis; it may be strictly used to define the onset of yield which occurs when the crack width is very small. The basic concept of strain compatibility overcomes automatically the problem of kinematic inadmissibility which has hitherto beset attempts to explain the observed increases in normal moment of resistance of an isotropic slab at angles to the reinforcement directions, but in doing so it raises the problem of equilibrium. Prince, though, claims that the out of balance tangential forces are small and hence negligible. He produced no experimental results to justify this statement. The other objections to his theory are, a diameter of bar to crack width ratio must be assumed; this of course is quite arbitrary and cannot be accepted; and of course the major objection is the basic assumption that strain takes place normal to the crack; in fact,

Downham [3] and the author showed that strains do not behave in that manner at yield.

2.8 Experimental work by Prince.

In his thesis, Prince [8] mentions a series of experiments carried out at University College, London. Out of thirteen slabs tested, three had a degree of orthotropy of 0.5, the rest unity. The loading arrangement for the slabs and their dimensions are shown in figures 2.13 and 2.14. Cracks were allowed to develop in an unrestricted manner in a specified region of the slab. The object of the tests was to investigate the variation of yield normal moment with different arrangements of steel, and hence test his newly developed criterion. The results obtained did not generally verify his theoretical prediction, although his predicted results appeared better than those by the theories developed by Johansen [2] and Wood [6].

Prince encountered three problems during his experiments.

(i) Difficulty in determining at what load yield actually occurred, since with the constant strain loading device used the load fell rapidly as yield was approached due to the effect of large creep strain.

(ii) Loss of bond in some tests.

(iii) Difficulty in calculating the theoretical yield moment of the slab with a relatively small number of inclined bars.

Prince assumed that failure would occur at the section containing the least area of steel, and he calculated his yield moment on this basis. He attributed the discrepancy of his results to difficulties (i) and (ii). It is very surprising that he had bond trouble, specially when he provided hooks to avoid this particular

trouble. Downham [3] carried out about 48 tests and the author another 28, and Downham only had bond trouble in one test. The difficulty (i) could have been avoided by providing steel with a definite yield point followed by a horizontal plateau, i.e. with no strain hardening.

2.9 Tests by Baus and Tolaccia.

Baus and Tolaccia [10] in 1963 carried out tests at Liege University under the direction of Professors H. Louis and Ch. Massonnet. These tests were carried out to establish experimentally the yield criterion for reinforced concrete slabs subjected to pure biaxial bending. In order to eliminate the effect of shear, it was decided to conduct tests on model slabs subjected to pure bending as shown in figure 2.15. In the first place, the test frame left the edges to deflect freely to avoid any extraneous stresses. Secondly, any combination of principal moments could be applied of either like or unlike sign, to facilitate investigations in each quadrant of the yield locus. The most satisfactory testing arrangement is shown schematically in diagram 2.15. The test rig comprises sixteen levers numbered 1, 2, 3, 4 and distributed four along each side of the model slab. These levers are encastered onto the edges of the slab by jaws lined with rubber sheet to spread the load. The moments are applied through the levers by jacks acting at each end. The eight jacks A are connected in parallel to pump 1, the eight jacks B in parallel to pump 2, and the sixteen jacks C to the third pump. The jacks C apply the couple say M_2. The eight outside jacks C act upwards, whilst the inner ones downwards. If the couple say M_1 has the same sign as M_2 this is applied by jacks A acting downwards. The jacks B then support the dead weight plus the reaction from jacks A. If the couple

M_1 is the opposite sign to M_2 then this is applied by jacks B acting downwards, jacks A taking the dead weight and reaction from B. The applied moments can be either the same or different signs and can have any combination of relative values. The moments are applied uniformly along the edges. Shear stress is non-existent except for that due to the dead load and that is relatively small.

The model slabs were 1300 mm. square by 80 mm. thick. Between the orthogonal reinforcing mats were 10 mm. bars at 60 mm. spacing. These bars were spot welded round the outside, onto which the reinforcing bars which strengthen the edges were in turn fixed. About 40 slabs were tested in all, with the inclination of the orthogonal mesh at 0°, 22.5°, 30° and 45° to the sides of the slab. Some of the slabs tested had top and bottom reinforcement. From data given in the paper the degree of orthotropy was calculated and found to be 0.815.

The experimental results of Baus and Tolaccia [10] are shown graphically in figure 2.16. The experimental criterion is always outside the rectangular one and the extra safety (strength) increases as the absolute value of the ratio between M_1 and M_2 becomes closer to the value of the ratio between the individual yield moments calculated as for a beam. The discrepancy of the experimental results in the first quadrant in relation to the theoretical values is attributed to the Poisson's ratio effect. The concrete of the compression face is subjected to biaxial stresses, which has an effect on the reinforcement analogous to prestressing. This effect becomes more important when the transverse stresses are increased and the quality of concrete is improved, since the Poisson's ratio increases. The discrepancy of values in the fourth quadrant was attributed to tensile stresses in the concrete around the steel. The concrete in tension

around the steel is subjected to transverse compression; this improves the bond and retards the onset of cracking. Baus and Tolaccia [10] state that if it is accepted that the concrete does not crack before the steel yields, the moment required for steel yield is all the more important when the modulus of rupture is large.

In conclusion, Baus and Tolaccia showed that the yield criterion is not rectangular but of the shape shown in figure 2.16. The criterion is concave.

It seems that Baus and Tolaccia put an enormous amount of work and thought into these experiments. They do not mention though how the important factor of membrane forces was eliminated, neither do they mention whether or not the ratio of the two applied moments was maintained constant through the experiment. This condition of proportional loading is of great importance in plastically yielding structures. The membrane forces will have a tendency to increase the moment strength of the slabs. The increase of strength in the first quadrant was attributed to Poisson's ratio, although Morley [7] showed that the effect is negligible. Obviously, here there is a contradiction. The increase in strength in the fourth quadrant was attributed to transverse forces hindering development of cracking. Although this could be true to a small extent, it will never hinder cracking until the steel yields. The strains developed in the steel at yield are so high that no concrete will sustain them without cracking. The extra reinforcement provided around the edges, which amounts to doubling the strength in these regions, and the spot welding, will produce sizeable forces in a direction perpendicular to the one in which the moment is acting. Also, there is a difference in level between the two neutral axes in the heavily and lightly reinforced

regions; this will have a tendency to produce membrane forces in the lightly reinforced test area due to the restraint on it from the more heavily reinforced region.

2.10 Work by Morley.

C. T. Morley [7], in a thesis submitted to the University of Cambridge in 1965, describes two series of tests which were designed to investigate the ultimate load behaviour of slabs subjected to uniaxial or biaxial moments with or without the presence of membrane forces, and in particular to assess the importance of kinking of the reinforcement. In the first series of tests, a number of long rectangular slabs with a single set of bars inclined at various angles between 0° and 75° were subjected to uniaxial bending about the long axis, with various ratios of membrane forces to bending moment. Deflections due to the shearing force along the crack were measured and eliminated by the application of restoring forces as shown in figure 2.17. From the ultimate moment and the shearing force required to restore the slab to a state of uniaxial strain, graphs of normal force and shearing force per unit crack length were drawn against the inclination of the reinforcement. Figure 2.18 shows the curves obtained for the case of zero membrane force, and for comparison purposes, the theoretical curves for the unkinked and fully kinked theories.

From his experiments, Morley [11] points out that the measured values of normal force agree very closely with those obtained from the Johansen [2] theory, but offers no explanation of the discrepancy between the measured and expected values of the shearing force. Morley [7] concluded that the amount of kinking in the bars, if any, is negligible and that the Johansen criterion is closely correct.

Morley took great care in measuring the shearing force along the crack, but failed completely to explain discrepancies of the order of 25%.

The second series of tests was carried out upon rhomboid slabs in the manner suggested by Johansen, this loading system theoretically producing biaxial moments where the ratio $\frac{M_1}{M_2}$ is negative and equal to the square of the ratio of the diagonal lengths. These slabs were isotropically reinforced and the inclination of the bars varied between 0^o and 45^o to the direction of applied principal moments. The ultimate moments obtained from this series of experiments were found to agree closely with the Johansen criterion.

From the experimental results obtained, Morley concluded that the Johansen square criterion is entirely justified, and that bending of the steel across a crack as suggested by Wood [6] and others is insignificant. These results are used to justify the assumptions made in developing a generalized yield criterion for a slab element acted upon by both bending moments and membrane forces. He uses the device of replacing the reinforcement by a thin sheet of material having same area per unit length of the slab element as the original bars, and having stress properties which represent the steel which it replaces. The yield criterion of this plate is such that it can provide uniaxial stress, fy, in the original bar directions. The concrete is assumed to have perfect elastic-plastic behaviour. In turn, Morley describes three methods of applying the limit theorems using the following assumptions.

(i) Statically admissible stress distributions are assumed at all levels of the slab and integrated over the slab depth to obtain stress resultants in the same manner as Nielsen [13].

(ii) A distribution of plastic strain rate is assumed leading to an upper bound solution.

(iii) An alternative upper bound is obtained by replacing the concrete with a material of infinite compressive strength.

These three methods are developed and a number of solutions are obtained by the use of a computer. In a slab with $\mu=0.2$ and equal top and bottom reinforcement, the difference between the infinite strength solution and the upper bound obtained by the second method amounts to about 6.5%, while the difference between the lower bound solution and the second solution is said to be 3%. In a slab with $\mu=0.3$ and no top steel, these two figures become 2.8% and 1% respectively. These solutions are for pure moments. In the general case with membrane action, similar agreement between the three solutions is claimed.

2.11 Work by Downham.

The work carried out by Downham [3] at the University of Aston in Birmingham under the direction of Professor Holmes was of an experimental nature. In his thesis, Downham describes two separate series of tests. The first group are called 'plank tests', in which the slab elements were subjected to uniaxial moment, and the second group, which are called the 'general moment tests', in which the slab elements were subjected to combined bending and torsional moments. For both series of tests, the testing rig was designed in such a way so as to exclude transverse shear forces and membrane forces from the test areas.

The main variables controlled in both series of tests were

(i) The angle, β, between the main reinforcement mesh and the span direction of X-direction.

(ii) the degree of orthotropy μ.

(iii) the ratio of applied bending moment to applied torque.

The steel properties were also held constant. This was achieved by cutting the steel from the same roll and heat treating all the steel at one attempt. In fact, after heat treatment, it was found that the steel exhibited a sharp yield point and little strain hardening during yield. Downham's [3] attempt to control the strength of the concrete was less successful. This he claims was mainly due to the variation of the quality of the cement.

(a) Plank Test.

A total of seventeen specimens were tested in this series. Each one of the seventeen slab elements was subjected to uniaxial moments till collapse. The slab element was set up on rollers in the same way as a beam. One roller was fixed, the other allowed to move so that membrane forces did not occur. Rigid line loads were applied across the specimens 150 mm. on either side of the centre line. Thus the region between the line loads was subjected to a pure maximum bending moment. The results of all the seventeen tests are shown in Table 2.1.

The main criticism of this series of tests is the severe restriction on the freedom of deformation imposed on the slab elements since deformation can only take place in one direction. Downham realised that this restriction was being imposed, but agreed that its effect on the test zone would be of little significance. Also, no precautions were taken to avoid the tendency of the corners to lift up; presumably because this eventuality was not forseen.

(b) General Moment Tests.

A total of thirty-one specimens were tested in this series. The test set-up was arranged in such a way that the ratio of the torsional moment to the bending moment was maintained constant throughout the experiment. Referring to figure 2.19, the only restriction imposed to freedom of deformation was to the curvature in the Y-direction in the vicinity of the jaws.

The whole set-up of the experiment was as follows:-

Two opposite edges were fitted with extra reinforcement and clamped in heavy steel channel jaws. These heavy jaws were welded to a thick plate, triangular in shape, which acted as a lever arm to provide the bending and torsional moments. Referring to figure 2.19, the supports for the whole set-up consisted of two ball bearings, one of which was bearing on a fixed steel column, the other on a proving ring which was set on rollers to prevent membrane stresses occurring. A central hydraulic jack transmitted load to a cross beam, which in turn transmitted the load to the jaws. By adjusting the position of the cross beam on the jaws, the ratio of torsional moment to bending moment could be altered. Downham [3] carried out tests for three ratios of torsional to bending moments. Namely, 0.2, 0.75 and 1.167. The results of his tests are shown in Table 2.2.

Downham, apart from measuring collapse loads, took enormous care to measure the strains on the compression face of the slab by means of strain gauges and also the curvature of the slab by measuring deflections on the tension side of the slab. Two typical graphs are shown in figures 2.20 and 2.21. These results assisted Downham [3] to come to three important conclusions:

(i) the yield lines do not occur in the direction of the principal moments,

(ii) or principal curvatures.

(iii) Also, since the principal concrete strains on the compression face of the slab element do not occur in the direction of the steel bars, then the steel bars must be subjected to axial and shear stresses.

Effective length concept.

Downham [3] realized that the concrete slab elements are reinforced along discrete lines forming a step-wise non-homogeneous structure. Moreover, the width of a slab is not a multiple of an actual bar spacing taken in the direction of a yield line and cannot be even designed this way because of the variable angle α. Therefore, he put forward the effective length concept. The effective length concept had also been used by Kwiecinski [4] and Lenschaw and Sozen [12].

To use the concept of effective length of yield line, it is necessary to compare the actual number of bars acting with the theoretical number of bars acting. Downham used the Johansen expression for normal moment at failure as a datum, which led to the expression for effective length of yield line

$$b^1 = \frac{(n_1 S_1)\cos\alpha + \mu (n_2 S_2)\sin\alpha}{\cos^2\alpha + \mu \sin^2\alpha} \quad .$$

The effective length b^1 was used to reduce total ultimate moments to moments per unit length.

The main criticism to an effective length derived in this way is that it is based on the Johansen expression, an expression that is criticised as conservative by as much as 16% when the slabs are

isotropic. Surely this error is re-introduced in the experimental quantities through the effective length. The author proposes to derive a new effective length that is independent of any theoretical expression for normal moments.

In conclusion, Downham produced a quantity and of good quality of results for a variety of degrees of orthotropy, orientation of main reinforcement to free side of slab elements, and torsional to bending moments ratios, that reinforce the necessity for a new criterion.

2.12 Discussion and Conclusions.

Although Johansen's [2] criterion is accepted universally, there is considerable evidence which shows that his criterion is rather conservative. There are a number of causes for the increased load carrying capacity of the slab elements. The theoretical work carried out by Wood [6] showed the great importance of membrane action. In certain circumstances, membrane action could enhance the load carrying capacity of slab elements by two or three times the predicted load by the Johansen theory. If specific measures are taken to ensure that membrane action is removed, it is still necessary to show the effect of bar orientation and biaxial moments. Wood [6] reported that isotropic slab elements subjected to uniaxial moments showed a moment enhancement by as much as 16% when the bar orientation was 45° to the normal of the crack.

Baus and Tolaccia claim moment increases by as much as 20%-30% when $M_1 = \pm M_2$ for all inclinations of reinforcement to principal axes.

Downham reported that orthotropic slab elements of $\mu = 0.275$ subjected to uniaxial moments showed moment increase by 42%.

Contrary to the above evidence, Morley [7] claims that his experimental results on slab elements subjected to uniaxial bending are in good agreement with the Johansen criterion. The same agreement is claimed by Lenschaw and Sozen [12] for slabs subjected to uniaxial and combined torsional and bending moments.

It is obvious that there is some confusion here. More tests are required to bring new evidence to light.

It is the purpose of this thesis to examine the physical behaviour of reinforced concrete slab elements subjected to combined torsional and bending moments. It is also the purpose of this thesis to study the behaviour of the steel bars crossing a crack. Further, a new criterion will be proposed for a slab element which attempts to satisfy both equilibrium and displacement compatibility of reinforcement.

SLAB	$\alpha^\circ=\beta^\circ$	μ	Effective width in	m_{n1}/m_{nj}
P 1	0	1.00	30	1.005
P 2	30	0.99	25.69	1.054
P 3	45	0.99	24.34	1.059
P 4	0	0	30	0.877
P 5	30	0	24.25	1.030
P 6	45	0	16.97	1.282
P 7	60	0	10.39	1.432
P 8	0	0.275	30	0.966
P 9	30	0.275	22.56	0.256
P10	45	0.275	19.71	1.384
P11	60	0.274	20.26	1.319
P12	90	0.275	31.5	1.062
P13	0	0.543	30	1.032
P14	30	0.546	23.26	1.060
P15	45	0.542	22.95	1.099
P16	60	0.547	24.66	0.905
P17	90	0.545	32.37	1.001

Table 2.1. ULTIMATE MOMENT RESULTS PLANK TEST SERIES (DOWNHAM)

TB	μ	$\frac{Mxy}{Mx}$	$\frac{m_n}{m}$	$\frac{m_t}{m}$	$\frac{m_{nt}}{m}$	α°	β°
1	0.99	0.2	1.07	-0.030	-0.076	7.0	0
2	0.99	0.2	0.95	-0.021	-0.071	35.8	30
3	1.00	0.2	0.99	-0.021	-0.095	49.6	45
4	1.00	0.75	1.14	-0.290	-0.179	20.3	0
5	0.98	0.75	1.06	-0.261	-0.180	49.5	30
6	0.99	0.75	1.17	-0.290	-0.210	64.3	45
7	1.00	1.167	1.23	-0.480	-0.260	24.1	0
8	0.98	1.167	1.20	-0.475	-0.210	57.5	30
9	0.99	1.167	1.30	-0.480	-0.386	65.8	45
28	0.97	0.2	0.96	-0.015	-0.110	72.1	67.5
29	0.96	0.75	1.10	-0.282	-0.108	90.2	67.5
30	0.92	1.167	1.15	-0.430	-0.292	89.7	67.5
31	0.99	1.167	1.22	-0.478	-0.274	23.7	0
10	0.55	0.2	0.945	-0.030	0.058	12.1	0
11	0.55	0.2	0.800	-0.007	0.224	48.6	30
12	0.55	0.2	0.660	-0.005	0.217	64.0	45
13	0.54	0.2	0.626	-0.017	0.042	71.7	60
14	0.54	0.2	0.554	-0.008	-0.127	93.5	90
25	0.54	0.2	0.800	0.012	-0.348	133.1	135
15	0.54	0.75	1.15	-0.308	-0.025	26.8	0
16	0.55	0.75	0.835	-0.212	-0.038	55.7	30
17	0.54	0.75	0.710	-0.177	-0.048	70.1	45
18	0.55	0.75	0.650	-0.148	-0.167	80.0	60
19	0.55	0.75	0.676	-0.161	-0.294	106.9	90
26	0.54	0.75	1.02	-0.158	-1.130	140.1	135
20	0.54	1.167	1.28	-0.520	-0.025	32.2	0
21	0.55	1.167	0.86	-0.337	-0.061	63.5	30
22	0.54	1.167	0.76	-0.288	-0.044	75.5	45
23	0.54	1.167	0.745	-0.247	-0.367	80.8	60
24	0.55	1.167	0.845	-0.314	-0.415	112.4	90
27	0.54	1.167	1.26	-0.431	-1.120	149.9	135

Table 2.2. ULTIMATE MOMENT RESULTS General Moment Series (DOWNHAM) .

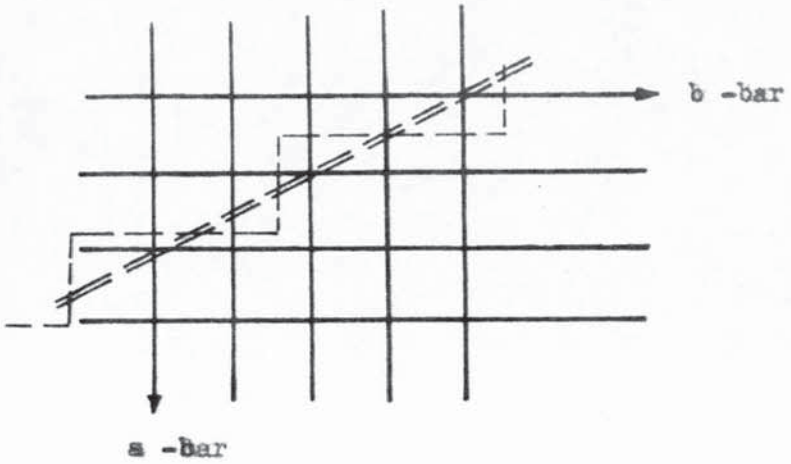

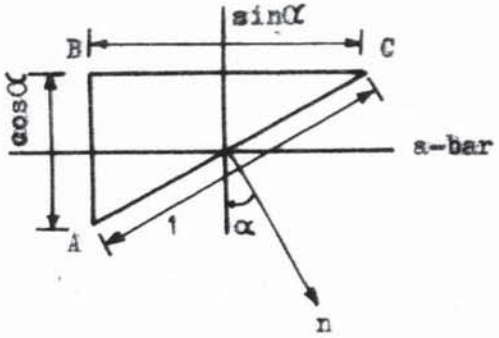

Wood's Basic Assuptions

Figure 2.1

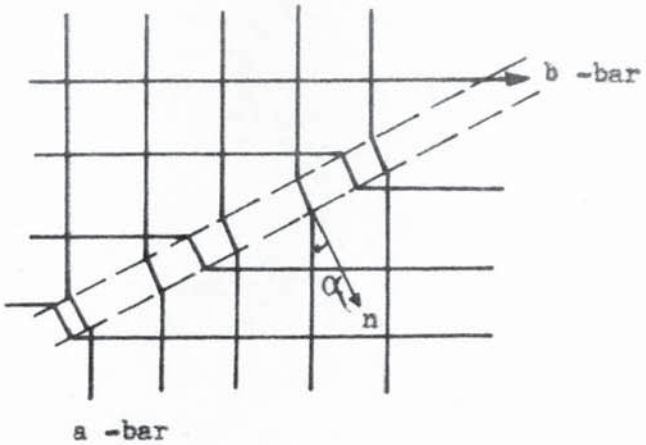

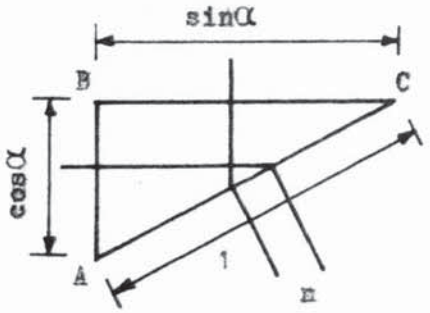

Johansen's Step Assumption

Figure 2.2

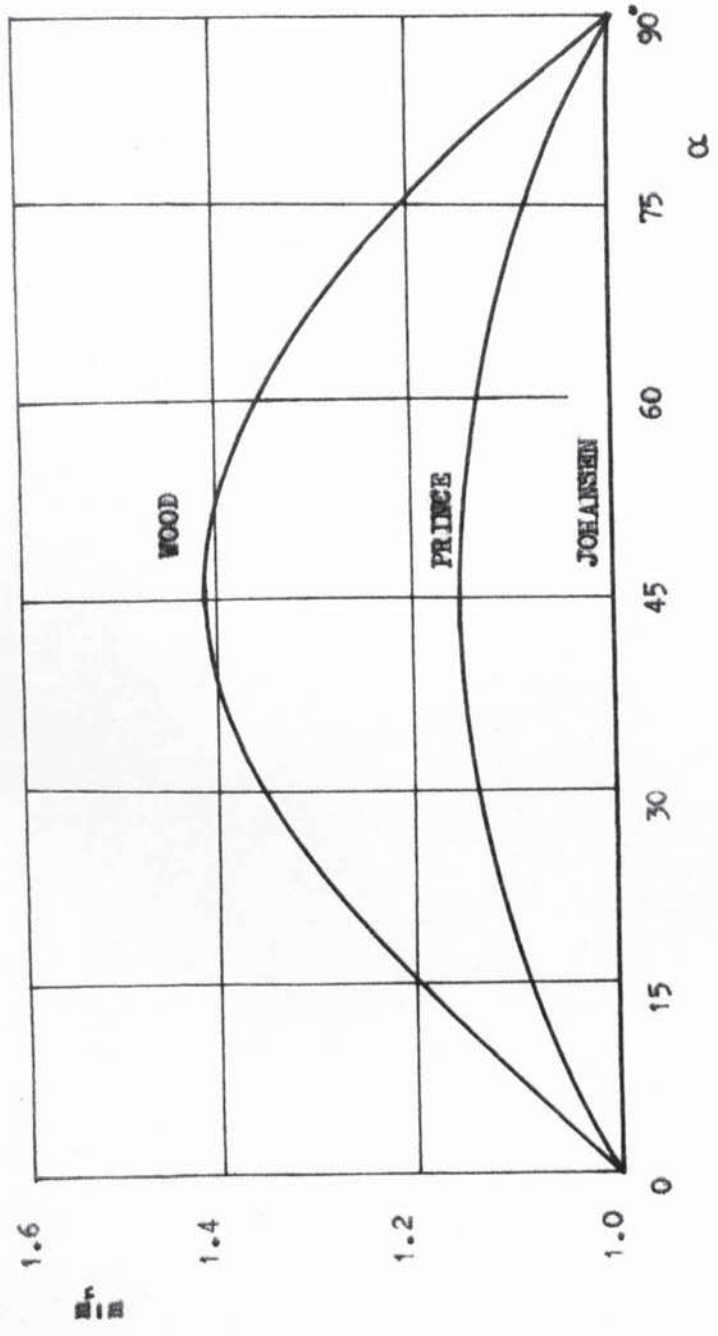

Figure 2.3 NORMAL BENDING MOMENTS ($\mu = 1$)

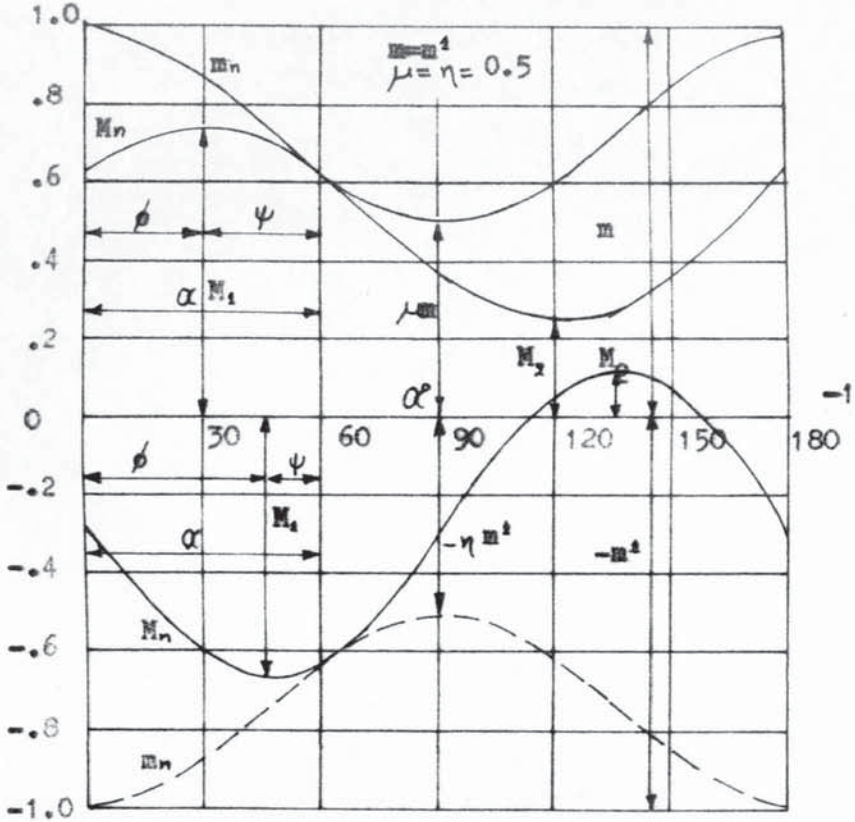

Figure 2.4 FAILURE IN SLAB -KEMP

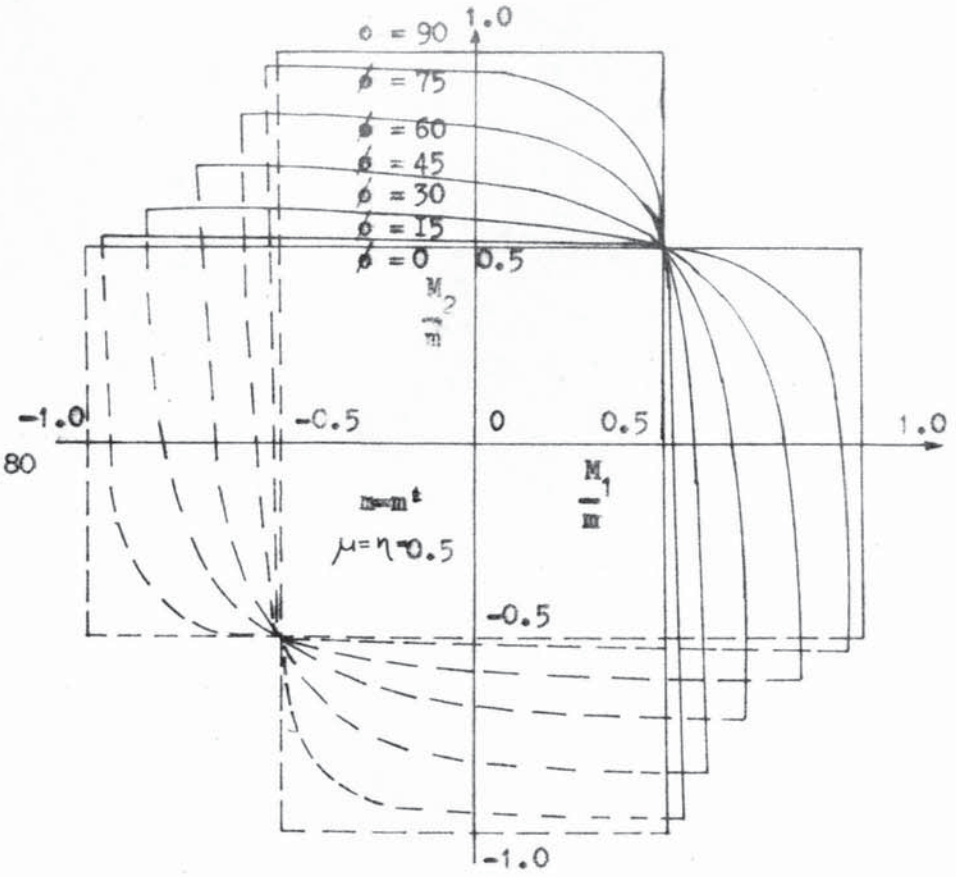

Figure 25 YIELD CONDITION - KEMP

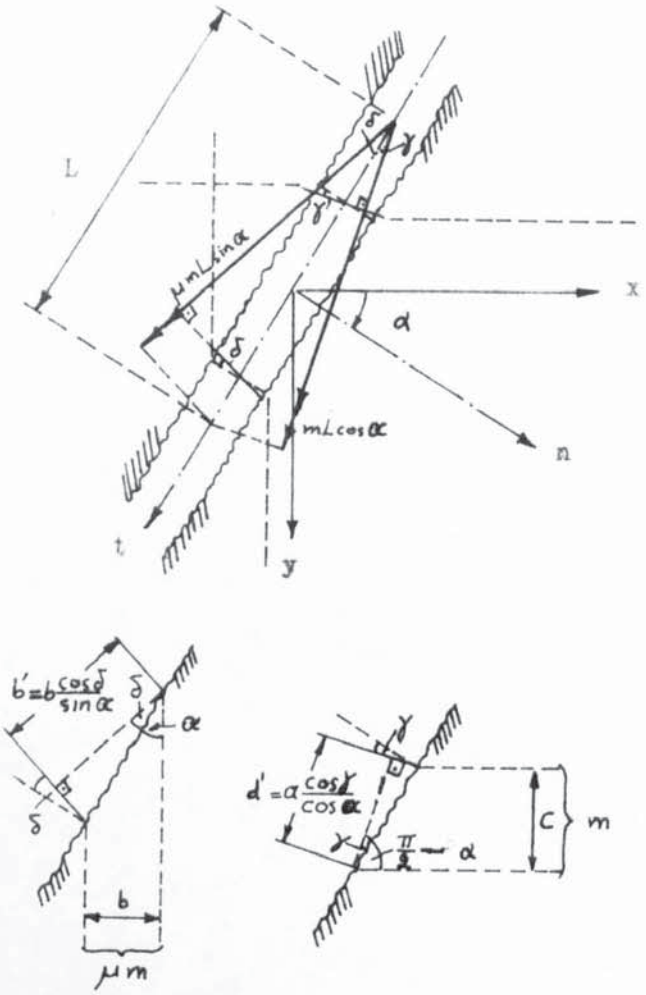

Figure 2.6 Geometrical pattern and yield moment components for an elastically orthotropic reinforced concrete slab.

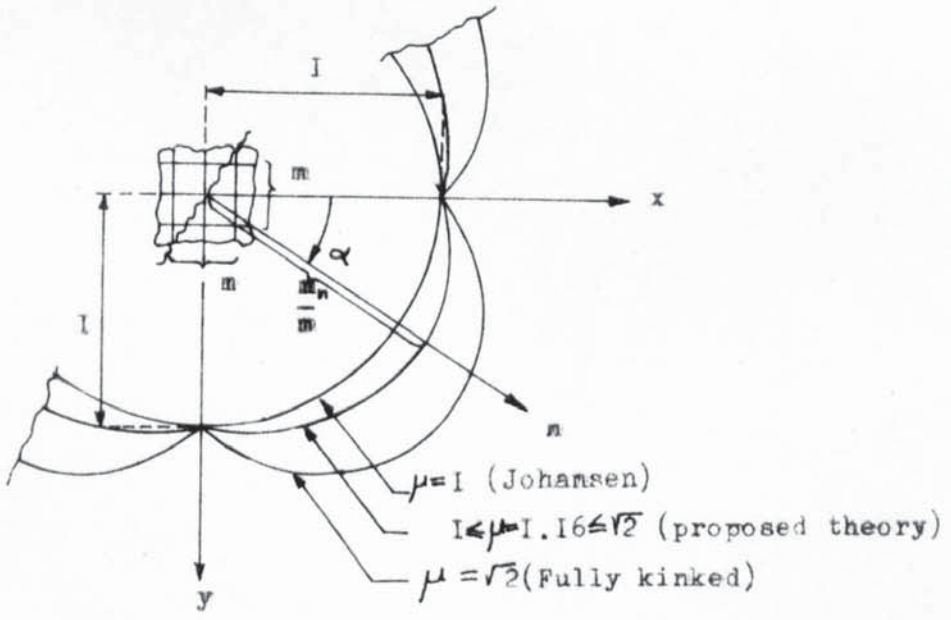

Figure 2.7 Graphical representation of the Kwiecinski criterion in polar co ordinates

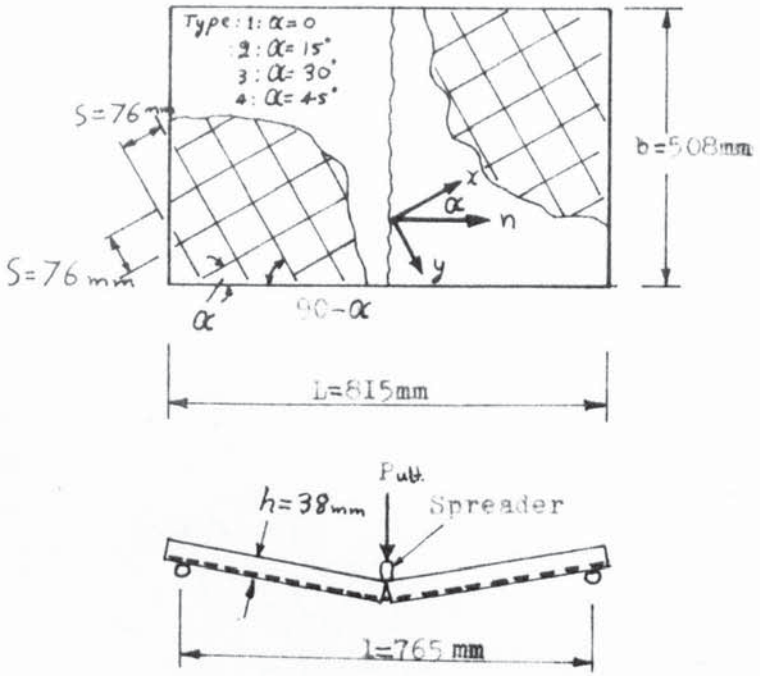

Figure 2.8 Details of slabs

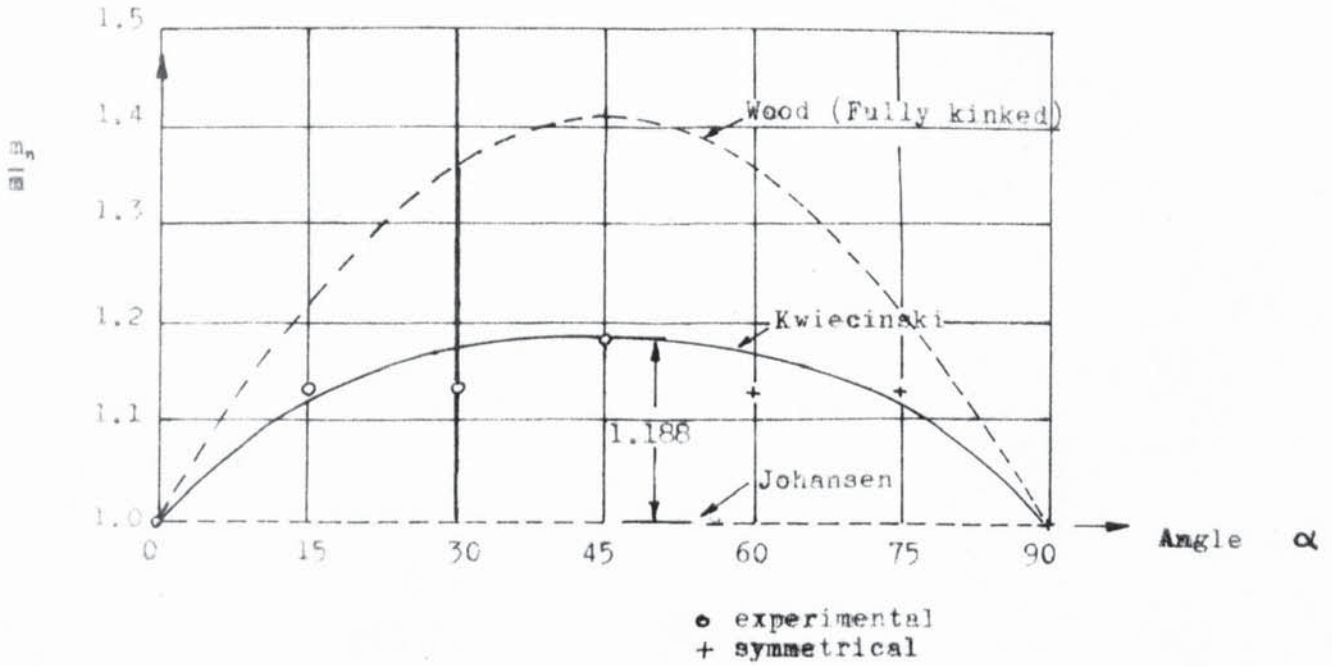

Figure 2.9 Theoretical and experimental results.

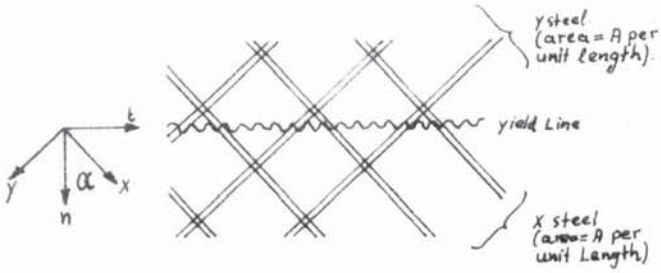

Co_ordinate directions in a isotropic slab

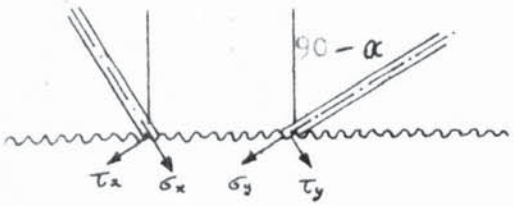

Postulated stess system in the reinforcement

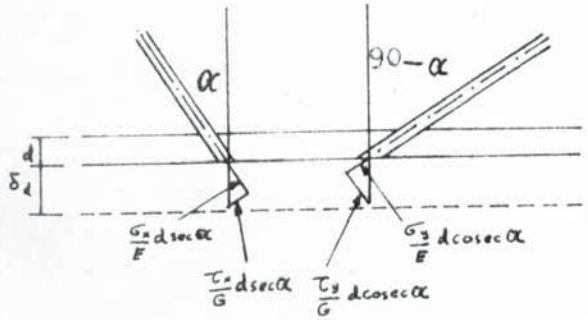

Figure 2.10 Elastic deformation of the reinforcement a crack

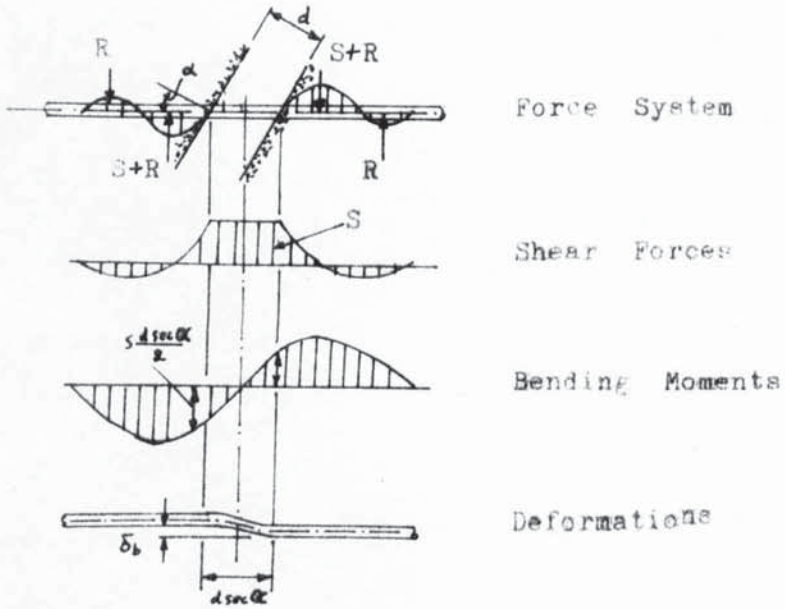

Figure 2.11 Bending deformions of a bar crossing a yield line obliquely

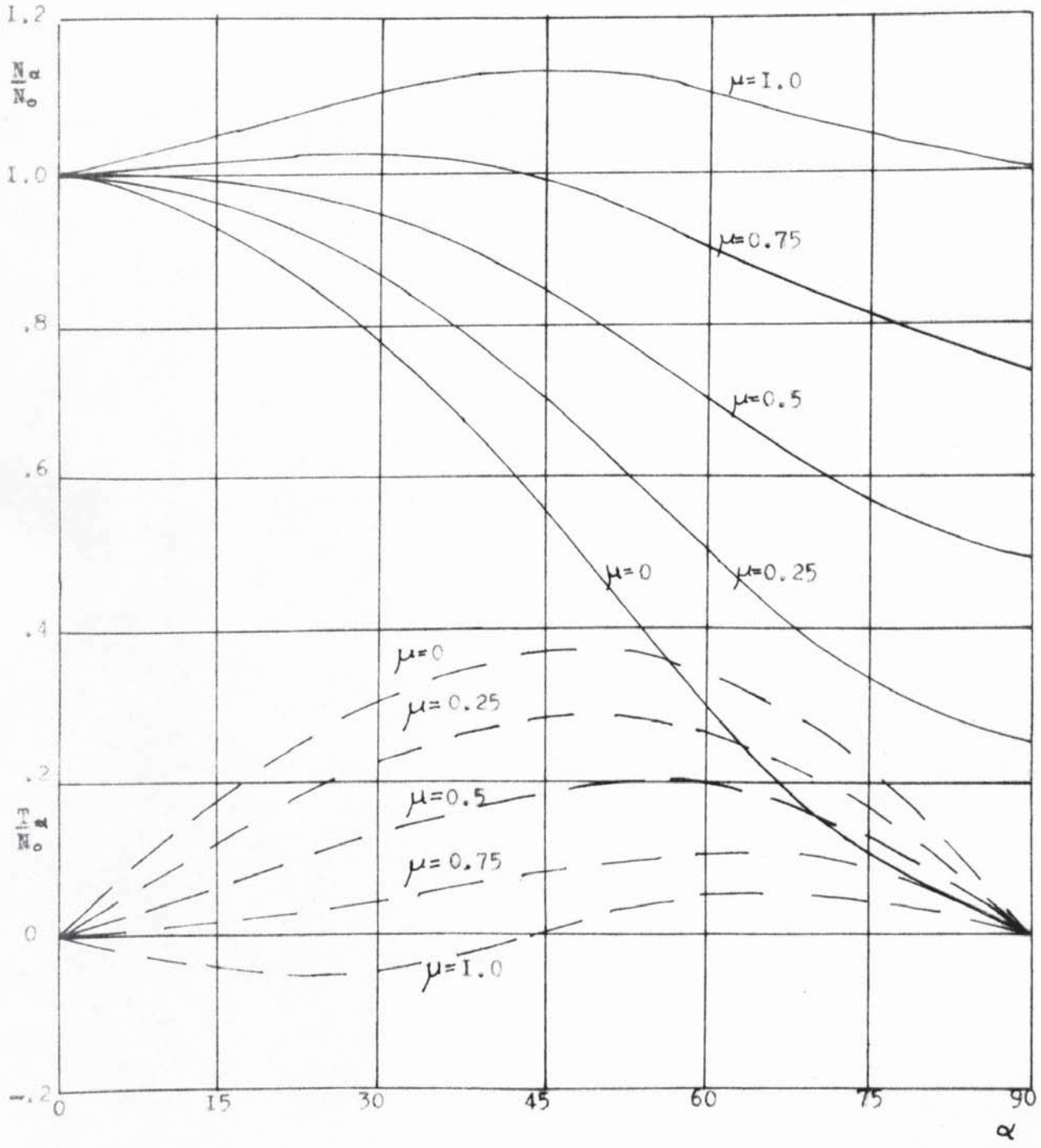

Figure 2.12 EQNS. DESCRIBING N and T BENDING ALLOWED PRINCE

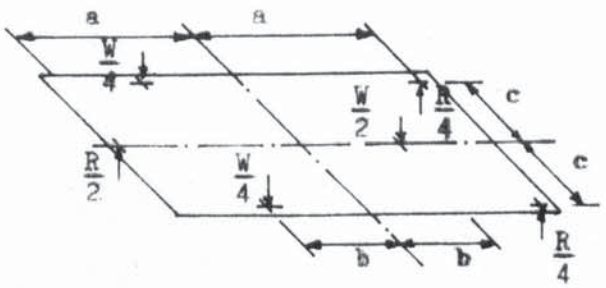

Figure 2.13 Testing rig used to produce uniform uniaxial bending

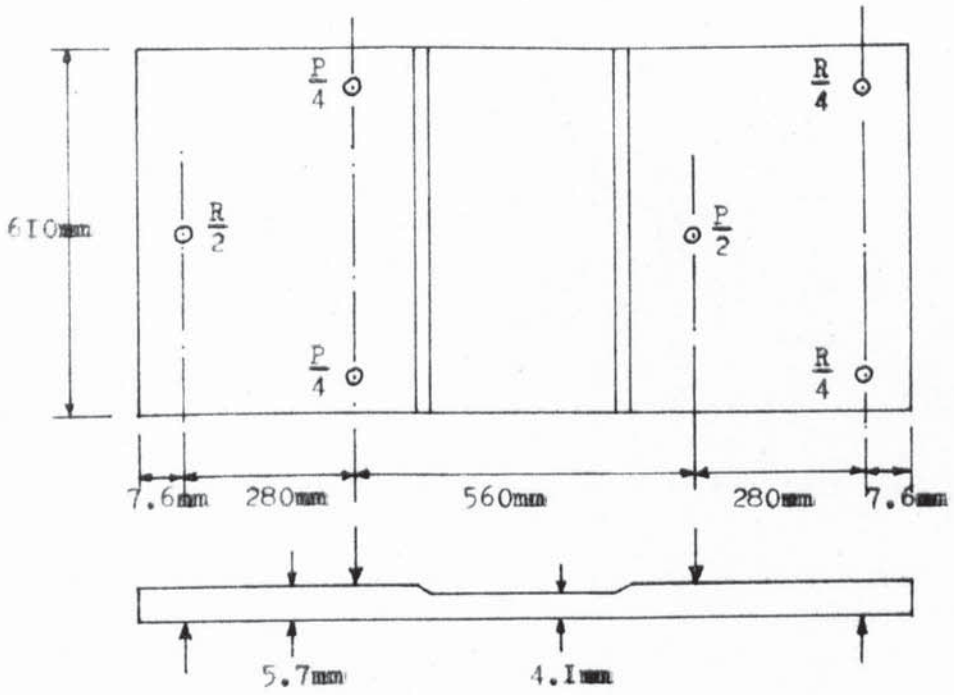

Figure 2.14 PRINCE TESTS

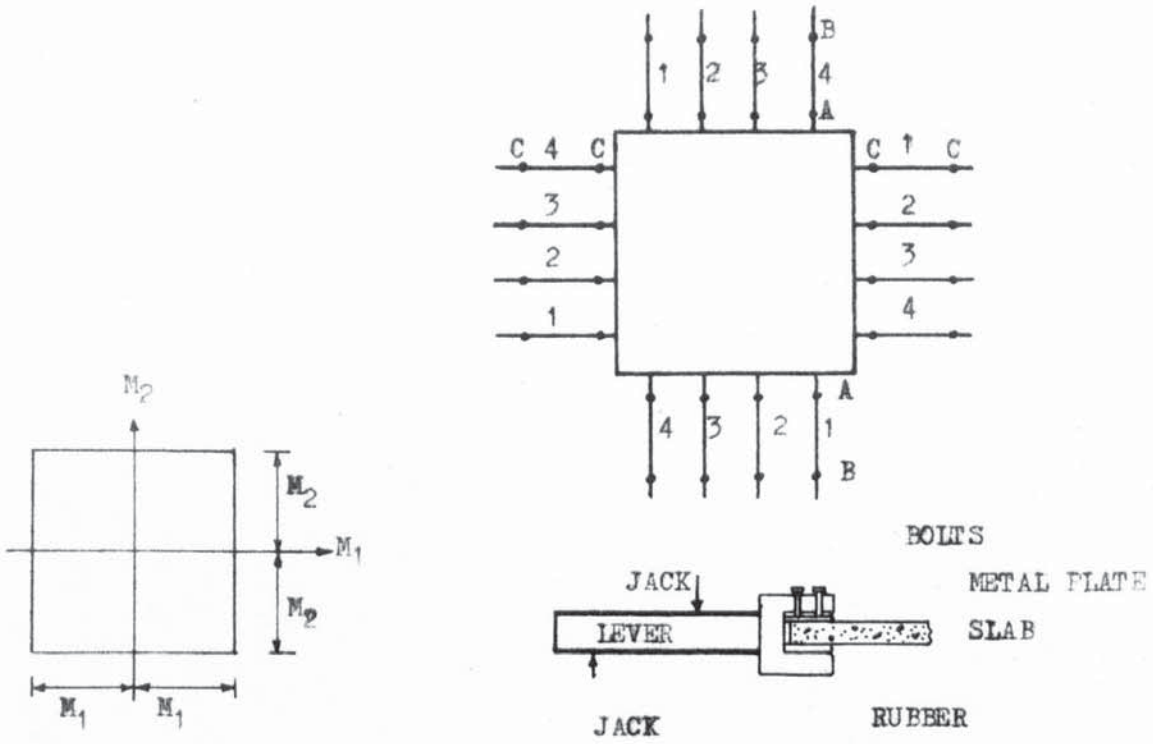

Figure 2.15

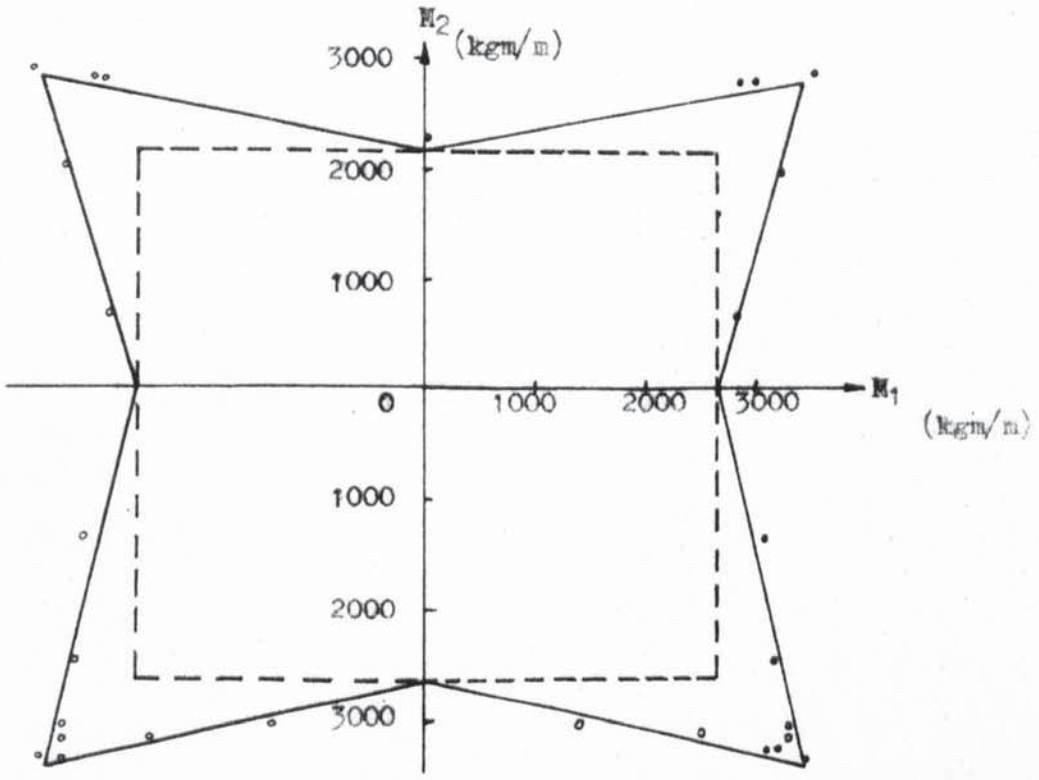

Yield Criterion $\phi = 0$

Figure 2.16

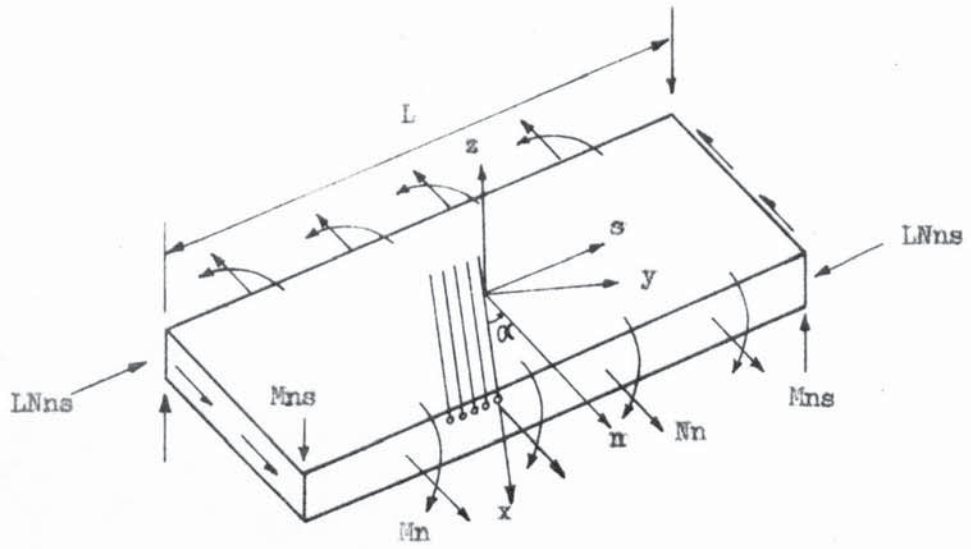

Nn=Membrane force per unit length
Mn=moment per unit length

Figure 2.17

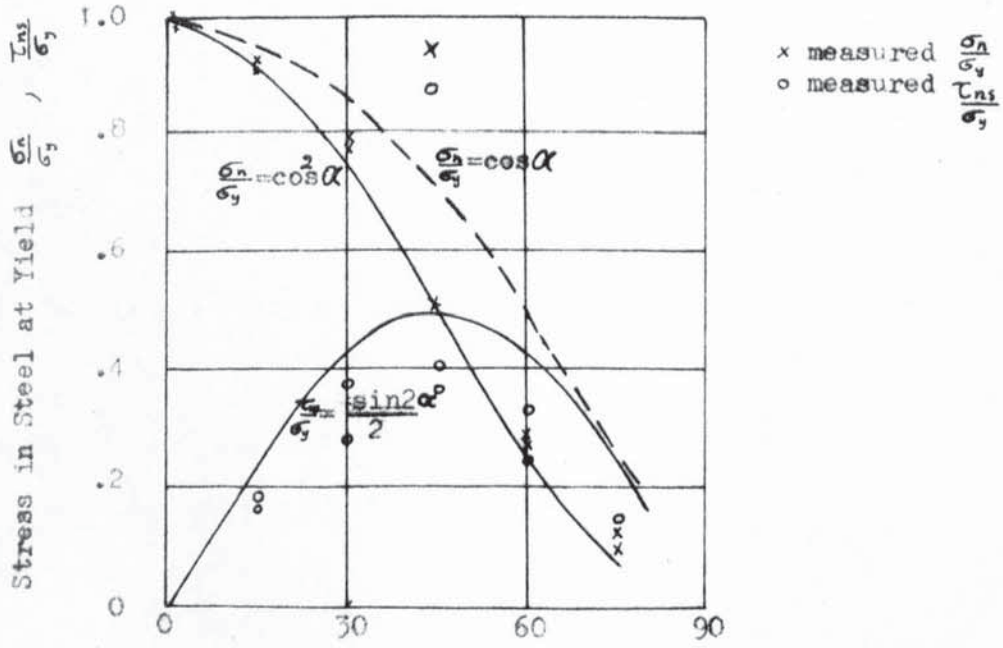

Angle of Reinforcement α

MORLEYS EXPERIMENTS

Figure 2.18

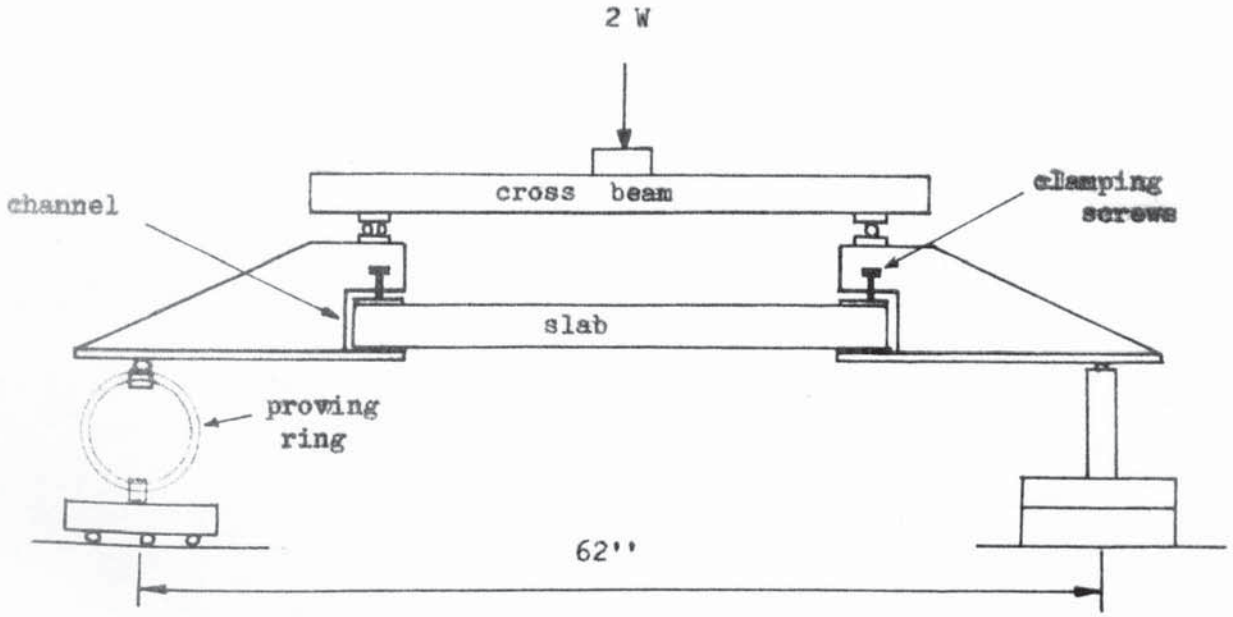

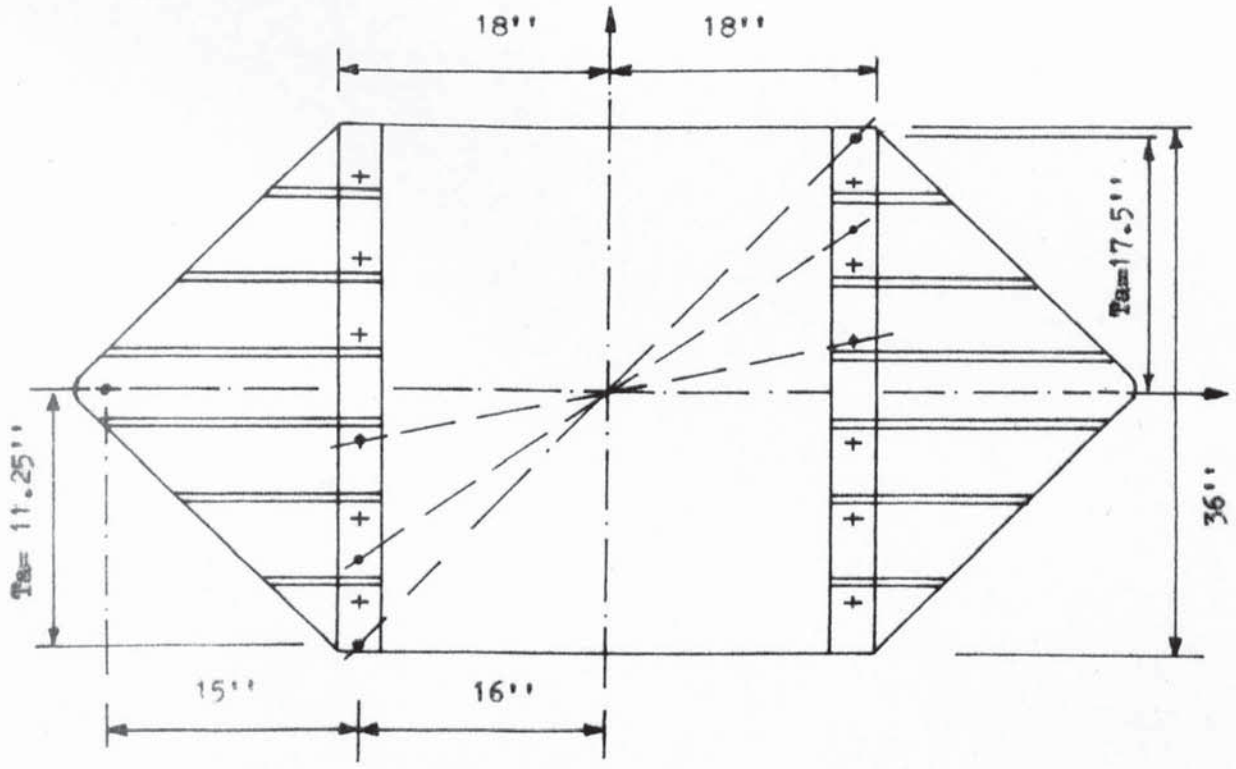

Figure 2.19 **TEST SET UP**

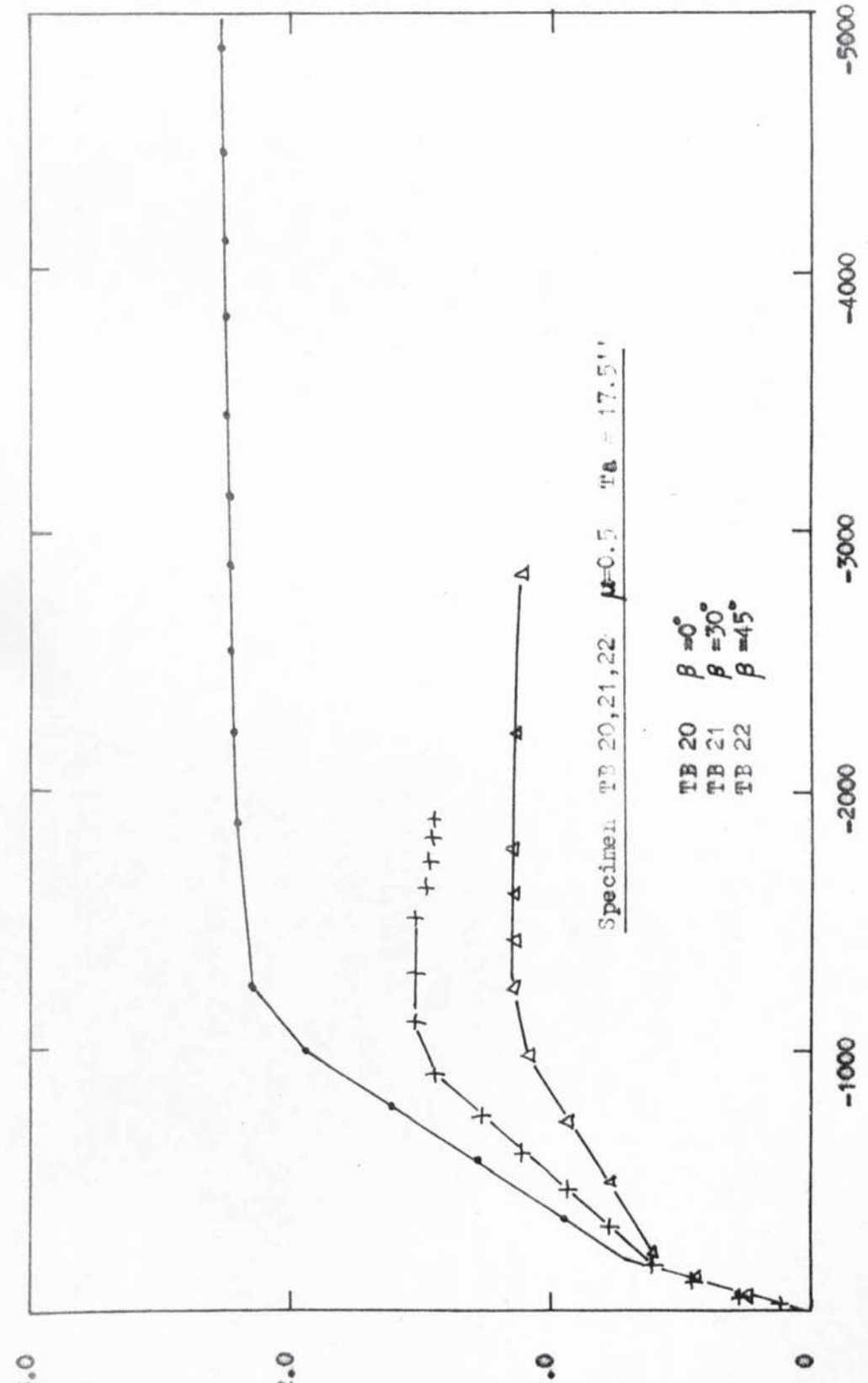

Figure 2.20 **PLOT OF PRINCIPAL CONCRETE STRAINS** (DOWNHAM)

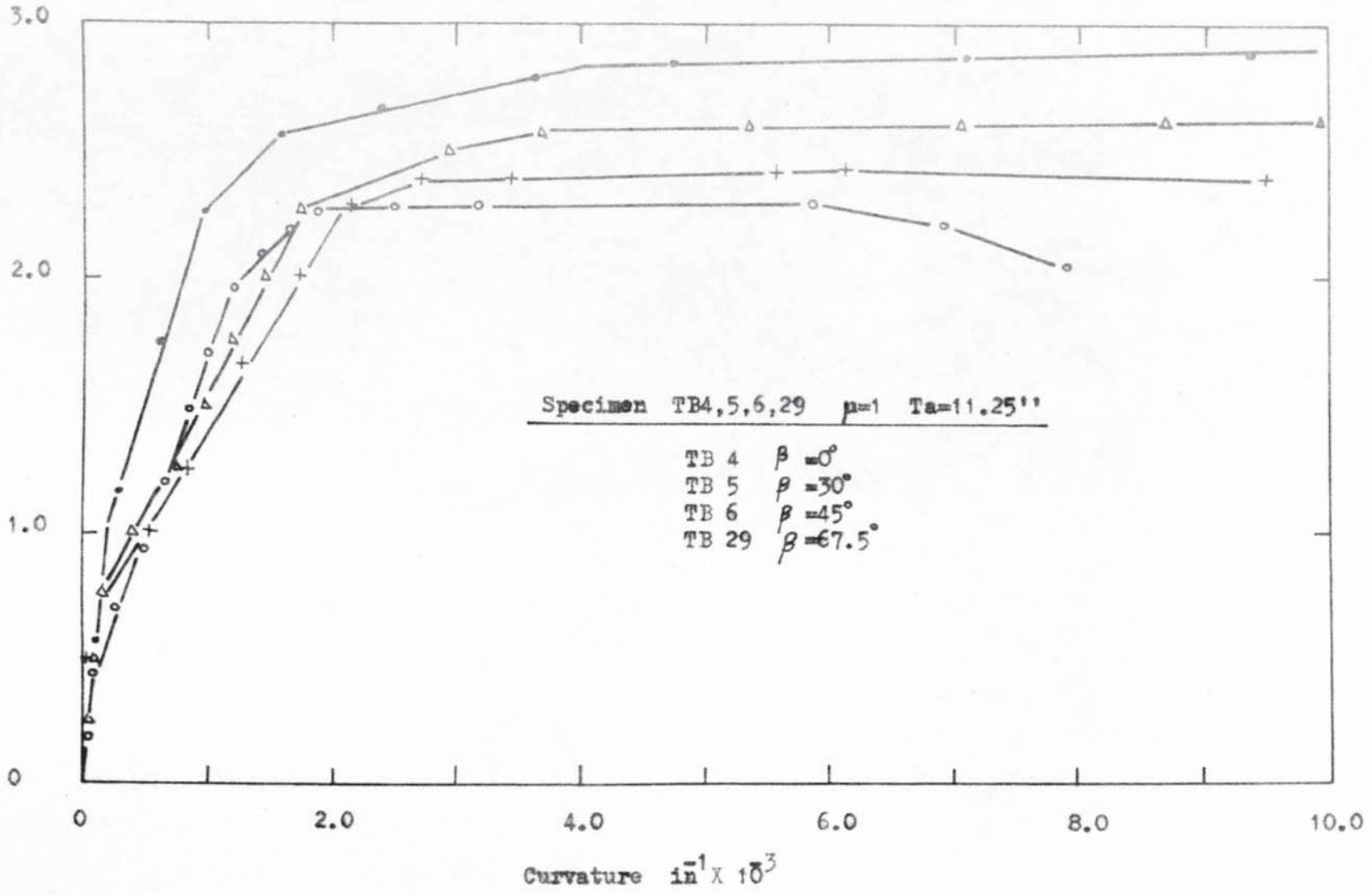

Figure 2.21 **PLOT MAXIMUM PRINCIPAL CURVATURE** (DOWNHAM)

CHAPTER 3

A NEW CRITERION FOR THEORETICAL YIELD

3.1 Introduction.

It is the purpose of any yield criterion to predict the ultimate load carrying capacity of a slab element subjected to any combination of biaxial moments.

The yield criterion considered in this chapter refers to the flexural yield condition of a reinforced concrete slab element, and is valid only if the steel is the governing factor. In other words, the section is under-reinforced.

Firstly, it is necessary to derive an equation for the normal yield moment on a yield line traversing a slab element at some oblique angle to the reinforcement. In order to make comparisons with the results of previous researchers, the normal and tangential moments are reduced to dimensionless quantities.

3.2 The Ideal and Perfect crack.

Consider a reinforcing bar which is inclined to the direction of the crack as shown in figure 3.1.

As the crack opens, assuming the concrete does not crush and is inelastic in the vertical plane containing the bar, the direction of the bar changes.

If the crack width becomes infinitely large, the bar becomes normal to the crack.

Naturally, the bar would have yielded when the crack width was only one or two mm. wide, and the change of direction of the bar was only a fraction of a degree. The Ideal crack should be straight and

should not crush. The stiffness of the concrete elements adjacent to the bar should be large.

Such a crack is realized by steel plates as shown in plates 3.1 and 3.2. Detailed description is given in Chapter 4.3.1.

3.2.1 Normal and tangential stresses on a steel bar traversing Ideal crack.

Consider Figure 3.2. From the geometry, it can be concluded that the reinforcing bar is antisymmetric with respect to the intersection between the centre lines of the crack and the bar. Therefore, this point of intersection will remain fixed independently of the width of the crack and the condition on either side of the crack. This same point is also free of bending moments, and is only subjected to shear and axial forces.

From the geometry of Figure 3.2, the half length of the bar is

$$l_o = \frac{L}{\sin\theta} \qquad .. \quad .. \quad 3.1$$

Using the triangle properties for triangle ABC

$$\frac{\Delta}{\sin\delta\theta} = \frac{l_o}{\cos(\theta+\delta\theta)} \qquad .. \quad .. \quad 3.2$$

From 3.1 and 3.2

$$\frac{\Delta}{\sin\delta\theta} = \frac{L}{\sin\theta\cos(\theta+\delta\theta)} \qquad .. \quad .. \quad 3.3$$

let $$\frac{\Delta}{L} = S$$

then from equation 3.3

$$\tan\delta\theta = \frac{S\sin 2\theta}{2(1+S\sin^2\theta)} \qquad .. \quad .. \quad 3.4$$

Consider half the bar in figure 3.2 subjected to a shear force F and an axial force P.

Using the co-ordinate system shown in figure 3.2, and the curvature relationship $\frac{dy^2}{dx^2} = -\frac{M_0}{EI}$

(the shear deformation will be considered later)

$$EI\frac{dy^3}{dx^3} - P\frac{dy}{dx} = -V \qquad .. \quad .. \quad 3.5$$

$$EI\frac{dy^4}{dx^4} - P\frac{dy^2}{dx^2} = q \qquad .. \quad .. \quad 3.6$$

Since the bar is subjected to axial and shear forces only, $q=0$, hence 3.5 reduces to

$$\frac{dy^3}{dx^3} - \mu^2\frac{dy}{dx} = -\mu^2\frac{V}{P} \qquad .. \quad .. \quad 3.7a$$

and 3.6 to

$$\frac{dy^4}{dx^4} - \mu^2\frac{dy^2}{dx^2} = 0 \qquad .. \quad .. \quad 3.7b$$

where $\mu^2 = \frac{P}{EI}$.

The general solution of equation 3.7b is

$$y = Ae^{\mu x} + Be^{-\mu x} + Cx + D \qquad .. \quad .. \quad 3.8$$

where A, B, C, and D are constants of integration, and can be found from the boundary conditions. The boundary conditions are:-

(i) at x=0 $\quad y=0$

(ii) at x=0 $\quad \frac{dy}{dx}=0$

(iii) at x=lo $\quad EI\frac{dy^2}{dx^2}=0$

(iv) at x=lo $\quad \frac{dy^3}{dx^3} - \mu^2\frac{dy}{dx} = -\mu^2\frac{F}{P}$

Applying the boundary conditions each in turn in the general solution 3.8 :-

$$\left.\begin{aligned} &A+B+D = 0 \\ &\mu A - \mu B + C = 0 \\ &A\mu^2 e^{\mu lo} + B\mu^2 e^{-\mu lo} = 0 \\ &A\mu^3 e^{\mu lo} - B\mu^3 e^{-\mu lo} - \mu^3 A e^{\mu lo} + \mu^3 B e^{-\mu lo} - \mu^2 C = -\mu^2 \frac{F}{P} \end{aligned}\right\} \quad .. \quad 3.10$$

Solving equation 3.10 for A, B, C, D

$$C = \frac{F}{P}$$

$$A = -\frac{F}{\mu P} \frac{e^{-\mu lo}}{(e^{\mu lo} + e^{-\mu lo})}$$

$$B = \frac{F}{\mu P} \frac{e^{\mu lo}}{(e^{\mu lo} + e^{-\mu lo})}$$

$$D = -\frac{F}{\mu P} . \tanh(\mu lo).$$

The general solution giving the deflection of bar is

$$y = \frac{F}{\mu P(e^{\mu lo} + e^{-\mu lo})}\left[- e^{\mu(x-lo)} + e^{-\mu(x-lo)}\right] + \frac{F}{P} x - \frac{F}{\mu P} \tanh \mu lo \quad .. \quad .. \quad 3.10a$$

The deflection of bar at centre of crack relative to original direction of bar, figure 3.2, due to bending only is δ_B.

From general solution 3.10a

$$\delta_B = \frac{F}{P} lo - \frac{F}{\mu P} \tanh \mu lo = \frac{Flo}{P}\left[1 - \frac{\tanh \mu lo}{\mu lo}\right] \quad .. \quad .. \quad 3.11$$

The equation 3.11 should be corrected for shear deformation.

The shear deformation $\delta_s = \frac{KloF}{AG}$ 3.12

where K is a constant depending on the shape of the steel bar. For a round solid bar $K = \frac{10}{9}$.

The total deformation due to shear and bending is obtained by adding 3.11 and 3.12.

$$\delta = \frac{KloF}{AG} + \frac{Flo}{P}\left[1 - \frac{\tanh \mu lo}{\mu lo}\right] \quad .. \quad .. \quad 3.13$$

Referring to figure 3.2,

$$\delta = lo \tan \delta\theta \quad .. \quad .. \quad 3.14$$

From equations 3.13 and 3.14

$$\frac{F}{P} = \frac{\tan\delta\theta}{\left(\frac{KP}{AG} + 1 - \frac{\tanh(\mu lo)}{\mu lo}\right)} \qquad .. \quad .. \quad 3.15$$

Assuming that τ is the average shear stress and σ is the average axial stress $\frac{F}{P} = \frac{\tau}{\sigma}$

Equation 3.15 can be re-written in the form

$$\frac{\tau}{\sigma} = \frac{\tan(\delta\theta)}{\left(\frac{KP}{AG} + 1 - \frac{\tanh(\mu lo)}{\mu lo}\right)} \qquad .. \quad .. \quad 3.16$$

From equation 3.4 $\tan(\delta\theta) = \frac{S\sin 2\theta}{2(1+S\sin^2\theta)}$ 3.17

From figure 3.2 $\frac{e}{lo} = \frac{\Delta}{L}\sin^2\theta$ (axial strain ε)

$$\varepsilon = \frac{\Delta}{L}.\sin^2\theta \qquad .. \quad .. \quad 3.18$$

The axial force $P = EA\varepsilon = EA\frac{\Delta}{L}\sin^2\theta$ 3.19

but $\mu lo = \sqrt{\frac{P}{EI}}.lo = \sqrt{\frac{\Delta}{L}} \cdot \frac{L}{r_G}$

where $r_G = \frac{D}{4}$ radius of gyration of section (round bar),

hence $\mu lo = 4.\sqrt{S} \cdot \frac{L}{D} = 2\sqrt{S}\,\varrho$ 3.20

where $\varrho = \frac{2L}{D}$ crack width/diameter.

The quantity $\frac{KP}{AG}$ may be transformed into known quantities, thus:-

let $3G = E$ (Young's modulus of steel)

then $\frac{KP}{AG} = 3K.\frac{P}{EA} = 3K.S\sin^2\theta$ (from 3.19) 3.21

Substituting 3.17, 3.20 and 3.21 in equation 3.16

$$\frac{\tau}{\sigma} = \frac{S\sin 2\theta}{2(1+S\sin^2\theta)\left[3KS\sin^2\theta + 1 - \frac{\tanh(2\sqrt{S}\varrho)}{2\sqrt{S}\varrho}\right]} \qquad .. \quad .. \quad 3.22$$

Examining equation 3.22, it is obvious that for a given bar orientation, the ratio $\frac{\tau}{\sigma}$ depends only on the value of ϱ and S.

Since the crack is Ideal, the value of ϱ at yield could be measured directly or, as in our case, in the steel analogue series, design ϱ for a particular value. For practical cases, the value of ϱ at yield could be evaluated analytically as will be shown later.

For ordinary reinforcing steel, the S, $(\frac{\Delta}{L})$, value cannot exceed 0.002 units because the steel will yield.

To investigate the effect of S on the $\frac{\tau}{\sigma}$ ratio, a computer program was written and the equation 3.22 was solved for a range of angles ranging from 0° to 90°, and also for a range of S values ranging from 0 to 0.04.

It was found that for a given bar orientation, the ratio $\frac{\tau}{\sigma}$ was independent of S.

It has been concluded, therefore, that the shear stress to axial stress ratio depends only on the bar orientation for a given value of crack width to diameter ratio.

Figure 3.3 shows the variation of $\frac{\tau}{\sigma}$ with α for a given ϱ where α is the angle between the direction of a bar and the normal to the crack ($\alpha = 90-\theta$).

3.3 The concrete crack traversed by a steel bar.

Contrary to the ideal crack is the ordinary concrete crack. According to the size of shear and axial stresses acting on the bar, the concrete adjacent to the bar would act elastically or plastically. As the crack opens, the steel bar has a tendency to normalize itself to the yield line.

A shear force is transmitted from the bar onto the concrete

adjacent to the bar. Such a crack is shown in figure 3.4. The bar then re-orientates itself. The re-orientation effect of the bar on the overall bending moment of resistance is negligible, as will be shown later the overall re-orientation at yield is only a small fraction of a degree.

3.3.1 Normal and Tangential stresses on a steel bar traversing a concrete crack.

The basic assumption in this theory is that the stress-strain curve for the concrete adjacent to the bar is rigid-plastic.

This assumption implies that the pressure, q, exerted by the reinforcing bar on the concrete, is constant over a length, l_p, which is required for equilibrium.

Consider a bar inclined at an angle θ to the crack as shown in figure 3.5. Using the co-ordinate system as shown in figure 3.5 and the arguments of Chapter 3.2.1, the equilibrium conditions require that

$$EI \frac{dy^3}{dx^3} - P \frac{dy}{dx} = -V \qquad .. \quad .. \quad 3.23a$$

$$EI \frac{dy^4}{dx^4} - P \frac{dy^2}{dx^2} = +q \qquad .. \quad .. \quad 3.23b$$

modifying the above equation by letting $\mu^2 = \frac{P}{EI}$

$$\frac{dy^3}{dx^3} - \mu^2 \frac{dy}{dx} = -\mu^2 \frac{V}{P} \qquad .. \quad .. \quad 3.24a$$

$$\frac{dy^4}{dx^4} - \mu^2 \frac{dy^2}{dx^2} = +\mu^2 \frac{q}{P} \qquad .. \quad .. \quad 3.24b$$

The differential equation 3.24b has the general solution

$$y = Ae^{\mu x} + Be^{-\mu x} + Cx + D + \frac{qx^2}{2P} \qquad .. \quad .. \quad 3.25$$

The constants of integration A, B, C, and D can be found from the boundary conditions and the equilibrium equations.

The boundary conditions are:-

$$\left.\begin{array}{ll} \text{(i)} & \text{at } x=0 \quad y=0 \\ \text{(ii)} & \text{at } x=0 \quad \frac{dy}{dx}=0 \\ \text{(iii)} & \text{at } x=lp \quad EI\frac{dy^2}{dx^2}=0 \\ \text{(iv)} & \text{at } x=lp \quad \frac{dy^3}{dx^3}-\mu^2\frac{dy}{dx}=-\mu^2\frac{F}{P} \end{array}\right\} \quad .. \quad .. \quad 3.26$$

The horizontal equilibrium of the bar requires that

$$F = q\,lp \quad .. \quad .. \quad 3.27$$

where q is the pressure exerted by the concrete on the bar and 2lp is the effective crack width.

It is assumed that q is acting uniformly through the half effective crack width lp. It is not far from the truth since at yield, and this is the point of investigation, the concrete near the crack will have a tendency to crush, and hence creating a zone of constant stresses at the vicinity of the crack. As long as the effective crack is not large in relation to the diameter of the bar, the equation 3.27 is valid.

Applying the boundary conditions 3.26, equilibrium equation 3.27 in the general solution 3.25

$$\left.\begin{array}{l} A+B+D=0 \\ A\mu-B\mu+C=0 \\ A\mu^2e^{\mu lp}+B\mu^2C^{-\mu lp}+\frac{q}{P}=0 \\ -\mu^2C-\mu^2q\frac{lp}{P}=-\mu^2\frac{F}{P} \\ F=q\,lp \end{array}\right\} \quad .. \quad .. \quad 3.28$$

Solving above equation

$$C=0$$

$$A=B=-\frac{q}{2\mu^2P\cosh\mu lp}=-\frac{F}{2\mu^2lpP}\frac{1}{\cosh\mu lp}$$

$$D = -2A = \frac{F}{\mu^2 lpP} \quad \frac{1}{\cosh \mu lp}$$

Hence the general solution is

$$y = \frac{F}{P}\left[\frac{1}{\mu^2 lp \cosh \mu lp}(1 - \cosh \mu x) + \frac{x^2}{2lp}\right] \quad .. \quad .. \quad 3.29$$

The deflection of the bar at the centre of the crack (x=lp)

$$\delta_B = \frac{Flp}{P}\left[\frac{\cosh(\mu lp) - 1}{\mu^2 lp^2} + \frac{1}{2}\right] \quad .. \quad .. \quad 3.30$$

The deflection given by equation 3.30 is due to bending only and a correction is required for the shear deformation.

For a bar subjected to a uniformly distributed load q and a point load F, the shear deformation is given by equation

$$\delta_S = \frac{K}{AG} \cdot \frac{Flp}{2} \quad .. \quad .. \quad 3.31$$

the notation having the same meaning as before. The total deformation is obtained by adding up 3.30 and 3.31

$$\delta = \frac{F.lp}{P}\left[\frac{\cosh(\mu lp) - 1}{\mu^2 lp^2} + \frac{1}{2} + \frac{PK}{2AG}\right] \quad .. \quad .. \quad 3.32$$

From 3.14 $\delta = l_o \tan\theta$

In this case the half length of bar in the crack is lp instead of lo

hence $\delta = lp\tan\theta$ 3.33

From equation 3.20 $\mu lp = 2\sqrt{S}\,\varrho$ 3.34

From equation 3.21 $\frac{KP}{AG} = 3.KS\sin^2\theta$ 3.35

Substitute 3.33, 3.34 and 3.35 in equation 3.32

$$\tan\theta = \frac{F}{P}\left[\frac{\cosh(2\sqrt{S}\,\varrho) - 1}{(2\sqrt{S}\,\varrho)^2} + \frac{1}{2} + \frac{3}{2} \cdot KS\sin^2\theta\right] \quad .. \quad .. \quad 3.36$$

Let the average shear stress be τ and the average axial stress σ then $\frac{F}{P} = \frac{\tau}{\sigma}$.

Re-arranging 3.36 -

$$\frac{\tau}{\sigma} = \frac{\tan(\delta\theta)}{\left[\frac{\infty\,\mathrm{sech}(2\sqrt{S}\,\varrho) - 1}{(2\sqrt{S}\,\varrho)^2} + \frac{1}{3} + \frac{3}{2}\cdot KS\sin^2\theta\right]} \quad .. \; .. \; 3.37$$

From 3.4 $$\tan(\delta\theta) = \frac{S\sin 2\theta}{2(1+S\sin^2\theta)} \quad .. \; .. \; 3.38$$

Substitute 3.38 in equation 3.37

$$\frac{\tau}{\sigma} = \frac{S.\sin 2\theta}{2(1+S\sin^2\theta)\left[\frac{\infty\,\mathrm{sech}(2\sqrt{S}\,\varrho)-1}{(2\sqrt{S}\,\varrho)^2} + \frac{1}{3} + \frac{3}{2}.\ KS\sin^2\theta\right]} \quad 3.39$$

The equation 3.39 will give the ratio $\frac{\tau}{\sigma}$ provided ϱ and S are known. S has a range of values from (0–0.002).

Let $\frac{\tau}{\sigma} = \eta$

at yield from Von-Mises $fy^2 = \sigma^2 + 3\tau^2$

hence $$\frac{\tau}{fy} = \frac{\eta}{\sqrt{1 + 3\eta^2}} \quad .. \; .. \; 3.40$$

To study the effect of ϱ and S on equation 3.40, a computer program was written to solve equation 3.40 for a range of values for ϱ, S and θ. From the results it was concluded that for a given bar orientation the value $\frac{\tau}{fy}$ was independent of S, for the given range of S values, and dependent on ϱ. The value of ϱ must be found.

The equilibrium equation $F = q\,lp$ (3.28) will be used in conjunction with equation 3.40 to evaluate ϱ.

$$F = q\,lp$$

$$F = \tau\pi\frac{D^2}{4},\quad lp = \frac{L}{\sin\theta},\quad q = D.U.$$

hence $$\tau\,\pi\,\frac{D^2}{4} = DU.\frac{L}{\sin\theta}$$

Re-arrange $$\frac{2L}{D} = \varrho = \frac{\tau}{U}\cdot\frac{\pi}{2}\cdot\sin\theta$$

$$\varrho = \frac{\tau}{fy}\cdot\frac{fy}{U}\cdot\frac{\pi}{2}\cdot\sin\theta$$

For a given bar orientation the above equation relates the crack width diameter ratio to the shear stress on the bar.

For ordinary reinforced concrete and in particular the one used in our experiments the $\frac{fy}{U}$ is 10.

Therefore $\varrho = \frac{\tau}{fy} \cdot 5\pi \sin\theta$ 3.41

If, for a given bar orientation, the equations 3.40 and 3.41 are solved simultaneously, ϱ can be found.

A computer program was written to solve numerically the equation 3.40 for a range of ϱ and θ values. S was given a value (0.004) since $\frac{\tau}{fy}$ is independent of S.

A family of curves ϱ v.s. $\frac{\tau}{fy}$ were plotted for a range of θ values.

Also, the equation 3.41 was plotted on the same axes for the same range of θ values (see Fig. 3.6). For a particular value of θ, the intersection point of the two curves (3.40 and 3.41) gave the ϱ value. Figure 3.7 shows the variation ϱ with respect to angle θ.

A computer program was written to investigate the contribution of $(\frac{\tau}{fy})$ ratio to the total normal and twisting moments along the yield line for the average ϱ_o value and the correct ϱ as shown in figure 3.7 for a range of θ values. It was found that the variation was only 1.5%. Since variation was small, therefore, it has been decided that in future calculations the average ϱ_o value is to be used.

Let $\varrho = \varrho_o = 1.413$, equation 3.39 can be re-written:

$$\frac{\tau}{\sigma} = \frac{S\sin 2\theta}{2(1+S\sin^2\theta)\left[\frac{\cosech(2\sqrt{S}\,\varrho_o) - 1}{(2\sqrt{S}\,\varrho_o)^2} + \frac{1}{2} + \frac{3}{2}K\sin^2\theta\right]} \qquad 3.42$$

The equation 3.42 gives the shear/axial stress ratio of a bar inclined at an angle θ to the crack. Figure 3.8 and 3.9 show the variation of

$\frac{\tau}{\sigma}$ v.s.α and $\frac{\tau}{f_y}$ v.sα where α is the angle between the direction of a bar and the normal to the crack. ($\alpha = 90-\theta$).

3.4 Development of Theoretical Normal and Twisting moments at yield.

It is the purpose of any yield criterion to predict the ultimate load carrying capacity of a slab element subjected to any combination of biaxial moments.

Firstly, it is necessary to derive an equation for the normal yield moment on a yield line traversing a slab element at some oblique angle to the reinforcement.

In section 3.3, it was proved that

$$\frac{\tau}{\sigma} = \frac{S\sin 2\theta}{2(1+S\sin^2\theta)\left[\frac{\cosech(2\sqrt{S}\,e_o)-1}{(2\sqrt{S}\,e_o)^2} + \frac{1}{2} + \frac{3}{2}K\sin^2\theta\right]}$$

where θ was the direction of the bar relative to the crack.

It is customary, though, to express direction relative to the normal to the crack.

Let $\alpha = 90-\theta$, (Figure 3.5)

The ratio of stresses in bar a is

$$\frac{\tau_a}{\sigma_a} = \frac{S\sin 2\alpha}{2(1+S\cos^2\alpha)\left[\frac{\cosech(2\sqrt{S}\,e_o)-1}{(2\sqrt{S}\,e_o)^2} + \frac{1}{2} + \frac{3}{2}K\cos^2\alpha\right]} \quad .. \; 3.43$$

The ratio of stresses in bar b is

$$\frac{\tau_b}{\sigma_b} = \frac{S\sin 2\alpha}{2(1+S\sin^2\alpha)\left[\frac{\cosech(2\sqrt{S}\,e_o)-1}{(2\sqrt{S}\,e_o)^2} + \frac{1}{2} + \frac{3}{2}K\sin^2\alpha\right]} \quad .. \; 3.44$$

Let $k_a = \frac{\tau_a}{\sigma_a}$ and $k_b = \frac{\tau_b}{\sigma_b}$ 3.45

From Von-Mises criterion and equation 3.45 at yield

$$\sigma_a = \frac{f_y}{\sqrt{1+3k_a^2}}, \qquad \tau_a = \frac{k_a f_y}{\sqrt{1+3k_a^2}} \qquad .. \quad .. \quad 3.46a$$

$$\sigma_b = \frac{f_y}{\sqrt{1+3k_b^2}}, \qquad \tau_b = \frac{k_b f_y}{\sqrt{1+3k_b^2}} \qquad .. \quad .. \quad 3.46b$$

From figure 3.10, the normal and tangential forces per unit length on the yield line are given by:-

$$N = A\sigma_a \cos^2\alpha + \mu A\sigma_b \sin^2\alpha + (\tau_a + \mu\tau_b)A\sin\alpha\cos\alpha \quad .. \quad 3.47a$$

$$T = A(\sigma_a - \mu\sigma_b)\sin\alpha\cos\alpha + \mu A\tau_b \sin^2\alpha - A\tau_a \cos^2\alpha \quad .. \quad 3.47b$$

It is obvious that if both sets of bars yield, the equations 3.46a and 3.46b can be substituted in equations 3.47a and 3.47b, and the normal and tangential forces will be obtained in terms of yield stresses. For large deformations to take place, certainly both sets of bars should yield, and in exceptional circumstances yield will occur in both sets of bars simultaneously. In general, one set of bars will yield first, and then deform plastically until the second set yields.

According to the law of plastic potential, there will hardly be any change in the stress distribution on the bars after yield.

Therefore, from equations 3.46a, 3.46b and 3.47a

$$N = \frac{Af_y}{\sqrt{1+3k_a^2}}\cos^2\alpha + \mu\frac{Af_y}{\sqrt{1+3k_b^2}}\sin^2\alpha + \frac{k_a f_y}{\sqrt{1+3k_a^2}} + \mu\frac{k_b f_y}{\sqrt{1+3k_b^2}} A\sin\alpha\cos\alpha$$

From equations 3.46a, 3.46b and 3.47b

$$T = A\left(\frac{f_y}{\sqrt{1+3k_a^2}} - \frac{\mu f_y}{\sqrt{1+3k_b^2}}\right)\sin\alpha\cos\alpha + A\left(\frac{\mu k_b f_y}{\sqrt{1+3k_b^2}}\sin^2\alpha - \frac{k_a f_y}{\sqrt{1+3k_a^2}}\cos^2\alpha\right)$$

The two above equations give the normal and twisting forces on the yield line at yield.

For under-reinforced slabs, for which the above theory is applicable, the compression concrete zone is small and it could be argued that the lever arm in any direction is constant and equal to l_a.

If both equations are multiplied by the lever arm, the normal and twisting forces are reduced to moments:

$$m_n = \frac{m}{\sqrt{1+3k_a^2}}\cdot\cos^2\alpha + \frac{\mu\, m}{\sqrt{1+3k_b^2}}\sin^2\alpha + \left(\frac{ka}{\sqrt{1+3k_a^2}} + \frac{\mu\, kb}{\sqrt{1+3k_b^2}}\right)\frac{m}{2}\sin 2\alpha \quad 3.48a$$

$$m_{nt} = \frac{m}{2}\left(\frac{1}{\sqrt{1+3k_a^2}} - \frac{\mu}{\sqrt{1+3k_b^2}}\right)\sin 2\alpha - m\left(\frac{ka}{\sqrt{1+3k_a^2}}\cdot\cos^2\alpha - \frac{\mu kb}{\sqrt{1+3k_b^2}}\cdot\sin^2\alpha\right) \quad 3.48b$$

The development of the above equations is based upon an elastic analysis; they may strictly only be used to define the onset of yield.

It has, however, been argued previously that the plastic distribution of stress on the bars are not likely to be different from the elastic.

The formulae 3.48a and 3.48b could be used to determine the actual failure of the slab without any significant error.

A computer program was written to solve the equations for the normal and twisting moments; the results are shown in a graphical form in figures 3.11 and 3.12.

3.5 The Yield Criterion

Having determined the normal and tangential moments existing on a yield line for a variety of reinforcement conditions, it remains to determine the relationship between these moments and any set of applied principal moments. It has been shown by Kemp [9] using the normal and twisting moments derived by Johansen [2], that the yield criterion for isotropically or orthotropically reinforced concrete slabs is essentially an envelope of normal bending moments. Kemp has postulated that if m_n is the normal moment of resistance of the concrete slab acting at some angle α to the reinforcement axes, and M_n is the applied normal bending moment acting at some angle $(\phi + \psi)$, figure 3.13, to the reinforcement axes, then:

$$M_n = m_n$$

$$\frac{dM_n}{d\psi} = \frac{dm_n}{d\alpha}$$

This condition is shown graphically in figure 3.13. The criterion that is to be developed in this chapter will be based on the above philosophy; in addition, some more requirements will have to be satisfied.

3.5.1 The Yield Criterion in the Isotropic and Orthotropic case.

It has been mentioned earlier that the basic requirements at yield are :-

$$M_n = m_n \qquad .. \quad .. \quad 3.49$$

$$\frac{dM_n}{d\psi} = \frac{dm_n}{d\alpha} \qquad .. \quad .. \quad 3.50$$

It is also necessary that nowhere does M_n exceed m_n, nor M_{nt} exceed m_{nt}. In other words

$$m_n \geq M_n \qquad .. \quad .. \quad 3.51$$

$$m_{nt} \geq M_{nt} \qquad .. \quad .. \quad 3.52$$

It seems that the Johansen expression used by Kemp automatically satisfies all four conditions.

It does not necessarily mean that any moment expressions developed will satisfy all the conditions automatically; a certain control will therefore be required to make sure that all four conditions are satisfied.

The external normal moment acting on a yield line may be expressed in terms of the principal moments M_1 and M_2, and the angle between the direction of M_1 and the normal to the yield line by the following expression:

$$M_n = M_1\cos^2\psi + M_2\sin^2\psi \qquad .. \quad .. \quad 3.53$$

The external twisting moment can be expressed in the following form:

$$M_{nt} = \frac{(M_1 - M_2)}{2}\sin 2\psi \qquad .. \quad .. \quad 3.54$$

For an orthogonal orthotropically reinforced concrete slab, the normal moment of resistance at yield from equation 3.48a is

$$m_n = \frac{m}{\sqrt{1+3k_a^2}}\cos^2\alpha + \frac{\mu m}{\sqrt{1+3k_b^2}}\cdot\sin^2\alpha + \left(\frac{ka}{\sqrt{1+3ka^2}} + \frac{\mu kb}{\sqrt{1+3k_b^2}}\right)\frac{m}{2}\sin 2\alpha \quad .. 3.55$$

The equivalent twisting moment of resistance from equation 3.48b is

$$m_{nt} = \frac{m}{2}\left(\frac{1}{\sqrt{1+3k_a^2}} - \frac{\mu}{\sqrt{1+3k_b^2}}\right)\sin 2\alpha - m\left(\frac{ka}{\sqrt{1+3ka^2}}\cos^2\alpha - \frac{\mu kb}{\sqrt{1+3k_b^2}}\sin^2\alpha\right) .. 3.56$$

It must be mentioned here again that k_a and k_b are functions of α.

Let $\frac{M_n}{m} = Fe$ and $\frac{m_n}{m} = Fr$

Also let $\frac{M_{nt}}{m} = Re$ and $\frac{m_{nt}}{m} = Rr$.

The equation 3.53 can be re-arranged in the form

$$Fe = \frac{M_1}{m}\left(\frac{1+f}{2}\right) + \frac{M_1}{m}\left(\frac{1-f}{2}\right)\cos 2\psi \qquad .. \quad .. \quad 3.57$$

where $f = \frac{M_2}{M_1}$

also $$\frac{dFe}{d\psi} = Fe^1 = -\frac{M_1}{m}(1-f)\sin 2\psi \qquad .. \quad .. \quad 3.58$$

The equation 3.55 can be written in the form

$$Fr = \frac{\cos^2\alpha}{\sqrt{1+3k_a^2}} + \frac{\mu\sin^2\alpha}{\sqrt{1+3k_b^2}} + \left(\frac{ka}{\sqrt{1+3ka^2}} + \frac{\mu kb}{\sqrt{1+3k_b^2}}\right)\frac{\sin 2\alpha}{2} \qquad .. \quad 3.59$$

also $$\frac{dFr}{d\alpha} = Fr^1 = -\frac{\sin 2\alpha}{\sqrt{1+3k_a^2}} + \frac{\mu\sin 2\alpha}{\sqrt{1+3k_b^2}} + \left(\frac{ka}{\sqrt{1+3k_a^2}} + \frac{\mu kb}{\sqrt{1+3k_b^2}}\right)\cos 2\alpha -$$

$$-\frac{3ka}{(1+3ka^2)^{3/2}}\frac{dka}{d\alpha}\cdot\cos^2\alpha-\frac{3\mu kb}{(1+3kb^2)^{3/2}}\cdot\frac{dkb}{d\alpha}\cdot\sin^2\alpha+\left(\frac{\frac{dka}{d\alpha}}{\sqrt{1+3ka^2}}+\frac{\mu\frac{dkb}{d\alpha}}{\sqrt{1+3kb^2}}\right)\frac{\sin2\alpha}{2}$$

$$-\left[\frac{3ka^2\frac{dka}{d\alpha}}{(1+3ka^2)^{3/2}}+\frac{3\mu kb^2\frac{dkb}{d\alpha}}{(1+3kb^2)^{3/2}}\right]\frac{\sin2\alpha}{2} \qquad .. \quad .. \quad 3.60$$

where ka and kb are given by equations 3.43 and 3.44, hence:

$$\frac{dka}{d\alpha}=\frac{\left[2\cos2\alpha+\frac{S\sin^2 2\alpha}{(1+S\cos^2\alpha)}+\frac{\frac{3}{2}KS\sin^2 2\alpha}{\left(\frac{\cosh(2\sqrt{S}\rho_o)-1}{(2\sqrt{S}\rho_o)^2}+\frac{1}{2}+\frac{3}{2}KS\cos^2\alpha\right)}\right]S}{2(1+S\cos^2\alpha)\left(\frac{\cosh(2\sqrt{S}\rho_o)-1}{(2\sqrt{S}\rho_o)^2}+\frac{1}{2}+\frac{3}{2}KS\cos^2\alpha\right)}$$

and

$$\frac{dkb}{d\alpha}=\frac{\left[2\cos2\alpha-\frac{S\sin^2 2\alpha}{1+S\sin^2\alpha}-\frac{\frac{3}{2}KS\sin^2 2\alpha}{\left(\frac{\cosh(2\sqrt{S}\rho_o)-1}{(2\sqrt{S}\rho_o)^2}+\frac{1}{2}+\frac{3}{2}KS\sin^2\alpha\right)}\right]S}{2(1+S\sin^2\alpha)\left(\frac{\cosh(2\sqrt{S}\rho_o)-1}{(2\sqrt{S}\rho_o)^2}+\frac{1}{2}+\frac{3}{2}KS\sin^2\alpha\right)}$$

The conditions of equations 3.49 and 3.50 require that

$$M_n = m_n \text{ and } \frac{dM_n}{d\psi}=\frac{dm_n}{d\alpha}$$

Then equating equation 3.57 to 3.59 and 3.58 to 3.60, we get

$$Fr=\frac{M_1}{m}\left(\frac{1+f}{2}\right)+\frac{M_1}{m}\left(\frac{1-f}{2}\right)\cdot\cos2\psi \qquad .. \quad .. \quad 3.61$$

$$Fr^1=\frac{M_1}{m}(1-f)\sin2\psi \qquad .. \quad .. \quad 3.62$$

From equations 3.61 and 3.62

$$\tan2\psi=\frac{Fr^1}{2Fr-\frac{M_1}{m}(1+f)} \qquad .. \quad .. \quad 3.63$$

Again, from equations 3.61 and 3.62 eliminating ψ by squaring and adding

$$\left[2Fr-\frac{M_1}{m}(1+f)\right]^2+Fr^{1\,2}=\left[\frac{M_1}{m}(1-f)\right]^2$$

This equation is quadratic in $\frac{M_1}{m}$ and can be solved. Therefore

$$\frac{M_1}{m} = Fr\,\frac{1+f}{2f} \pm \frac{1}{2f}\left[Fr^2(1-f) - Fr^{1^2} f\right]^{\frac{1}{2}} \quad .. \; .. \; 3.64$$

This solution could provide two real values of $\frac{M_1}{m}$ or two imaginary values of $\frac{M_1}{m}$.

Of course, imaginary values have no meaning here, and a restriction should be inserted to avoid imaginary solutions. For real values of $\frac{M_1}{m}$

$$Fr^2(1-f) - Fr^{1(2)} f \geqslant 0$$

hence $$\left(\frac{Fr}{Fr^1}\right)^2 \geqslant \frac{f}{(1-f)^2} \quad .. \; .. \; 3.65$$

Examining equation 3.65, it can be seen that $\frac{Fr}{Fr^1}$ is independent of the external moments, and f depends on the ratio $\frac{M_2}{M_1}$.

Values of Fr and Fr^1 can be calculated for any values of μ and α, inserted in equation 3.65 and f determined. The values of Fr, Fr^1 and f are substituted in equation 3.63 and 3.64, to obtain values of $\frac{M_1}{m}$ and ψ.

Since $\frac{M_1}{m}$, f and ψ are known, the external moment normal to the yield line and the twisting moment can be determined. Of course, the moment of resistance and twisting moment of resistance are known too since α is an assumed value for determining ψ and f.

The next two yield conditions have to be tested, and these conditions are given by equations 3.51 and 3.52.

i.e. $$\frac{m_n}{m} \geqslant \frac{M_n}{m} \quad .. \; .. \; 3.66$$

and $$\frac{m_{nt}}{m} \geqslant \frac{M_{nt}}{m} \quad .. \; .. \; 3.67$$

The values of $\frac{m_n}{m}$ and $\frac{M_n}{m}$ found by the described process are tested against the condition 3.66; also the values of $\frac{m_{nt}}{m}$ and $\frac{M_{nt}}{m}$ are tested against condition 3.67. Any two sets of values not satisfying both conditions simultaneously are rejected.

The method of determining the yield criterion appears indirect and laborious. Consequently, a computer program was written for solving the required equations and testing the four yield conditions. In that manner, the work was reduced to a minimum.

The complete yield criterion for a given degree of orthotropy was constructed by drawing curves of $\frac{M_2}{m}$ against $\frac{M_1}{m}$ for a range of ϕ values where ϕ is the angle between the direction of the main reinforcement and the principal moment M_1.

Figure 3.14 shows the yield criterion in a graphical form when the degree of orthotropy is unity for top and bottom steel. It is interesting to note that when ϕ is 45° the moment enhancement over the square yield criterion is 13.4%. Figure 3.15 shows the yield criterion when the degree of orthotropy is 0.5 for top and bottom steel.

3.6 Discussion and Conclusions.

A new expression for the normal and twisting moments of resistance acting on the yield line has been developed. For the first time a normal and twisting moment of resistance has been developed and incorporates the stiffness of the steel bar in the concrete crack and also the crushing strength of the concrete.

The new expression for the normal moment of resistance is justified by experimental results produced by R. Downham [3], Kwiecinski [4] and the author.

The expression developed shows a moment enhancement of 13.4%

above the Johansen expression when the bars are inclined at 45° to the yield line and the degree of orthotropy is unity.

The basic objection to the Johansen expression, the kinematic inadmissibility, is overcome by considering the shear stresses in the bar.

By considering the shear stress in the bar in addition to the axial stresses, the observed increases in normal moment of resistance of an isotropic slab at oblique angles to the reinforcement directions is fully explained. The Johansen expression fails to explain the observed increase in normal moments.

The new expression developed would appear to be acceptable, from the theoretical considerations and also from the experimental evidence produced by the author and other experimentors.

The expression appears to be slightly complex from the arithmetical point of view, otherwise it presents no other difficulty.

Earlier, it was shown that the effective crack width varies with the orientation of the bar, and a mean value was taken. In fact, the effective crack width varies sharply when the bar inclination to the normal is of the order of 0°- 15° and 75°- 90°. (See figure 3.7). Since the shear contribution to the overall normal moment is small and is even smaller when the bars are inclined at an angle to the normal, it justifies taking an average value for the effective crack width.

It was found that when the effective crack width was varied between 1.0 and 1.413, the variation of the normal moment was only 1.5%.

The approach used to develop the yield criterion was similar to that of Kemp [9]. Two extra conditions were used in addition to those of Kemp's, and the reason was explained during the development

of the criterion. The criterion developed by Kemp using the Johansen expressions is very simple from the algebraical point of view because the normal moment is a simple trigonometrical expression.

The criterion put forward by the author appears complex, only because the expressions are complex.

For isotropic slabs, Kemp developed the "square" yield criterion and the maximum ratio of the external moment to that of the moment of resistance is /1/.

The ratio of the same variables obtained from the yield criterion put forward by the author is /1.134/. This shows a definite increase in the strength of the slab. Comparing the two criteria for orthotropic slabs, figure 3.15 and figure 3.16, they appear to be of similar shape, but always the Johansen criterion lies within the criterion developed by the author. This is an indication that the new criterion yields higher values than the old one.

In conclusion, the new criterion reinforces the reliability of the old criterion and an estimate of the divergence of the new criterion to the old is provided.

In developing the new criterion, certain assumptions were made; it was thought essential to carry out a test program to justify the assumptions and the overall agreement of the normal moment of resistance to experimental values obtained by the author. To carry out a full testing program to test the theory in full seems impracticable.

It was decided to carry out three series of tests. Firstly, to idealize a crack using steel plates, hence the steel analogue series. Secondly, to study the implications of real cracks, hence the mono-steel bar concrete strip series. Thirdly, to test the overall expression for normal moments of resistance at yield, hence the Bending

and Torsion of Slabs series.

The next section describes the tests and results of the first two series.

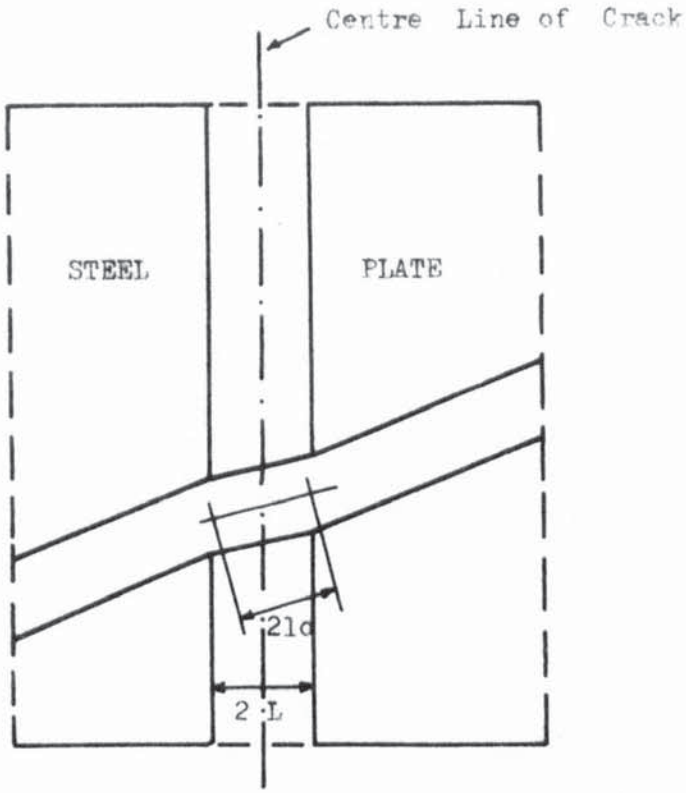

Figure 3.1 IDEAL CRACK

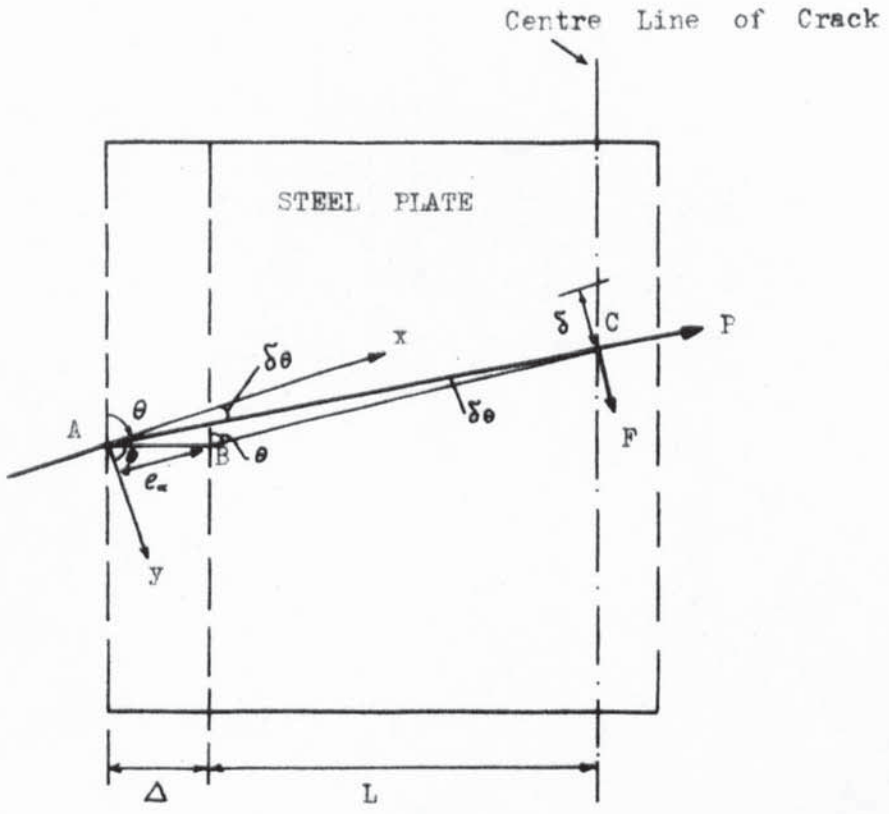

Figure 3.2 GEOMETRY OF BAR IN IDEAL CRACK AND FORCES ON BAR

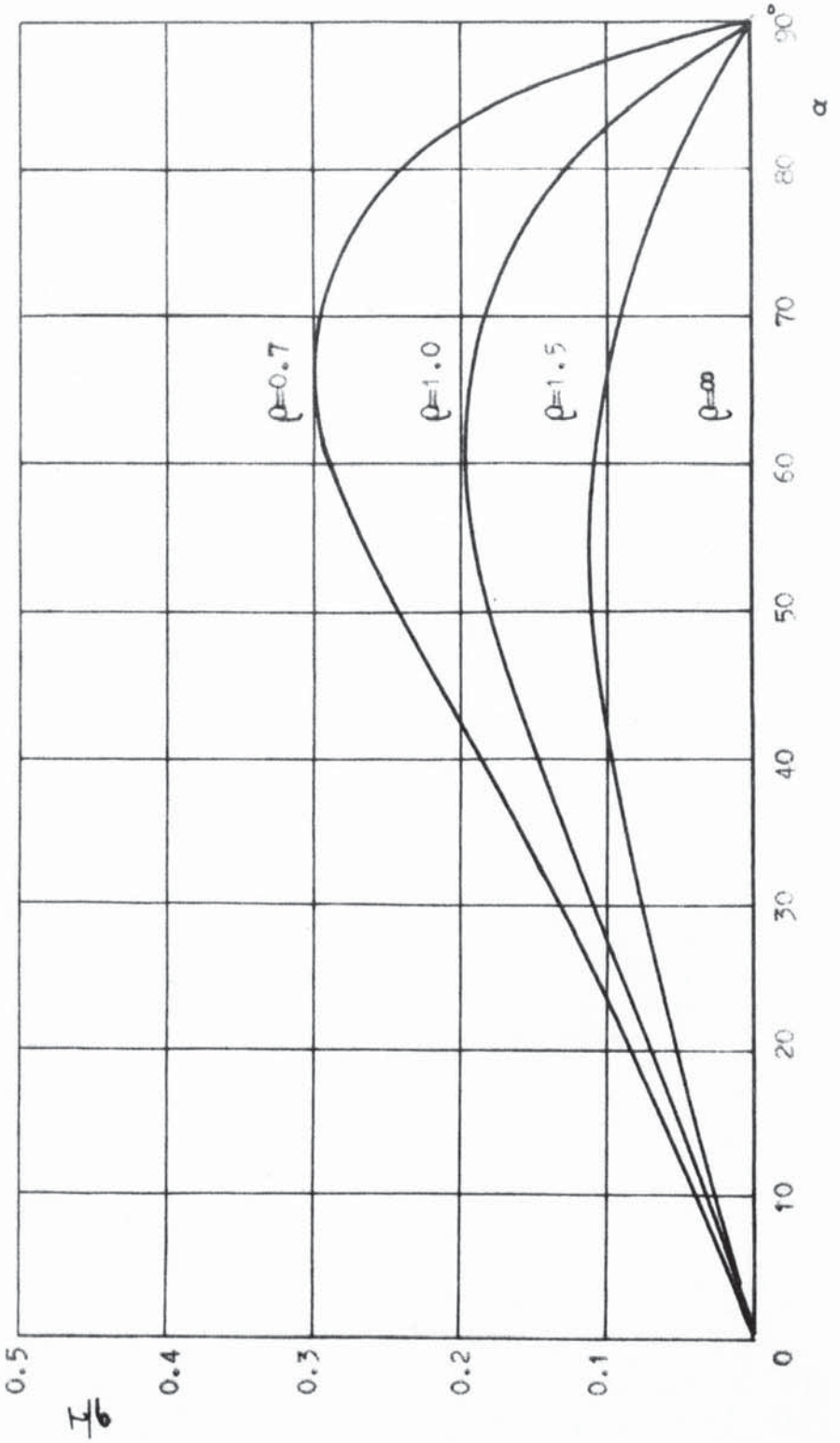

Figure 3.3 SHEAR/AXIAL STRESS IN BAR V.S ALPHA (STEEL ANALOGUE)

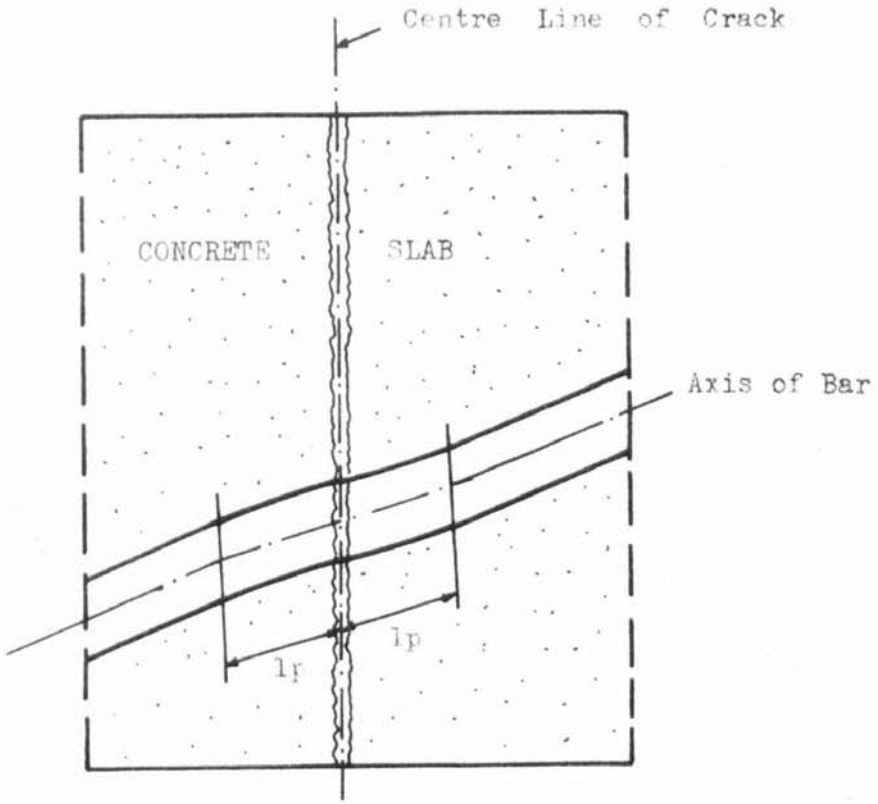

Figure 3.4 CONCRETE CRACK

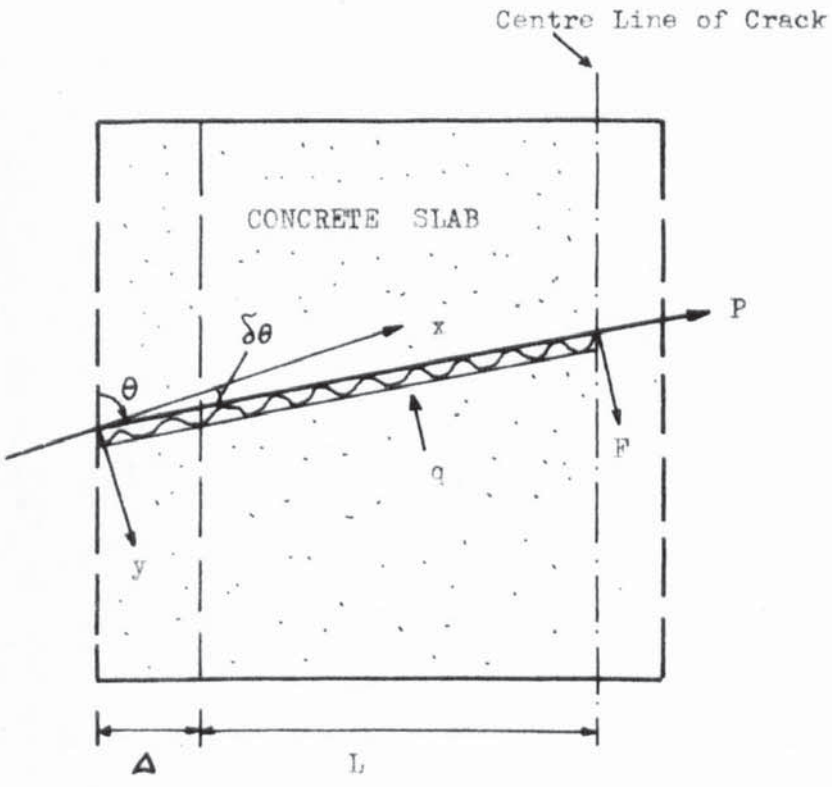

Figure 3.5 GEOMETRY OF BAR IN CONCRETE CRACK AND FORCES ON BAR

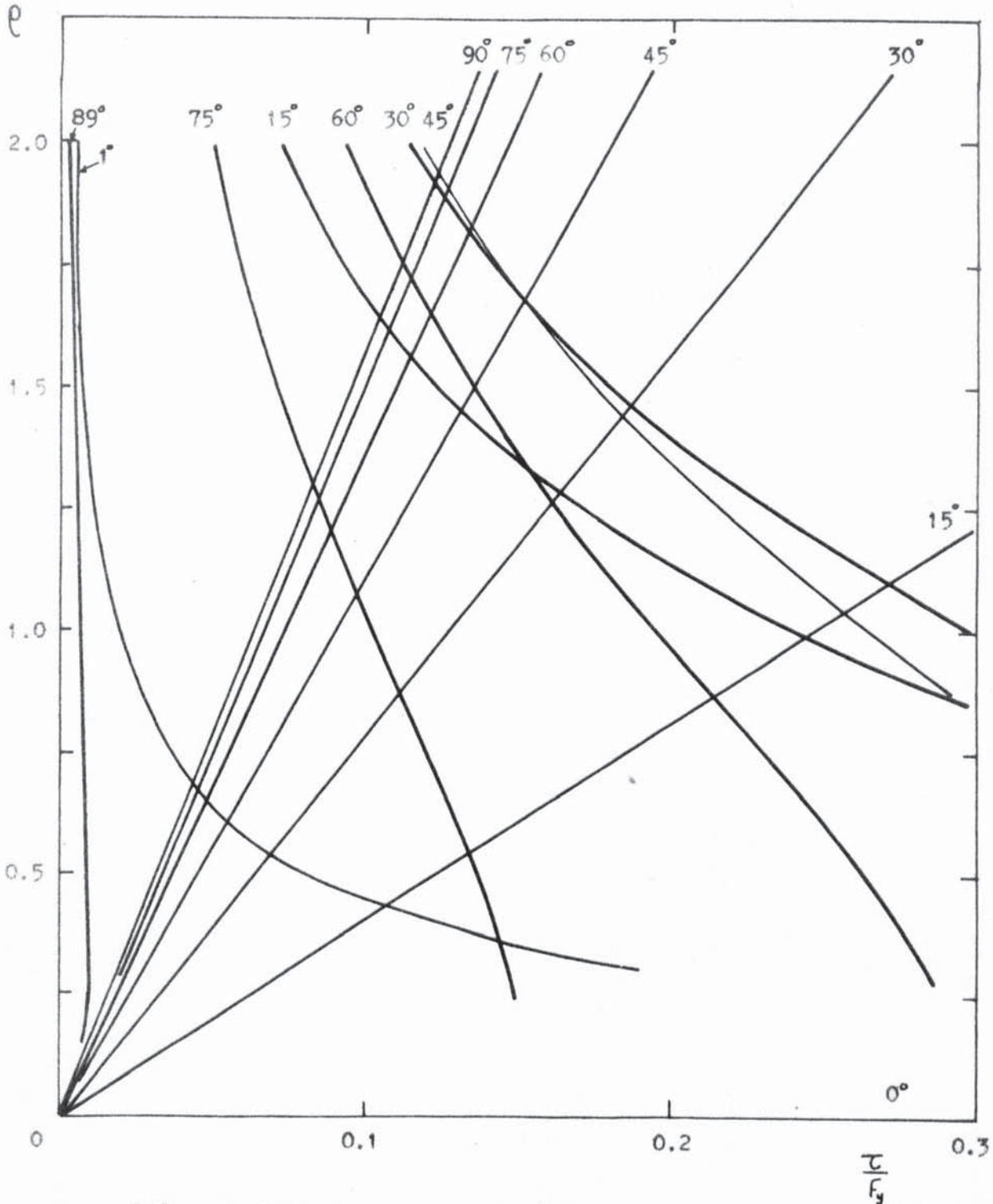

Figure 3.6 EFFECTIVE CRACK WIDTH/BAR DIAMETER V.S SHEAR/AXIAL STRESS

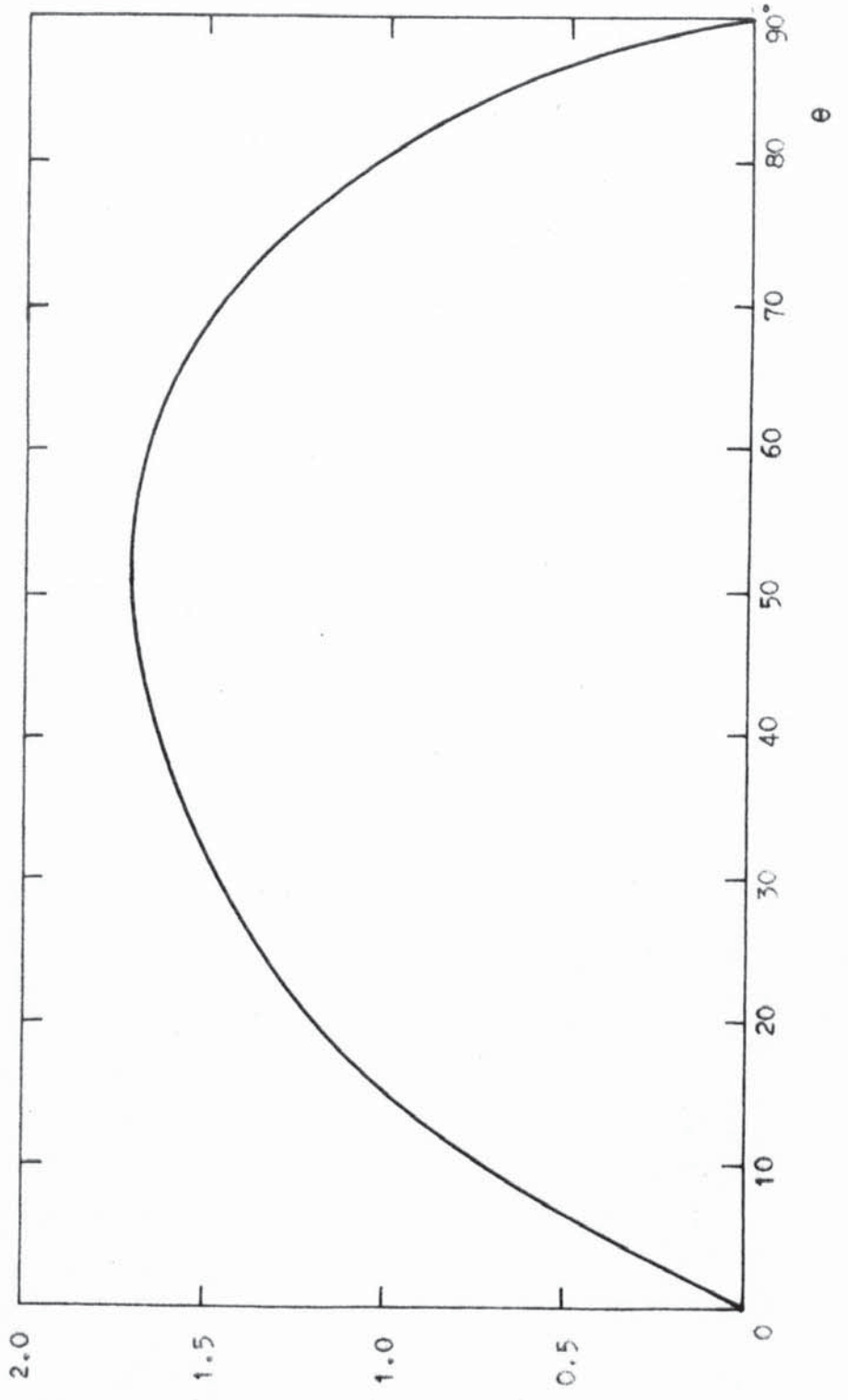

Figure 3.7 EFFECTIVE CRACK WIDTH/BAR DIAMETER V.S THETA

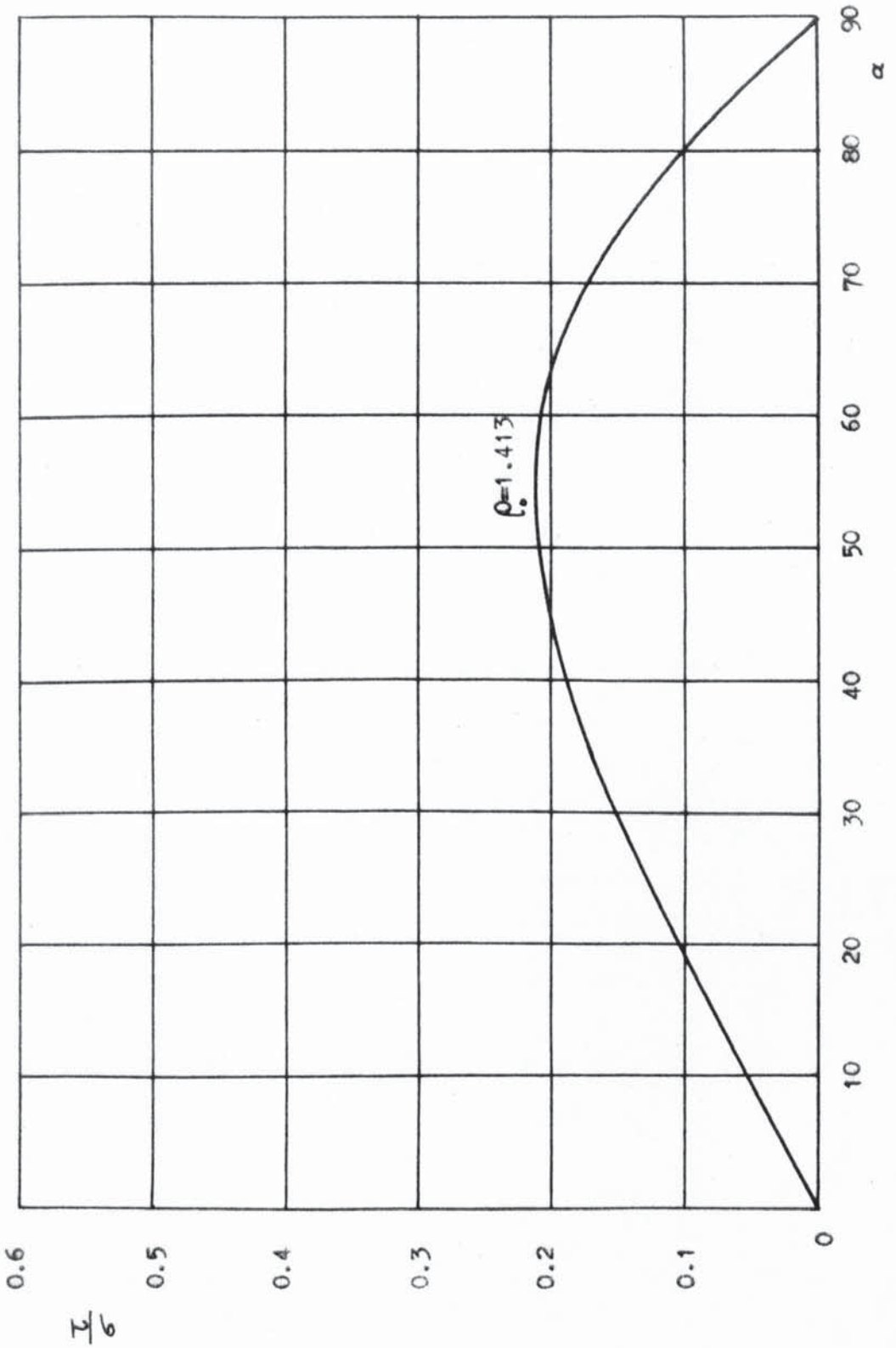

Figure 3.8 SHEAR/AXIAL STRESS IN BAR V.S ALPHA (CONCRETE)

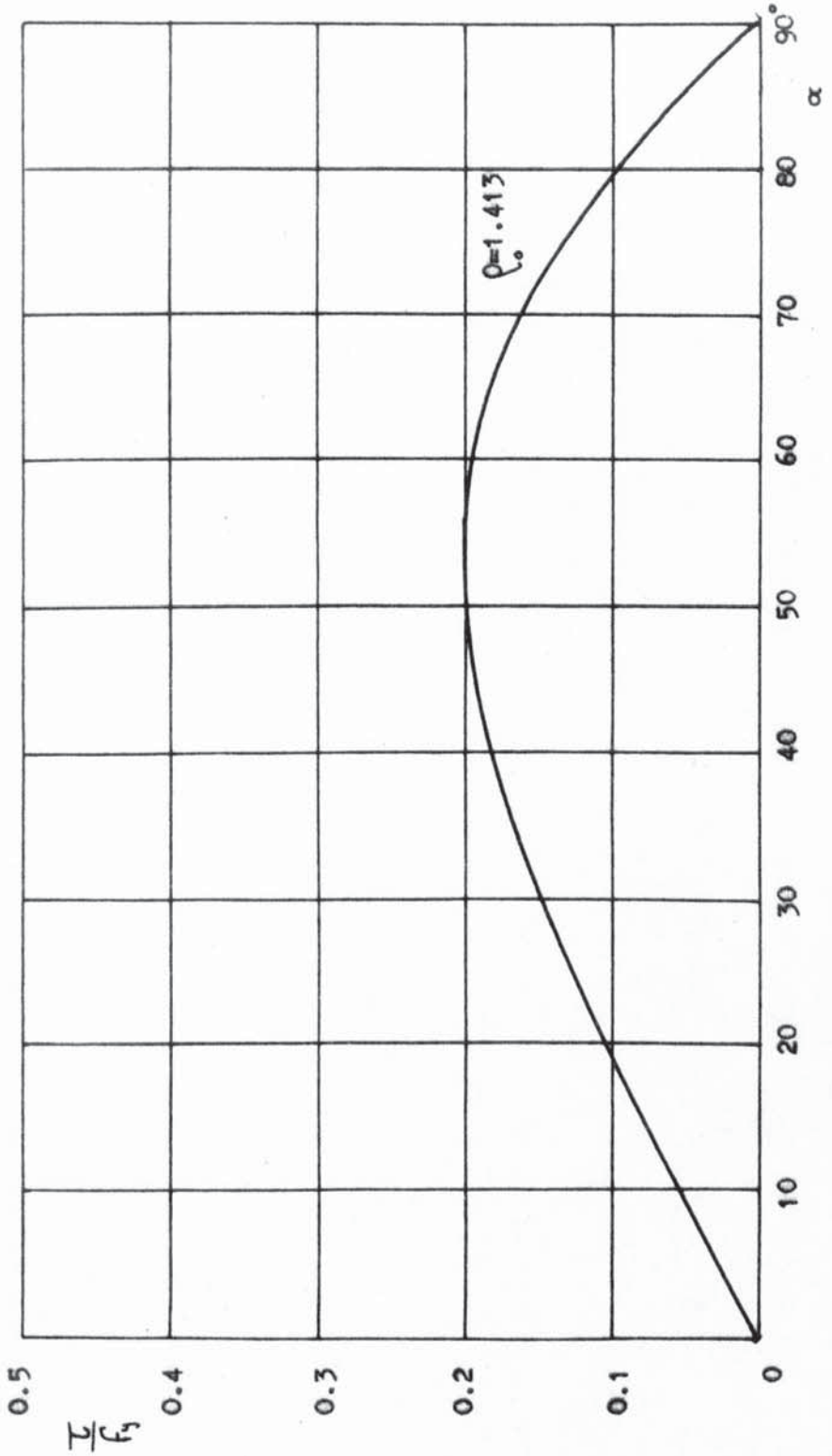

Figure 3.9 SHEAR/AXIAL YIELD STRESS IN BAR V.S ALPHA (CONCRETE)

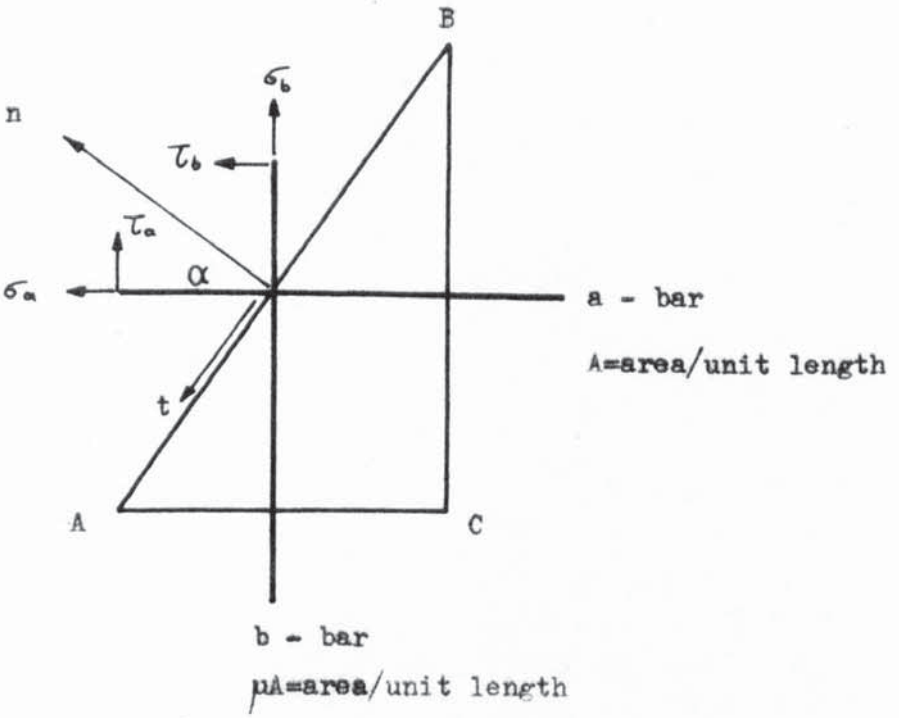
B
σ_b
n
τ_b
τ_a
α
σ_a
a - bar
A=area/unit length
t
A
C
b - bar
μA=area/unit length

Figure 3.10

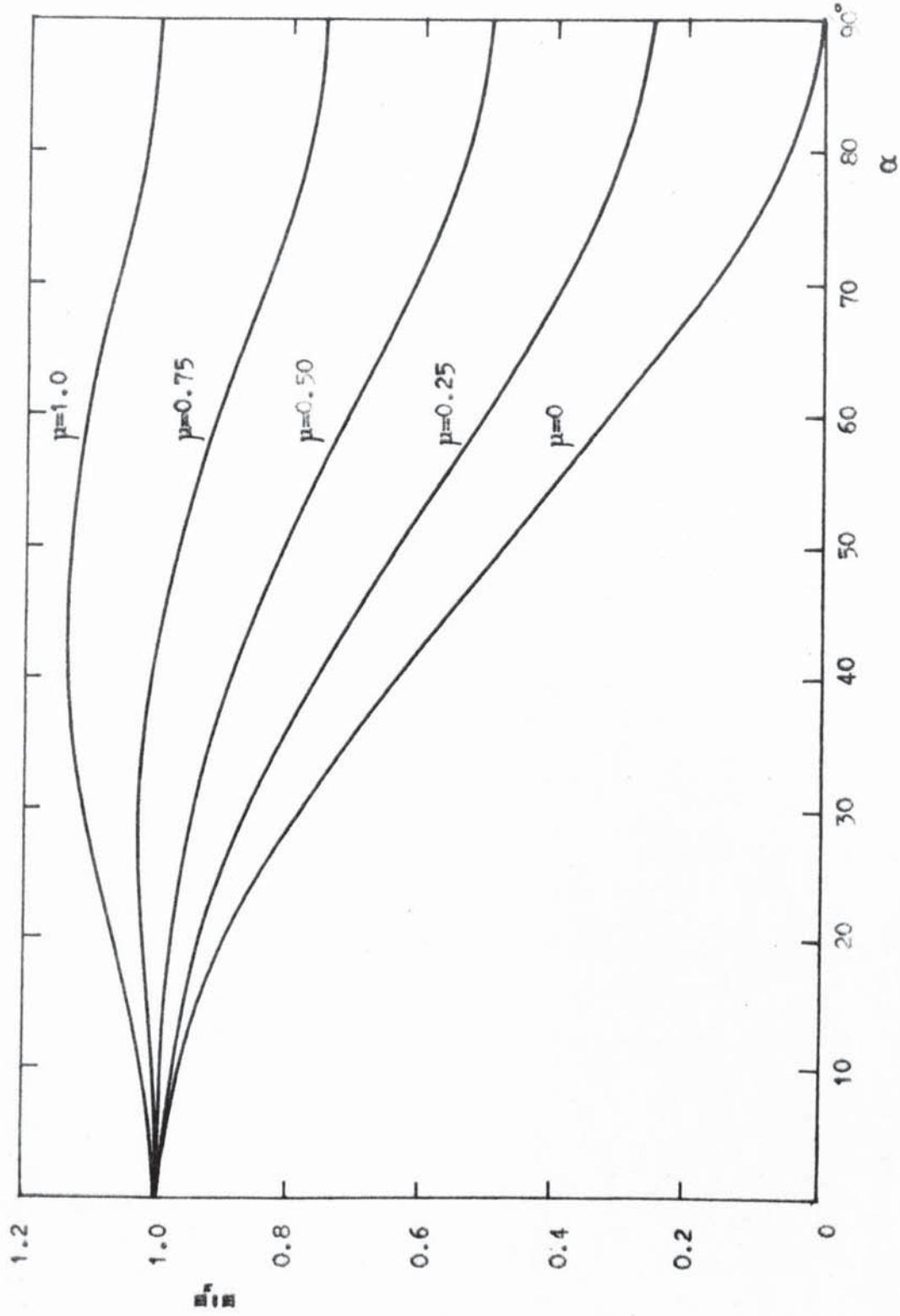

Figure 3.11 THEORETICAL NORMAL MOMENT V.S ALPHA (AUTHOR)

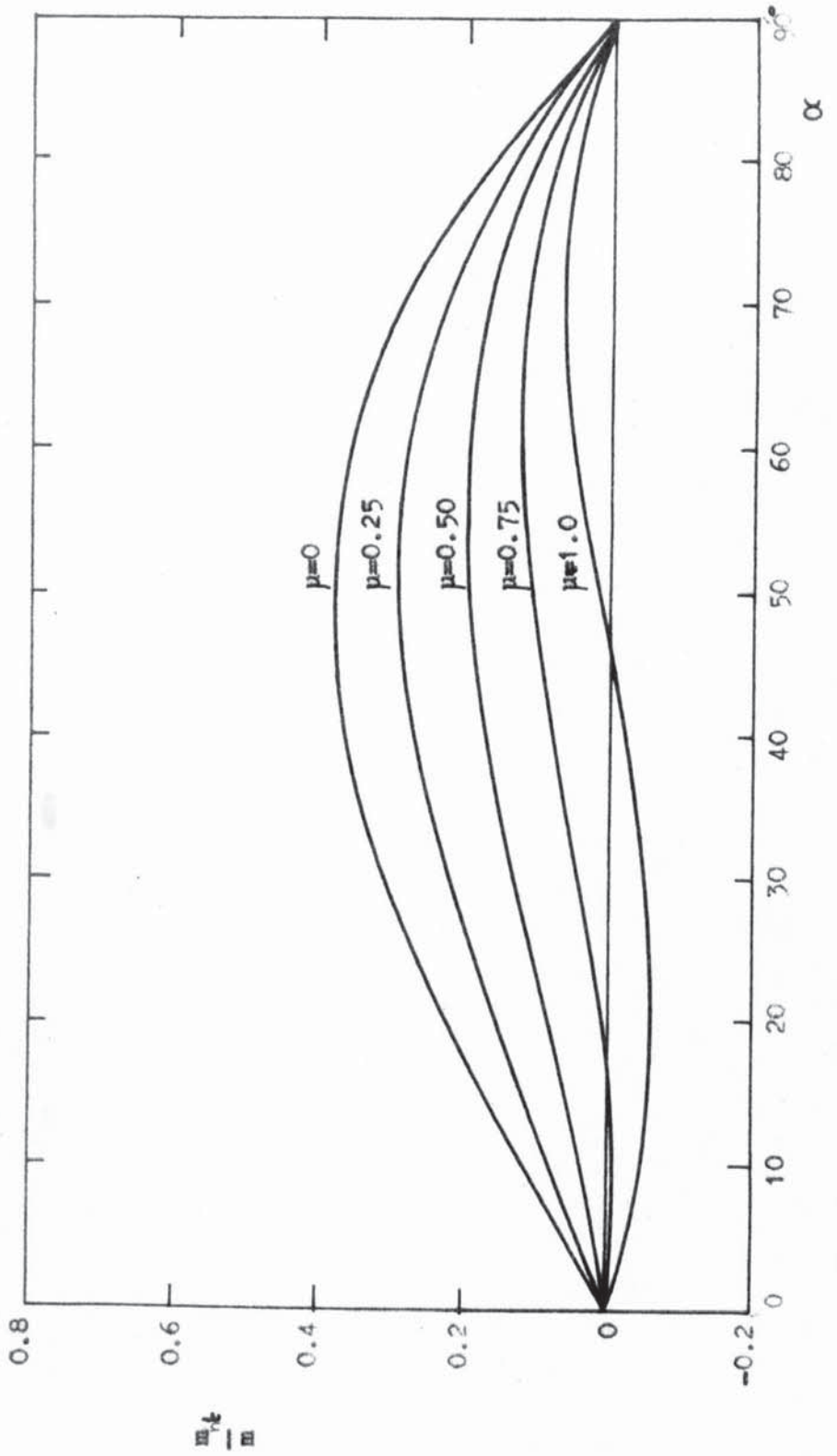

Figure 3.12 **THEORETICAL TWISTING MOMENT V.S ALPHA (AUTHOR)**

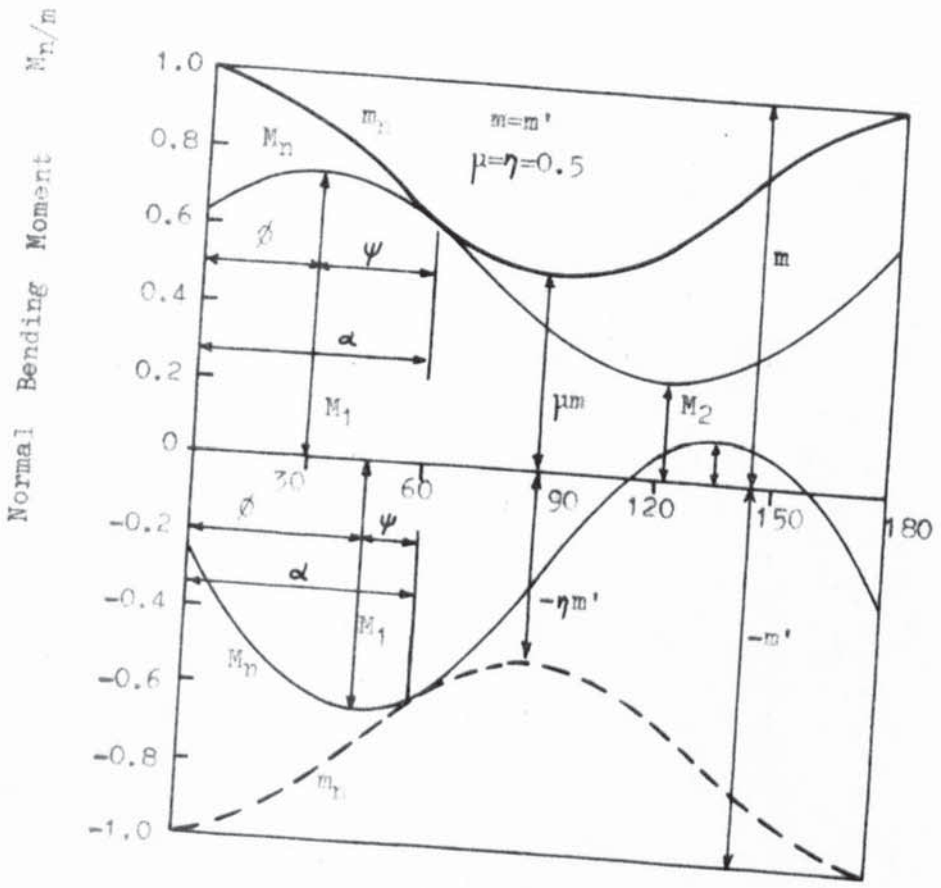

Figure 3.13 FAILURE IN SLAB

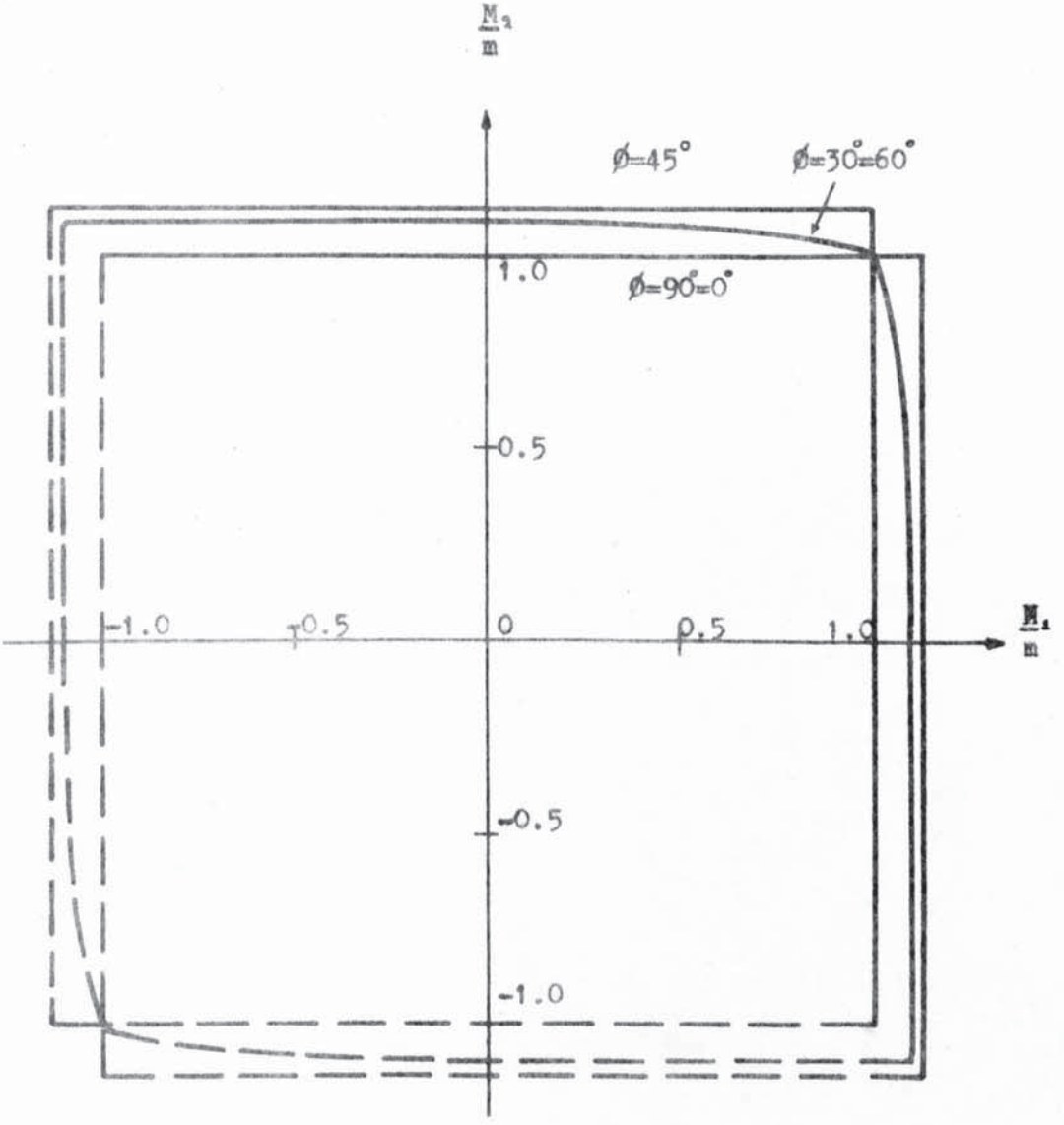

Figure 3.14 YIELD CRITERION FOR ISOTROPIC SLABS (AUTHOR)

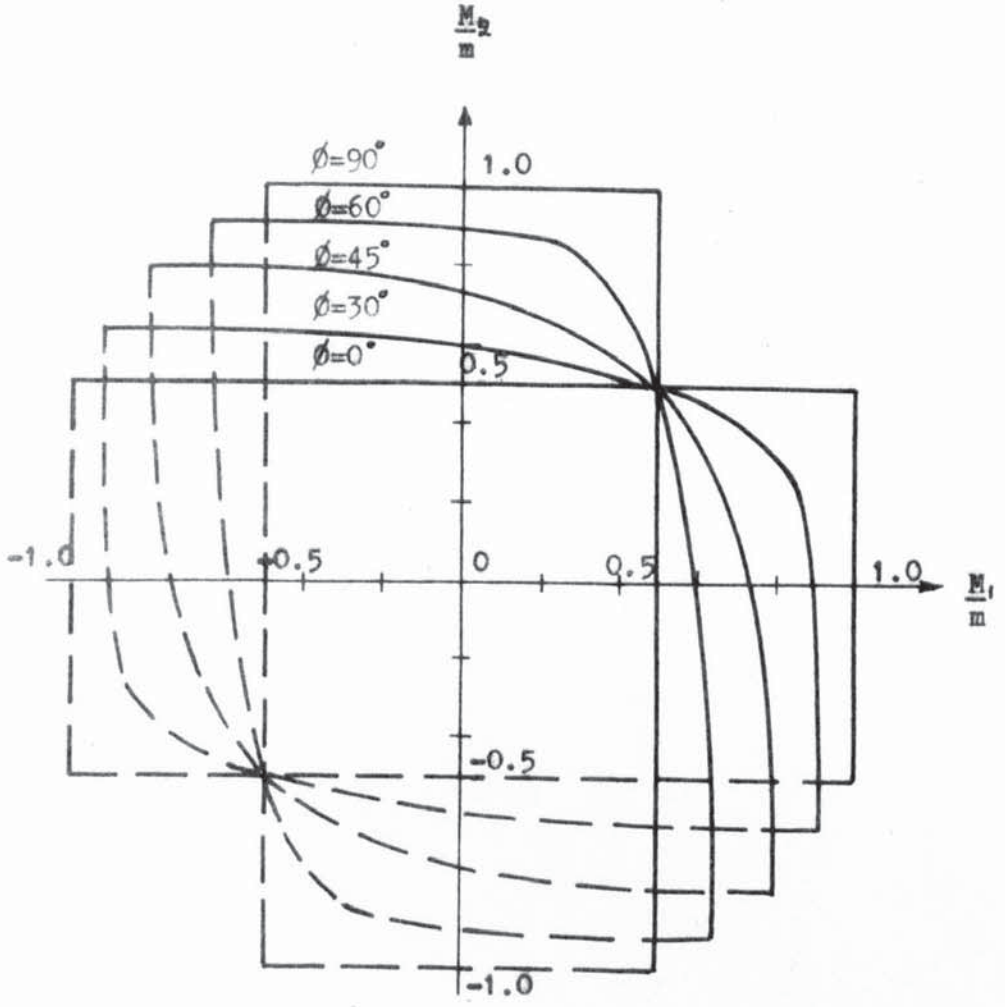

Figure 3.15 YIELD CRITERION FOR AN ORTHOTROPIC SLAB ($\mu=\eta=0.5$)
(AUTHOR)

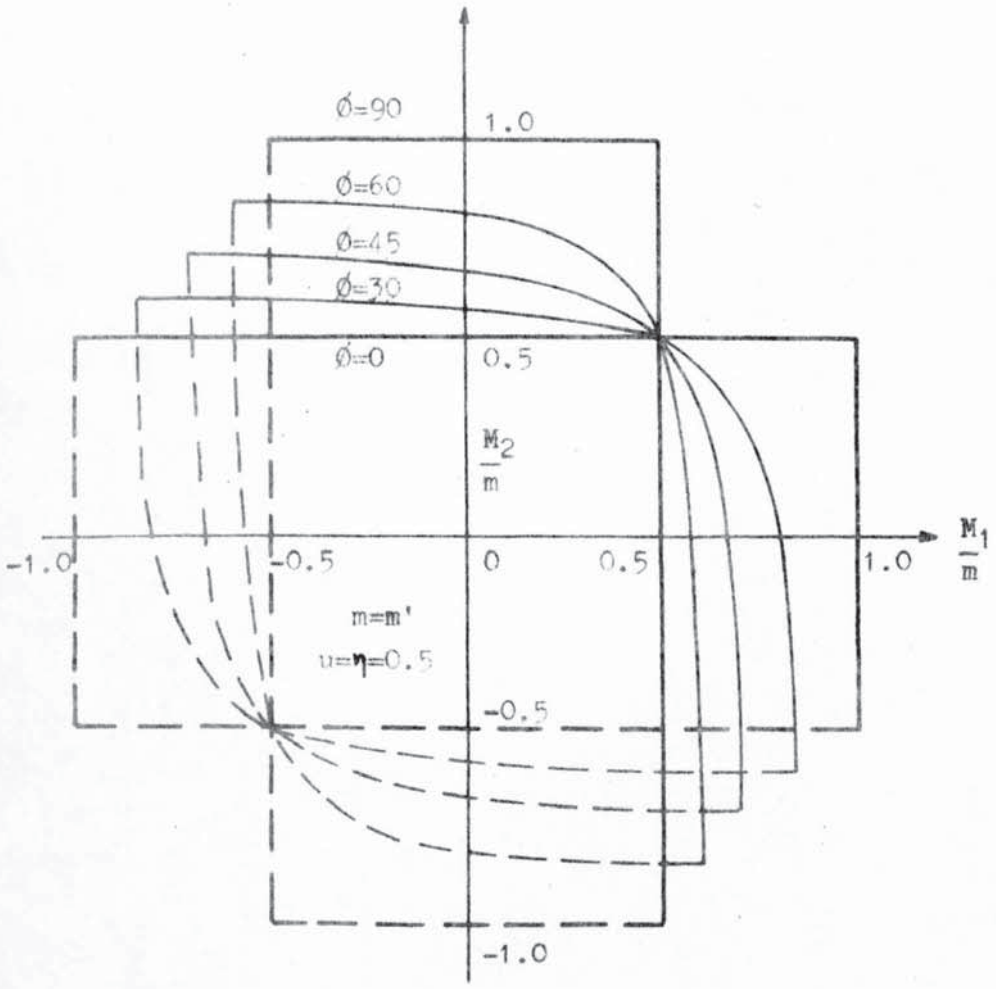

Figure 3.16 YIELD CONDITION - KEMP

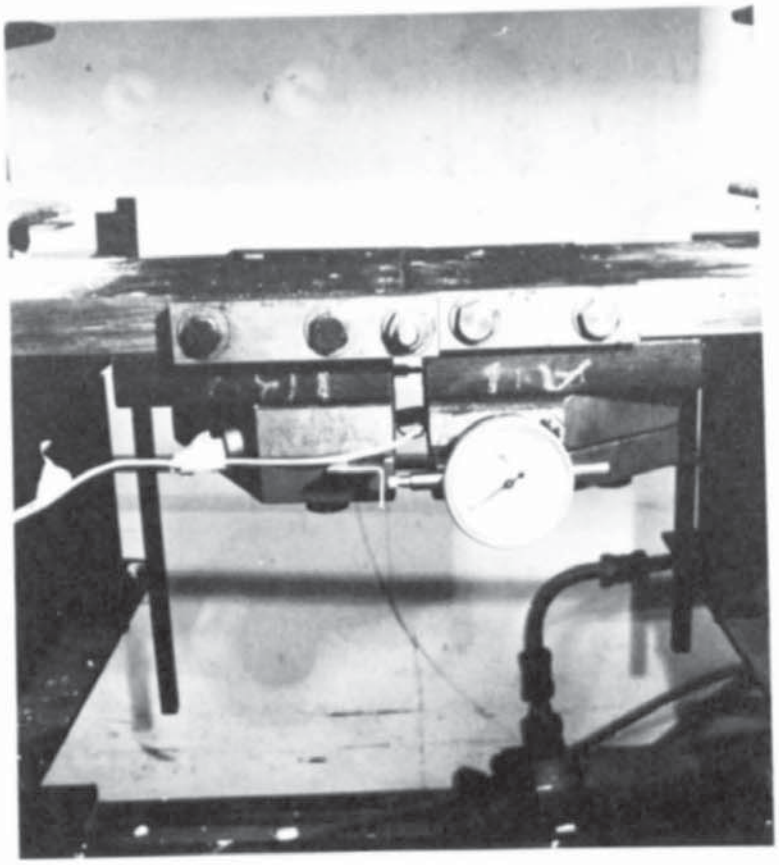

PLATE 3.1 SIDE VIEW (STEEL ANALOGUE)

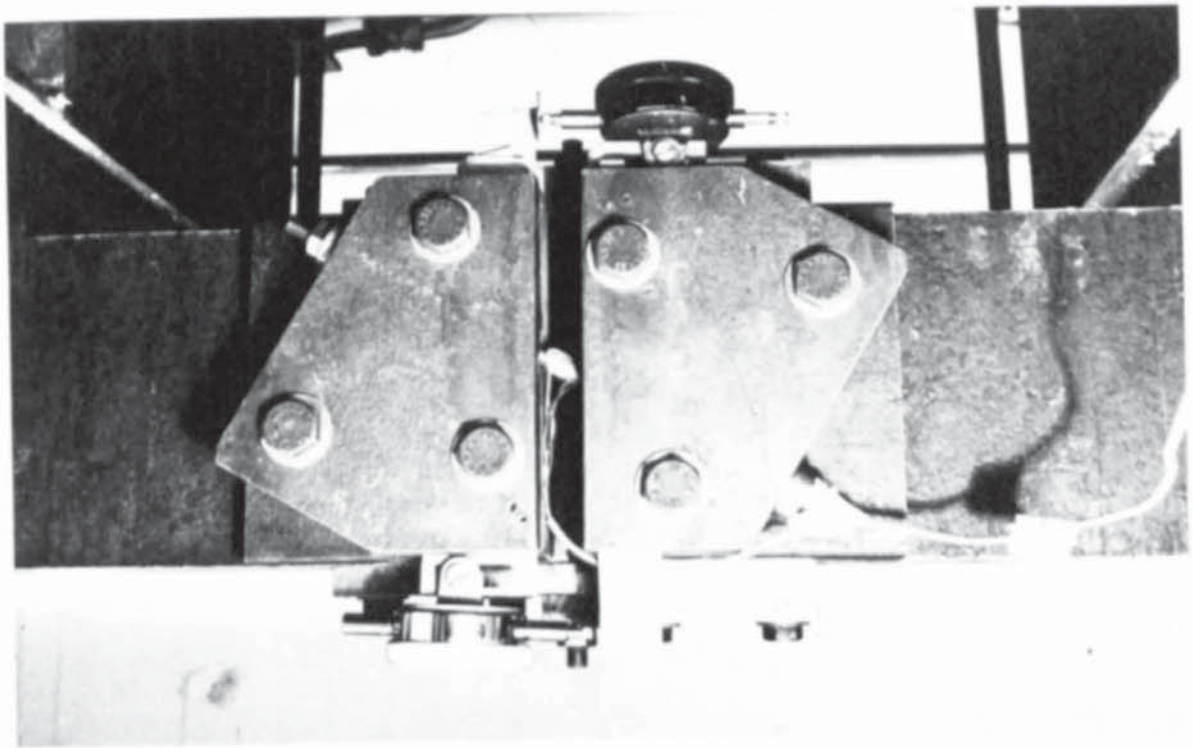

PLATE 3.2 PLAN VIEW, TENSION FACE (STEEL ANALOGUE)

CHAPTER 4.

THE DEVELOPMENT OF EXPERIMENTAL TECHNIQUES.

4.1 Introduction.

The theory developed in the previous chapter is based upon certain assumptions concerning the state of stress in the reinforcing steel at yield, and also on the existence of an 'effective crack width'.

Concerning the state of stress in the reinforcing bar crossing the yield line at some oblique angle, this is difficult to assess directly. What is proposed in this chapter is to show visually and experimentally that both shear and axial stresses do exist on a bar crossing a yield line at some oblique angle. The concept of the 'effective crack width' over the overall strength of a slab element will be demonstrated by comparing the strength of a steel analogue slab to the strength of a concrete slab strip both having originally the same crack width. It was necessary, therefore, to design a steel analogue slab that could be subjected to bending in the same manner as a simply supported concrete slab. The steel analogue slab was built in such a way that a single steel bar could be placed at various angles to the normal to the artificial crack. The steel analogue slab enabled the author to determine the normal moment to the crack. The object of using a steel analogue slab was to eliminate the effects of concrete crushing which will occur in a concrete slab in the acute angle formed by the bar and the yield line.

When the first series of tests on the steel analogue slab was completed, a second series of tests was carried out, where the steel analogue slab was replaced by concrete. This series of experiments

was intended to investigate the importance of the crushing effect mentioned above, and to obtain a more realistic appraisal of the actual behaviour of the reinforcing bar crossing a yield line at an oblique angle in a concrete slab. To avoid any interference of concrete around a steel bar, an artificial crack was created at the centre of the bar across its width. This concrete crack width was of the same size as the artificial crack created in the steel analogue slabs.

The first series of tests was called the Steel Analogue Series, and the second series of tests the Mono-Steel bar Concrete Strip Series.

4.2 Steel Analogue Series.

4.2.1 Description of Apparatus.

The steel analogue slab shown in Plates 4.1 and 4.2 consisted principally of two large plates 457 mm long, 152 mm wide and 25.4 mm thick, hinged together along the 152 mm side. The hinge between the two plates was rather unique. This hinge had the property of keeping both plates together while complete rotational movement was allowed. When the testing rig was subjected to pure bending, the hinge was subjected to compression only. Steel bars to be tested were held in position by two sets of plates as shown in plates 4.1 and 4.2. These plates holding the bar in position provided the lever arm between the compression zone (axis of hinge) and the centroidal axis of the bar. This lever arm was the same in all tests and equal to 63.5 mm. Each set of plates was grooved in a predetermined position dictating the direction of the bar to the normal to the artificial crack direction. The depth of the groove on each plate was 0.03 mm less than the radius of the bar, and the purpose of this tolerance was to create a grip on

the bar when the six bolts were tightened. A new set of plates was required for different bar orientations to the normal to the artificial crack direction.

All tests were carried out within a large permanent portal frame testing rig. Details of construction of the portal testing rig is described in Chapter five, section 5.5.1. Plate 4.3 shows the portal testing rig and the steel analogue slab ready for testing. The steel analogue slab was supported on rollers to eliminate membrane effects, and was subjected to pure uniaxial moment by means of two line loads symmetrically placed on either side of the artificial crack. Both line loads were supplied by a single hydraulic jack having a 100 KN capacity, and measured by a prooving ring placed between the hydraulic jack and an I beam placed transversely across the position of the line loads. Details of the position of the loads and supports is shown in figure 4.1. In the same figure, the dimensions of the plates are shown. The increase in the gap between the two sets of plates (i.e. the increase in width of the artificial crack) during the test was read on two dial gauges. These gauges (see plate 4.1) on either side of the plates were mounted at the same level as the steel bar. Since the stiffness of the plates was relatively large in relation to the stiffness of the bar crossing the gap, it was assumed that the reading on the gauges was the actual elongation of the bar normal to the gap direction.

The material chosen for the tests was 9.5 mm diameter mild steel, turned down to 8.0 mm over the critical length. Here the length of the bar transversing the gap between the plates (i.e. the artificial crack width) is considered as the critical length. The exact diameter for each bar was measured with a micrometer screw gauge, the results of such measurements are shown in table 4.1. At the centre of each bar,

two electrical resistance gauges were fixed parallel to each other as described in the Instrumentation section of Chapter five. These gauges were basically used as a guide to indicate the yield of the bar. Each steel bar also had screw threads on either end so that nuts could be tightened for security against slip of the bar.

4.2.2 Testing Procedure.

The testing procedure was basically simple. Each bar to be tested was placed in the grooves of the two sets of plates described earlier. The position of the bar was adjusted to ensure that the strain gauges fixed on the steel bar were in the centre of the vertical plane bisecting the gap and also the electrical resistance gauges were parallel to the vertical plane containing the axis of the steel bar. These adjustments were important. The point where the vertical plane that bisects the gap meets the steel bar, is the point of antisymmetry, hence the bending moment is zero and the gauges read only axial strains. If the gauges are at the same level, then they should record the same strain readings.

The two end nuts were tightened until strain readings on the gauges recorded 20 microstrains. After this, the dial gauges were fixed in position, and readings were taken on all gauges.

The steel analogue slab was gently lifted into position, avoiding any disturbance of the dial gauges and was aligned so that the span direction would lie in the same plane as the hydraulic jack, and perpendicular to the centre of the line loads and line supports. Load was applied in small increments, and dial gauge readings and strain gauge readings were taken until the strains recorded on both the strain gauges exceeded the axial yield strain of the bar and free flow of strain was occuring with no load increase. Free flow of strains with

no load increase is the horizontal part of the graph in figures 4.3 - 4.6. A standard tensile test was used to determine the yield strain of the material of the bar. Each test was considered as finished when the strains recorded exceeded the axial yield strain and free flow of strain was occuring at constant load. The test was not continued beyond this point as changes in geometry tended to become significant, so invalidating the results.

After completion of each test, the steel analogue slab was dismantled and the steel bar was examined. Plate 4.4 shows a steel bar before test, and plate 4.5 shows the same steel bar after test. There is no doubt that the bar 'kinked'. The actual kinking of a bar at yield, which was inclined at 60° to the normal to the crack, was no more than a few degrees. Moment enhancement due to kinking is then small and negligible. There is no doubt, however, that if the experiment had been continued well beyond yield of the bar, then the bar re-orientation could have been considerable.

4.2.3 Results.

The results obtained in the Steel Analogue Series are summarised in tables 4.1 and 4.2, and figures 4.2 - 4.6. Figure 4.2 plots the variation of the ratio (the applied moment per unit width normal to the crack) to (design moment in bar direction per unit width) against the crack width; for various inclinations of the bar to the normal. From the graph, it can be seen that the least crack width required for yield to occur is when the steel bar is normal to the crack. The graph when α is zero, shows fully elastic-fully plastic behaviour. This is the usual behaviour of a steel bar having a definite yield point and subjected to an axial load. The graph when α is 30°, 45°, and 60°, consists of three parts. The first part appears to be a

straight line, the second part a curve, and the third part a horizontal line. Departure from linearity in the moment-crack curves for non zero α values, figure 4.2, occurs at low loads. This could be due to two reasons. Firstly, it could be due to yielding of the specimen and secondly, it could be due to sporadic slipping of the specimen through the bearing plates. The first reason must be discarded since the strain gauges fixed on either side of the bar recorded strains much lower than the yield strains obtained from a simple axial test. The second possibility appears more reasonable, since small load drops were recorded during the test. However, this effect will not invalidate the results in any way, since yield in the bar specimen will be decided by the excess of strains over and above the yield strain leading to free flow of strains as shown in figures 4.3-4.6.

Figures 4.3-4.6 plot the variation of the ratio (the applied moment per unit width normal to the crack) to (design moment in bar direction per unit width) against the strains on either side of the bar, for various inclinations of the bar to the normal. From the graphs, it can be seen that the gauges on either side of the bar did not record the same strain. There is no apparent reason why these gauges should record different readings. The difference in strain for test SA1, figure 4.3, could only be attributed to a slight difference in level between the gauges. This error could have taken place during placing the bar in position. Difference in strain between the two gauges placed on either side of the bar for tests SA2, SA3, SA4, figures 4.4, 4.5, and 4.6 could be attributed to two reasons. The first reason is identical to that given for test SA1. The second reason is the possibility that the centre of both strain gauges was not at the point of skew symmetry of the bar. Slight misplacement of the

gauges would have caused one gauge to read higher readings than the other. Again, these small experimental errors have no effect on the overall performance of the steel analogue slab or the ultimate result. Again, from figures 4.3-4.6, it can be seen that although the strain readings recorded by the gauges are higher than the axial yield strain, the bar did not yield. This is due to the fact that the gauges recorded strains along the axis of the bar, the top fibres of the steel did not reach yield strain until later in the loading sequence. This difference of strains is due to the difference of level in relation to neutral axis of bending.

Table 4.1 shows the properties of the steel bars used for all four tests, whilst table 4.2 shows the yield moments normal to the crack per unit length. Also, these yield moments are compared with those predicted by the Johansen [2] criterion. It can be seen that when α is 60°, the moment enhancement is over 36%.

4.3 Mono-Steel bar Concrete Strip Series.

4.3.1 Description of Slab Strips.

Altogether, six specimens were tested in this series. Each slab bears the reference mark CS (concrete strip) followed by the number of the specimen. All specimens were 914 mm long and 152 mm wide. The nominal thickness of the slab was 76 mm, but thickness of each slab was measured by means of a micrometer screw gauge at ten different points, and the mean value was used for further calculations.

All slabs were reinforced with a single bar inclined at different directions relative to the uniaxial moment direction. Figure 4.7 shows a typical reinforcing arrangement. The reinforcing steel chosen was 9.5 mm diameter mild steel turned down to 8.00 mm over the test length.

Hooks were provided at the end of the bar to eliminate the possibility of bond failure. Also, two additional bars were introduced in the slab, but not crossing the test area, to make sure the slab will fail at a particular cross section. On each bar, two electrical resistance gauges were fixed. These gauges were fixed at the centre of the bar and parallel to each other. The procedure of fixing and waterproofing the strain gauges is described in the Instrumentation section of Chapter five. The bar was placed in a plywood mould in such a position that the strain gauges were in a vertical plane and at the centre of the artificial crack (to be described shortly in this section). These gauges were intended to be used as a guide to indicate the yield of the bar.

In this test series, an artificial crack was created on the tension face of the slab at the centre of the span across the width of the slab. This crack was of the same width as the artificial crack in the Steel Analogue Series. The width of the crack was 15.9 mm, and the depth measured from the tension face was 25.4 mm. Plates4.6 and 4.7 show a typical crack. The crack exposes the bar and also creates a weak zone at this particular section. The crack was created by placing polystyrene in the mould, in the form of a prism measuring 152 mm long, 25.4 mm deep and 15.9 mm wide. A micrometer screw gauge was used to measure the actual crack width of each slab, and the results are shown in table 4.4.

Casting was carried out on a variable speed vibrating table after the concrete had been mixed in a mixer of the non-tilting drum type, manufactured by Linear Concrete Machinery Co. Ltd.

Details of the concrete mix ingredients are given in Chapter five, section 5.2. The 9.5 mm cover to the reinforcing steel was maintained

by affixing 9.5 mm mortar spacing blocks to the reinforcing steel. In addition to the concrete slabs, control specimens were prepared. Concrete cylinders were used for determination of Youngs modulus and modulus of rupture and concrete cubes for determination of the crushing strength of the concrete. All slabs and control specimens were stripped twenty-four hours after casting and cured for twenty-four days in a controlled humidity curing tank.

4.3.2 Testing Procedure.

The tests were carried out within a large permanent portal frame testing rig, which is described in detail in Chapter five, section 5.5.1. Plate 4.8, however, shows enough details of the testing rig to facilitate the description of the testing procedure. Before the slab was placed on the testing rig, two dial gauges reading to 25×10^{-5} mm were fixed on either side of the slab on steel inserts embedded in the concrete during casting. These inserts may be seen near the ends of the crack on plate 4.6. Plate 4.9 shows one of the dial gauges fixed on the steel inserts, which were accurately adjusted before casting so that the dial gauges were reading crack increases at the same level as the reinforcing bar. When the dial gauges were fixed in position, zero readings were taken on all the gauges.

The slab was gently lifted into position as shown in plate 4.8, and supported in rollers to eliminate membrane forces. Loads were applied to the upper surface in the form of two line loads transmitted through steel rollers plastered transverely onto the upper surface 229 mm to either side of the slab centre line. Three I beams of large cross section (127 mm x 76 mm) were placed perpendicular to the steel rollers and along the span direction. A vertically aligned, centrally positioned, 100 kN capacity, long travel jack acted on the upper block

of a prooving ring and was operated by a hand pump system. Before each test began, checks were made to ensure that the span direction, I beams and hydraulic jack were all in the same vertical plane. The whole set up is shown in plate 4.8, and figure 4.8 shows all the important slab dimensions and the position of the loads.

Since the slabs were reinforced with a single bar and were thus lightly reinforced, the loading was carried out in small increments. Readings on all the gauges were taken for each load increment, and the test was continued until the slab failed.

After completion of test, the slab was brought down from the testing rig and placed on a table and examined. Plate 4.7 shows tensile cracks along the depth of the slab, and it can also be seen that the compression zone is very small. Plate 4.6 shows the tensile face of the slab, where it can be seen that tensile cracks exist in the same direction as the bar. Crushing of concrete was also seen at the same level as the bar, but is not obvious on the photograph. This is further evidence that a bar crossing a yield line at some oblique angle is subjected to axial and shear forces. However, it must be emphasised here that at yield, 'kinking' of any measurable quantity was not observed, but the tensile cracks along the bar show that the bar has a tendency to 'kink'. Extensive crushing of concrete was observed when the bar was inclined at 60° and 75° to the normal to the artificial crack.

4.3.3 Results.

The results from the Mono-Steel bar Concrete Strip Series are summarised in tables 4.4 and 4.5, and graphically in figure 4.9. Table 4.4 shows the actual slab thickness, concrete cube crushing strength, the original artificial crack width and the design strength of the slab

per unit width in the direction of the reinforcing bar. Table 4.5 shows the bar orientation relative to the normal to the crack, the prooving ring reading at yield, and also the ultimate moment at yield (this includes dead weight of slab and the load spreader). In addition, table 4.5 shows the ratio of ultimate normal yield moment to the Johansen [2] normal yield moment. It can be seen that this ratio is greater than unity when α is 15°, 30° and 45°. When α is 60°, the ratio is much less than unity. The reduction in moment when α is 60° is due to the large amount of concrete crushing around the reinforcing bar. Crushing of concrete and subsequent failure of slab started at low loads. The author believes that the reinforcing bar ($\alpha = 60^{\circ}$) did not yield at all when failure took place. Specimen CS5, bar orientation 75° to the normal to the yield line, failed immediately after the application of the second load. Failure of this specimen was entirely due to the crushing of the small side cover of concrete. It was felt that this test should be discarded.

Figure 4.2 (4.97) illustrates the variation of the ratio (ultimate moment per unit width at yield) to (design moment per unit width in the direction of the bar) plotted against the crack width. The first part of the trilinear graph represents the elastic behaviour of the bar before any tensile cracks develop in the concrete below the neutral axis. The second part of the graph shows the linear behaviour of the bar after the shift of the neutral axis due to the development of tensile cracks in the concrete. The third part of the graph, which is horizontal, shows that the reinforcement has yielded, or that the slab failed because of extensive crushing of concrete.

Although precautions were taken to ensure the normal operation of the strain gauges on either side of the bar, the strain gauges did

not operate satisfactorily. Results obtained were erratic and unreliable. This abnormal behaviour of the strain gauges was due to insulation failure of the gauges.

4.4 Effects of the 'effective crack width'.

In Chapter three, the effective crack width was defined as the length of the bar required for equilibrium. The forces in equilibrium were the shear force on the bar and the concrete pressure generated by the shear force. The effective crack width will always be greater than the visible tensile concrete crack. Also in Chapter three, it was shown theoretically that when the effective crack width becomes large, the predicted normal moments by the author's theory coincide with those predicted by the Johansen theory. In both the Steel Analogue Series and the Mono-Steel bar Concrete Strip Series, the original nominal artificial crack width was 15.9 mm. Also, the steel bars used in both series for a particular bar orientation had the same diameter, the same strength, and the same Youngs modulus. In theory then, both series should have produced the same m_n/m ratio for a particular bar orientation. Examining m_n/m values in tables 4.2 and 4.5, it can be seen that this is not the case. Since, in both series, all the parameters controlling the m_n/m ratio are constant except the effective crack width, then the variation of m_n/m obtained in both series for a given bar orientation must be due to the effective crack width. It must be emphasised here that the increase in the width of the artificial crack (SA series) during the test was very small; amounting to no more than 2 mm, which was entirely due to the elongation of the bar. Changes in the artificial crack created in the Mono-Steel bar Concrete Strip Series were due to three reasons. First, the elongation of the bar due to stress which, at yield, was no more than 1 mm (see figure 4.9). Second,

crushing of the concrete around the bar alters the crack width, and third, yielding of concrete adjacent to the bar also alters the crack width.

The effects of the effective crack width will be defined here as the following ratio:

$$C_f = \frac{(\frac{m_n}{m})_{SA} - (\frac{m_n}{m})_{CS}}{(\frac{m_n}{m})_{SA}}$$

where $(\frac{m_n}{m})_{SA}$ is the ratio of the experimental normal yield moment/design moment in the bar direction in the Steel Analogue Series, and $(\frac{m_n}{m})_{CS}$ is the experimental ratio of the normal yield moment/design moment in the bar direction in the Mono-Steel bar Concrete Strip Series.

Table 4.6 shows the $(\frac{m_n}{m})_{SA}$ and $(\frac{m_n}{m})_{CS}$ values, also the factor C_f. The C_f value is approximately zero when α is zero, and increases gradually when α is increased. The C_f value should be zero again when α is 90°.

4.5 Conclusions on Results.

The object of this chapter was twofold. Firstly, it was to show the existence of axial and shear stresses on a steel bar crossing a yield line at some oblique angle , and secondly, to show the existence of the effective crack width and the overall effect on the moment strength of a concrete slab.

The existence of axial stresses on the bar no-one doubts; however, the strain gauges placed on the bar at the point of antisymmetry showed their existence. Both the tensile cracks which developed on the tension face of the slab along the length of the reinforcing bar, and the

concrete crushing which occurred at the same level as the bar, demonstrated beyond any doubt that shear stresses on the bar do exist when the bar is inclined at an oblique angle to the yield line. Also, plate 4.5 shows slight kinking of the steel bar; this kinking could only be caused by shear forces on the bar.

By keeping constant all the parameters effecting the moment strength except the crack width during the test in the Steel Analogue and Mono-Steel bar Concrete Strip Series (initially both series had the same crack width), it has been shown that the effective crack width exists and has a detrimental effect on the overall moment strength of the slab. The overall effect of the effective crack width and concrete crushing has been demonstrated by comparing the experimental normal moment obtained from the Steel Analogue Series to that obtained in the Mono-Steel bar Concrete Strip Series. The C_f factor as defined by equation 4.1 is as much as 0.411 when α is 60°. In practice, the C_f factor would be smaller since only two bars out of a large number of bars would have a small side concrete cover.

Series number	α°	Original crack width mm	Bar diameter mm	Axial yield stress fy N/mm	Axial yield strain ε microstrain	m kNm/m
SA 1	0	16.36	7.82	341.2	1400	6.87
SA 2	30	15.57	7.97	341.2	1400	8.24
SA 3	45	14.60	7.91	348.1	1650	10.08
SA 4	60	15.95	7.90	348.1	1650	14.22

Table 4.1 STEEL ANALOGUE SERIES

Series number	Prooving ring reading kN	Ultimate moment kNm/m	$\frac{m_n}{m}$	$\frac{m_n}{m_{nj}}$
SA 1	10.32	6.88	1.001	1.001
SA 2	9.90	6.62	0.803	1.071
SA 3	8.71	5.92	0.587	1.174
SA 4	6.87	4.85	0.341	1.364

Table 4.2 STEEL ANALOGUE SERIES

Series Number	α°	Bar diameter mm	Axial Yield stress fy N/mm^2	Axial Yield strain ε
CS 1	0	7.84	341.2	1400
CS 2	30	7.84	341.2	1400
CS 3	45	7.81	348.1	1650
CS 4	60	7.57	348.1	1650
CS 5	75	7.88	348.8	1570
CS 6	15	7.88	348.8	1570

TABLE 4.3 CONCRETE SLAB STRIPS

Series Number	Slab thickness mm	Concrete strength U N/mm^2	Original crack width mm	m KNm/m
CS 1	76.48	44.25	15.06	6.63
CS 2	76.61	44.25	15.21	7.65
CS 3	77.27	39.72	14.82	9.45
CS 4	76.76	39.72	15.29	12.32
CS 5	77.32	55.70	14.68	7.19

TABLE 4.4 CONCRETE SLAB STRIPS

Series number	α	Prooving ring reading kN	Ultimate moment at yield kNm/m	$\frac{m_n}{m}$	$\frac{m_n}{m_{nj}}$
CS1	0	11.08	6.59	0.994	0.994
CS2	30	9.44	5.97	0.780	1.040
CS3	45	7.80	5.01	0.530	1.060
CS4	60	3.62	2.48	0.201	0.804
CS5	75	1.57	----	-----	----
CS6	15	10.99	6.86	0.955	1.025

Table 4.5 MONO - STEEL BAR CONCRETE STRIPS

Series number		α°	$\left(\frac{m_r}{m}\right)_{SA}$	$\left(\frac{m_r}{m}\right)_{CS}$	C_f
SA1	CS1	0	1.001	0.994	0.006
SA2	CS2	30	0.803	0.780	0.029
SA3	CS3	45	0.587	0.530	0.097
SA4	CS4	60	0.341	0.201	0.411

Table 4.6

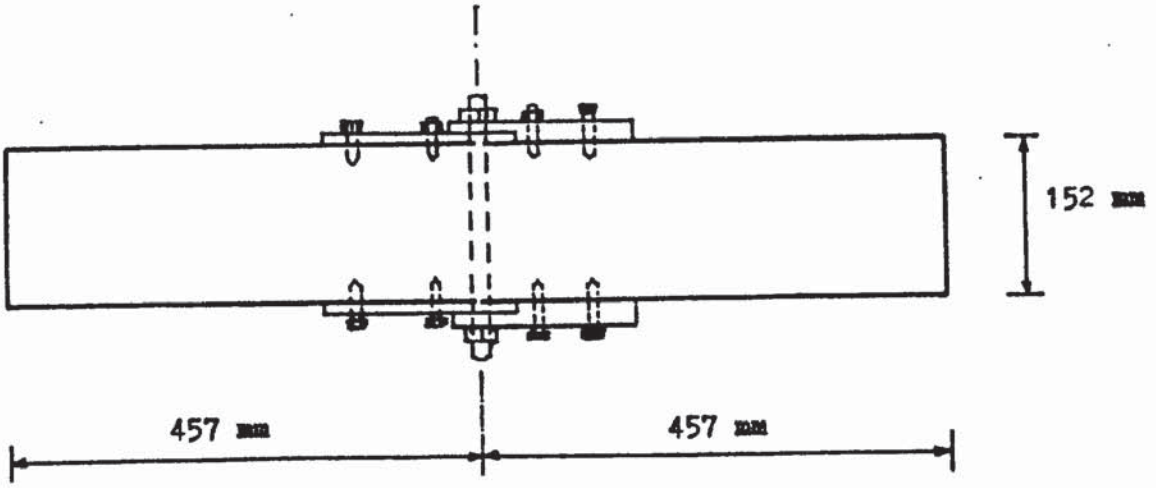

PLAN VIEW OF RIG

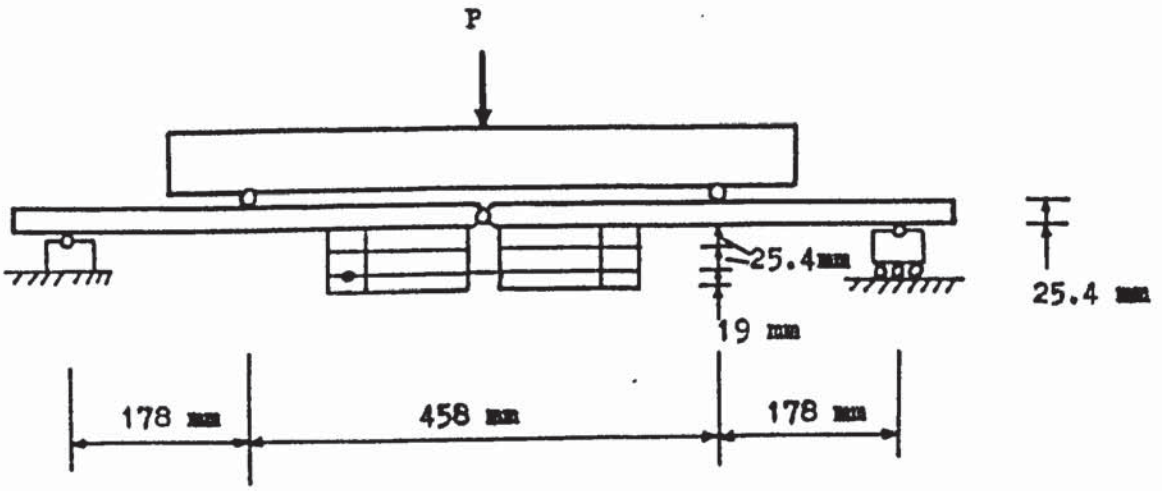

Figure 4.1 TEST SET UP (STEEL ANALOGUE)

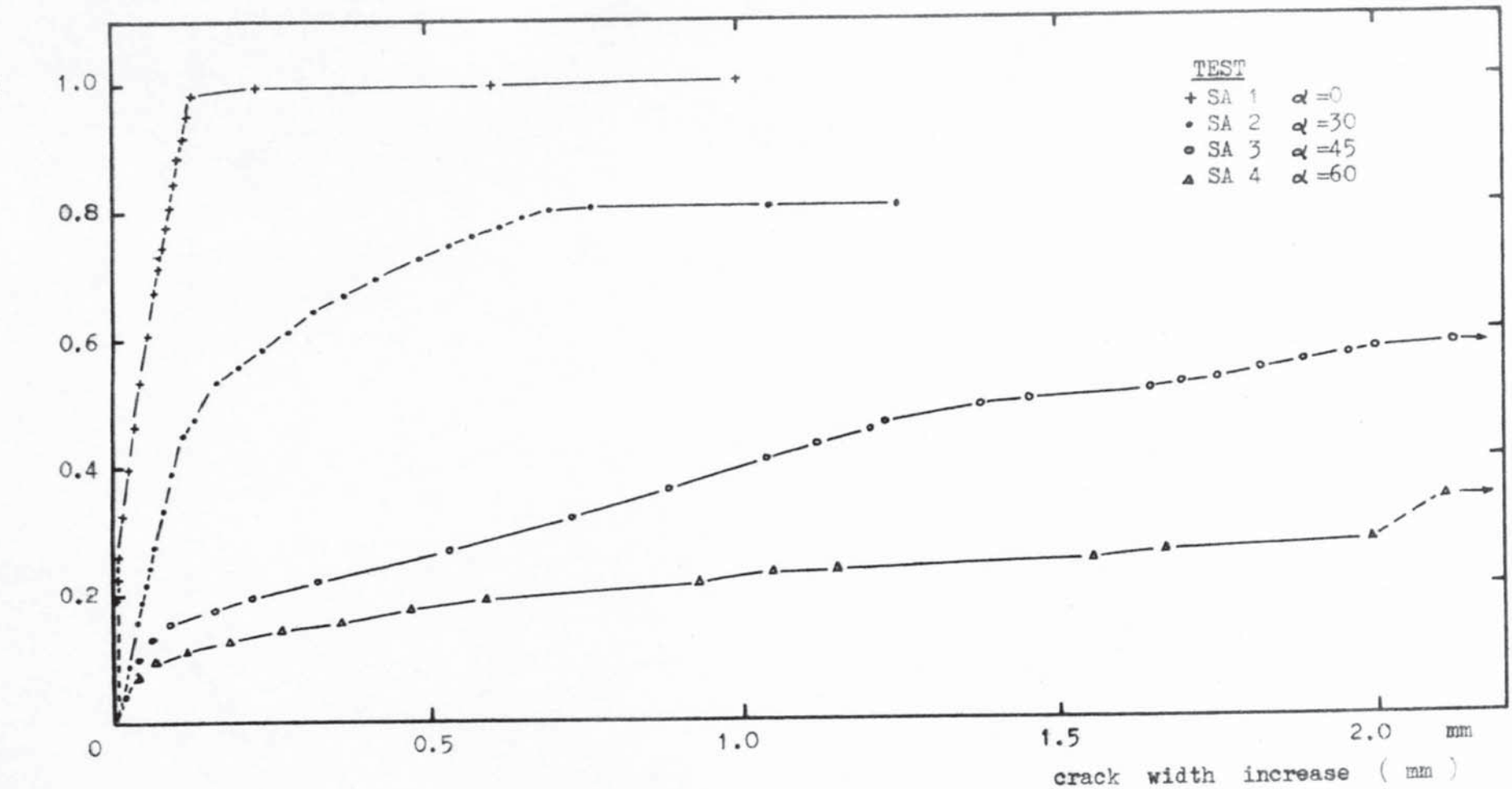

Figure 4.2 PLOT OF CRACK WIDTH INCREASE (STEEL ANALOGUE)

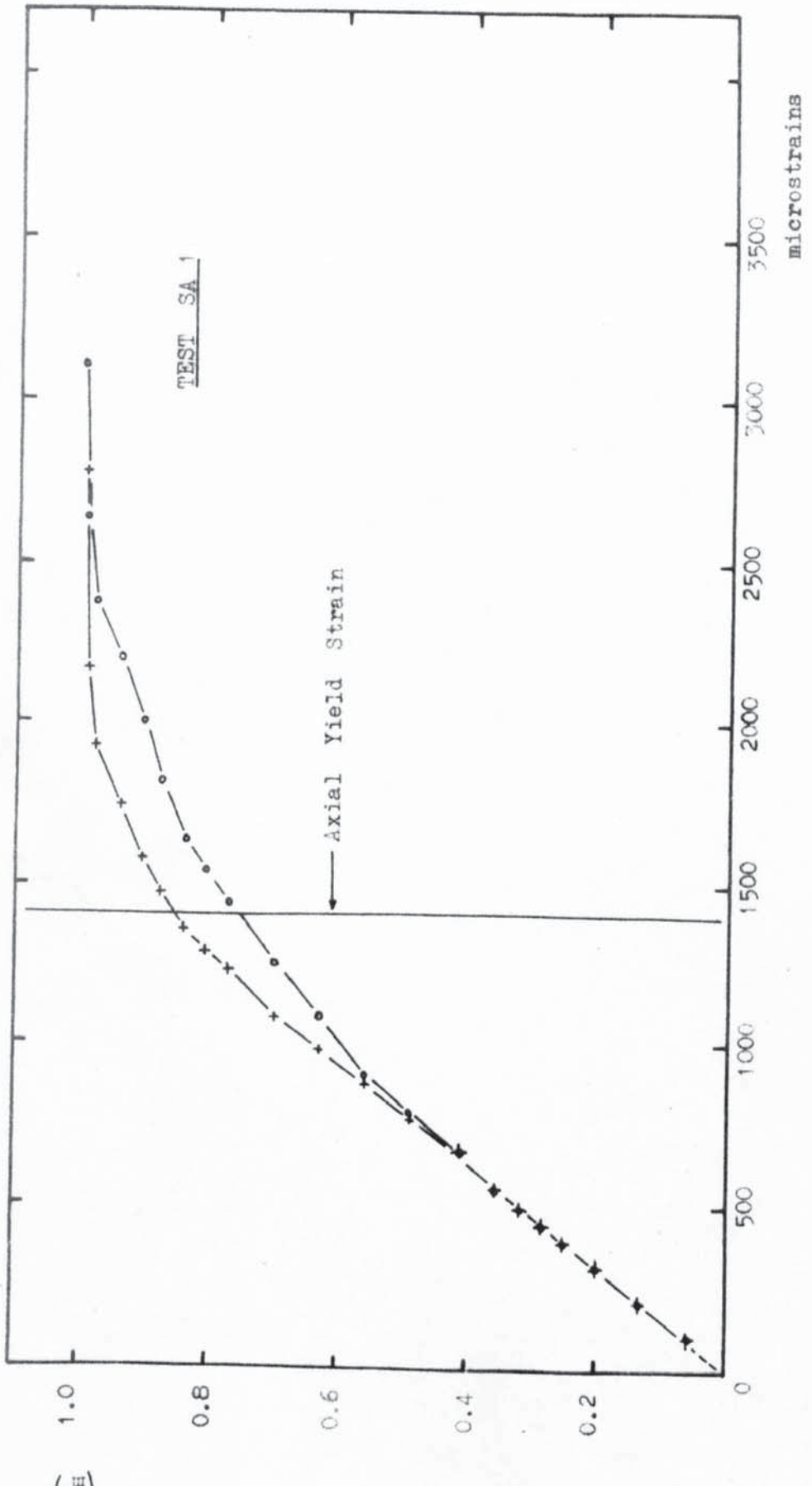

Figure 4.3 PLOT OF STEEL STRAIN (STEEL ANALOGUE)

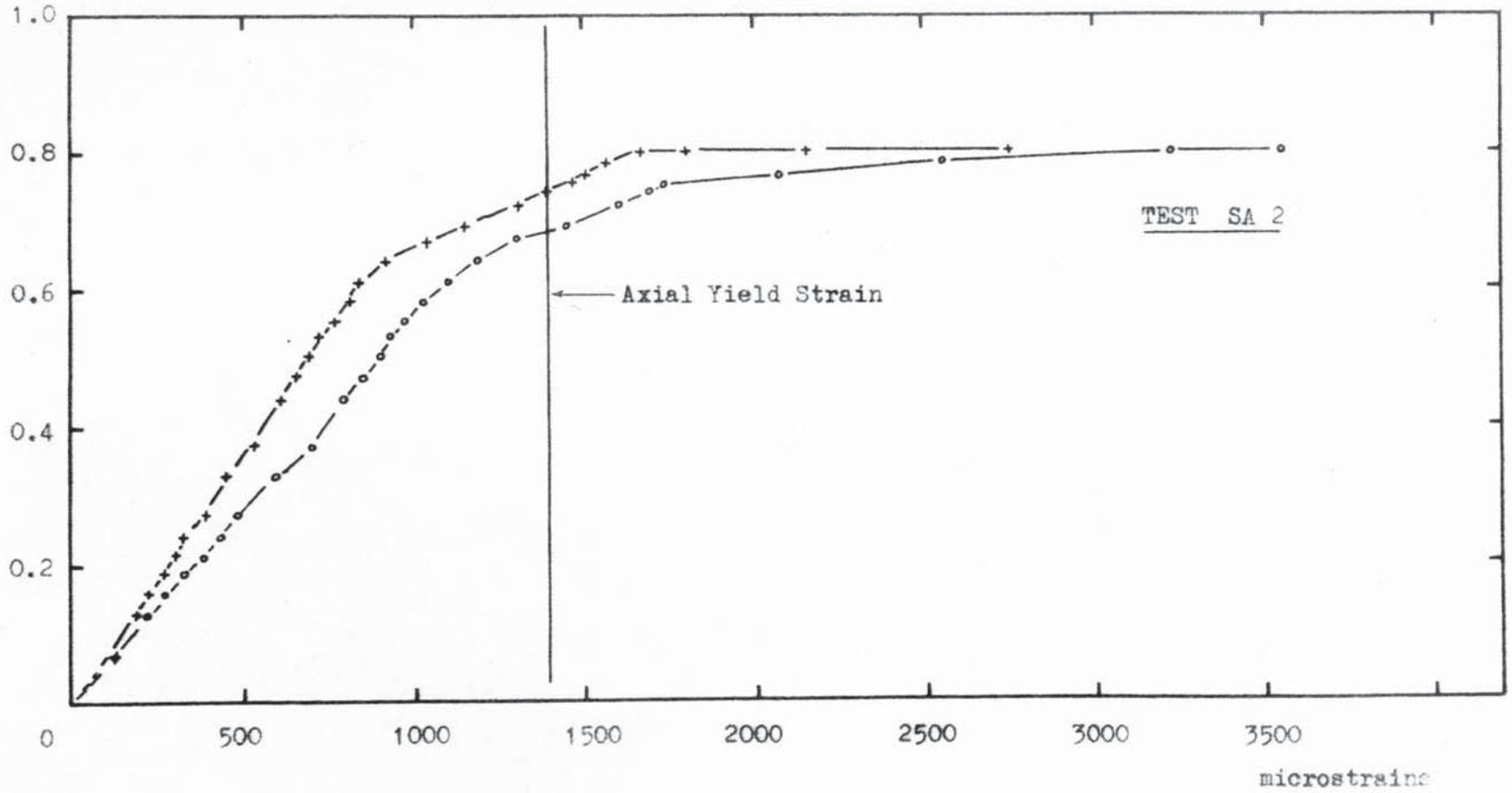

Figure 4.4 PLOT OF STEEL STRAIN (STEEL ANALOGUE)

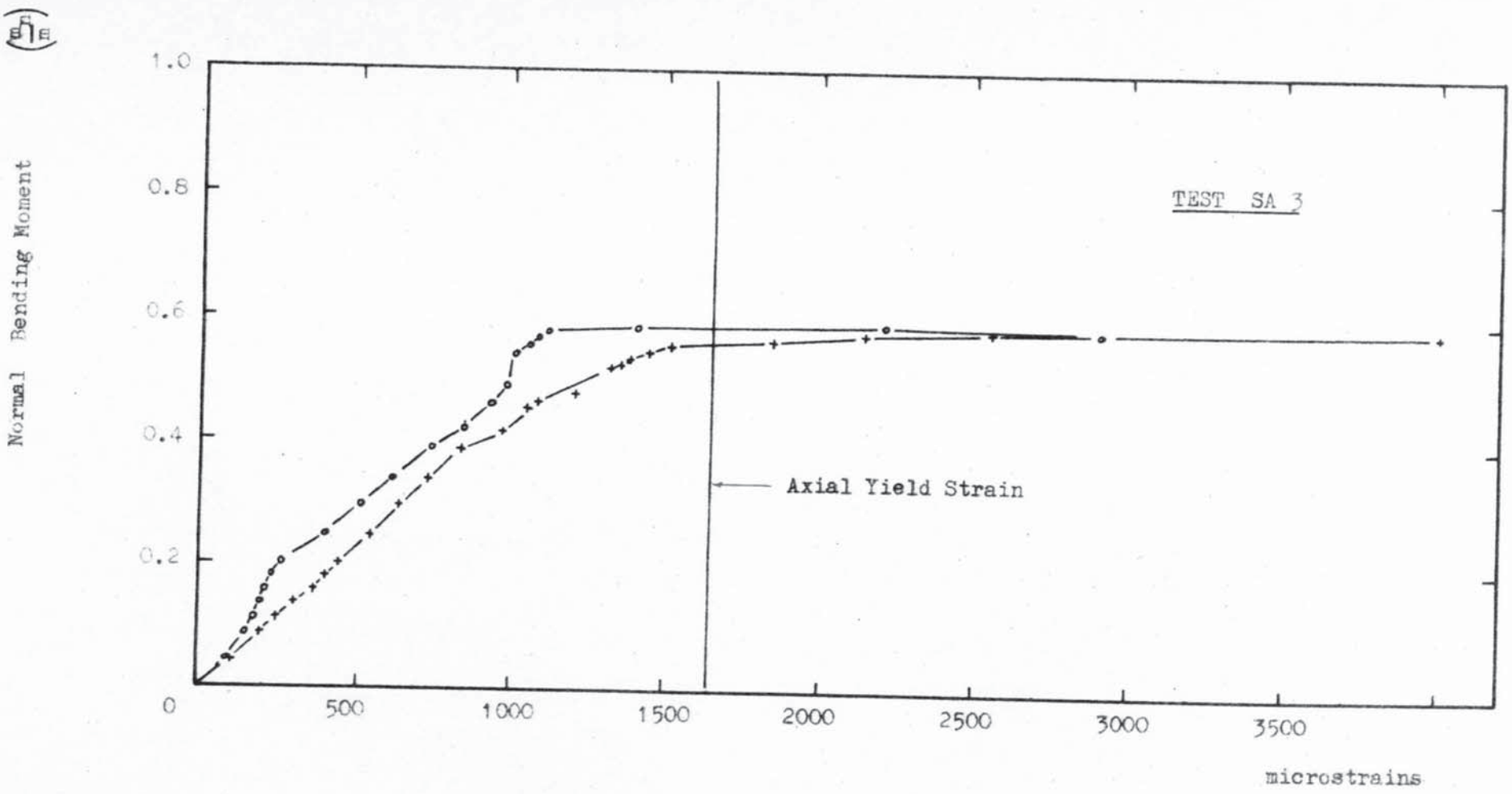

Figure 4.5 PLOT OF STEEL STRAIN (STEEL ANALOGUE)

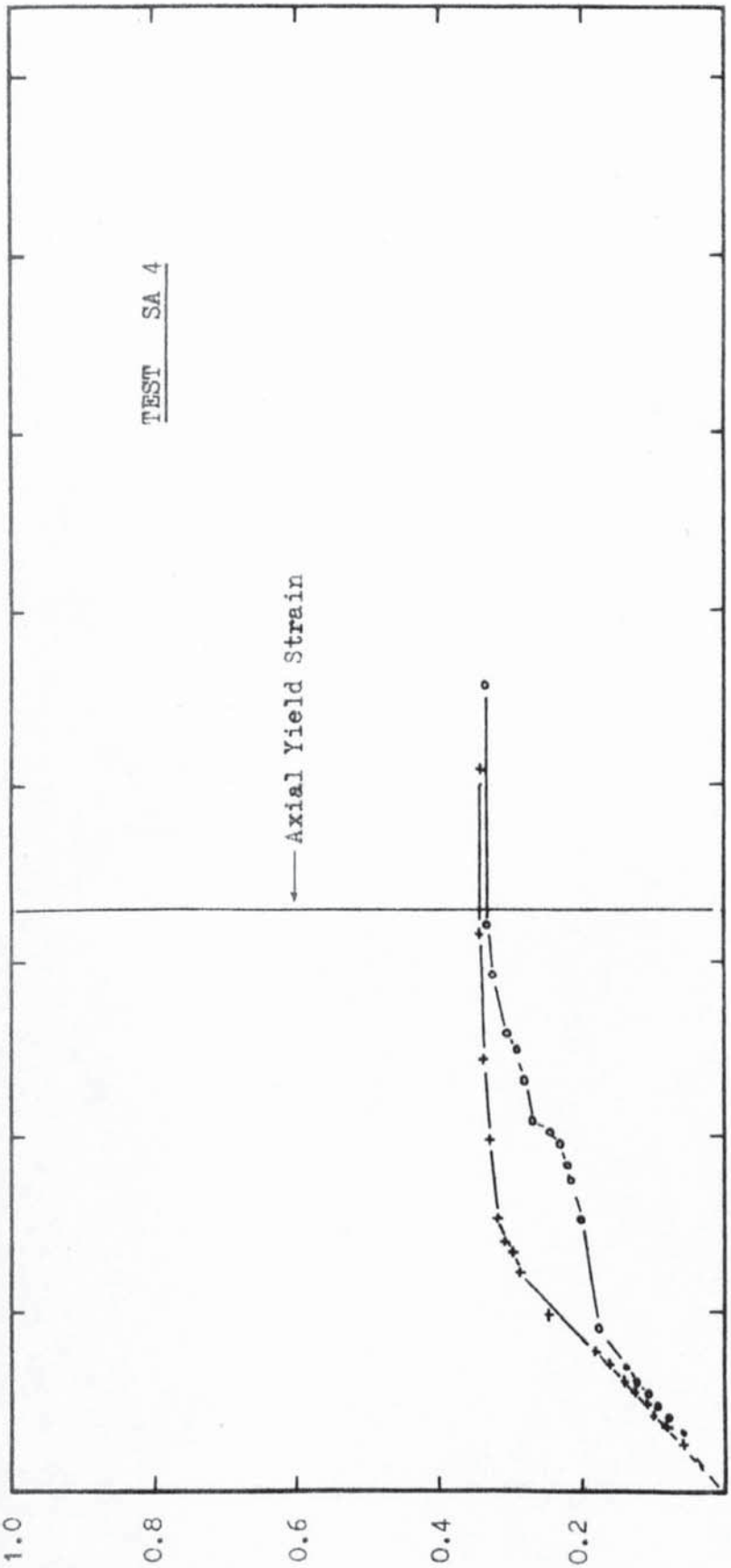

Figure 4.6 PLOT OF STEEL STRAIN (STEEL ANALOGUE)

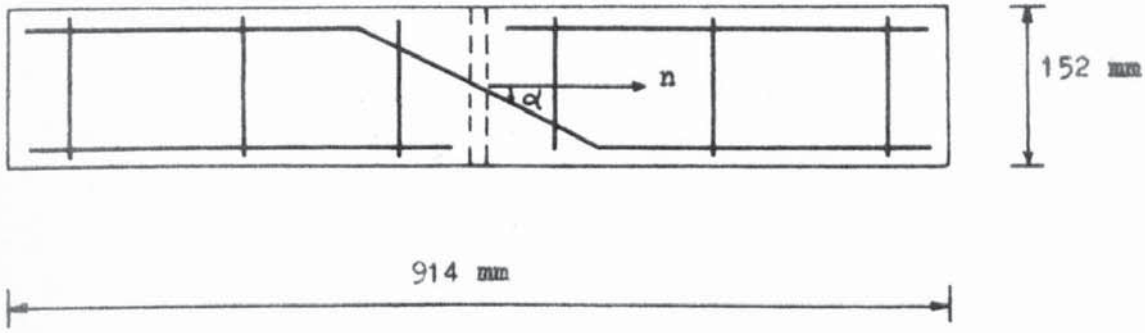

Figure 4.7 TYPICAL REINFORCING ARRANGEMENT

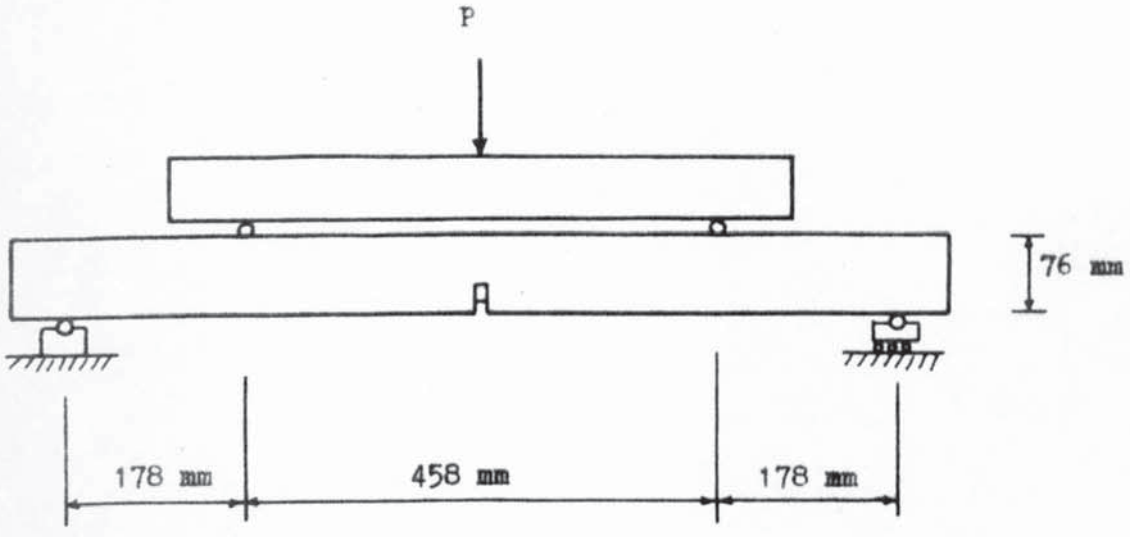

Figure 4.8 TEST SET UP (CS)

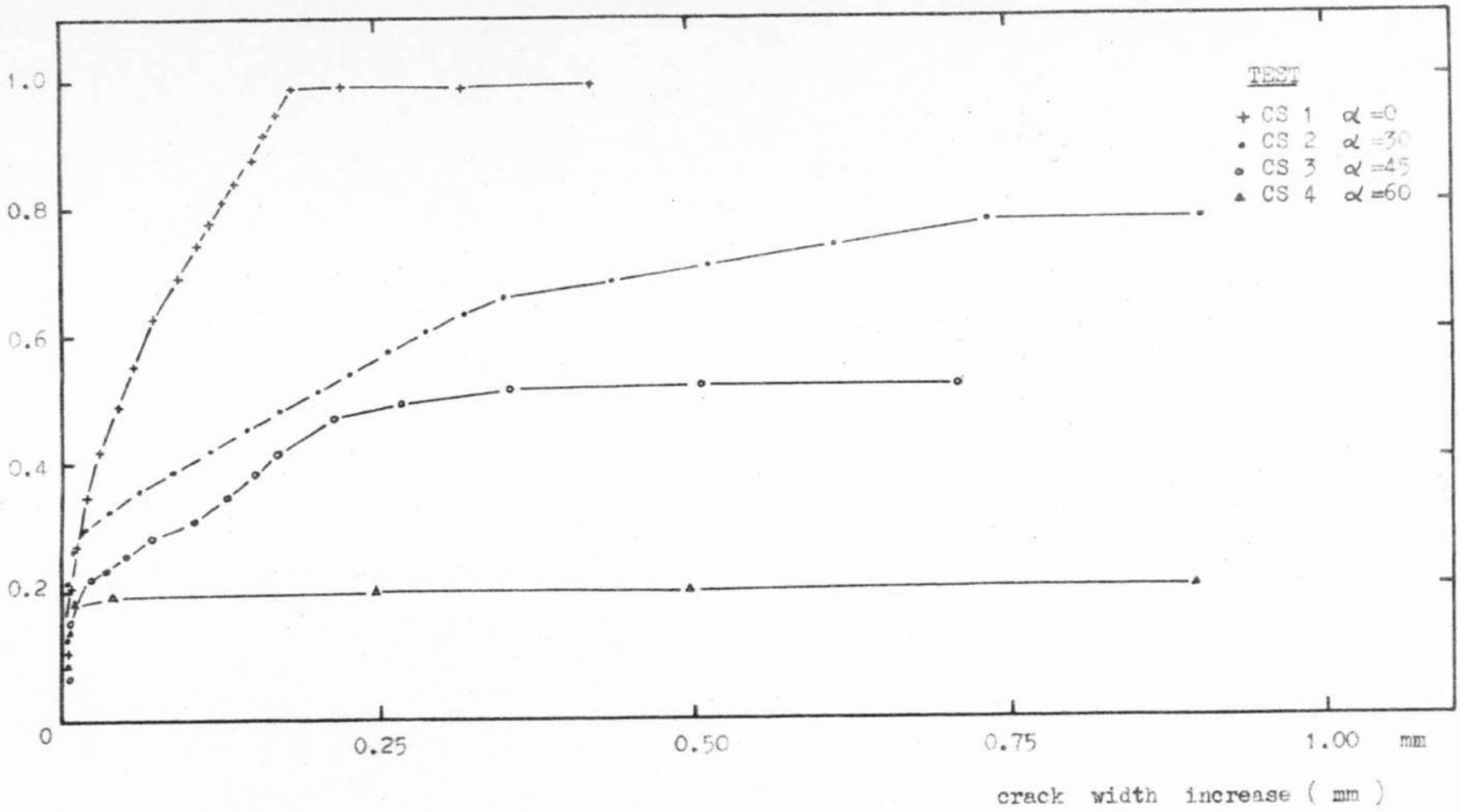

Figure 4.9 PLOT OF CRACK WIDTH INCREASE (MONO—STEEL BAR CONCRETE STRIP)

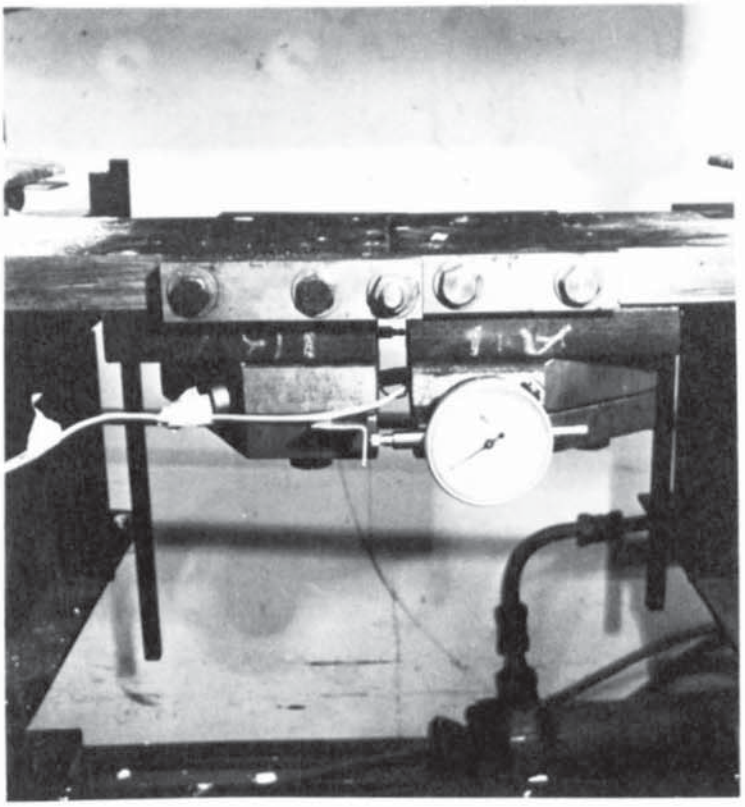

PLATE 4.1 SIDE VIEW (STEEL ANALOGUE)

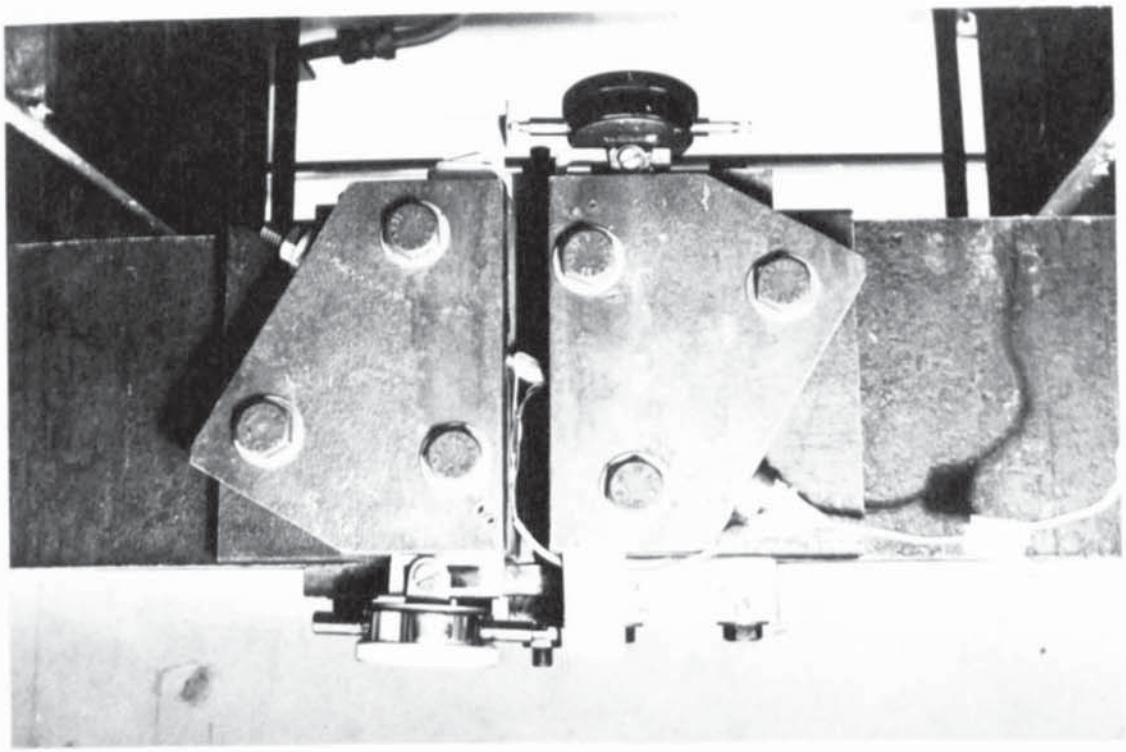

PLATE 4.2 PLAN VIEW, TENSION FACE (STEEL ANALOGUE)

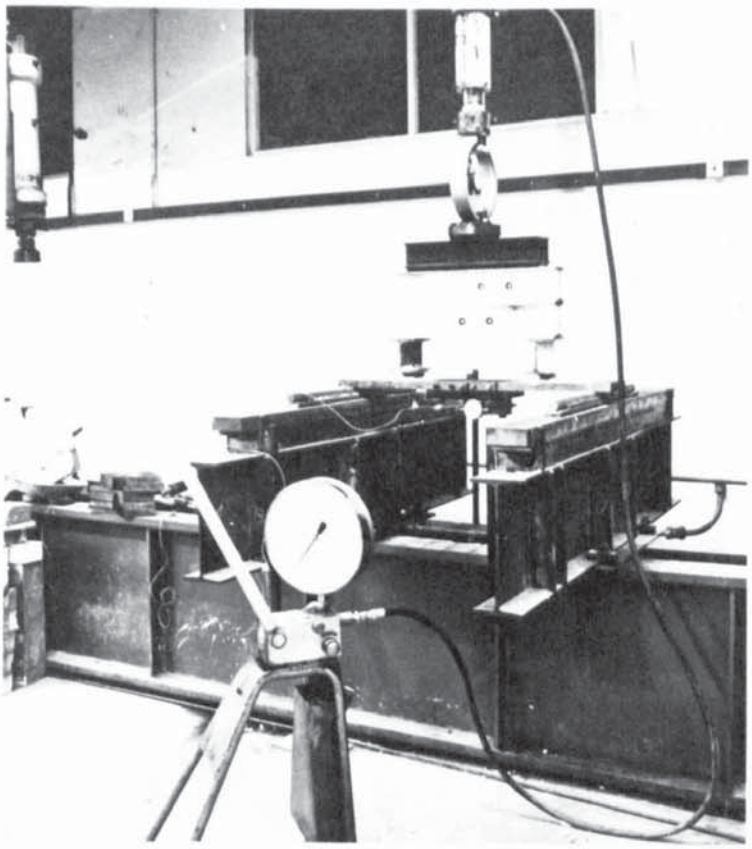

PLATE 4.3 TEST SET UP (STEEL ANALOGUE)

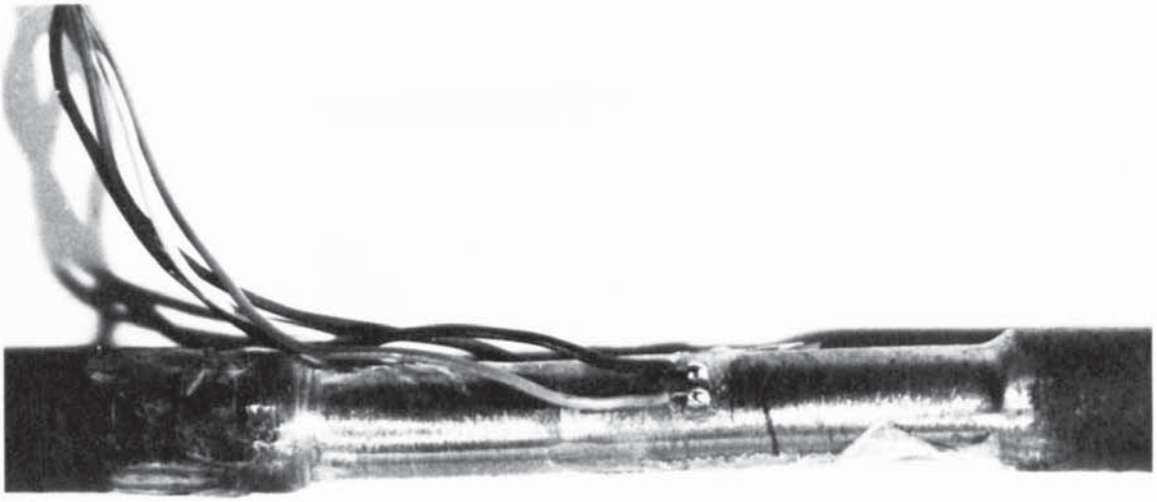

PLATE 4.4. STEEL BAR WITH STRAIN GUAGE

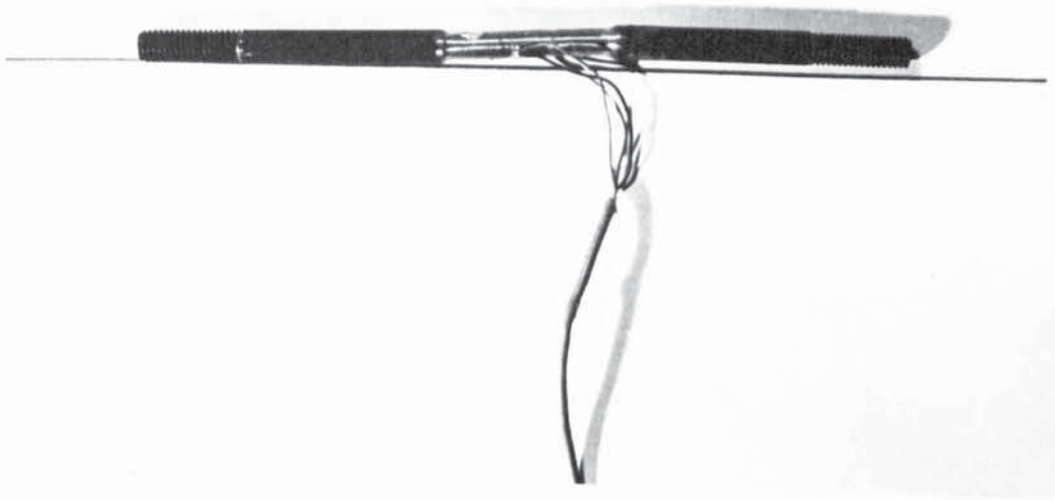

PLATE 4.5 STEEL BAR AFTER TEST (STEEL ANALOGUE, α = 60)

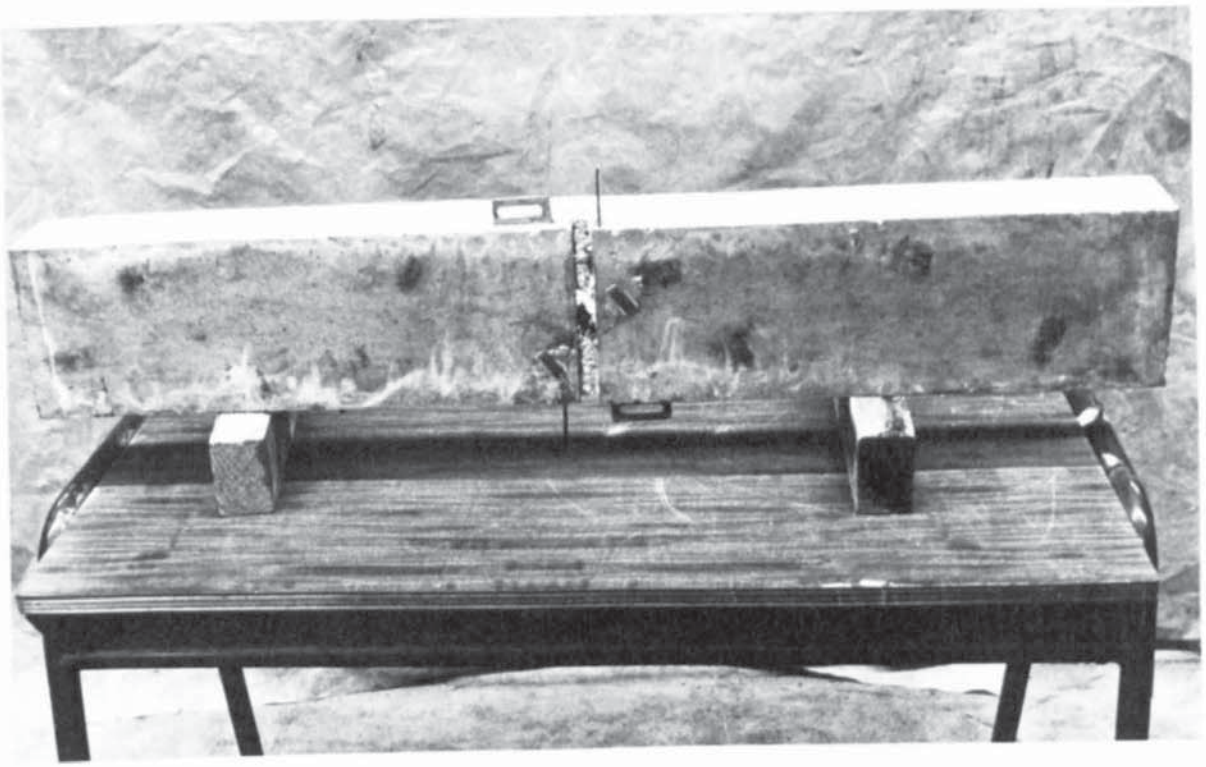

PLATE 4.6 ARTIFICIAL CRACK (MONO - BAR CONCRETE STRIP)

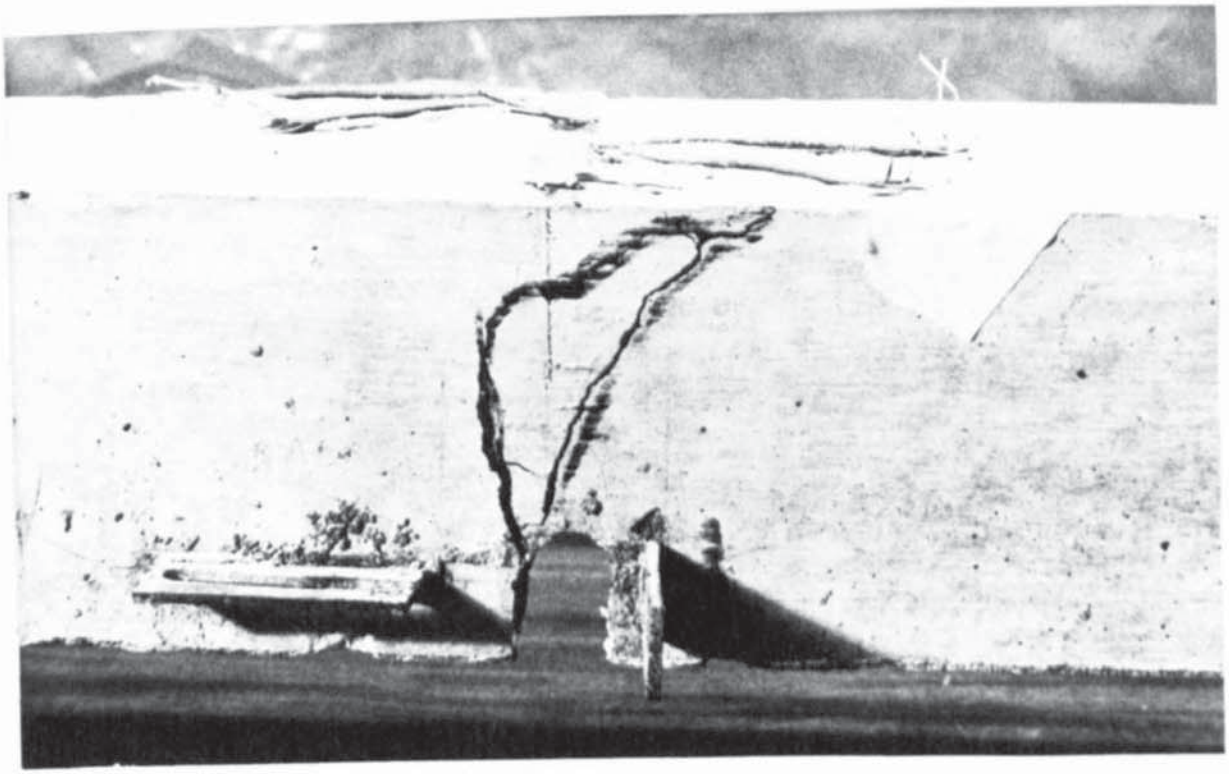

PLATE 4.7 TENSILE CRACK ALONG DEPTH OF CONCRETE STRIP

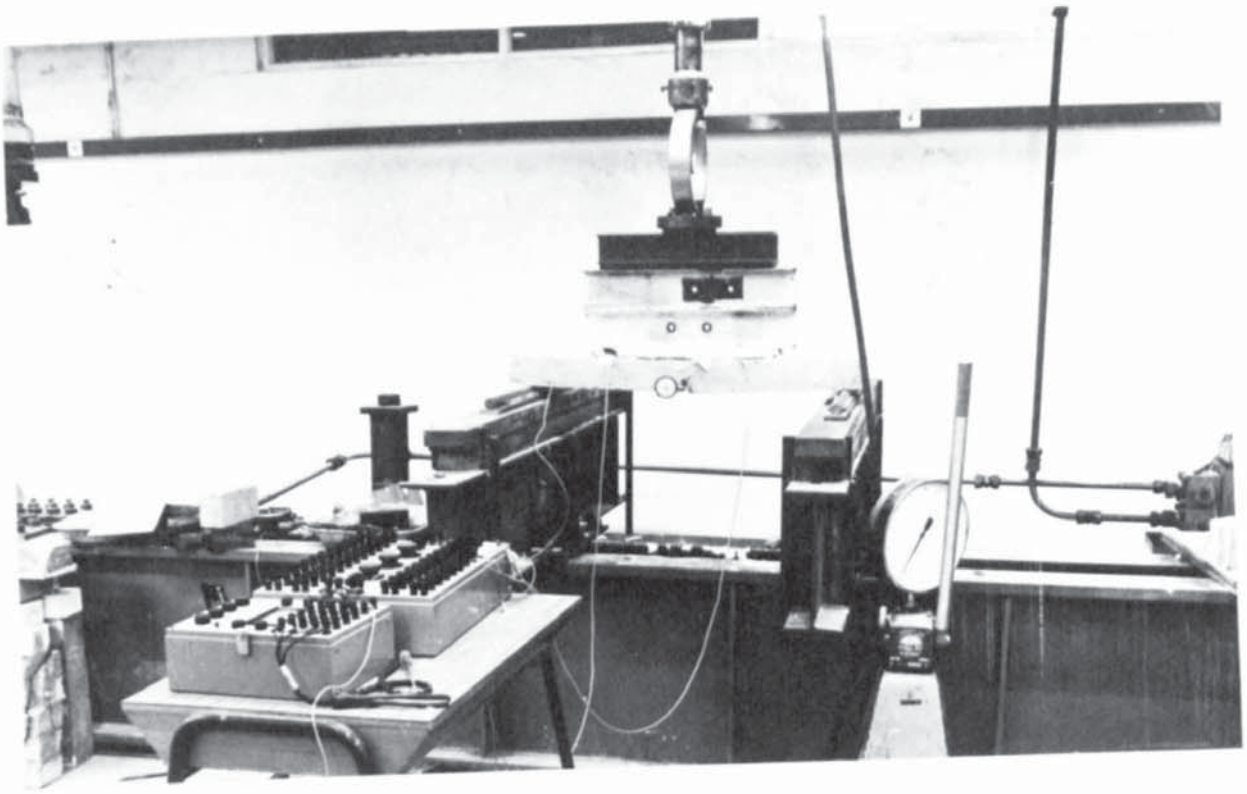

PLATE 4.8 TEST SET UP (MONO - BAR CONCRETE STRIP)

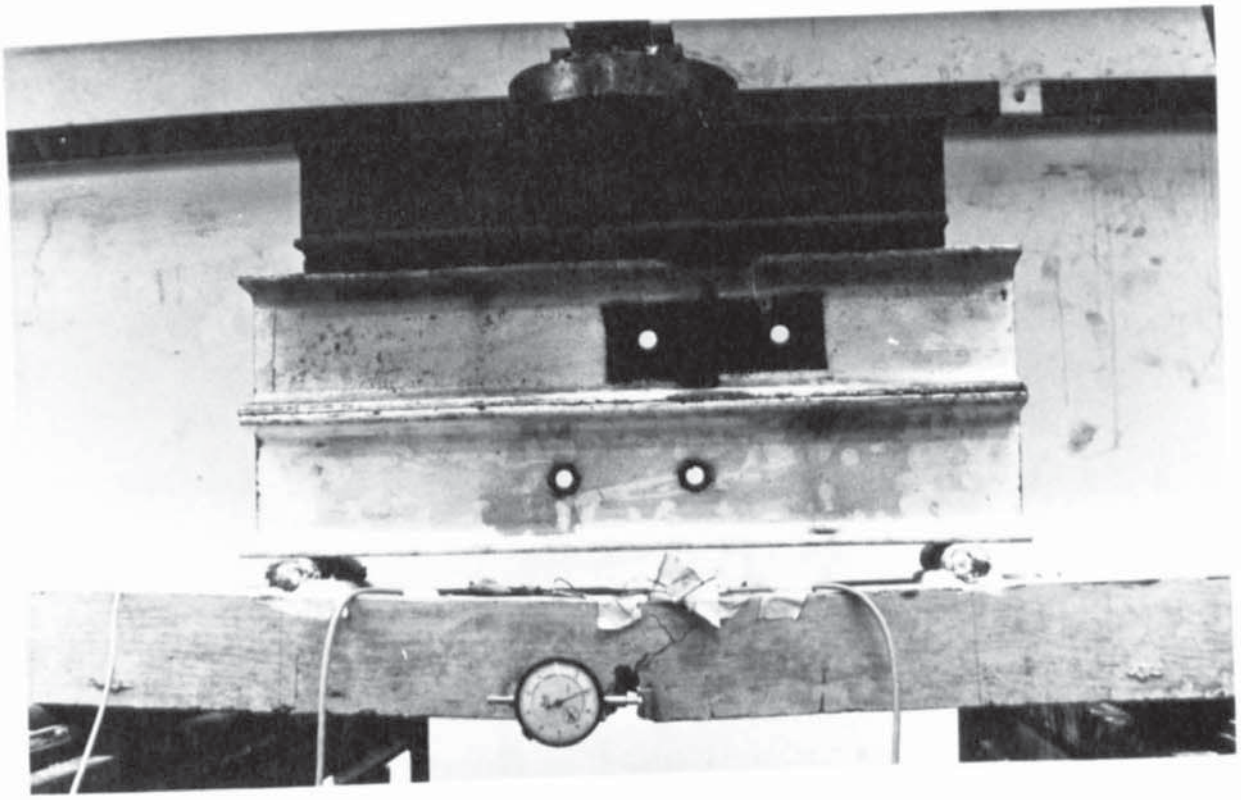

PLATE 4.9 TEST SET UP

CHAPTER 5

TESTS ON REINFORCED CONCRETE SLABS SUBJECTED TO BENDING AND TORSION

5.1 Introduction

The object of these experiments was to investigate the behaviour of reinforced concrete slab elements subjected to combined bending and torsional moments.

All other effects, such as transverse shear forces and membrane forces, were to be eliminated.

Apart from one single restriction, the slab elements tested had complete freedom to deform according to the shape dictated by the loads. The single restriction was the curvature adjacent to the jaws. This curvature was zero because of the large stiffness of the jaws. This restriction was considered insignificant since the jaws are some distance from the critical test region.

The main variables controlled in the series of tests were:-

(a) The angle, β, between the main reinforcement and the span direction.

(b) The "degree of orthotropy", μ, which is defined as the ratio of ultimate moments of resistance in the bar direction and will always lie within the range

$$-1 \leq \mu \leq 1$$

(c) The ratio of the torsional moment to that of the bending moment.

(d) The steel stress-strain characteristics.

Other variables such as concrete strength, slab thickness, were held constant as far as possible.

All slab elements had bottom reinforcement only.

5.2 Materials used for the test series.

5.2.1 Cement

Typical Portland Cement produced by the Blue Circle Group was used in all test specimens.

5.2.2 Aggregates

Zone III sand and 3/8 inch crushed gravel supplied by the Midland Gravel Co. Ltd. from pits in the Birmingham area was used in all specimens.

Sieve analysis of both the sand and the gravel was carried out according to the B.S.812 and the results are presented in tabular form in Table 5.1 and 5.2 respectively.

5.2.3 Concrete Mixes.

A concrete mix was designed to produce a strength of 35 MN/m^2 at 28 days with a medium workability. Trial mixes were prepared and tested for strength and workability and adjusted to produce the desired properties. The accepted ingredient dry proportions were 1:2:4 by weight, and the water-cement ratio was 0.55.

5.2.4 Concrete Control Specimens.

With each mixing a set of concrete control specimens was cast. This set of control specimens consisted of:-

(a) Three 100 mm cubes.

(b) Three 500 mm x 100 mm x 100 mm prisms.

(c) One 300 mm x 150 mm Cylinder.

On certain occasions only one set of control specimens was cast, for it was possible to test two slabs on the same day. The control

specimens were tested according to B.S.1881. The concrete cubes yielded the compressive strength of the mix, the prisms the modulus of rupture, and the cylinder the Youngs Modulus. The loading of all specimens was applied by means of a 1200 KN Capacity Denison Compression testing machine.

Tables 5.3 and 5.4 show the serial number of tests, angle of orientation of steel, compression strength and modulus of rupture of the concrete mix, and the nominal degree of orthotropy of the slabs. The average Youngs modulus of the concrete was found to be 27.1 KN/mm^2.

5.2.5 Reinforcement.

Three types of steel were used, referenced A, B, and C. The original intention was to use only two types of steel, type A and C, but because of shortage of type A steel, type B had to be used. Tensile tests were performed on the steel supplied by G.K.N.; the tests showed that its characteristics were not the desired ones. To improve the properties of the steel, the steel had to be annealed. The heat treatment was carried out by the British Heat Treatment Company. After annealing, the steel exhibited the desired characteristics, that is fully elastic, fully plastic, with a definite yield point and no strain hardening. Twelve tensile tests were performed on random samples of each type of steel, and the average tensile strength and Young's modulus were obtained. The properties of all three types of steel are shown in table 5.5 and figure 5.1.

The 7 mm steel was used to provide the upper layer of reinforcement for the concrete slabs having a nominal degree of orthotropy of 0.25. By using smaller diameter bars a larger number of bars were used to provide the same degree of orthotropy.

5.3 Instrumentation.

5.3.1 Steel strains.

Apart from reading the collapse loads, it was required to study the steel and concrete behaviour during the whole loading cycle.

The steel strains were measured by means of electrical resistance strain gauges attached to the reinforcing steel within the central region of the slab measuring 150 mm square. Eight gauges in all were placed in this region, four on the upper reinforcement and four on the lower reinforcement. The gauges (type CG-121) were originally cemented onto the steel with Budd G.A.2 strain gauge cement, but this type of cement was subsequently found to be completely unsatisfactory. The setting time of this cement was over 24 hours, and a number of gauges failed even before casting the slab. Consequently, the Budd G.A.2 strain gauge cement was replaced by Eastmans glue made by Kodac, and this produced satisfactory results. The rate of failure of gauges was decreased and the setting time was less than 5 minutes. The cementing procedure to be described is that for Eastmans glue. Firstly, the metal was polished bright by means of emery paper and after degreasing the surface with Trichlorethylene, the metal surface was neutralized with ammonia solution of 0.1 normality. The gauges were also degreased and neutralized by dipping the gauges in the same solutions. After this they were placed upside down on a glass plate and pieces of cellotape, much larger than the gauges, were fixed on them. The metal surface and gauges were treated with an accelerator (catalyst) provided by Kodac with the Eastmans glue, and two minutes later a spot of glue was placed on the metal surface. The gauge and cellotape were placed on the glue and pressed gently to improve contact, and then

left for five minutes to set. Finally, the cellotape was gently removed while the gauge was left stuck on the metal surface.

The gauges were placed on the top side of the lower bars and the bottom side of the upper bars to ensure that the gauges were reading strains at the same level. Wire leads were soldered to the exposed tabs of gauges, the wires then being led across the top of reinforcement mesh to the side of the specimen. Eventually, the gauges were waterproofed using a synthetic rubber coating compound "Gagekote 2". Eventually, the colour code of each gauge was noted and numbered according to detailed drawings.

5.3.2 Concrete strains.

The investigation of concrete strains, and hence the direction of principal strains, is of great importance. These results were used to show whether or not the steel bars were subjected to axial and shear stresses. The concrete gauges were placed in a central region of the slab measuring 152 mm square. This region was completely free from any edge effects introduced by the jaws, since it was about 270 mm away from the jaws.

Twelve gauges making four forty-five degree rosettes were fixed on each corner of the square (see figure 5.2). It was hoped that at least one rosette would be in the vicinity of a crack. H. Tinsley and Co. Ltd. type 7A gauges of length 62 mm and width 2.5 mm were used on the concrete and were found to function very satisfactorily. Out of the 350 gauges used, only 2 gauges failed, and these were replaced before the experiment began.

The rosette positions were smoothed by means of emery paper and degreased with trichlorethylene solution. F88 dental cement manufactured by Tridox Products, Philadelphia, U.S.A. was used to fix the

gauges to the concrete surface. The steel and concrete strains were read on a Peekel strain recorder. This particular instrument converts resistance changes directly to microstrains, and requires only one dummy gauge to complete the bridge.

5.3.3 Mechanical dial gauges.

The radius of curvature of the concrete slab elements and also the direction of the principal radius of curvature were required in order to make a comparison of principal moment directions, principal strain directions, and principal curvature directions. Of course, all the three principal directions must be compared at the same point on the slab. To determine the curvature, it was necessary to know the deflection at three colinear points. Since it was uncertain where the slab would fail, sixteen deflection gauges were used, so that the principal curvatures and directions could be determined at four points. These four points corresponded to the four rosette positions. The maximum deflection reading of each gauge was 50 mm.

An adjustable frame was designed and built on which the deflection gauges were fixed. The frame had the shape of a hollow prism with the lower face fixed on the test machine base and the upper face could be adjusted at any level. Details of the frame are shown in Plate 5.1, and the position of all sixteen gauges in figure 5.3.

5.4 Description of specimens.

Twenty-eight reinforced slabs were constructed and tested; one of these slabs was a repeat. The slabs carry the reference mark TB, followed by the number of the test. All the slabs measured 914 mm x 914 mm. The thickness of each slab was measured by means of a micrometer gauge at twenty different points spread over the slab, and the

average taken. The average thickness of each slab was used to calculate the strength of the slab. Assuming the concrete strength was constant, the degree of orthotropy was controlled by the spacing of the reinforcing bars. For all slabs, the bottom reinforcement was supplied by 9.5 mm diameter steel bars having a concrete cover of 9.5 mm. For the slabs having a nominal degree of orthotropy of 1.0 and 0.5, the upper reinforcement was supplied by 9.5 mm diameter steel bars having a concrete cover of 19.0 mm. For the slabs having a nominal degree of orthotropy of 0.25, the upper reinforcement was supplied by 7.0 mm diameter steel bars having a concrete cover of 19.0 mm.

Figures 5.4, 5.5, 5.6, 5.7, 5.8, and 5.9 show details of the spacing and arrangement of the steel bars. Plates 5.2 and 5.3 show the completed steel reinforcement for two slabs in the moulds. The U reinforcement is also shown. The U bars were introduced at the support edges so as to eliminate the possibility of failure of the slabs at the jaws. The a-bars were orientated at an angle β to the X-axis and the b-bars at an angle $90-\beta$ to the X-axis.

Tables 5.3 and 5.4 show the mesh orientation to the X-axis for all twenty-eight slabs.

The construction of the mesh was aided by drawing a plan view of the bars on a plywood board, the bars were placed over this plan and the upper and lower layers of steel reinforcement wired together. To increase the bond of the bars and to diminish the possibility of bond failure, hooks were provided for all reinforcement. The depth of the concrete cover to the steel reinforcement was maintained by fixing mortar cubes 9.5 mm thick on the bottom reinforcement. The cast slabs and control specimens were stripped one day after casting and cured in a tank for twenty-four days.

5.5 Test Set Up.

5.5.1 Testing Rig.

The testing rig is quite complex to describe; however, an attempt will be made. Plate 5.1 will assist an understanding of the description.

The testing rig was constructed from I sections. Two I sections were fixed parallel to each other with a gap of 150 mm. These beams formed the base of the whole testing rig. Another two I beams were placed transversely to the length of the base I beams spaced at 1.575 m. from centre to centre of the flanges. All four beams, although of large cross section, were stiffened to create a solid testing rig. Overhead, another two large I beams were fixed, on columns, parallel to the base I beams. On the overhead I beams, the main hydraulic jack was suspended, which provided a downward thrust for load application. The upward thrust which exerted torsional moments on the slab specimens was supplied by two hydraulic jacks, fixed on short columns. The position of the columns could be varied at will. The testing rig was required to be designed in such a way that the following effects were eliminated:-

(a) Transverse shear forces.

(b) Membrane forces.

The first condition was achieved by applying two equal, symmetrically placed point loads. This arrangement created a zone between the point loads that was subjected to pure bending and torsional moments. The second condition was achieved by placing rollers on one of the two ball-bearing supports. These rollers were free to move horizontally, thus eliminating membrane forces.

The rig was also designed to enable the author to apply different combinations of bending and torsional moments. This was achieved by varying the position of the hydraulic jacks providing the upward thrust. Between the two I beams that were placed on the base beams a frame was built on which sixteen deflection gauges were placed. Plate 5.1 shows this arrangement.

The bending and torsional moments were transmitted to the concrete slab through two steel jaws of large stiffness. The steel jaws were an important feature of the testing rig. The jaw was constructed from stiffened plate 12 mm thick, which tapered from 920 mm wide at one end to a 100 mm radius arc at the other. A ball bearing recess was situated at the centre of this 100 mm radius circle. On top and along the 920 mm edge of the plate was welded a 100 mm x 100 mm x 6 mm channel which acted as a location and clamp for the edge of the slab element. The bottom, open edge of the channel was welded flush with the edge of the 12 mm plate and six holes were tapped in the upper leg of the channel at 150 mm centres. The channel-plate system was stiffened by welding 150 mm thick plates onto the channel and across the plate so that the stiffening plates were 200 mm deep at the front edge of the channel, tapering to 6 mm at the other edge. The jaws and slab formed a complete unit, which can be seen in Plate 5.1 and figure 5.10. The whole unit was supported on ball bearings at two points 1.575 m apart measured along the X-axis. The ball bearings at the support points fitted between recesses in the underside of the jaws, and on steel plates measuring 100 mm x 100 mm x 25 mm. One of these plates was resting on the transverse I beam while the other was resting on rollers made of hardened steel bars. The rollers were provided to allow the whole unit to move horizontally so as to eliminate

the membrane forces.

The bending and torsional moments on the slab element were transmitted through the jaws. Each jaw was loaded at two points. A 200 KN hydraulic jack loaded the centre of the channel through a spreader as shown in figure 5.10. This loading arrangement provided the bending moment along the X-axis of the slab. The torsional moment was supplied by two 50 KN hydraulic jacks which provided an upward thrust at two assymmetrical points, as shown in Plate 5.1 and figure 5.10. The hydraulic jacks were calibrated to ensure that the loading ratio of the large hydraulic jack to the smaller hydraulic jack was four. All three hydraulic jacks were connected to the same pump to ensure a constant load ratio between all three jacks. The maintenance of the above ratio is important because, as will be shown later, the direction of the principal external moments is function of the position of the loads only, provided that the magnitude of the loads remains at a fixed ratio.

5.5.2 Description of a typical test.

After the slab was removed from the curing tank, the position of the sixteen deflection gauges was marked with a felt pen. Then the slab was placed on a fork lift truck and the concrete strain rosettes were fixed, as described in the instrumentation procedure, item 5.3.2. The jaws were cleaned free from any pieces of concrete or any other obstacles with a vacuum cleaner, and afterwards were placed on four pieces of timber, two for each jaw, of the same thickness. The slab was brought forward between the two jaws, then the jaws were slid forward so that the two parallel edges of the slab containing the U reinforcement were inside the channel (see figure 5.10). The slab was

lowered on the channel of both jaws and the forks of the truck were removed. The two steel jaws were clamped together by means of two steel clamps so that the vertical side of the channel was in contact with the edges of the concrete slab. A wedging steel lamina was forced between the channel and the upper concrete face, and the hardened Allen screws were tightened slightly, and then tightened hard starting from the central screws moving outwards in both directions. The slab and jaws were lifted on the testing rig, the steel jaws were allowed to rest on the ball bearing supports and two pieces of timber running between the two transverse I beams and parallel to the base I beams. A Wild T6 theodolite was brought forward and the axis of the large hydraulic jack and supporting bearings were aligned in the same plane, the slab was levelled and the bearings and jack aligned again. The smaller, lower jacks were placed in position as dictated by the recesses on the plate of the jaws. A slight pressure was applied through all three hydraulic jacks, and the timber supports were removed. The oil valve was released to secure zero load and zero readings were taken on all gauges.

First 1 KN force was applied on the proving ring, and a reading was taken on all gauges. The rate of loading on the proving ring from then onwards was in increments of about 4 KN, and all gauges were read at each load increment. When the concrete slab was near collapse, and the gauge readings were becoming larger, the rate of loading was decreased.

When the maximum load was reached, another five sets of readings were taken. The readings were taken as fast as possible to decrease the effect of creep on the gauges. The testing time varied between $1\frac{1}{2}$ hours and $2\frac{1}{2}$ hours according to the strength of the slab.

After the testing procedure was completed, the slab was lowered down from the testing rig, the jaws were carefully removed, the direction of the major cracks relative to the X-axis were measured and recorded. For the sake of accuracy, the cracks were measured as follows. A large piece of perspex measuring 914 mm x 914 mm x 4 mm was placed over the lower face of the slab containing the tensile cracks with the free sides of the slab parallel to the sides of the perspex. The cracks were traced with a fine felt pen, and a best line was fitted through each crack and the direction of each line was measured by means of a protractor large enough to read to a tenth of a degree. Eventually, the average angle was obtained.

The slab was placed on its side, photographed and examined for any crushing of concrete along the cracks and adjacent to the steel bars. Eventually, the slab was placed flat on the floor, and by means of a sharp chisel, the cracks were chipped off to reveal the steel crossing the crack. The bars were examined very carefully to see if any "kinking" had taken place, and the number of bars crossing the cracks were recorded.

Finally, the slab was stored for any future use.

All twenty-eight tests followed the above procedure. Plates 5.4 to 5.15 show typical patterns of yield lines.

Sieve Analysis of Sand and Aggregate

Sieve Analysis of Zone III Sand

Sieve size or number		%
Retained	$\frac{3}{16}$ in	4.61
	7	7.39
	14	6.08
	25	8.92
	52	44.8
	100	22.8
Passing	100	5.75

Table 5.1

Sieve Analysis of $\frac{3}{8}$ Crushed Gravel

Sieve Size	%
Retained $\frac{3}{8}$ in.	2.24
$\frac{3}{16}$ in.	81.89
Passing $\frac{3}{16}$ in.	15.92

Table 5.2

Series number	Orthotropy μ (nominal)	Angle β	Compressive strength U MN/m^2	Modulus of rupture fu MN/m^2
TB1	1.0	0	39.2	3.59
TB2	1.0	60	43.2	3.74
TB3	1.0	45	43.2	3.74
TB4	1.0	30	38.3	3.76
TB16	0.50	90	37.9	4.22
TB17	0.50	60	32.7	3.89
TB18	0.50	45	35.4	3.55
TB19	0.50	30	32.7	3.89
TB20	0.50	0	37.9	4.22
TB31	0.25	90	38.3	3.76
TB32	0.25	60	37.7	3.87
TB33	0.25	45	38.8	3.73
TB34	0.25	30	38.8	3.73
TB35	0.25	0	37.7	3.87

Table 5.3 Ta = 0.445 m la = 0.381 m (R.C. slabs)

Series number	orthotropy μ (nominal)	angle β	compressive strength f_u MN/m^2	modulus of rupture f_u MN/m^2
TB6	1.0	90	35.5	3.54
TB7	1.0	60	33.7	3.13
TB8	1.0	45	43.8	4.12
TB21A	0.5	90	44.8	3.76
TB21	0.5	90	36.4	4.15
TB22	0.5	60	25.6	3.38
TB23	0.5	45	38,8	3.16
TB24	0.5	30	36.9	3.20
TB25	0.5	0	33.5	3.08
TB36	0.25	90	35.5	3.68
TB37	0.25	60	42.9	3.41
TB38	0.25	45	44.9	3.92
TB39	0.25	30	40.5	4.36
TB40	0.25	0	52.6	4.51

Ta = 0.286 m la = 0.381 m (R.C. Slabs)

Table 5.4

Tensile Tests on Heat Treated Steel

Type of Steel	Diameter mm	Yield Strain microstrain	Yield Stress N/mm^2	Youngs Modulus kN/mm^2
A	9.5	1310	285	217
B	9.5	1610	338	211
C	7.0	1260	278	220

Table 5.5

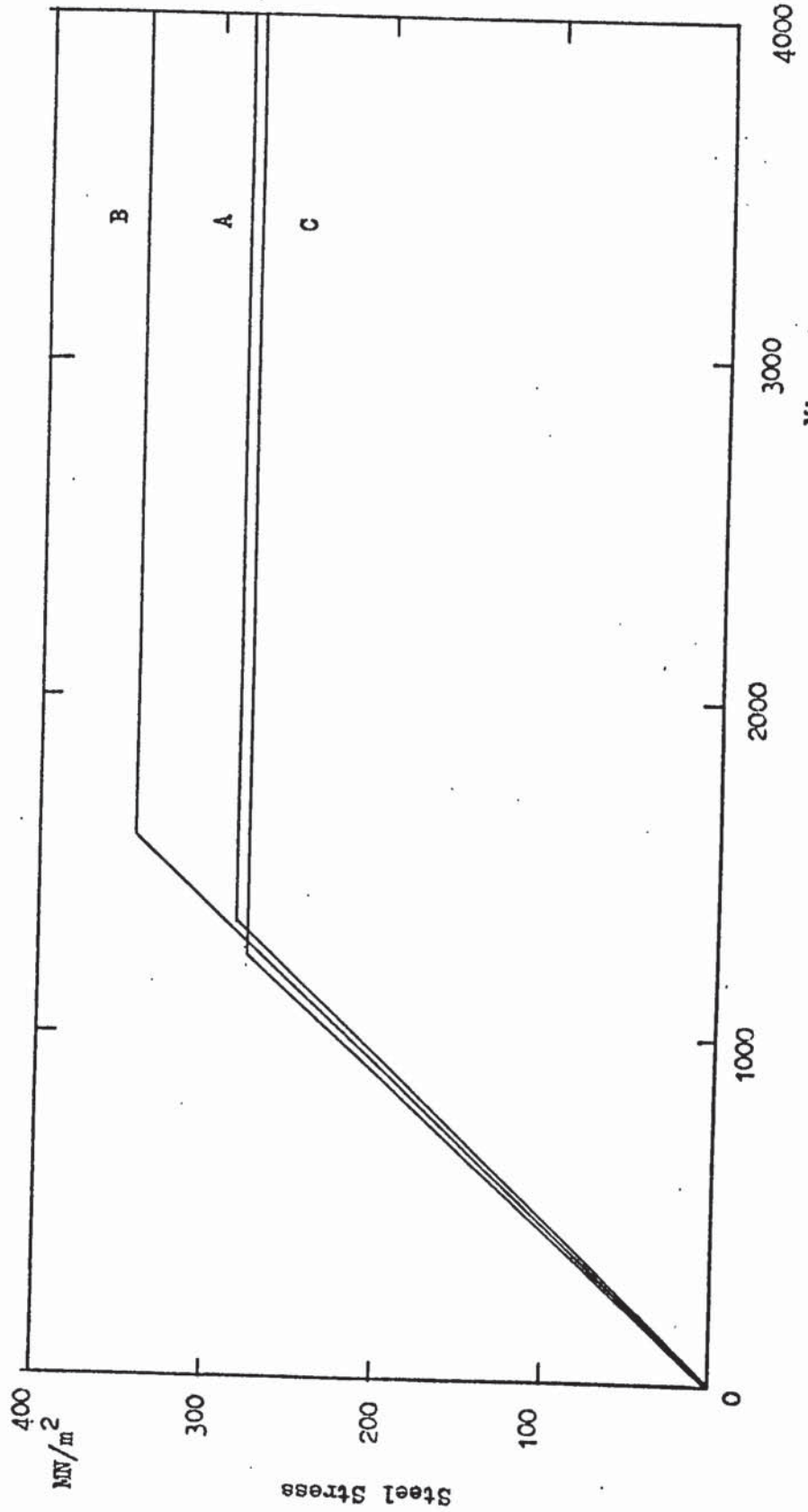

Figure 5.1 Steel Properties

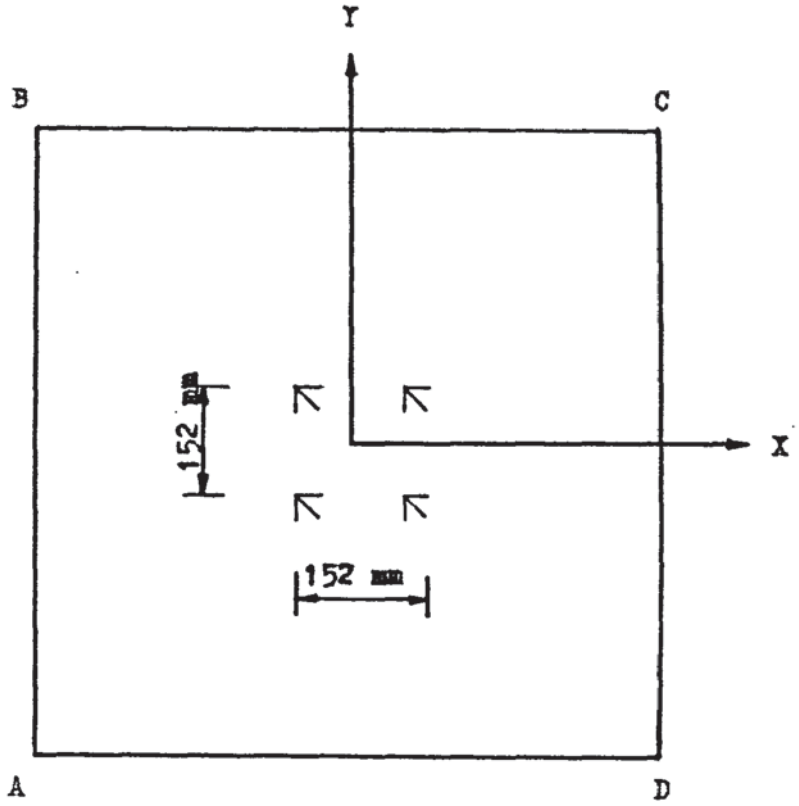

CONCRETE ROSETTE POSITIONS
(TOP SURFACE)

Figure 5.2

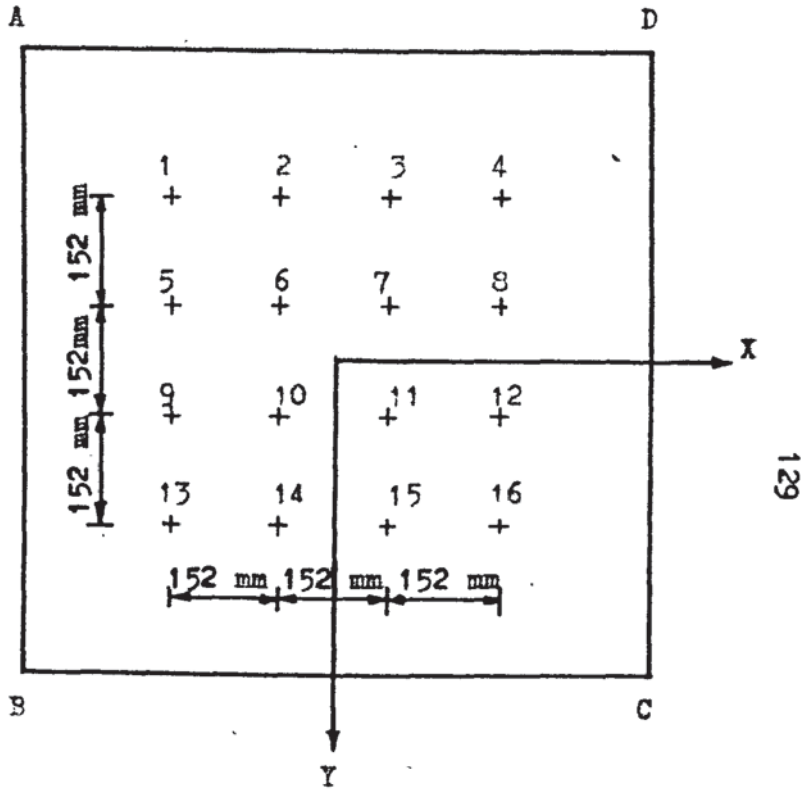

DEFLECTION POINTS PATTY GAUGES
(LOWER SURFACE)

Figure 5.3

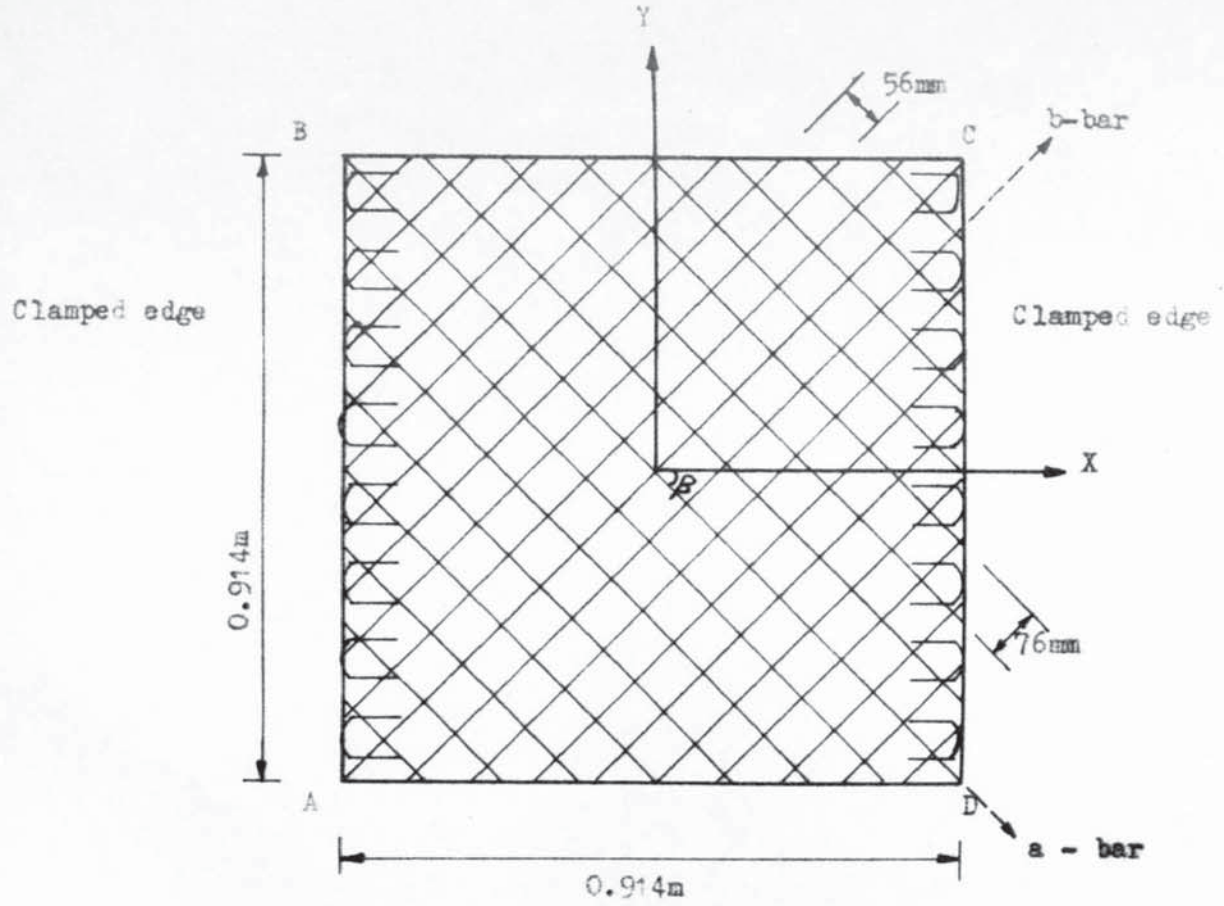

A Type Steel μ =1.0

Figure 5.4

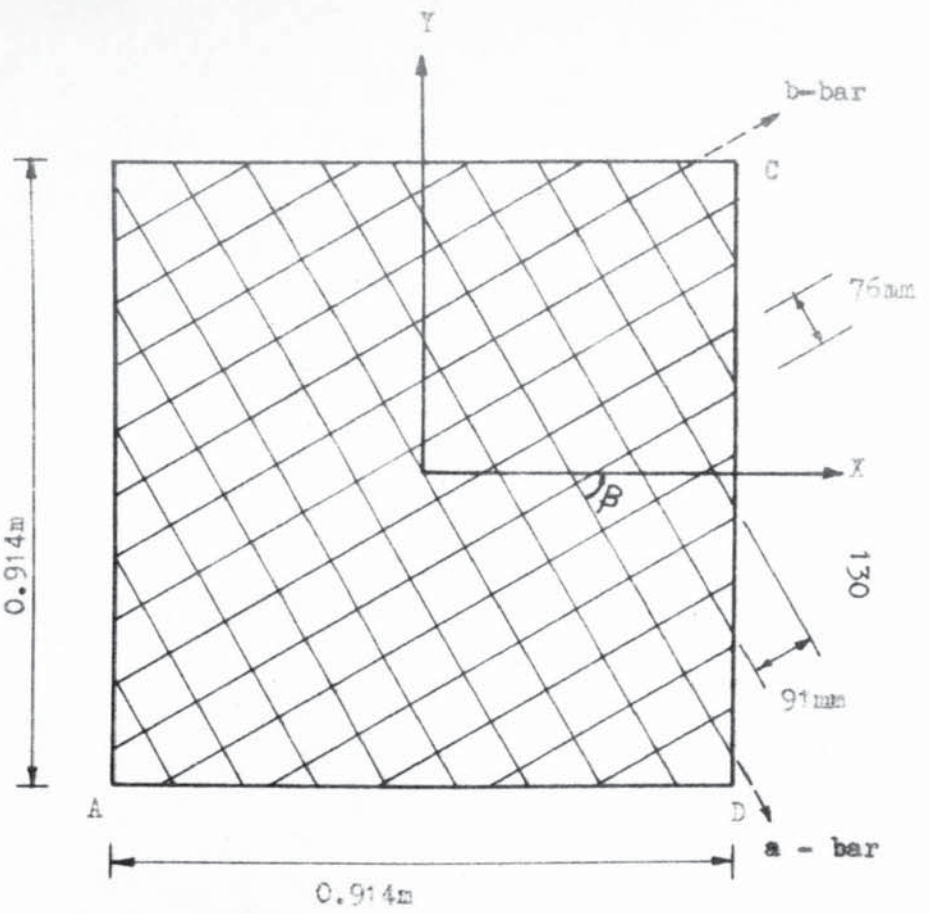

B Type Steel μ =1.0
(U reinforcement not shown)

Figure 5.5

TYPICAL MESH REINFORCEMENT

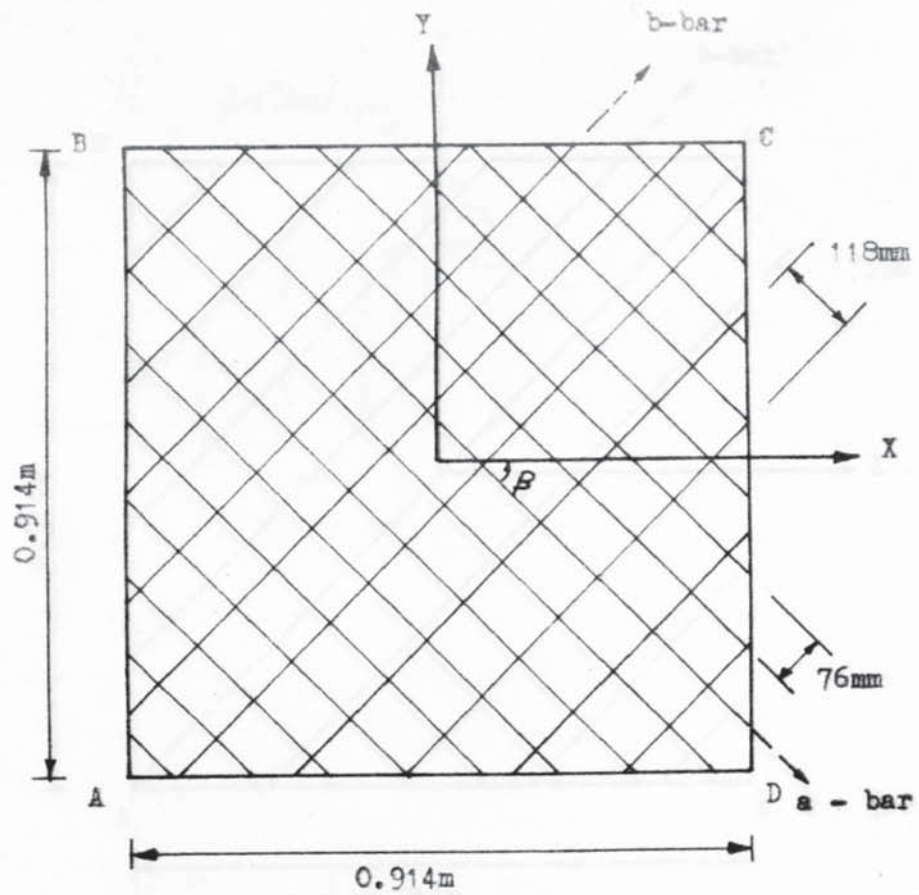

a-bars, b-bars, A Type Steel
μ =0.5

Figure 5.6

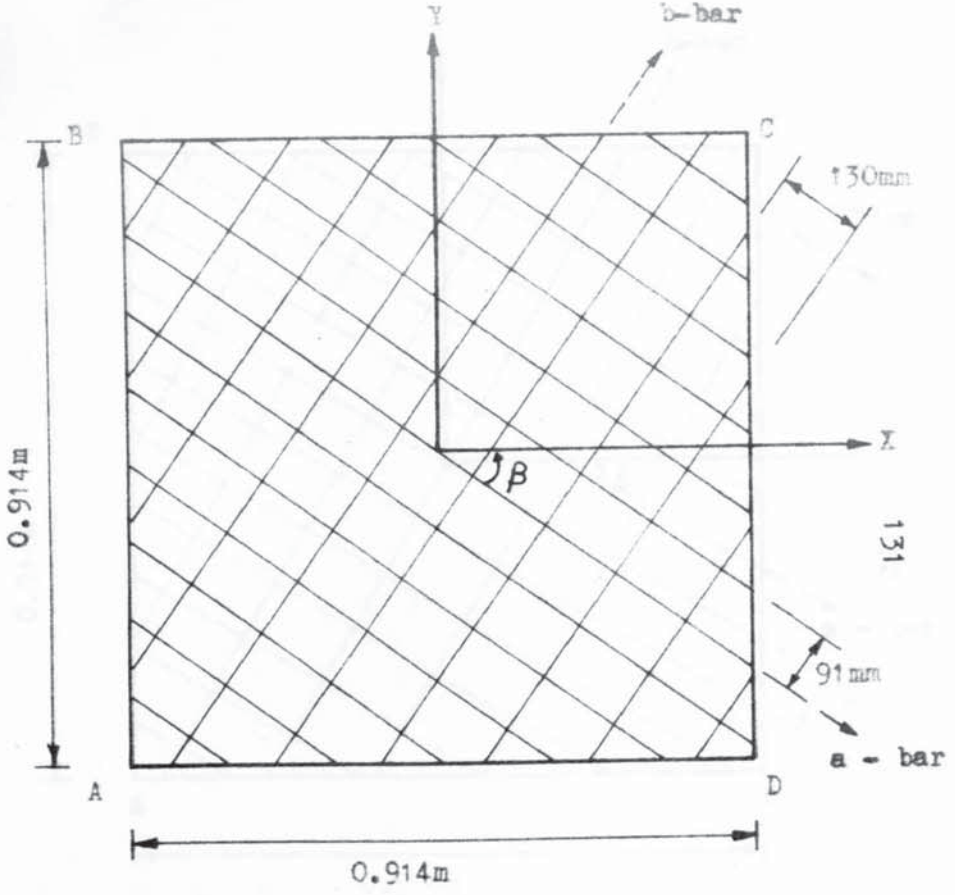

a-bars, b-bars, B Type Steel
μ =0.5

(U Reinforcement not shown)

Figure 5.7

TYPICAL MESH REINFORCEMENT

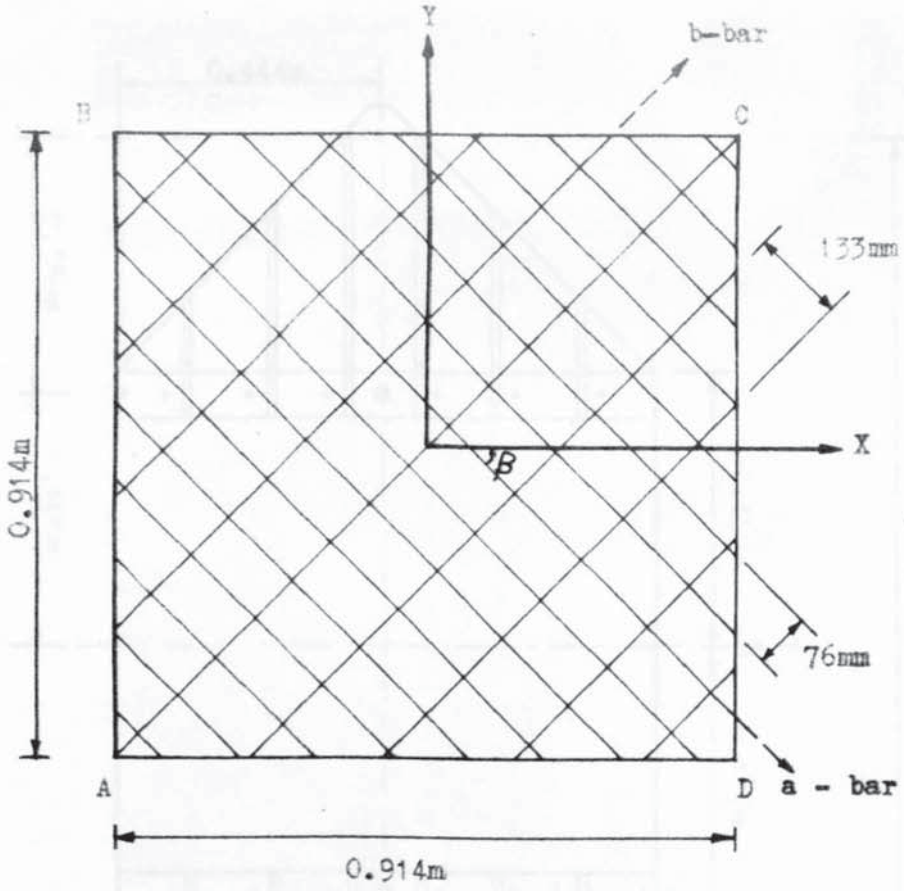

(U Reinforcement not shown)

a-bars A Type Steel
b-bars C Type Steel
μ =0.25

Figure 5.8

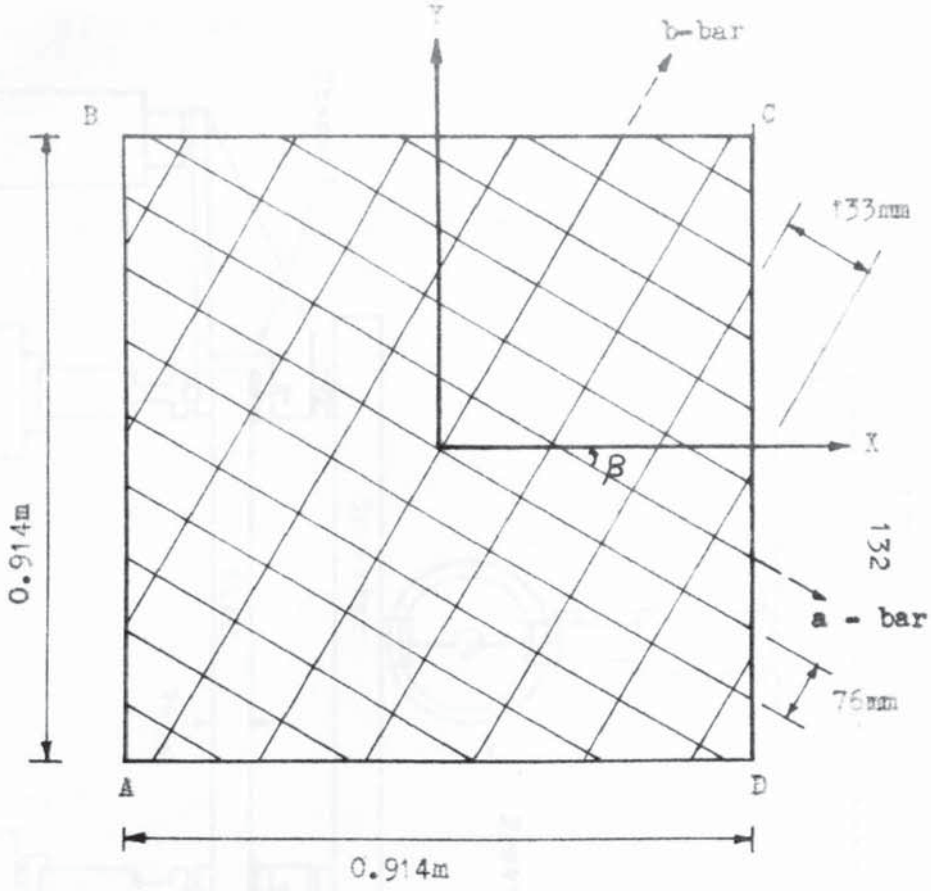

a-bars A Type Steel
b-bars C Type Steel
μ =0.25

Figure 5.9

TYPICAL MESH REINFORCEMENT

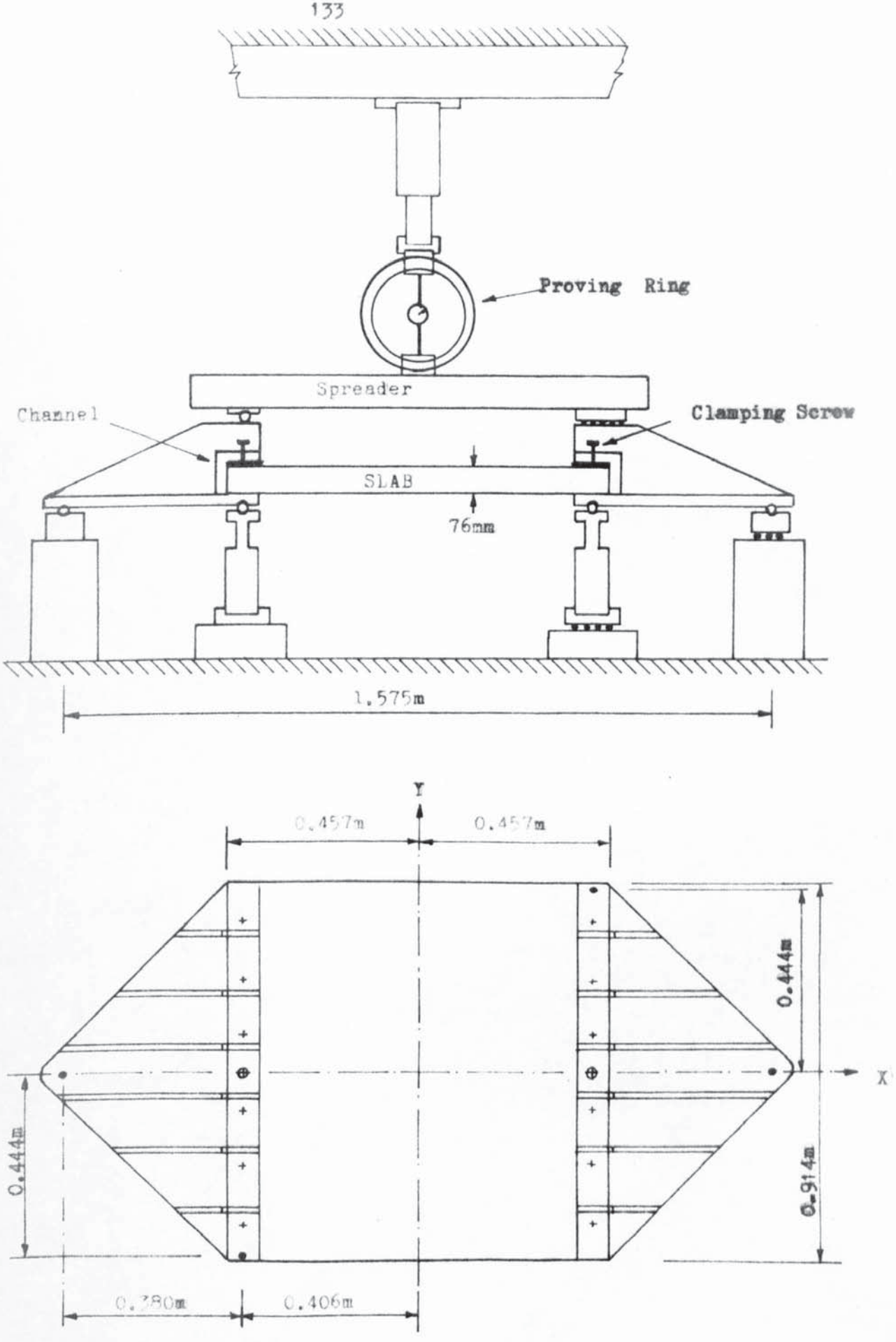

Figure 5.10 Test set up.

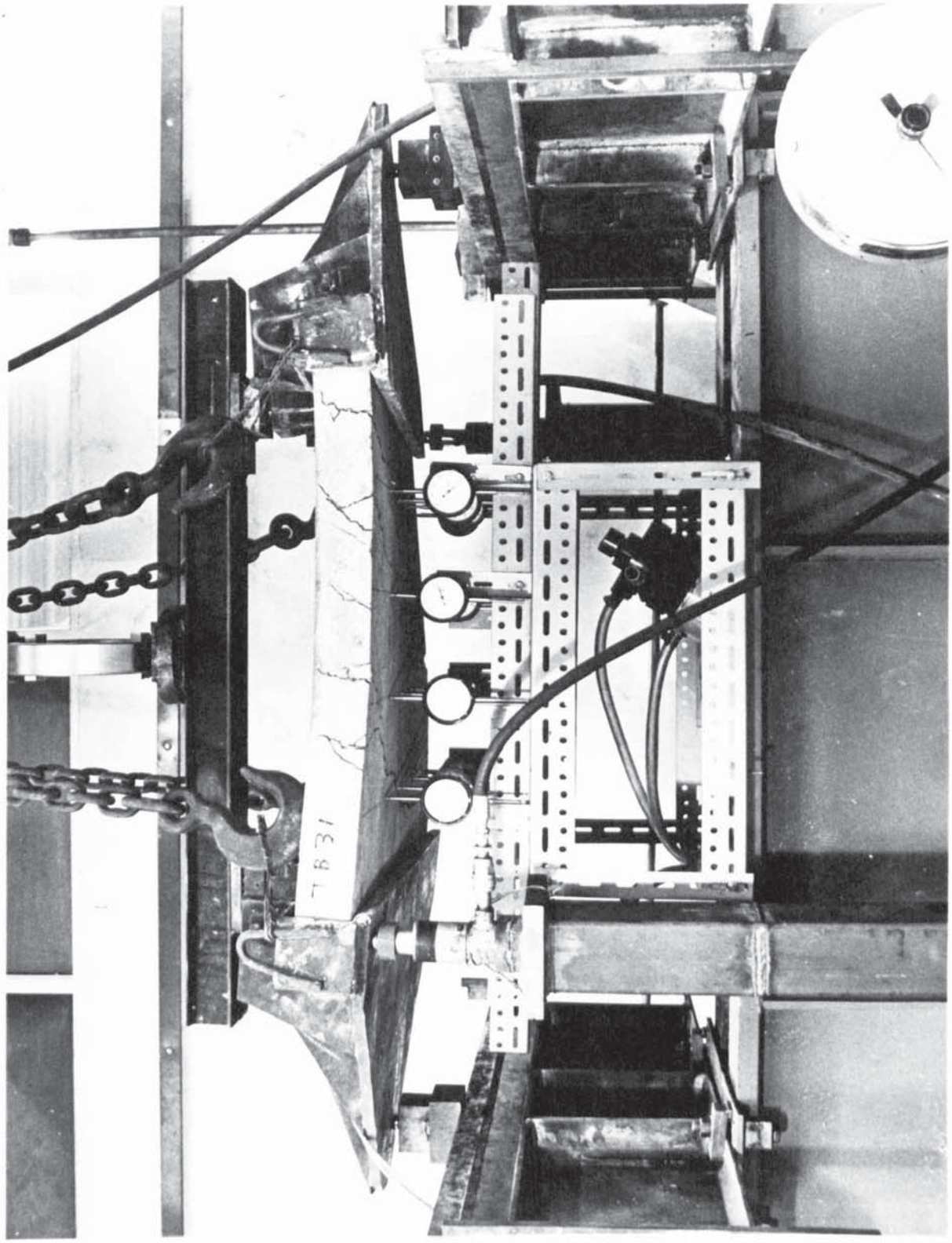

PLATE 5.1 TEST SET UP

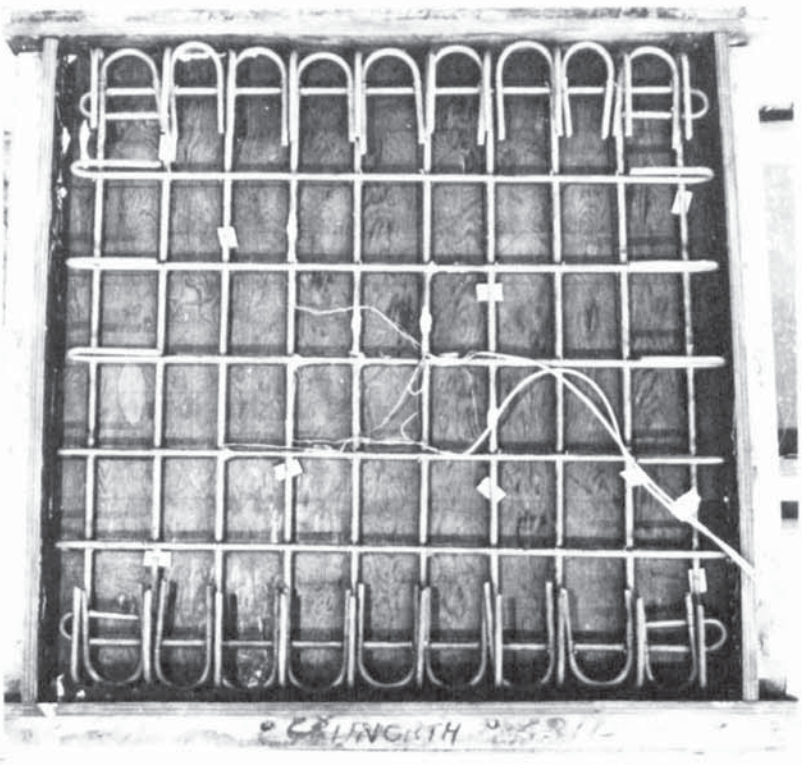

PLATE 5.2 STEEL REINFORCEMENT

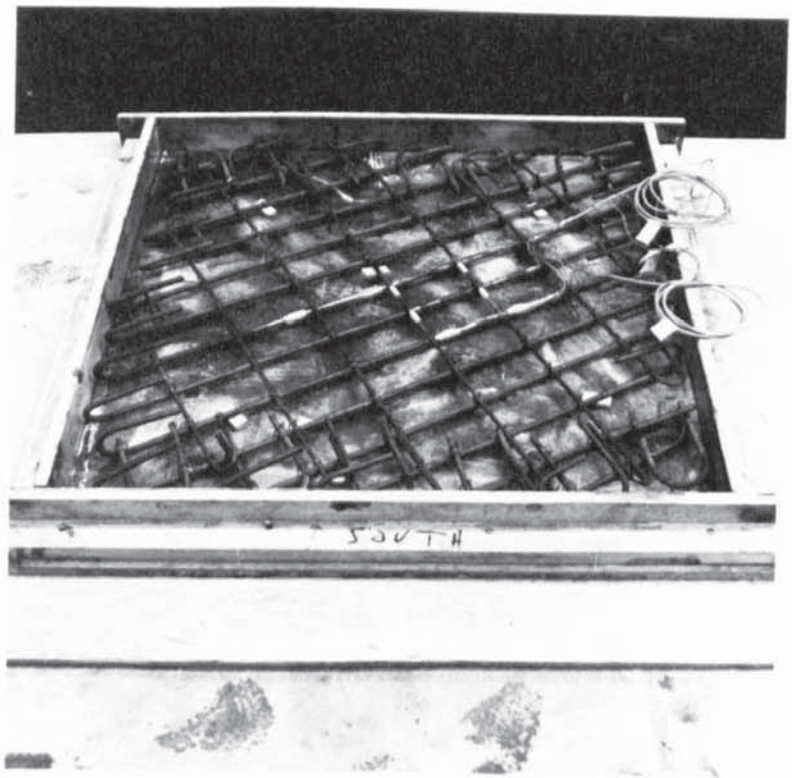

PLATE 5.3 STEEL REINFORCEMENT

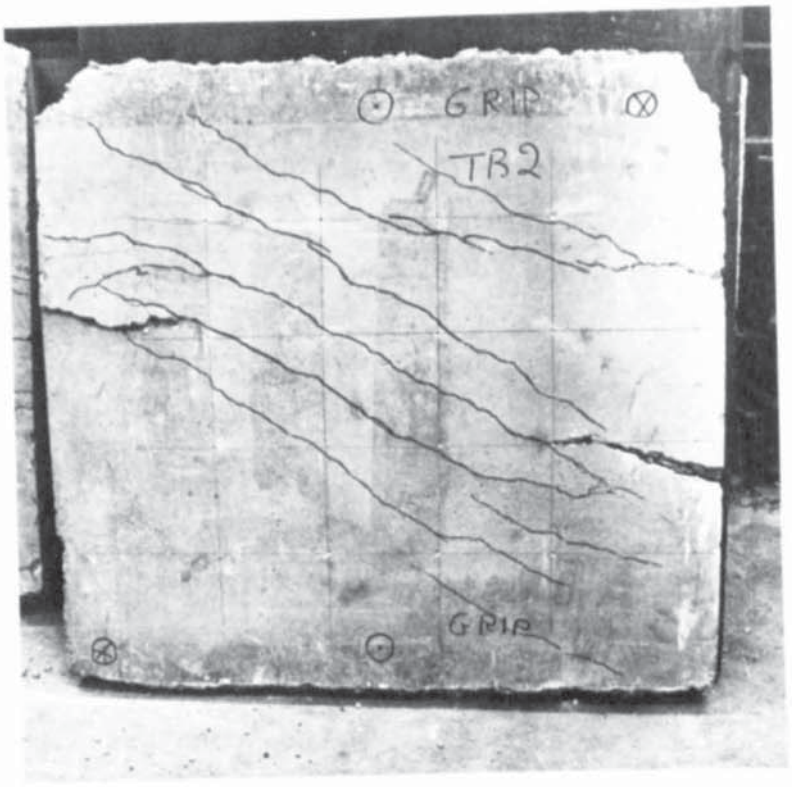

PLATE 5.4 SPECIMEN TB 2

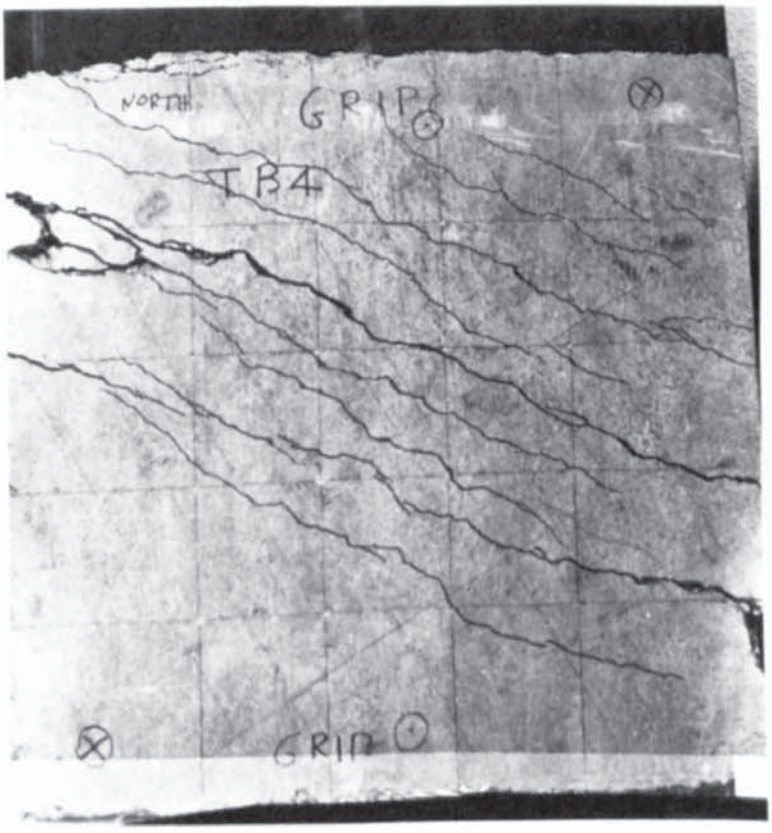

PLATE 5.5 SPECIMEN TB 4

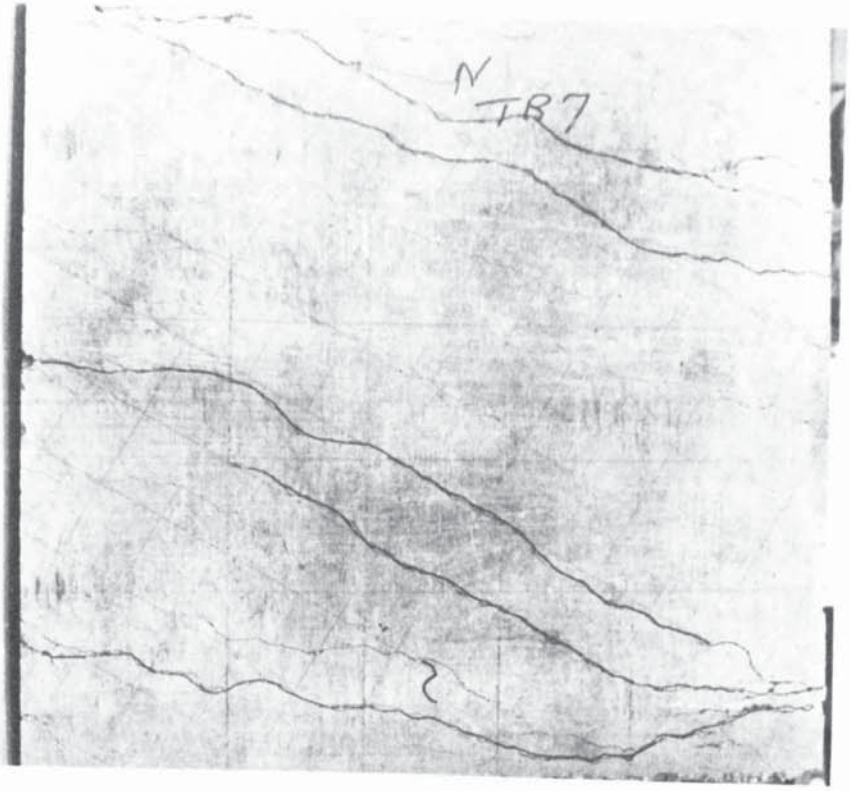

PLATE 5.6 SPECIMEN TB 7

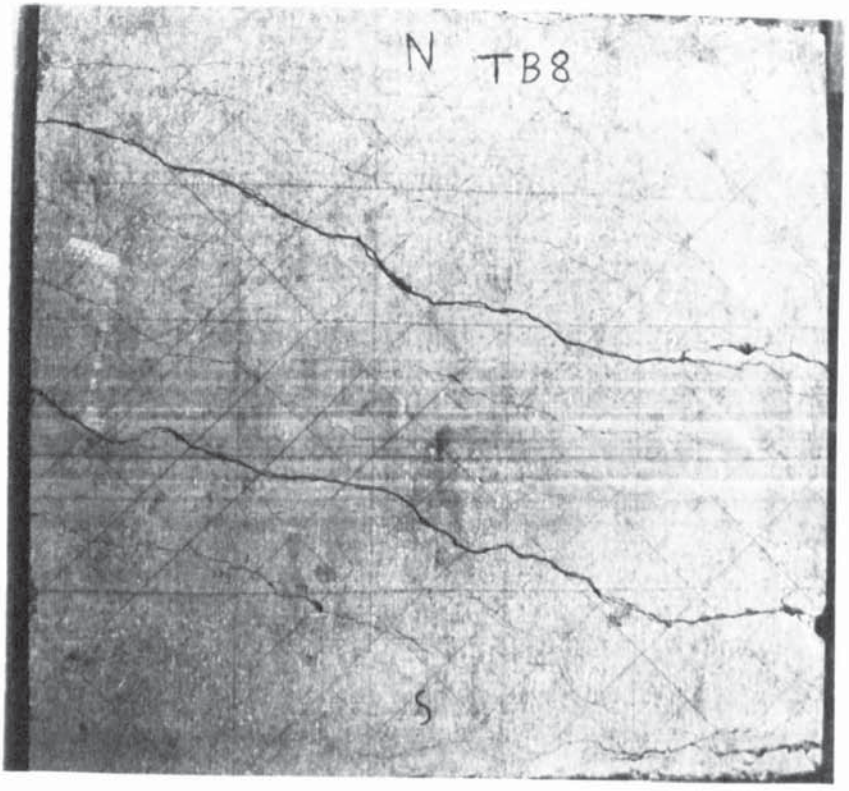

PLATE 5.7 SPECIMEN TB 8

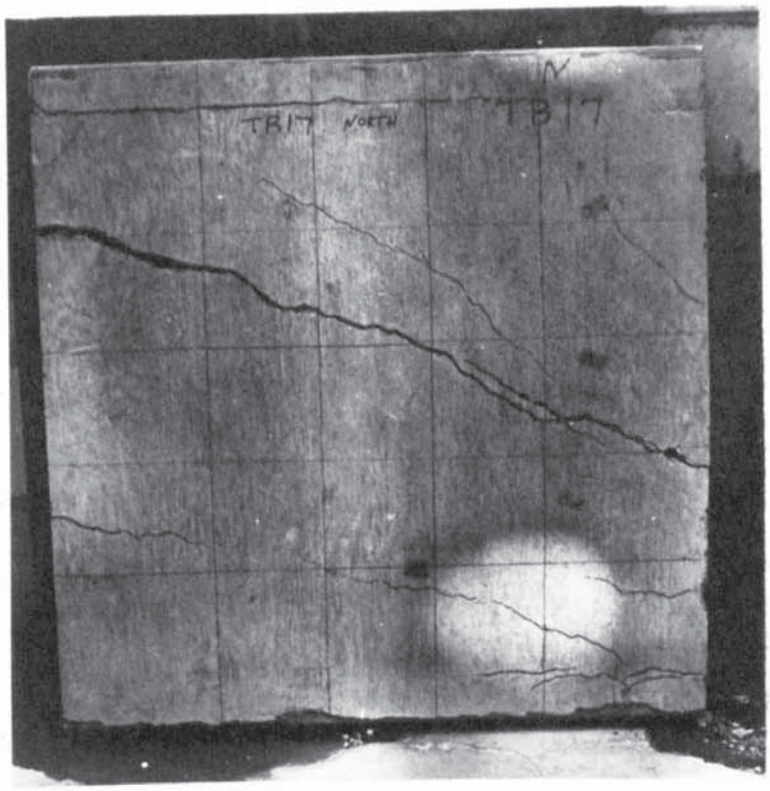

PLATE 5.8 SPECIMEN TB 17

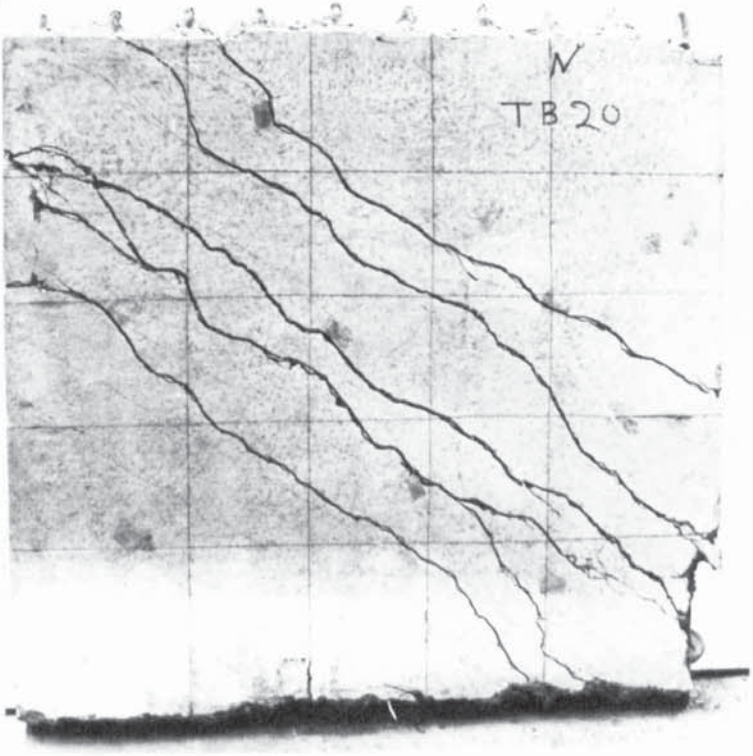

PLATE 5.9 SPECIMEN TB 20

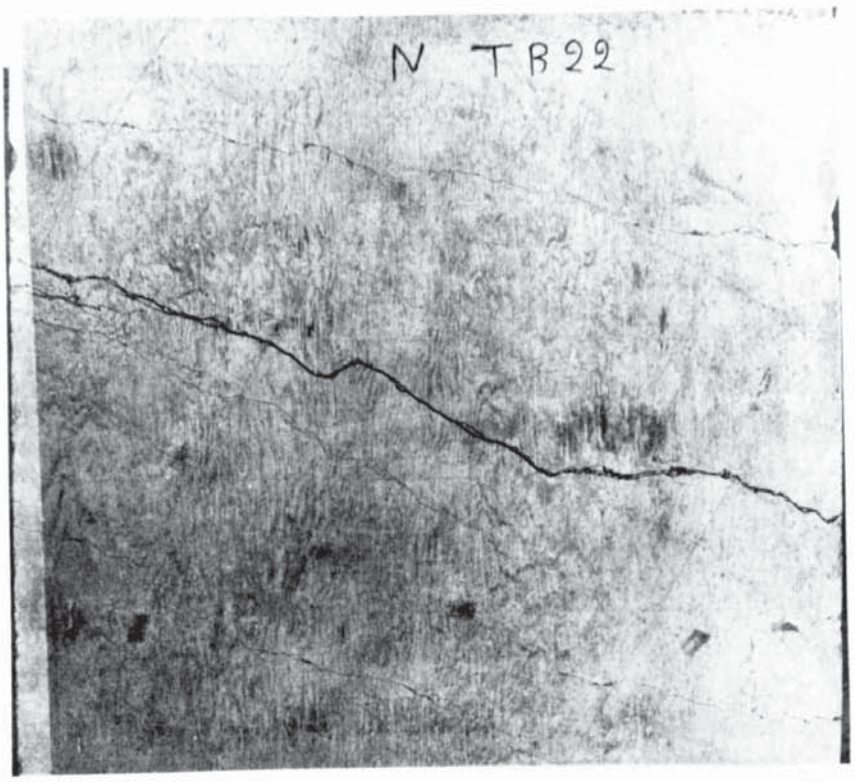

PLATE 5.10 SPECIMEN TB 22

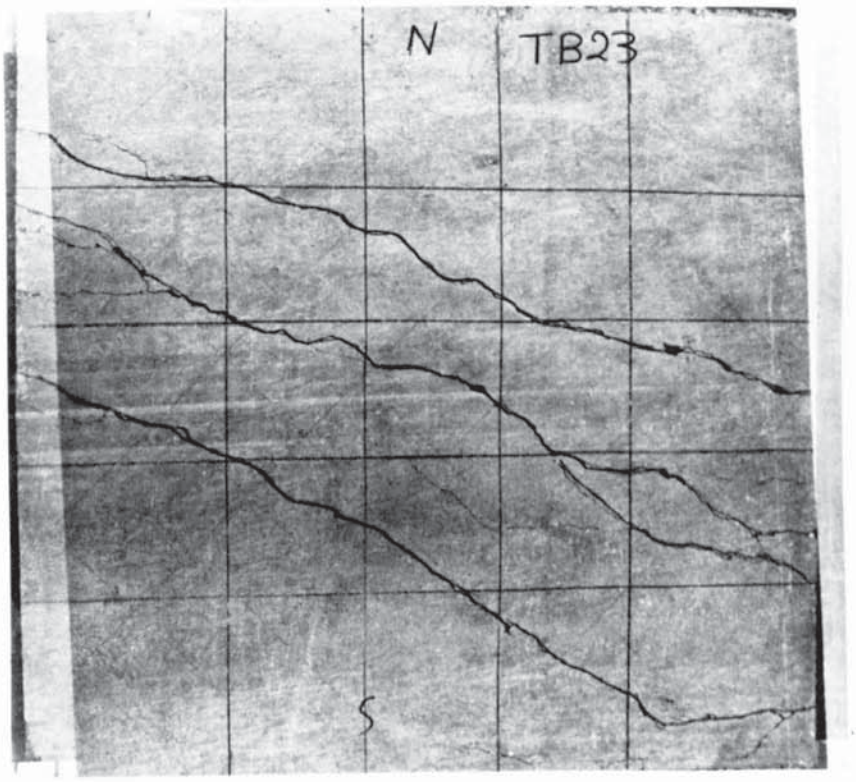

PLATE 5.11 SPECIMEN TB 23

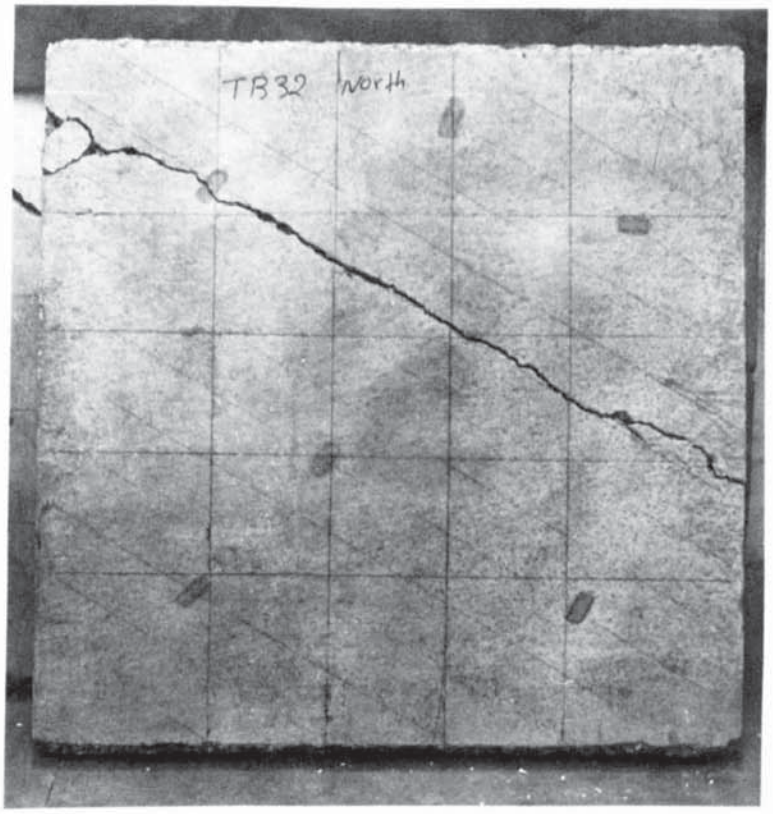

PLATE 5.12 SPECIMEN TB 32

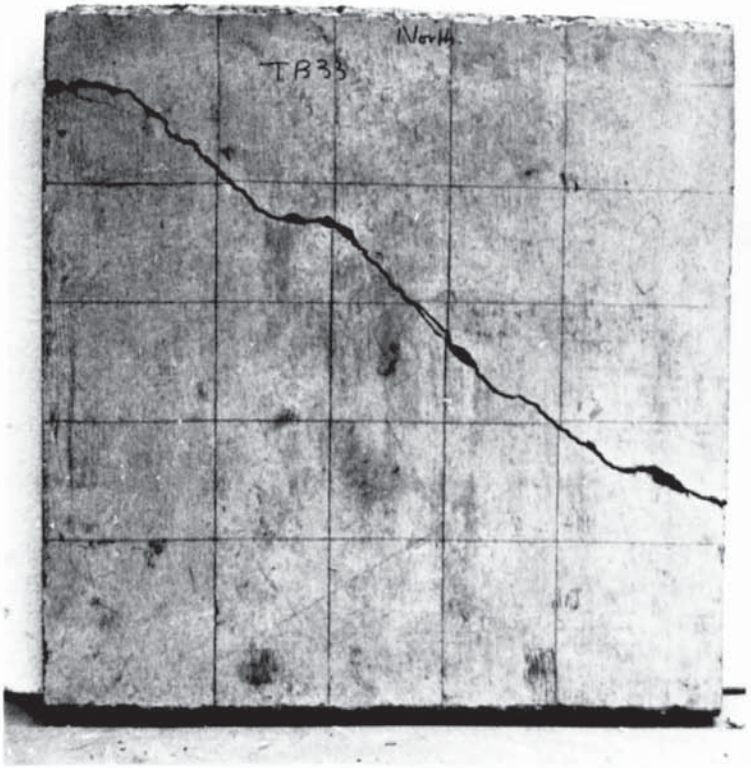

PLATE 5.13 SPECIMEN TB 33

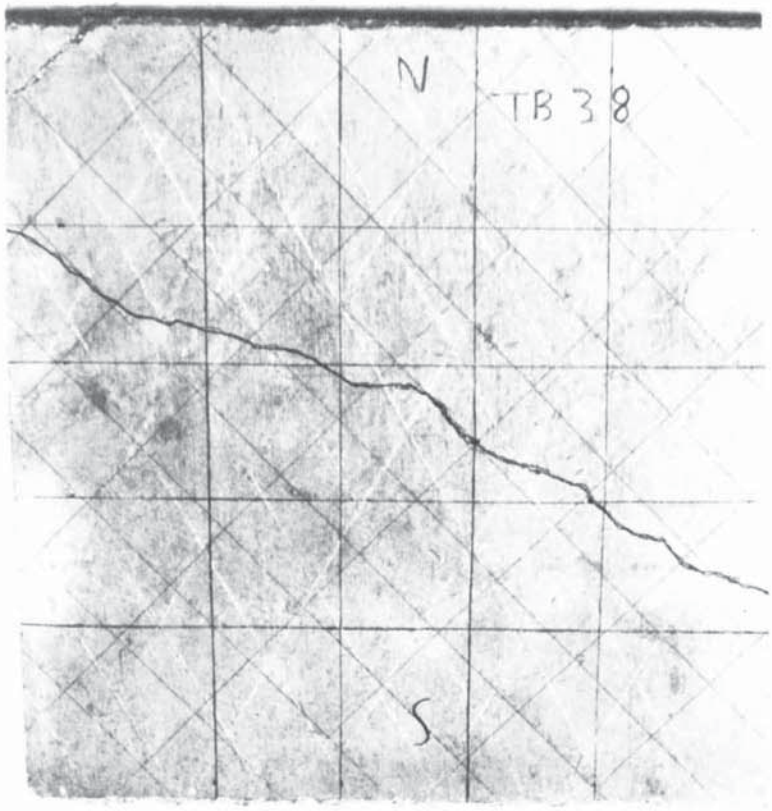

PLATE 5.14 SPECIMEN TB 38

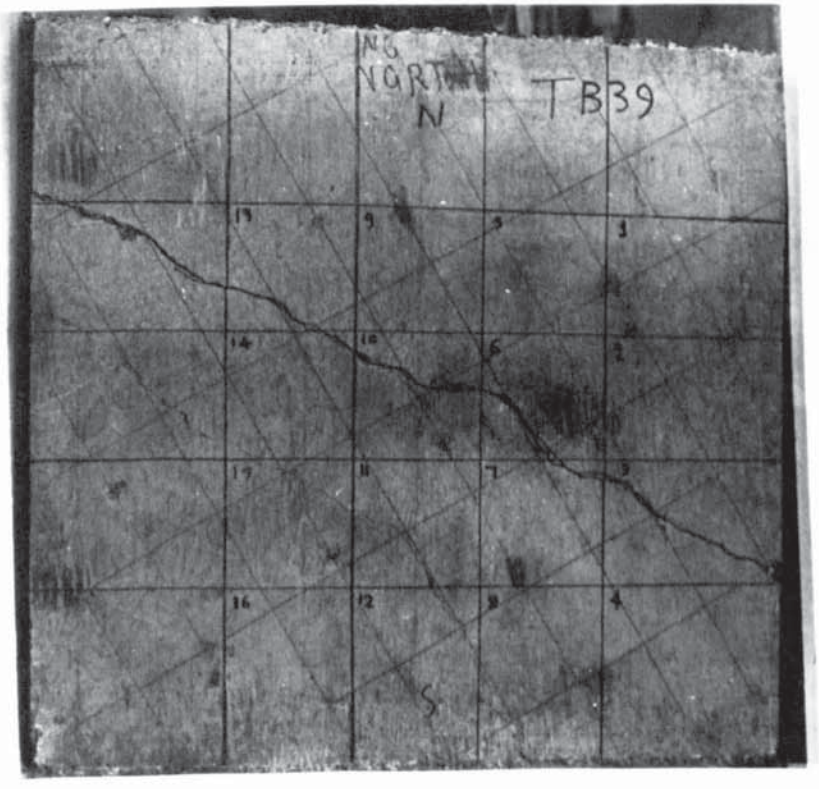

PLATE 5.15 SPECIMEN TB 39

CHAPTER 6

COMPARATIVE ANALYSIS OF RESULTS FROM THE COMBINED BENDING AND TORSION SERIES

6.1 Introduction.

It was the intention, when the above tests were designed, to determine the yield load and hence the yield moments per unit length of the crack for various angles of inclination of the reinforcement relative to the normal of the crack, and compare these values with those predicted by the new and old criterions. The experimental quantities measured gave the total normal and twisting moments on the yield line. Since the slabs are not homogeneous but are reinforced along discrete lines forming a step-wise non-homogeneous structure, the cracks tend to develop behind the bars at the edges of the slabs. Thus, the bars near the edges (which do not pass through the crack) do not contribute to the strength of the slab. Hence it is illogical to divide the total moments by the physical crack length to obtain moments per unit length. An effective crack length is required which takes account of these irregularities. Such an effective crack length concept has been developed by Kwiecinski [4,5] and Downham [3], but both these concepts are based on theoretical normal moment formulae. It was felt necessary to develop a new concept based on experimental values and hence independent of any theoretical criterion.

In this chapter, the variation of maximum principal curvature and maximum principal concrete strains in relation to moments and loads are also presented.

6.2 Effective crack length derived by Downham.

The effective crack length developed by Downham [3] is based on the Johansen [2] criterion. According to Johansen

$$m_{nj} = m_a \cos^2\alpha + m_b \sin^2\alpha \qquad .. \quad .. \quad 6.1$$

Let the crack length = l

then $$lm_{nj} = lm_a \cos^2\alpha + lm_b \sin^2\alpha \qquad .. \quad .. \quad 6.2$$

If the theoretical number of bars in the a-direction is n_a and the spacing is s_a, then

$$n_a s_a = l\cos\alpha \qquad .. \quad .. \quad 6.3a$$

Similarly, if the theoretical number of bars in the b-direction is n_b and the spacing is s_b, then

$$n_b s_b = l\sin\alpha \qquad .. \quad .. \quad 6.3b$$

Substituting equations 6.3a and 6.3b in equation 6.2

$$lm_{nj} = m_a(n_a s_a \cos\alpha + \mu n_b s_b \sin\alpha) \qquad .. \quad .. \quad 6.4$$

where $\mu = \frac{m_b}{m_a}$

but $$m_{nj} = m_a(\cos^2\alpha + \mu\sin^2\alpha) \qquad .. \quad .. \quad 6.5$$

Substituting equation 6.5 in equation 6.4

$$l = \frac{(n_a s_a \cos\alpha + \mu n_b s_b \sin\alpha)}{(\cos^2\alpha + \mu\sin^2\alpha)}$$

If the values of n_a, n_b and α are obtained from experiment

$$l = l_e = \frac{(n_a s_a)_{exp.}\cos\alpha + \mu(n_b s_b)_{exp.}\sin\alpha}{(\cos^2\alpha + \mu\sin^2\alpha)} \qquad .. \quad .. \quad 6.6$$

As already mentioned earlier in section 2.11, a number of similar effective lengths could be derived using similar arguments. An effective length is required that is independent of any theoretical criterion.

6.3 Effective crack length derived by the author.

The main use of the effective crack length is as a divisor for

the total moments at yield to obtain moments per unit length. Referring to figure 6.1 which shows a real crack, AB, of slab ABDE, the total moments of resistance perpendicular to lines BC and CA due to a-bars and b-bars is M^1_a and M^1_b respectively. The values of M^1_a or M^1_b may be obtained by means of the Formula

$$M^1_{a,b} = fyA_{st}(1 - \frac{KfyA_{st}}{bd_1U})d_1 \qquad .. \quad .. \quad 6.7$$

where A_{st} is the area of a-bars or b-bars crossing the yield line and b is equal to BC or CA. ($K = 0.475$).

Case (i) Only a-bars cross the yield line

The ratio $\frac{M^1_a}{m_a}$ is the effective length along the line BC, (see figure 6.2a).

Then $\frac{M^1_a}{m_a} = BC.\frac{m^1_a}{m_a}$

where m^1_a is the moment per unit length along BC due to the actual amount of steel crossing the yield line and m_a is the design moment per unit length along BC. The effective length along the yield line BA is then

$$l^1_a = BC\,\frac{m^1_a}{m_a} \cdot \frac{1}{\cos\alpha} = BA\,\frac{m^1_a}{m_a}$$

where BA is the physical crack length.

Let $BA = C$

The effective crack length is then

$$l^1_a = C.\frac{m^1_a}{m_a} \qquad .. \quad .. \quad 6.8$$

Let the external normal moment at yield be equal to M_{na}, and this strength is due only to the a-bars, then the external normal moment per unit length

$$m_{na} = \frac{M_{na}}{C.\frac{m^1_a}{m_a}} \qquad .. \quad .. \quad 6.9$$

All the quantities in the right hand side of equation 6.9 are experimental quantities.

Case (ii) Only b-bars cross the yield line.

The ratio $\frac{M^1_b}{m_b}$ is the effective length along the line CA (see figure 6.2b).

Then $\frac{M^1_b}{m_b} = CA\ \frac{m^1_b}{m_b}$

where m^1_b is the moment per unit length along CA due to the actual amount of steel crossing the yield line, and m_b is the design moment per unit length along CA.

The effective length along the yield line BA is then

$$l^1_b = CA.\frac{m^1_b}{m_b}\ \frac{1}{\sin\alpha}$$

$$l^1_b = BA\ \frac{m^1_b}{m_b} = C.\ \frac{m^1_b}{m_b} \qquad .. \quad .. \quad 6.10$$

If the external normal moment at yield is equal to M_{nb} and this strength is due only to the b-bars, then the external normal moment at yield per unit length

$$m_{nb} = \frac{M_{nb}}{C.\frac{m^1_b}{m_b}} \qquad .. \quad .. \quad 6.11$$

All the quantities on the right hand side of equation 6.11 are experimental.

Case (iii) Both a-bars and b-bars cross the yield line.

Cases (i) and (ii) deal with the effective lengths of cracks when a-bars or b-bars are crossing the yield line. In many cases, however, both a-bars and b-bars cross the yield line simultaneously. Therefore an effective length is required to accommodate for this case.

If equations 6.9 and 6.11 are added together:

$$m_n = m_{na} + m_{nb} = \frac{M_{na}}{C.\frac{m^1_a}{m_a}} + \frac{M_{nb}}{C.\frac{m^1_b}{m_b}} \qquad .. \quad .. \quad 6.12$$

The equation 6.12 is correct and valid, but it is impossible to differentiate M_{na} and M_{nb} when a-bars and b-bars are present. $(M_{na} + M_{nb})$ is measured experimentally.

A slight approximation is required and this approximation will be justified later. Let $M_n = M_{na} + M_{nb}$. For a large number of bars crossing the yield line, the ratios $\frac{m^1_a}{m_a}$ and $\frac{m^1_b}{m_b}$ are close to unity, and for a small number of bars, the ratios $\frac{m^1_a}{m_a}$ and $\frac{m^1_b}{m_b}$ are approximately equal. In these circumstances then

$$\frac{m^1_a}{m_a} \doteqdot \frac{m^1_b}{m_b} .$$

A better approximation will be obtained if $\frac{m^1_a}{m_a}$ and $\frac{m^1_b}{m_b}$ are averaged.

Let $r_m = \frac{1}{2}\left(\frac{m^1_a}{m_a} + \frac{m^1_b}{m_b}\right)$.

Then the effective length

$$l_{eo} = C.r_m \qquad .. \quad .. \quad 6.13$$

Therefore $m_n = \frac{M_n}{C.r_m}$ 6.14

Again the quantities of the right hand side of equation 6.14 are all obtained from experiments.

Tables 6.1 and 6.2 show the effective crack lengths derived using Downham's [3] concept and also the new concept put forward by the author. The values obtained from the two concepts are in good agreement and the approximation used earlier can be justified.

6.4 General formulae used in the proceeding analysis

In the proceeding analysis of this chapter a number of mathematical formulae were used. For clarity and convenience, it was felt necessary to include all these formulae in this section of Chapter six.

(a) External normal and twisting moments about the yield line.

Referring to figure 6.3, if moments are taken about the yield line AB,

$$M_n = P(la\sin\eta_1 + Ta\cos\eta_1) + 0.563\ \sin\eta_1 \quad .. \quad .. \quad 6.15$$

$$M_{nt} = P(la\cos\eta_1 - Ta\sin\eta_1) + 0.563\ \cos\eta_1 \quad .. \quad .. \quad 6.16$$

where the value 0.563 KNm is a constant depending on the weight of the jaws and the slab. If the width of the slab is b, then the crack length is $b/\sin\eta_1$. The external normal moment per unit length at yield is

$$m_{ne} = \frac{M_n}{b}.\sin\eta_1 = \frac{P}{b}\left(la\sin^2\eta_1 + \frac{Ta}{2}\sin 2\eta_1\right) + \frac{0.563}{b}\sin^2\eta_1 \quad .. \quad 6.15a$$

The external twisting moment per unit length at yield is

$$m_{nte} = \frac{M_{nt}}{b}.\ \sin\eta_1 = \frac{P}{b}\left(\frac{la}{2}\sin 2\eta_1 - Ta\sin^2\eta_1\right) + \frac{0.563}{2b}\sin 2\eta_1 \quad .. \quad 6.16a$$

The direction and the value of the principal applied moments can be derived from equation 6.15a. Differentiating equation 6.15a,

$$\frac{dm_{ne}}{d\eta_1} = \frac{P}{b}\left(la\sin 2\eta_1 + Ta\cos 2\eta_1\right) + \frac{0.563}{b}\sin 2\eta_1$$

For maximum or minimum (principal values) $\frac{dm_{ne}}{d\eta_1} = 0$

$$\tan 2\eta_1 = -\frac{PTa}{Pla + 0.563}$$ (principal direction relative to X-axis) 6.17

Since the direction of the principal applied moments is known, the angle η_1 substituted in equation 6.15 will yield the principal applied moments. From equation 6.17 it can be seen that $\tan 2\eta_1$ is not a linear

function of the load P. For large values of P though, the value of $\tan 2\eta_1$ becomes independent of P.

The equations 6.15 and 6.16 were also used to obtain the applied normal and twisting moments at yield. These values were divided by the effective crack length to obtain the applied normal and twisting moments per unit length at yield.

(b) Radius of curvature.

It has been mentioned earlier in the instrumentation section (5.3.3) that sixteen mechanical deflection gauges were placed underneath the concrete slabs and deflection readings were taken during the experiments. The objective of this was to obtain the maximum principal curvature. The curvature in a particular direction was obtained by means of the formula $K_r = \frac{w_2-2w_o+w_1}{h^2}$ where the w terms are the readings of three colinear gauges and h is the space between two consecutive gauges. Using the above formula, the curvature of a particular point was determined in three independent directions at 45° to each other. Using Mohr's circle, it was found that

$$\tan 2w = \frac{K_1+K_3-2K_2}{K_1-K_3} \quad \text{(principal directions relative to X-axis)}$$

$$K_p = (K_1+K_3) \pm \frac{(K_1-K_3)}{2\cos 2w} \quad \text{(principal curvatures)}$$

(c) Principal concrete strains

Concrete strain readings were read on four 45° rosettes. Each rosette provided enough information to use Mohr's circle of strains to obtain the principal concrete strains and their corresponding directions. The basic formulae are identical to those used for radius of curvature:-

$$\tan 2\gamma = \frac{\varepsilon_1 + \varepsilon_3 - 2\varepsilon_2}{\varepsilon_1 - \varepsilon_3}$$ (principal direction relative to X-axis) 6.18

$$\varepsilon_p = (\varepsilon_1 + \varepsilon_3) \pm \frac{(\varepsilon_1 - \varepsilon_3)}{2\cos 2\gamma}$$ (principal concrete strain).. 6.19

(d) Moments of resistance.

The ultimate moment of resistance of a unit width of slab in which the reinforcement is parallel to the uniaxial moment can be evaluated from the expression

$$m = f_y A_{st}\left(1 - \frac{K f_y A_{st}}{U d_1}\right) d_1 \qquad .. \; .. \; 6.20$$

where the constant K is a function of the shape of the compressive stress block at failure. Since the aggregates used in this test series were the same as those used by Downham [3], K was taken to be the same as that found experimentally by Downham (K = 0.475). This value is considerably less than the one used by Morley [7].

6.5 Comparison of results.

6.5.1 Introduction.

The results obtained in the combined bending and torsion series of experiments are classified into five groups, and each group is compared and discussed separately. This grouping has been adopted simply to facilitate and clarify the comparison. The five groups bear the following headings:

(i) the effect of mesh orientation on the ultimate strength of the concrete slab elements,

(ii) The effect of mesh orientation on the stiffness of the concrete slab elements,

(iii) maximum principal compression strains on concrete surface,

(iv) steel strain observations,

(v) formation of yield lines and comparison with principal directions.

6.5.2 The effect of mesh orientation on the ultimate strength of the concrete slab elements.

The work of Morley [7], Lenschow and Sozen [12], Prince [8], Baus and Tolaccia [10], Wood [6], Kwiecinski [4,5] and others is mainly concerned with the effect of mesh orientation relative to the principal moment directions on the ultimate moment strength of the slab element at yield. Morley and Lenschow and Sozen maintain that the Johansen criterion is acceptable while Prince, Baus and Tolaccia, Wood and Kwiecinski maintain that the Johansen criterion is unacceptable. The first two agree with Johansen that the bars carry only axial stresses. The others suggested that the bars 'kink' or are subjected to shear stresses in addition to axial stresses.

The ultimate test of any theory or hypothesis is experiment. Twenty-eight experiments were carried out on isotropically and orthotropically reinforced concrete slabs subjected to combined bending and torsion. The ultimate loads were reduced to normal and twisting moments at yield by means of equations6.15 and 6.16, and afterwards reduced to moments per unit length using the effective length concept developed by the author. All relevant information is shown in tables 6.1, 6.2, 6.3, 6.4, 6.5 and 6.6. The tables 6.7 and 6.8 show the normal and twisting moments per unit length at yield in a dimensionless form.

Figure 6.4 ($\mu = 0.225$) illustrates the results obtained from the author's experiments and also Wood's [6], Johansen's [2] and the author's theories. From the graph, it is obvious that the Johansen

criterion is definitely conservative while the Wood's criterion is on the unsafe side. The criterion put forward by the author seems to be in good agreement with the experimental values. Two experimental results for large values of alpha seem to be quite high relative to any of the three theories. This is due to the fact that the concrete in tension and not the steel controlled the slab element at failure, as in these two cases the percentage area of steel was at its lowest.

Figure 6.5 (μ= 0.596) illustrates Wood's [6], Johansen's [2] and the author's theories and also the experimental results obtained by the author. Again the results seem to lie between the two extreme theories; i.e. the Johansen and the Wood theories. The values for two experiments out of eleven seem to be fractionally less than that predicted by the author's theory. Also, another two values appear to be higher than those predicted by the author. In general, the author's predicted results seem to be in agreement with the experimental quantities.

Figure 6.6 (μ= 1.0) illustrates the experimental quantities obtained by the author and also the three distinct theories mentioned earlier. The experimental quantities here do not give a definite enough pattern to form a firm conclusion. What can be said with certainty is that there is a definite moment enhancement when the mesh orientation is increased from 0^{o} to 45^{o} relative to the normal to the crack, and also that the Johansen criterion is conservative. The scatter of results may be due to the fact that two experiments were not successfully carried out. One of them, TB 6, was the very first of the series carried out by the author, and the other, TB 3, tilted during testing and the slab had to be reset and tested again.

For further evidence against which the new theory could be compared, the author sought experimental results obtained by other researchers. Downham's [3] results obtained at the University of Aston in Birmingham were thought reliable enough to be used in this research. The results were re-analysed using the author's effective length concept. These results are shown in tables 6.9 and 6.10.

Figure 6.7 ($\mu = 0.275$) illustrates Downham's experimental values and the three distinct theories. Again the Johansen criterion is conservative. The author's criterion appears to yield satisfactory results. Only one value appears higher than that predicted by Wood. Figure 6.8 ($\mu = 0.54$) illustrates Downham's experimental values and also the three distinct theories. In this figure there are twenty-five experimental values. The trend is obvious. The Johansen criterion is again conservative while the Wood criterion is on the other extreme. The author's criterion seems to be closer to the experimental quantities than either of the other two.

Figure 6.9 ($\mu = 1.0$) illustrates Downham's [3] experimental quantities and the theories of Wood [6], Johansen [2] and of the author. The moment enhancement as the mesh direction is increased from 0° to 45° relative to the normal to the crack is obvious. Two results seem to be fractionally below the value predicted by the Johansen criterion, and one fractionally higher than that predicted by the Wood criterion. There is definite evidence that the trend of results has the same form as the theoretical expression put forward by the author.

6.5.3 The effect of mesh orientation on the stiffness of the concrete slab element.

The stiffness of an element can be considered as the ratio of moment to curvature in a given direction during any part of the loading

history of the specimen. The effective stiffness has three distinct points of change during the loading history of the specimen; it changes at first cracking, at first yield, and finally tends towards zero when plastic flow occurs.

Both Morley [7] and Lenschow and Sozen [12] have realized the importance of the stiffness of the slab elements and in their studies they showed that the stiffness is a function of the mesh orientation and the degree of orthotropy. Downham [3] also showed experimentally that the stiffness is a function of the mesh orientation and the degree of orthotropy.

The author, from his experiments, obtained results similar to Downham's. Figure 6.10 - figure 6.15 illustrate the behaviour of the test specimen up to complete yield. The figures show maximum principal moment per unit effective length plotted against maximum principal curvature.

Figures 6.10 and 6.11 illustrate the effect on stiffness of the mesh orientation for "isotropic" slab elements subjected to combined torsion and bending. From the figures it is obvious that before cracking takes place, the stiffness of the elements is not affected by the mesh orientation. After cracking, though, there is a considerable stiffness difference, although cracking was initiated at the same moment. The curvatures at first yield tend to increase as the mesh orientation was decreased from 90° to 45° relative to the normal of the crack. Again, from the figures 6.10 and 6.11 it can be seen that as plastic flow occurs, the stiffness decreases towards a zero value. The specimen TB 4 did not behave as the other specimens. This is due to the fact that the slab cracked while being lifted on the testing rig, and hence the initial cracking was not detected.

Figures 6.12 and 6.13 show the maximum principal moments per unit effective length plotted against maximum principal curvature for orthotropic slabs of degree of orthotropy one half ($\mu = 0.5$ Nominal). Again, before cracking occurs the stiffness seems to be completely unaffected by the mesh orientation. The cracking moment seems to be the same as for "isotropic" slabs. The slope, however, immediately after cracking seems to be different than the "isotropic" slabs. When plastic flow occurs, however, the stiffness decreases to zero.

Figures 6.14 and 6.15 show the variation of stiffness for slabs with $\mu = 0.25$. The behaviour of these slab elements is similar to the slabs having a degree of orthotropy $\mu = 0.5$.

In conclusion, it can be said that before cracking occurs, the stiffness of the slab elements is independent of the mesh orientation and the degree of orthotropy. In fact, there are indications that the stiffness depends only on the thickness of the slab and the concrete properties. The criterion of cracking is one based on stress conditions, and is controlled entirely by the tensile properties of concrete. However, once cracking has occurred, the stiffness of the slab element is controlled by the orientation of the mesh reinforcement relative to the normal to the crack and the degree of orthotropy.

As soon as plastic flow occurs, the stiffness of the slab elements decreases very rapidly towards zero.

6.5.4 Maximum principal compression strains on concrete surface.

On all the slabs tested, four concrete strain rosettes were placed on the top surface of the concrete. The location of the rosettes and the way they were fixed was described in section 5.3.2. The strains recorded on a rosette that was nearest to the crack plane were

reduced to principal strains using equation 6.19.

Figures 6.16 and 6.17 illustrate the variation of the principal concrete strains with the load P for "isotropic" slabs. The graphs are trilinear. The first part of the graph shows the elastic behaviour of concrete slab when there are no tensile cracks. The second part of the graph shows the elastic behaviour of the concrete slab when tensile cracks have developed. The break point between the first linear part of the graph and the second linear part denotes the load at which the first tensile cracks developed in the tension part of the slab. The third part of the trilinear graph shows the concrete strains on the compression face of the slab when the slab was yielding. The third part of the trilinear graph, which is practically horizontal, indicates that the slab has yielded and not that the concrete has reached its ultimate strength in compression. The load-strain characteristic before any cracks develop appears to be identical for all seven slabs. This is further evidence that the stiffness of the slab before any cracks develop is completely independent of the mesh orientation relative to the normal to the crack.

Figures 6.18 and 6.19 illustrate the behaviour of the compression principal strains on the surface of the concrete slabs during load increase, for a nominal degree of orthotropy of $\mu = 0.5$. Again, the load-strain characteristic of these slabs is trilinear.

Figures 6.20 and 6.21 illustrate the relationship between principal strains on the surface of the concrete slabs when the load on the slabs was varied. The degree of orthotropy for these slabs was $\mu=0.25$. The load-strain characteristic is trilinear. The second part of the trilinear graphs is very small. This is due to the low strength of the concrete slabs; these slabs have a low strength because of small

percentage of steel. For eight out of ten slabs, the failure of the slab occurred very shortly after the first tensile cracks appeared. For slabs TB 32, 33, 36 and 39, the maximum principal concrete strains were less than 800 microstrains. It is obvious then that the concrete has not reached its ultimate strength. For slabs with very small percentage of steel, failure occurs in a similar manner to an unreinforced concrete slab. It is not so much that the "concrete does not reach its ultimate strength", but rather that failure occurs so rapidly that the high strains which do develop in the concrete cannot be measured; i.e. the cracks moved upwards rapidly , eventually small remaining compression area crushes. In general, the maximum principal concrete strains seem to be controlled by the mesh orientation to the normal to the crack, the degree of orthotropy and the lever arm length.

6.5.5 Steel strain observations.

Electric resistance gauges were fixed on eight bars, four on the lower layer of reinforcement and four on the upper layer of reinforcement. These gauges were strategically placed to record strains on the reinforcement adjacent to the cracks. Unfortunately, the prediction of the crack locations proved difficult and most gauges recorded strains remote from the crack. The readings were influenced by the presence of uncracked concrete. Although load-strain graphs were plotted for all gauge readings and studied, only typical graphs will be presented in this chapter. A typical example of a load-strain characteristic is illustrated in figure 6.22. The graph is for specimen TB 1, the mesh orientation relative to the free side of the slab is zero, and the degree of orthotropy is unity. The axial yield strain of the bars was 1310 microstrains. The lower bar represented by gauge number two

seems to have yielded, the strains recorded are higher than the axial yield strain. The upper bar appears not to have yielded. This is due to the fact that the gauge numbered five was not located at the vicinity of the crack. It must be realized that the load-strain plots are not stress-strain characteristics, and a horizontal curve does not represent yield of the bar but a yield of the slab. The only criterion that can be used with certainty to indicate that the bar has yielded is the axial yield strain being exceeded by that recorded on the gauges.

Figure 6.23 illustrates another typical load-strain characteristic for two bars in specimen TB 17. Here the mesh orientation relative to the free side of the slab was 60^{o} and the degree of orthotropy one-half. Gauge number three was adjacent to the crack. This gauge recorded the three phase changes of the bar and the slab. The first linear part of the graph illustrates the load-strain behaviour of the bar before any cracks developed. The second part of the linear graph illustrates the load-strain behaviour of the bar after tensile cracks developed in the concrete. The interesting thing here is that the bar steel behaves linearly even after the yield strain was exceeded. This can be explained by the fact that the upper bars have not yielded simultaneously with the lower bars. The horizontal part of the graph denotes the total yield of the slab. Gauge number eight was located away from the crack and the strains recorded are low. The maximum strains recorded on this gauge were less than 700 microstrains. This does not mean that the bar did not yield at the crack.

Another typical load-strain behaviour is illustrated in figure 6.24. The axial yield strain of the upper bars was 1260 microstrains and that of the lower bars was 1310 microstrains. The two sets of bars

were from two different batches of steel. Specimen TB 33 had a mesh orientation of 45° to the free side and a degree of orthotropy one-quarter. Gauge number eight fixed on the upper bar recorded compression strains before any tensile cracks developed in the concrete. This can only be attributed to the Poisson ratio effect. Eventually, it seems that both bars yielded simultaneously.

6.5.6 Formation of yield lines and comparison with principal directions.

In the application of the yield line theory it may be more important and also more difficult to determine the location of the yield lines than to determine the moment capacity of a cross section. Lenschow and Sozen [12] developed an expression that determines the location of the yield lines and they claim that the expression is justified experimentally. Lenschow and Sozen also claim that the initial cracks appeared perpendicular to the maximum principal external moment. Further development of these cracks depends on the direction and distribution of the reinforcement.

Downham [3] agrees with the results of Lenschow and Sozen [12] in that all yield lines develop perpendicular to the maximum principal external moment but, contrary to them, suggests that any deviation of yield lines from the perpendicular to the maximum principal external moment is purely due to the self-weight of the slab elements. The self-weight of the slab elements alters the direction of the perpendicular to the maximum principal external moment. Kemp [9] in developing the yield criterion using the Johansen normal moment criterion and the curve describing the variation in applied moment between M_1 and M_2, postulated that yield occurs in the direction in which the curves first touch as the applied moment field is proportionally increased.

The author brought to light new experimental evidence concerning the behaviour of the yield lines. The development of cracks is of great importance. In this series of tests two types of failure occurred, failure due to a single crack (see plate 6.1 and 6.2) and failure due to multiple cracks (see plate 6.3 and 6.4).

(a) Single crack failure.

Single cracks basically developed in slabs that had a low percentage of steel perpendicular to the failure direction. The horizontal line in figure 6.25 shows the strength of the concrete slab neglecting reinforcement, which is independent of direction. The upper curve represents the strength of the concrete slab when the tensile strength of the concrete is neglected, which shows that the strength varies with direction. The lower curve represents the applied external moments. It can be seen that for α values between AB, the unreinforced slab has a higher strength than the reinforced slab, but for any other α value the reinforced slab has a higher strength than the unreinforced one. It is obvious then that the first tensile crack will appear where the external maximum principal moment has the same value as the moment of resistance of the unreinforced concrete slab. In other words, the first crack appears in the maximum moment principal direction. If the external maximum principal direction is within the AB range (as shown by full line Applied moment curve, figure 6.25), the slab will fail immediately after the propagation of the first crack; the sudden failure of the slab is followed by a load drop. If the maximum moment principal direction is outside the AB range (as shown by dotted line Applied moment curve, figure 6.25), multiple crack failure will occur; the behaviour is identical to slabs with high steel ratio and will be discussed shortly.

After the initial crack has propagated throughout the slab width, the stiffness of the slab is reduced across the crack length. Because of the stiffness reduction, concrete matrix and steel arrangement and distribution, it is possible to have single crack failure slightly outside the AB range.

(b) Multiple crack failure.

Multiple cracks basically developed in slabs that had a high percentage of steel perpendicular to the failure direction. In these slabs, the strength of the reinforced slab, when the tensile strength of the concrete is neglected, is larger than the strength of the unreinforced slab. Figures 6.26 and 6.27 illustrate the variation of strength in such slabs for two different values of degree of orthotropy. Referring to figures 6.26 and 6.27; as the combined bending and torsional moments were increased proportionally, the external maximum principal moment reaches the horizontal line first. Since the concrete reaches its limiting value first, the initial crack appears in the maximum principal direction. However, the slab has not yielded since reserve strength exists in the steel. The creation of the first crack has two major effects on the stress field. The first effect is the transfer of tensile stresses from the failed concrete to the steel and the second effect is the decrease of stiffness in the section across the crack. The above effects have a direct effect on the moment field adjacent to the crack. When the external moment is increased as shown in figures 6.26 and 6.27 (broken lines), it can be seen that in the directions lying between A and B, the slab is subjected to an external moment larger than the moment strength of the unreinforced concrete slab. Theoretically, cracks should develop in all the directions lying between A and B. Practically, though, cracks develop on

either side of the initial crack. The number and direction of these cracks will depend on the concrete matrix and steel arrangement and distribution, and they tend to propagate towards each other. The slab will only collapse when the external moment curve first touches the moment strength curve for the reinforced concrete slab.

The argument put forward in (a) and (b) above was substantiated experimentally. Tests TB 31, 32, 33, 34, 36, 37, 38 and 39 failed due to a single crack, the rest of the slabs failed due to multiple cracks. The argument put forward in (a) shows that slabs with low percentage of steel perpendicular to the failure direction will develop a yield line in the same direction as the direction of the applied principal moment. The argument put forward in (b) shows that slabs with high percentage of steel perpendicular to the failure direction develop yield lines which are not necessarily in the same direction as the applied principal moment. Further evidence in support of the argument in (a) and (b) is displayed in figures 6.28 to 6.55. Each figure shows the load variation with the tangent of the directions of the principal applied ~~principal~~ moment, principal compression concrete strain and principal curvature relative to the span direction for each specimen. There is also enough evidence to show that before any cracks develop the directions of maximum principal moment, maximum principal concrete strain and maximum principal curvature coincide. Once concrete cracks develop, the three principal directions do not necessarily coincide. At yield, however, the direction of the maximum principal compression strain of concrete moves towards the direction of the normal to the yield line. The direction of the maximum principal curvature also appears to move towards the direction of the normal to the yield line, it seems though, that this movement is not accomplished so readily.

The formation of multiple direction cracks in the tension face of the slab seems to hinder this movement. It is possible that with more sensitive instruments, this movement could be detected.

6.6 Conclusions on results.

The purpose of carrying out the tests described in the preceding sections was two-fold. The first purpose was to investigate the variation of normal moment of resistance of a slab element on a yield line with varying inclination of the reinforcement relative to the normal to the yield line, and to compare this value with that predicted by the new theory put forward by the author. The second purpose of the tests was to investigate the behaviour of a slab element subjected to combined bending and torsion. Both objectives have been successfully achieved.

The results obtained clearly showed that there is a definite increase in moment of resistance of an "isotropic" slab as the yield line becomes inclined to the steel, which reaches a maximum increase when the angle formed between yield line and steel is 45°. This trend seems to be in agreement with the predictions of the new theory developed in this thesis. Furthermore, it has been shown that the Johansen yield line theory is conservative, whilst the "full kink" theory developed by Wood overestimates the strength of the concrete slab elements. After the completion of the tests, the bars were examined for "kinking"; no measurable kinking was recorded but the tendency of the bars to kink was obvious. The experimental normal moments of resistance for isotropically and orthotropically reinforced concrete slab elements obtained were in good agreement with the values predicted by the new theory.

The second part of this test series was to investigate the behaviour of the slab elements subjected to combined bending and torsion.

The study of the maximum principal curvatures and concrete compression strains showed that the stiffness of the slab elements before any cracks develop is completely independent of the mesh orientation and degree of orthotropy. However, after cracking of the concrete takes place, it appears that the stiffness is controlled by the mesh orientation and the degree of orthotropy.

The study of the steel strains showed that the upper and lower steel reinforcement does not necessarily yield simultaneously. The direct observation of the first cracks during the test and the comparison of the direction of these cracks with the direction of the maximum principal moments showed that the first cracks take place in a direction perpendicular to the direction of the maximum principal moments. A study of the plot of the maximum principal directions of moments, compression concrete strains and curvatures, as well as the direction of the crack that caused yield, showed an interesting phenomenon. At first yield, the direction of the normal to the crack is not necessarily in the same direction as any of the three calculated principal directions. However, after some yielding has taken place, the principal direction of the maximum concrete compression strain and the maximum curvature tend to coincide with the normal to the crack. This can only be attributed to a change of the stiffness of the slab element at yield.

Series Number	Number of a - bars	Number of b - bars	Effective length m. (Author)	Effective length m. (Downham)
TB 1	11	5	0.804	0.875
TB2	0	13	0.839	0.825
TB3	5	11	0.876	0.784
TB4	7	10	0.866	0.826
TB16	4	8	0.859	0.936
TB17	1	7	0.924	0.917
TB18	4	6	0.835	0.878
TB19	4	6	0.823	0.838
TB20	9	3	0.863	0.926
TB31	3	7	0.811	0.830
TB32	0	6	0.805	0.799
TB33	3	7	0.941	0.987
TB34	4	6	0.822	0.817
TB35	12	4	1.017	1.160

Ta = 0.444 m la = 0.381 m (R.C. slabs)

Table 6.1

Series number	Number of a - bars	Number of b - bars	Effective length m. (Author)	Effective length m. (Downham)
TB 6	10	5	0.742	0.750
TB 7	0	10	0.794	0.744
TB 8	4	10	0.851	0.845
TB21A	2	7	0.730	0.861
TB21	3	7	0.926	0.950
TB22	1	6	0.756	0.788
TB23	4	6	0.960	0.877
TB24	5	5	0.821	0.805
TB25	10	3	0.925	1.010
TB36	1	7	0.961	0.844
TB37	0	6	0.822	0.680
TB38	4	6	0.940	0.922
TB39	5	5	0.827	0.829
TB40	10	5	1.131	1.144

Ta = 0.286 m la = 0.381 m (R.C. slabs)

Table 6.2

Series Number	Orthotropy (μ) Nominal	Twist Arm Ta m	Angle β	Crack Angle η	Angle α
TB1	1.0	0.444	0	56.6	33.4
TB2	1.0	0.444	60	59.3	89.3
TB3	1.0	0.444	45	63.8	71.2
TB4	1.0	0.444	30	64.5	55.5
TB16	0.50	0.444	90	63.1	63.1
TB17	0.50	0.444	60	67.0	83.0
TB18	0.50	0.444	45	63.7	71.3
TB19	0.50	0.444	30	60.9	59.1
TB20	0.50	0.444	0	58.5	31.5
TB31	0.25	0.444	90	67.4	67.4
TB32	0.25	0.444	60	60.9	89.1
TB33	0.25	0.444	45	49.2	85.8
TB34	0.25	0.444	30	54.0	66.0
TB35	0.25	0.444	0	48.0	42.0

Table 6.3

Series Number	Orthotropy (μ) Nominal	Twist Arm Ta m	Angle β	Crack Angle η	Angle α
TB6	1.0	0.286	90	63.8	63.8
TB7	1.0	0.286	60	72.4	77.6
TB8	1.0	0.286	45	70.7	64.3
TB21A	0.50	0.286	90	72.0	72.0
TB21	0.50	0.286	90	65.7	65.7
TB22	0.50	0.286	60	67.6	82.4
TB23	0.50	0.286	45	64.7	70.3
TB24	0.50	0.286	30	62.6	57.4
TB25	0.50	0.286	0	59.9	30.1
TB36	0.25	0.286	90	76.5	76.5
TB37	0.25	0.286	60	72.0	78.0
TB38	0.25	0.286	45	66.0	69.0
TB39	0.25	0.286	30	62.5	57.5
TB40	0.25	0.286	0	53.5	36.5

Table 6.4

Series number	Total normal moment on crack MT kNm (exp)	Total twist on crack MT kNm (exp)	Moment per unit length m_n kNm/m (exp)	Twist per unit length m_{nt} kNm/m (exp)
TB1	14.65	-3.76	18.22	-4.67
TB2	13.66	-4.17	16.27	-4.97
TB3	13.29	-5.23	15.80	-5.97
TB4	12.56	-5.10	14.50	-5.89
TB16	11.26	-4.20	13.18	-4.92
TB17	9.79	-4.38	10.59	-4.74
TB18	9.62	-3.64	11.51	-4.35
TB19	9.67	-3.12	11.74	-3.79
TB20	14.63	-4.28	16.97	-4.95
TB31	6.29	-2.70	7.75	-3.33
TB32	5.16	-1.45	6.41	-1.81
TB33	5.52	-0.40	5.86	-0.43
TB34	7.19	-1.27	8.74	-1.55
TB35	13.03	-1.26	12.81	-1.24

Table 6.5

Series number	Total normal moment on crack MT kNm (exp)	Total twist on crack MT kNm (exp)	Moment per unit length m_n kNm/m (exp)	Twist per unit length m_{nt} kNm/m (exp)
TB6	15.55	-2.59	20.96	-3.49
TB7	14.31	-4.65	18.02	-5.85
TB8	13.98	-4.07	16.42	-4.78
TB21A	10.96	-3.39	11.83	-3.66
TB21	10.44	-1.98	14.30	-2.71
TB22	8.32	-1.80	11.00	-2.38
TB23	9.39	-1.58	9.78	-1.64
TB24	10.30	-1.38	12.55	-1.66
TB25	14.70	-1.41	15.93	-1.52
TB36	5.49	-2.00	5.71	-2.08
TB37	5.30	-1.46	6.45	-1.77
TB38	5.52	-0.92	5.87	-0.97
TB39	6.75	-0.77	8.15	-0.93
TB40	14.36	+0.25	12.70	+0.21

Table 6.6

Series number	Degree of orthotropy (exp)	Moment of resistance m_a kNm/m	$\frac{m_n}{m_a}$	$\frac{m_{nt}}{m_a}$
TB1	0.992	15.72	1.159	-0.300
TB2	0.993	15.66	1.039	-0.320
TB3	0.992	15.63	0.970	-0.385
TB4	0.984	16.16	0.957	-0.395
TB16	0.570	16.12	0.818	-0.535
TB17	0.604	16.22	0.652	-0.483
TB18	0.600	15.78	0.730	-0.460
TB19	0.601	15.64	0.750	-0.403
TB20	0.597	16.00	1.059	-0.519
TB31	0.225	15.67	0.495	-0.944
TB32	0.226	16.36	0.392	-0.489
TB33	0.225	15.99	0.366	-0.118
TB34	0.225	15.98	0.547	-0.430
TB35	0.226	16.05	0.798	-0.342

Table 6.7

Series number	Degree of orthotropy (exp)	Moment of resistance m_a kNm/m	$\frac{m_n}{m_a}$	$\frac{m_{nt}}{m_a}$
TB6	0.983	15.14	1.384	-0.234
TB7	0.991	15.79	1.141	-0.374
TB8	0.994	15.74	1.043	-0.306
TB21A	0.598	15.84	0.730	-0.374
TB21	0.603	16.21	0.903	-0.287
TB22	0.599	14.81	0.743	-0.268
TB23	0.598	15.52	0.630	-0.177
TB24	0.600	15.79	0.794	-0.177
TB25	0.599	15.46	1.030	-0.164
TB36	0.225	16.06	0.356	-0.578
TB37	0.223	15.60	0.414	-0.509
TB38	0.223	15.62	0.376	-0.280
TB39	0.224	15.75	0.518	-0.264
TB40	0.222	15.85	0.801	+0.065

Table 6.8

Downham's results analysed using author's effective length concept.

Plank Series	μ	$\alpha = \beta$	l_{eo} m author	b' m Downham	$\frac{m_n}{m_{nj}}$
P 1	1.000	0	0.714	0.762	1.071
P 2	0.990	30	0.671	0.653	1.025
P 3	0.990	45	0.607	0.618	1.078
P 4	0	0	0.732	0.762	0.913
P 5	0	30	0.593	0.616	1.070
P 6	0	45	0.422	0.431	1.309
P 7	0	60	0.294	0.305	1.286
P 8	0.275	0	0.738	0.762	0.996
P 11	0.275	60	0.550	0.529	1.234
P 12	0.275	90	0.798	0.800	1.065
P 13	0.543	0	0.766	0.762	1.027
P 14	0.546	30	0.535	0.593	1.171
P 15	0.542	45	0.621	0.583	1.031
P 16	0.547	60	0.625	0.626	0.907
P 17	0.545	90	0.806	0.822	1.022

Table 6.9

Downham's results analysed using author's effective length concept.

TB series	μ	α	la m author	la m Downham	$\frac{m_n}{m_{nj}}$
1	0.99	7.0	0.914	0.908	1.070
2	0.99	35.8	0.826	0.853	0.982
3	1.00	49.6	0.810	0.830	1.016
4	1.00	20.3	0.773	0.924	1.348
5	0.98	49.5	0.820	0.827	1.113
6	0.99	64.3	0.891	0.852	1.106
7	1.00	24.1	0.769	0.912	1.463
8	0.98	57.5	0.909	0.847	1.139
9	0.99	65.8	0.821	0.820	1.334
10	0.55	12.1	0.920	0.912	0.957
11	0.55	48.6	0.877	0.862	1.046
12	0.55	64.0	0.827	0.849	1.066
13	0.54	71.7	0.728	0.802	1.164
14	0.54	93.5	0.962	0.935	1.000
15	0.54	26.8	1,074	0.900	1.080
16	0.55	55.7	0.911	0.819	1.133
17	0.54	70.1	0.884	0.835	1.151
18	0.55	80.0	0.860	0.790	1.062
19	0.55	106.9	0.903	0.954	1.196
20	0.54	32.2	1.017	0.932	1.324
21	0.54	63.5	0.941	0.845	1.239
22	0.54	75.5	1.024	0.856	1.111
23	0.54	80.8	0.934	0.794	1.146
24	0.54	112.4	0.976	0.965	1.356
25	0.54	133.1	0.906	0.851	0.996
26	0.54	140.1	0.851	0.850	1.259
27	0.54	149.9	0.837	0.853	1.448
28	0.97	72.1	0.950	0.880	0.913
29	0.96	90.2	0.976	0.889	1.031
30	0.92	89.7	1.040	0.889	1.056
31	0.99	23.7	0.967	0.921	1.155

Table 6.10

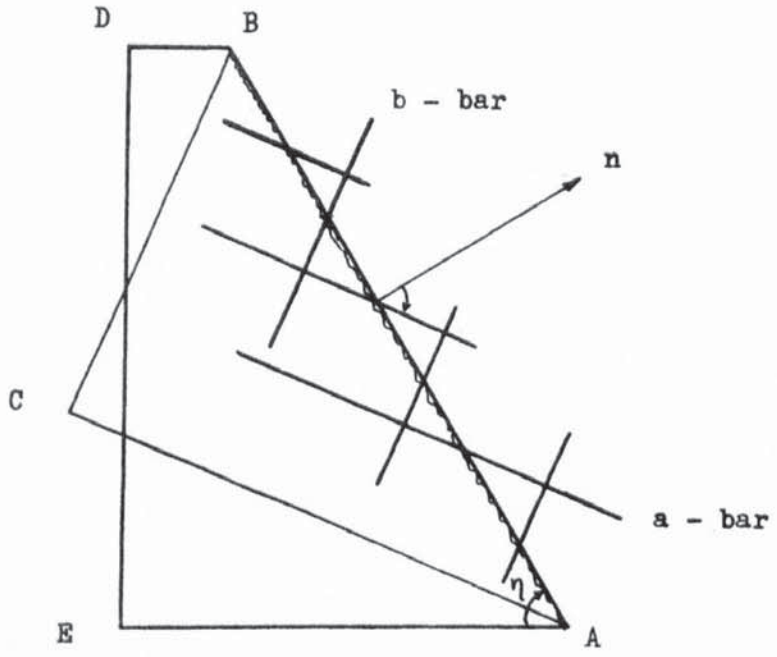

Figure 6.1

SLAB SECTION

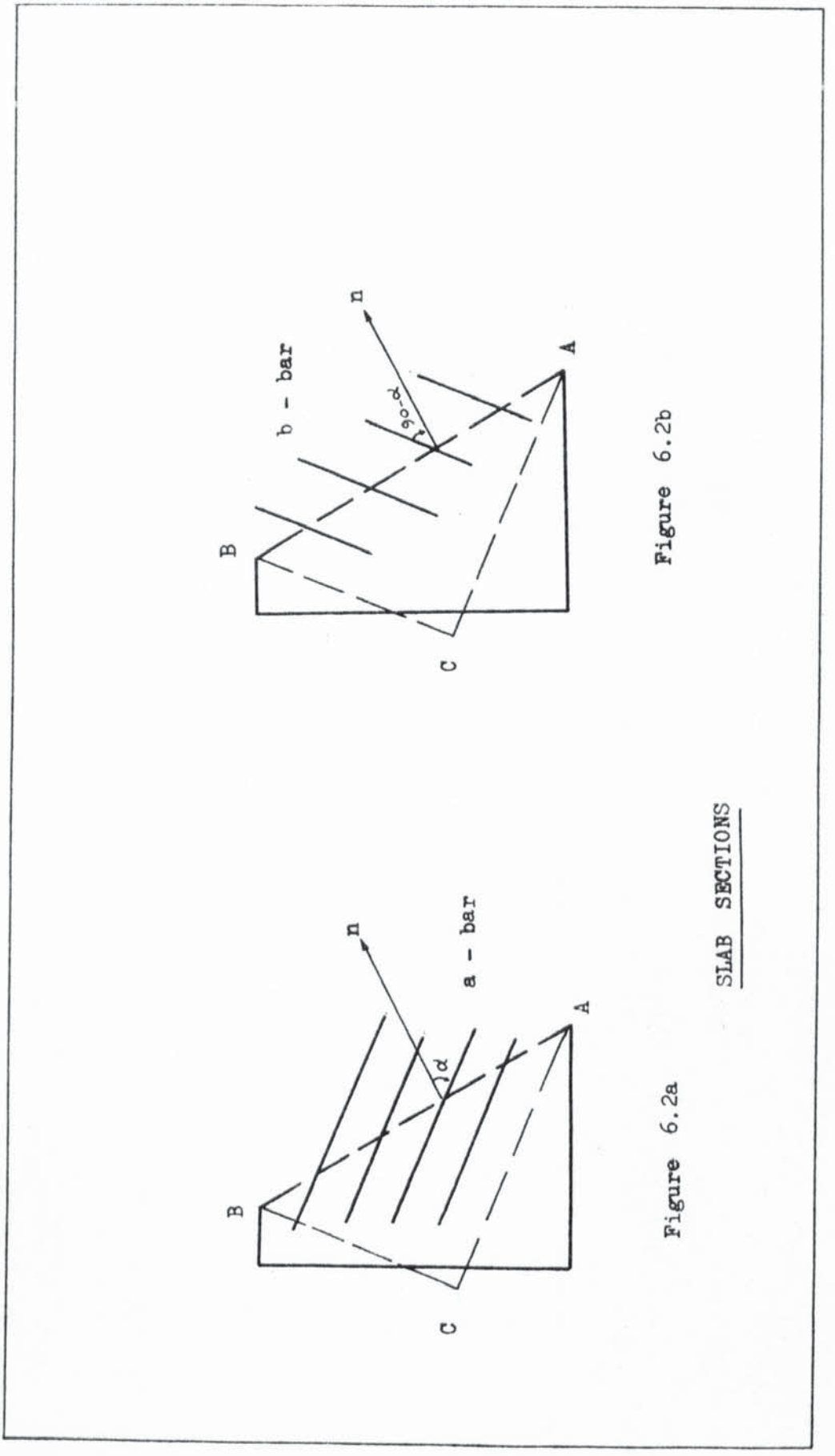

Figure 6.2b

Figure 6.2a

SLAB SECTIONS

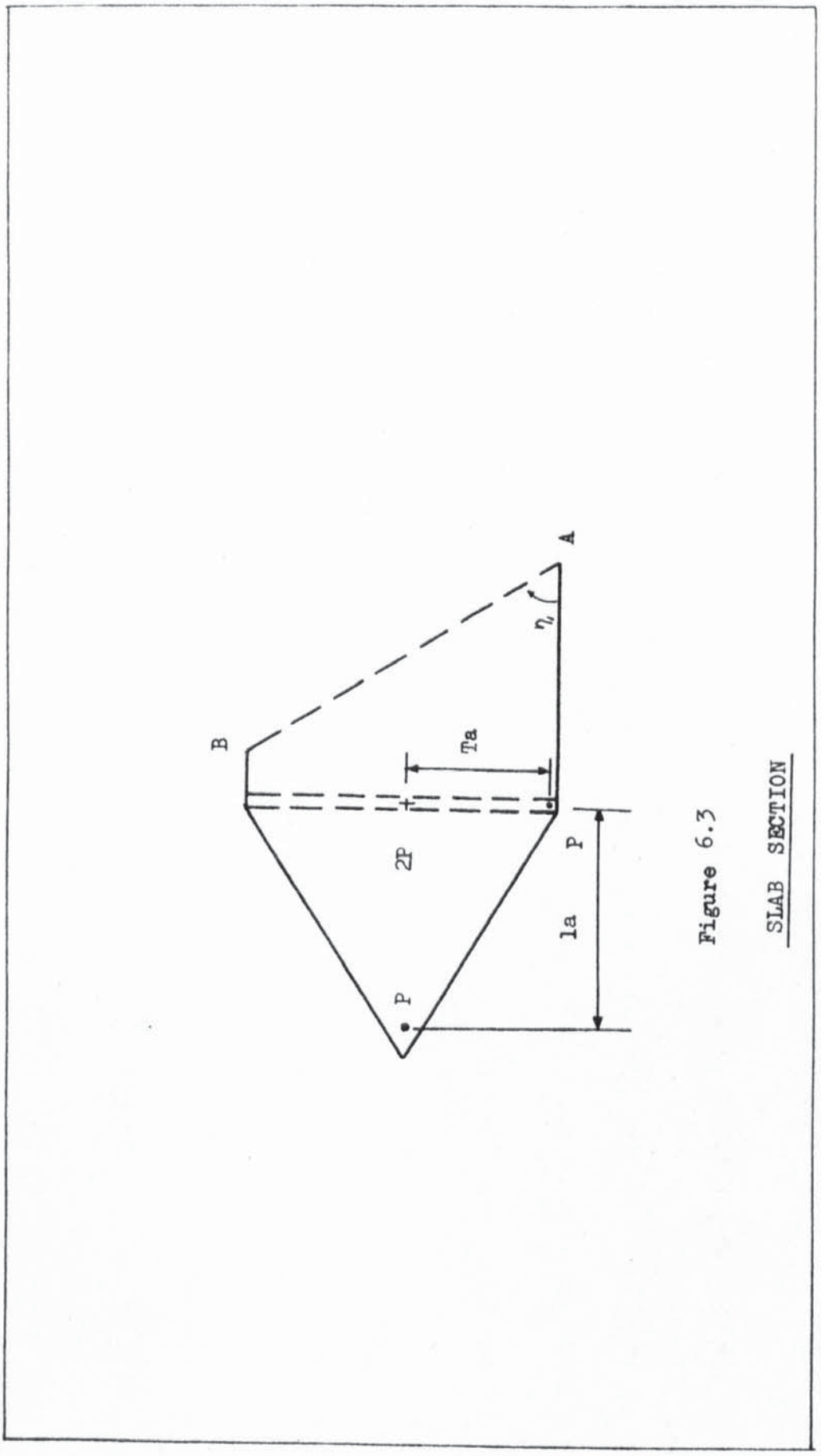

Figure 6.3

SLAB SECTION

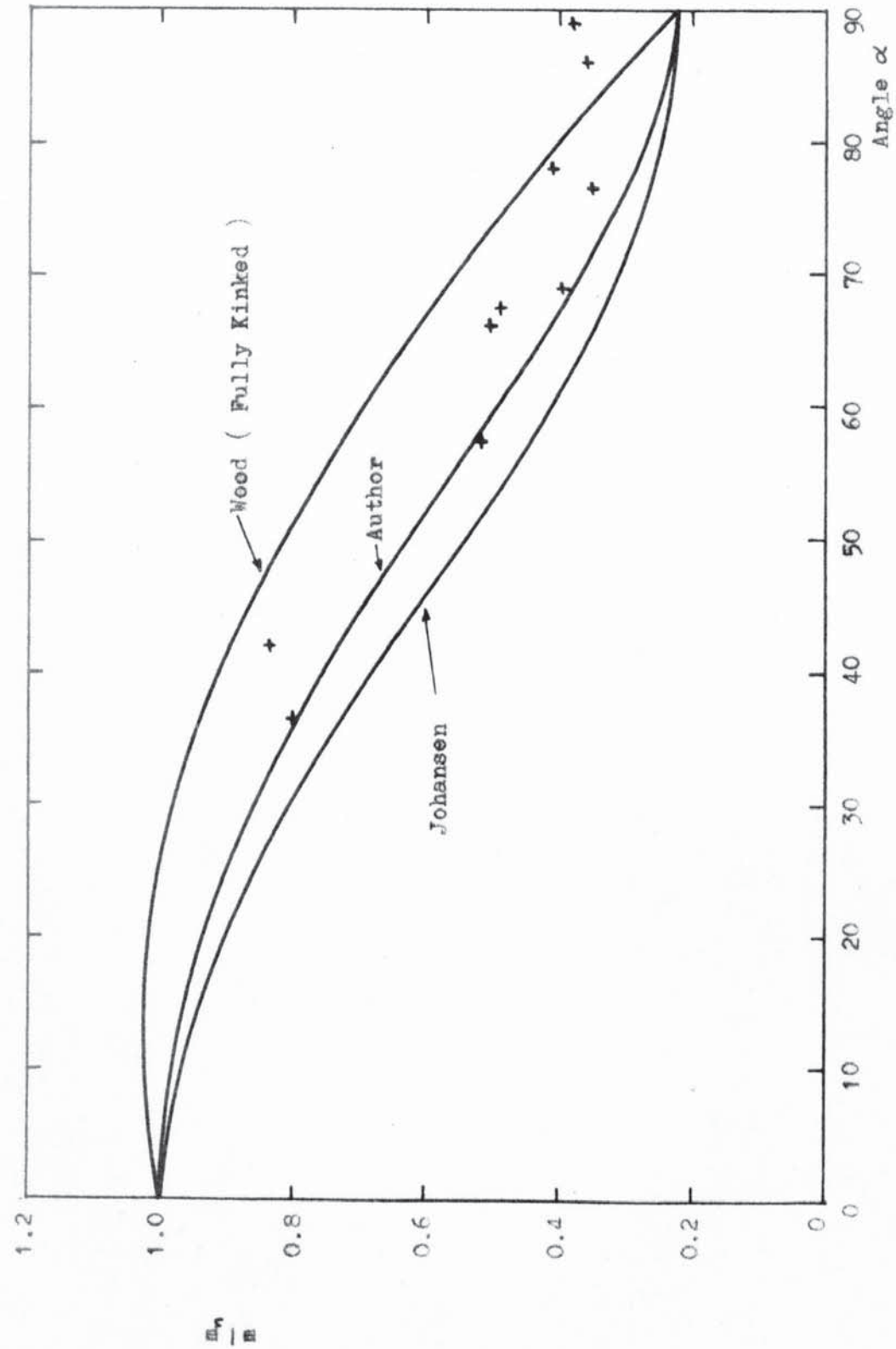

Figure 6.4 m_n/m V.S alpha at failure (μ=0.225) AUTHOR'S RESULTS

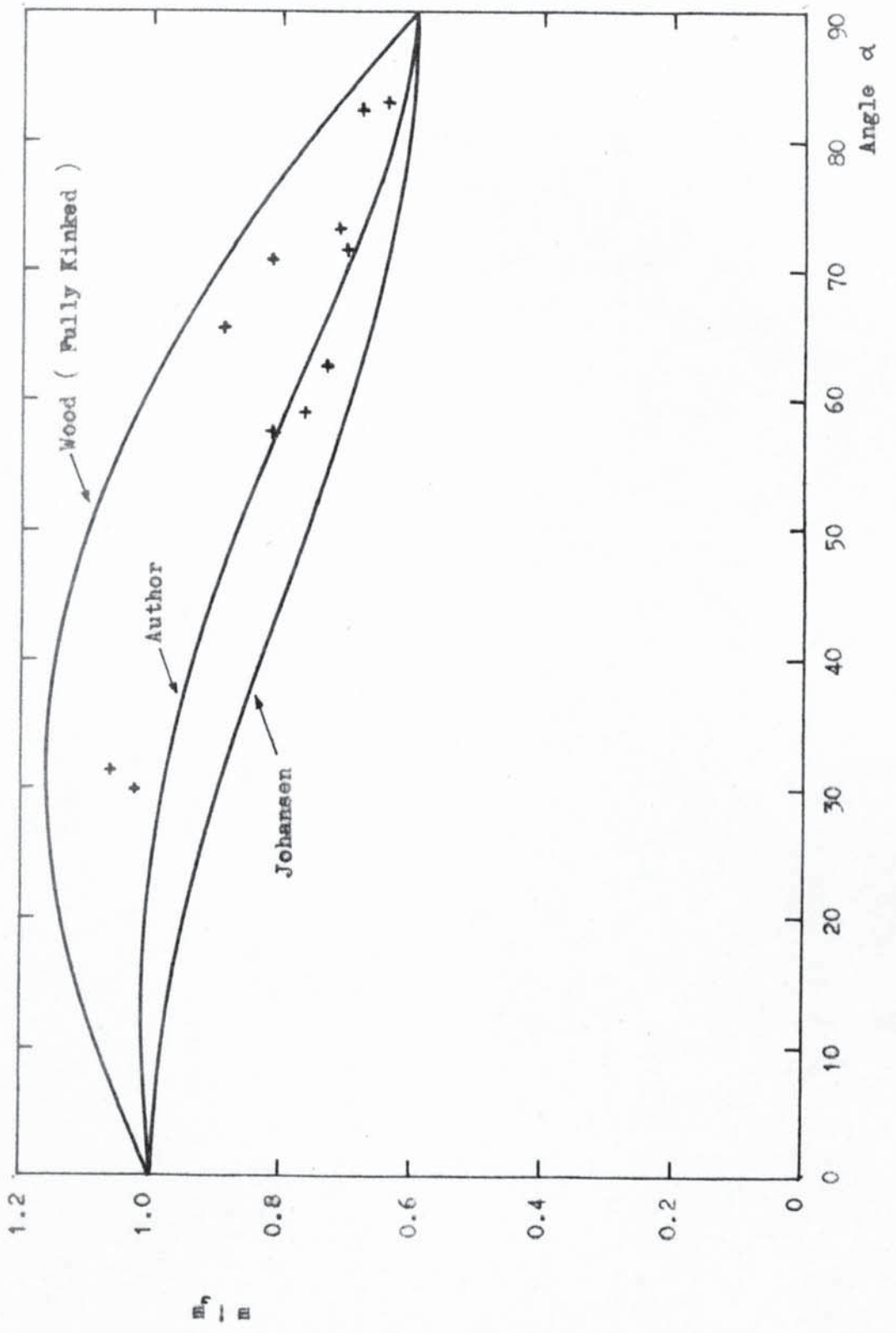

Figure 6.5 m_o/m V.S Alpha at failure (μ=0.596) AUTHOR'S RESULTS

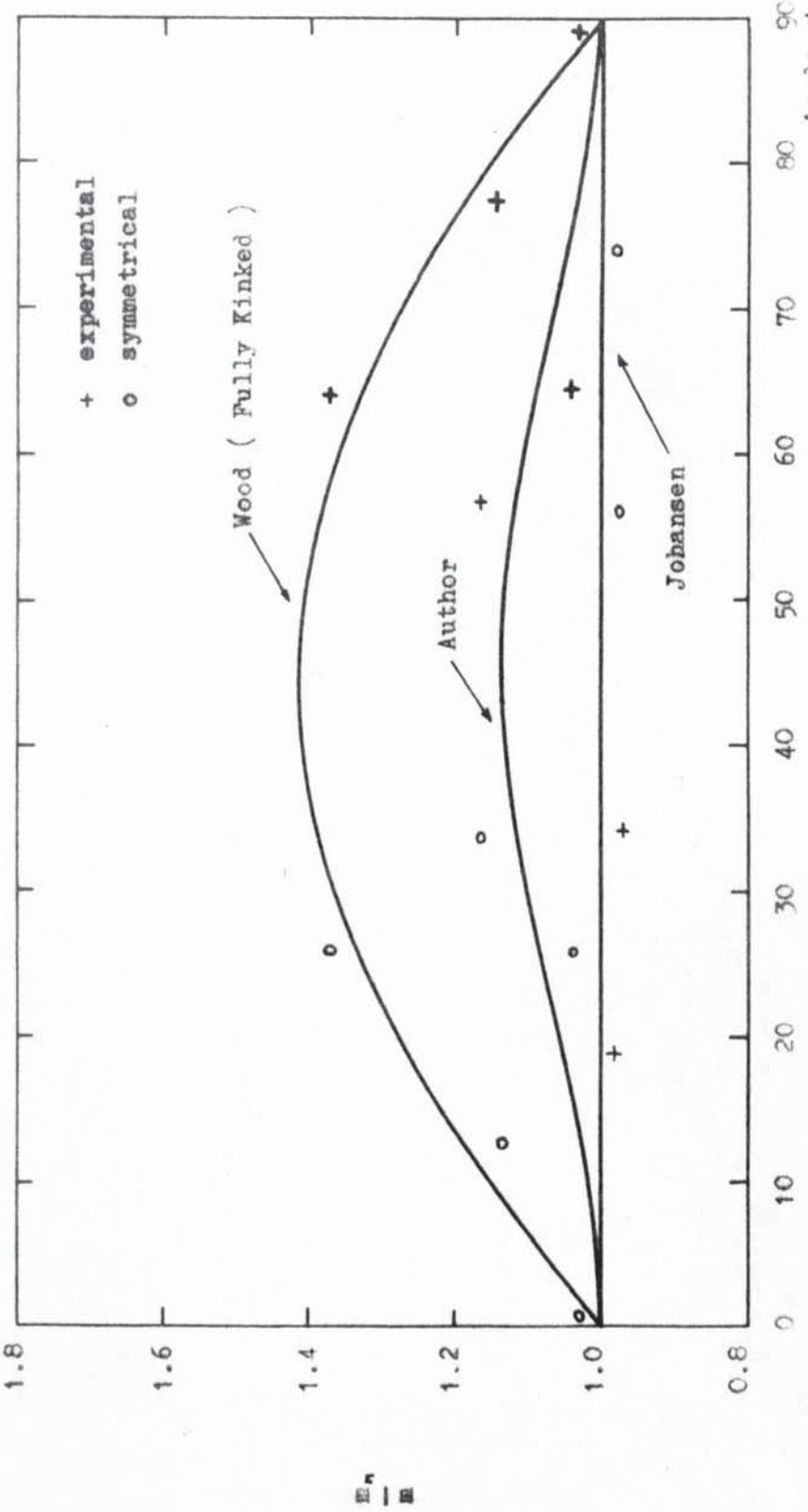

Figure 6.6 M_n/M V.S alpha at failure (μ=1.0) AUTHOR'S RESULTS

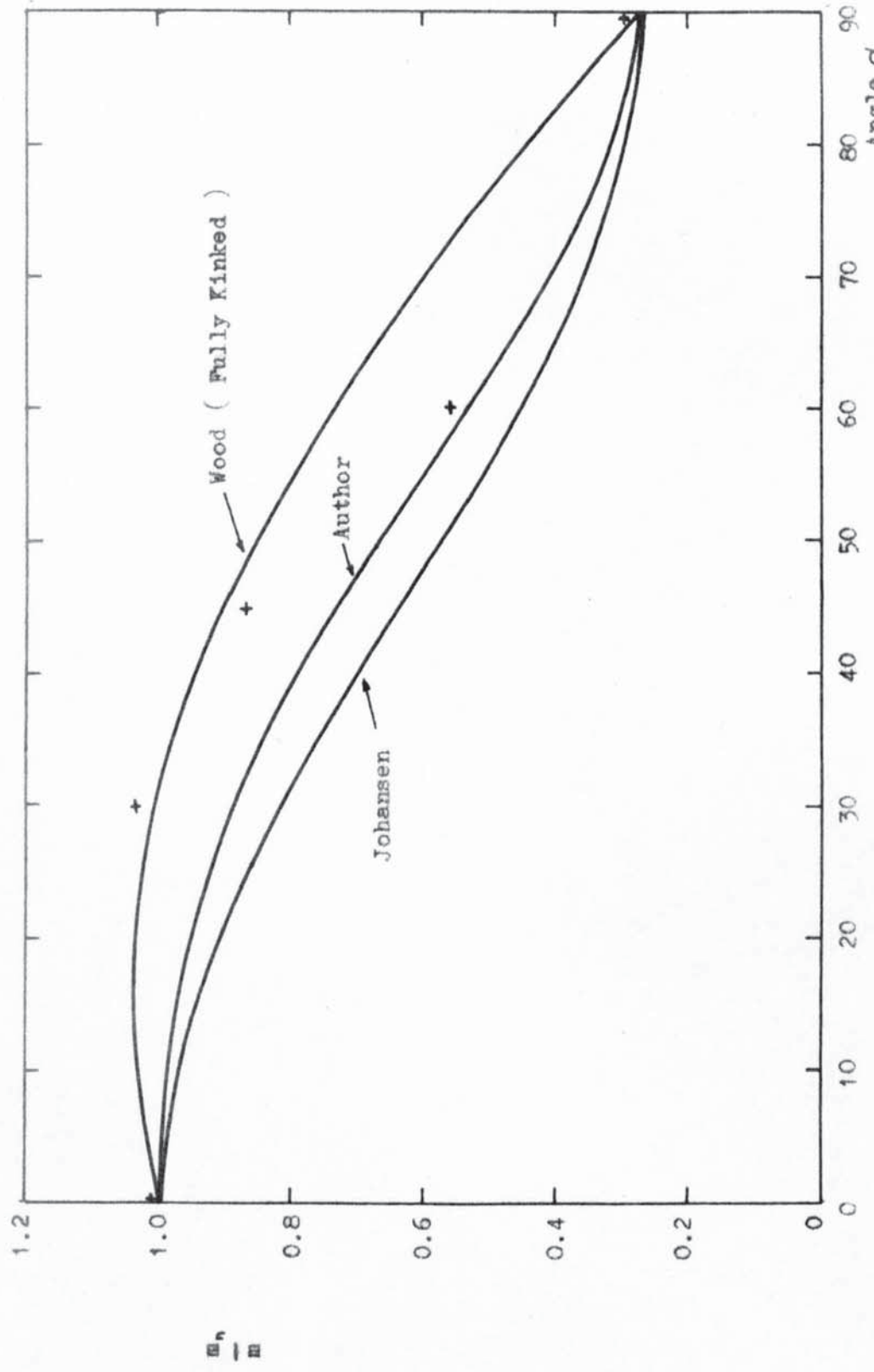

Figure 6.7 m_n/m V.S alpha at failure (μ=0.275) DOWNHAM'S RESULTS

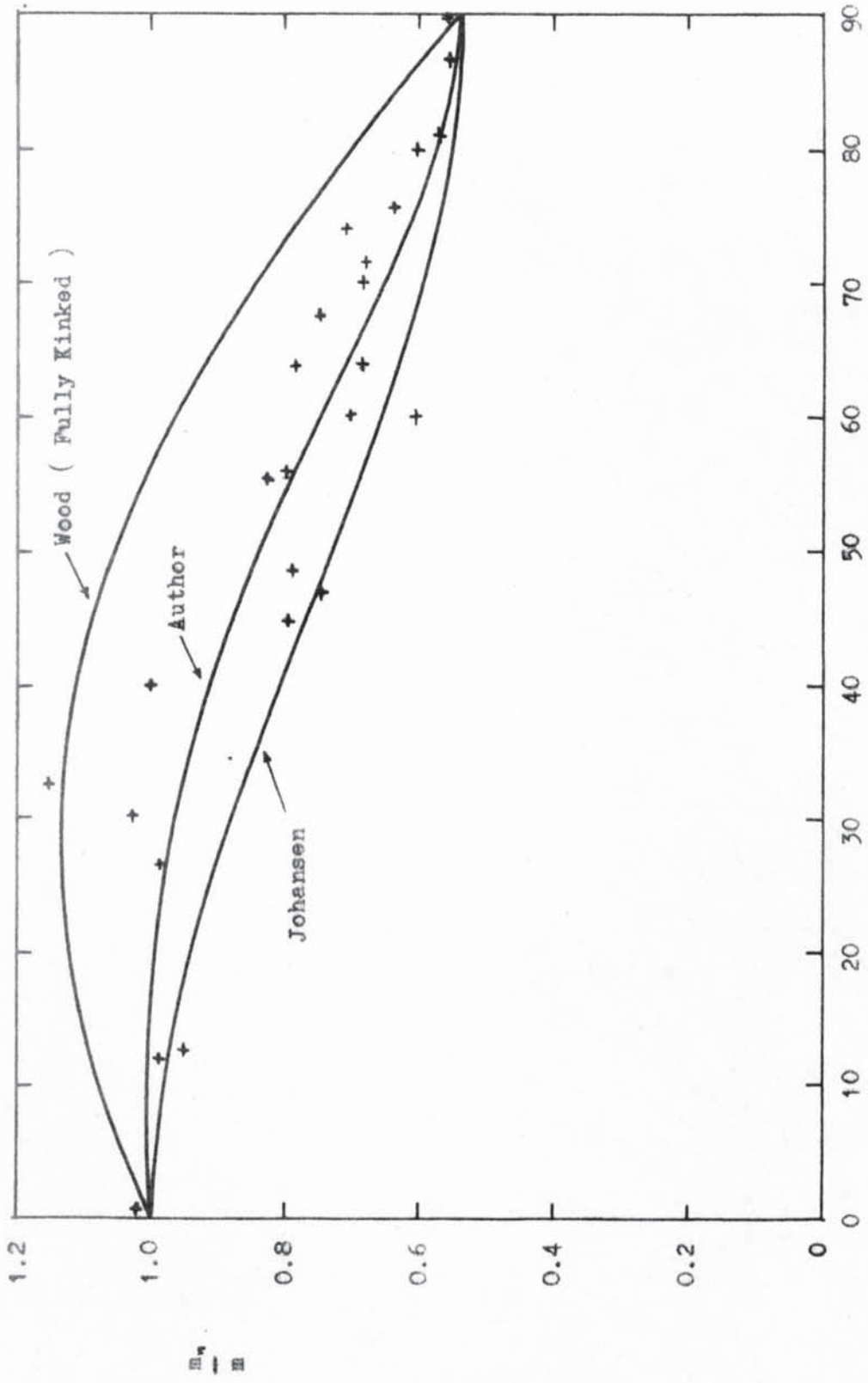

Figure 6.8 m_u/m V.S Alpha at failure (μ=0.54) DOWNHAM'S RESULTS

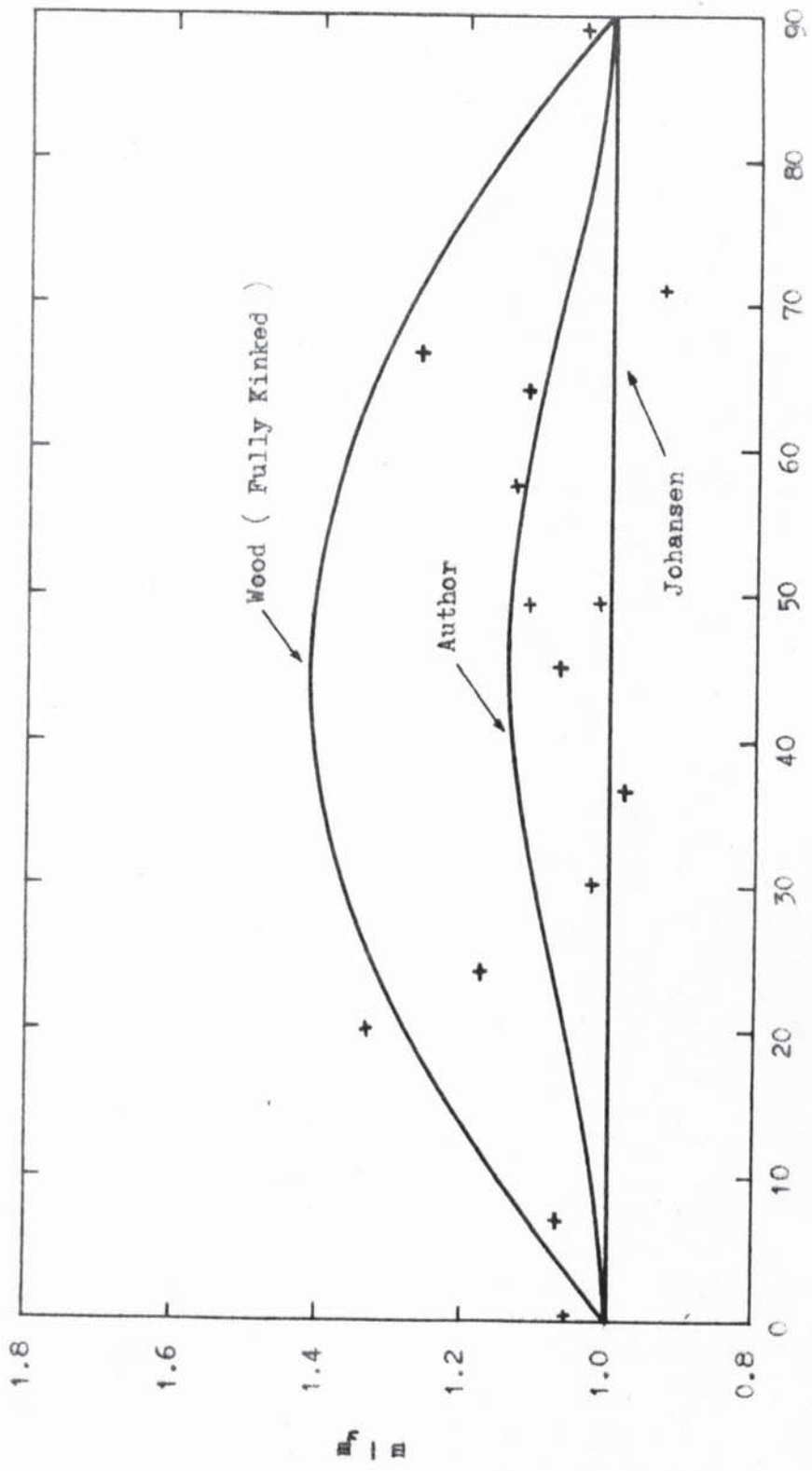

Figure 6.9 m_h/m V.S alpha at failure (μ=1.0) DOWNHAM'S RESULTS

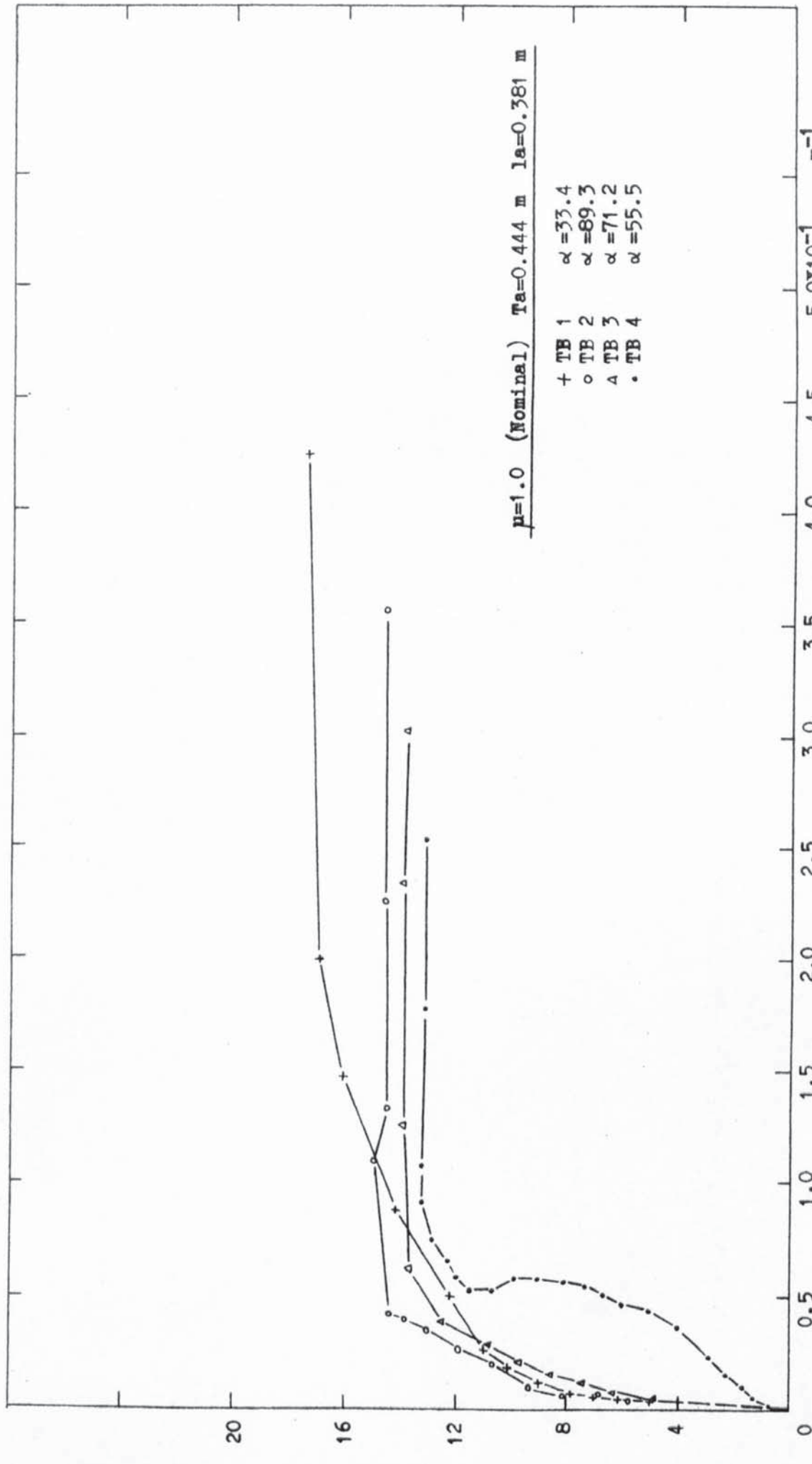

Figure 6.10 PLOT OF MAXIMUM PRINCIPAL CURVATURE

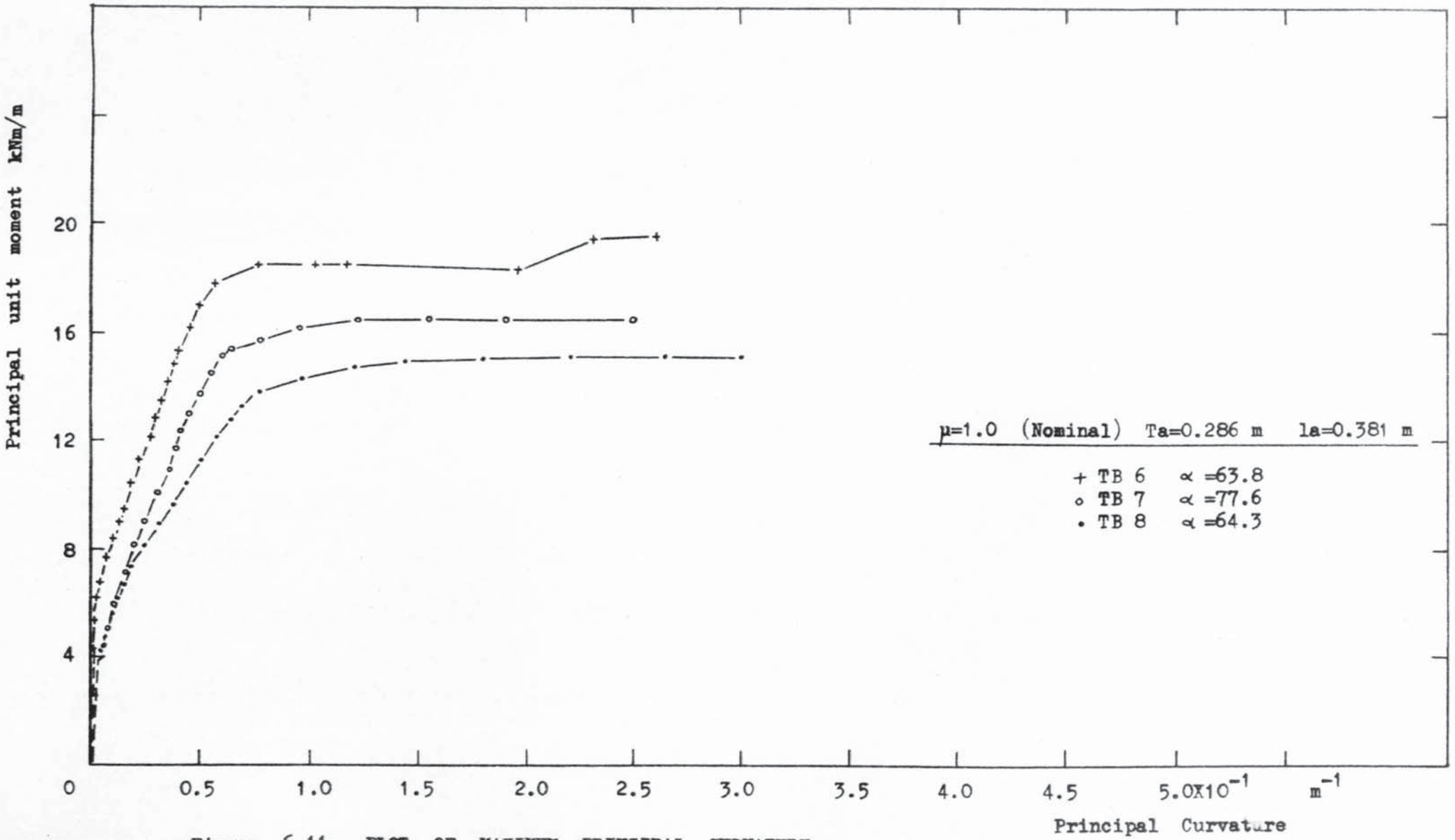

Figure 6.11 PLOT OF MAXIMUM PRINCIPAL CURVATURE

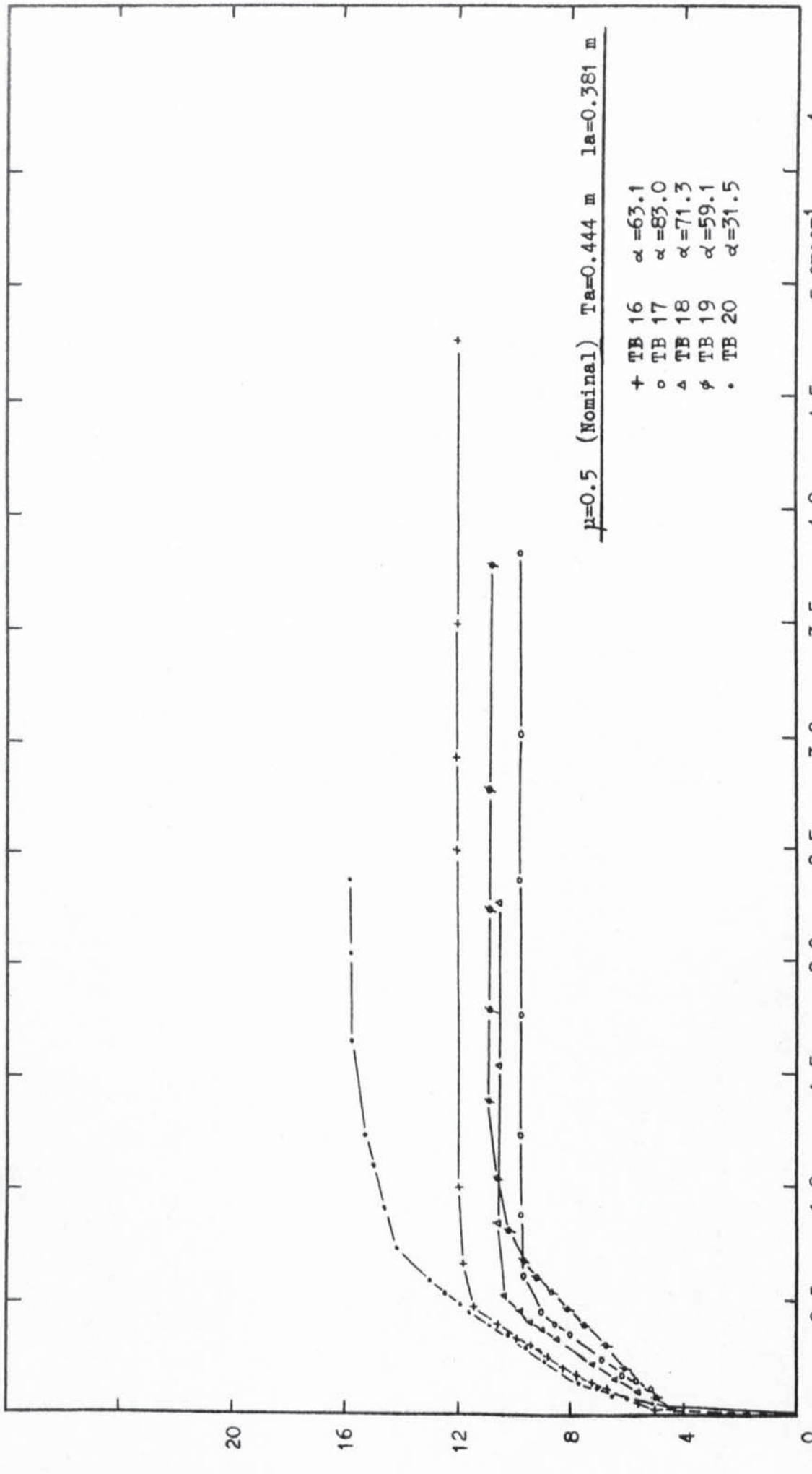

Figure 6.12 PLOT OF MAXIMUM PRINCIPAL CURVATURE

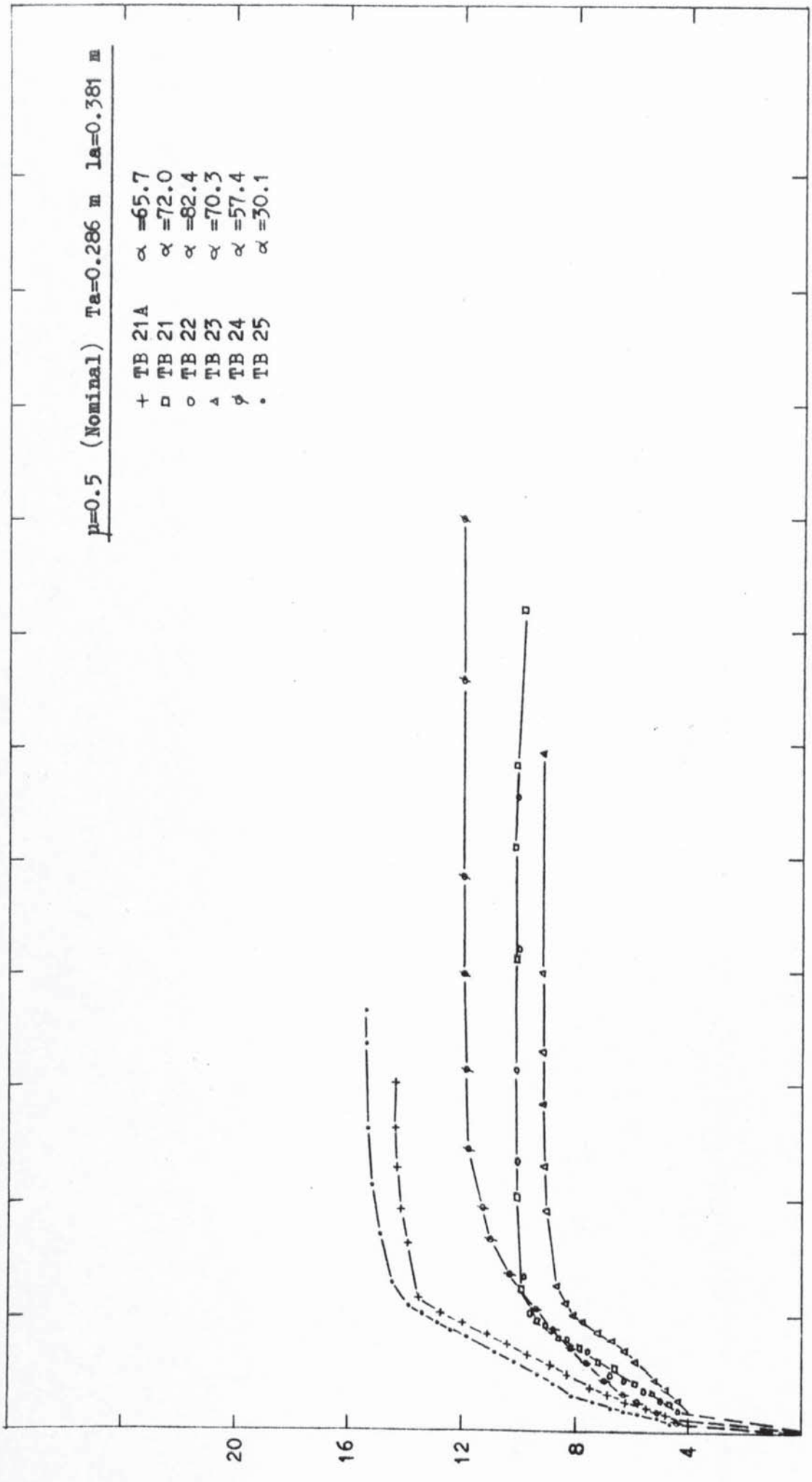

Figure 6.13 PLOT OF MAXIMUM PRINCIPAL CURVATURE

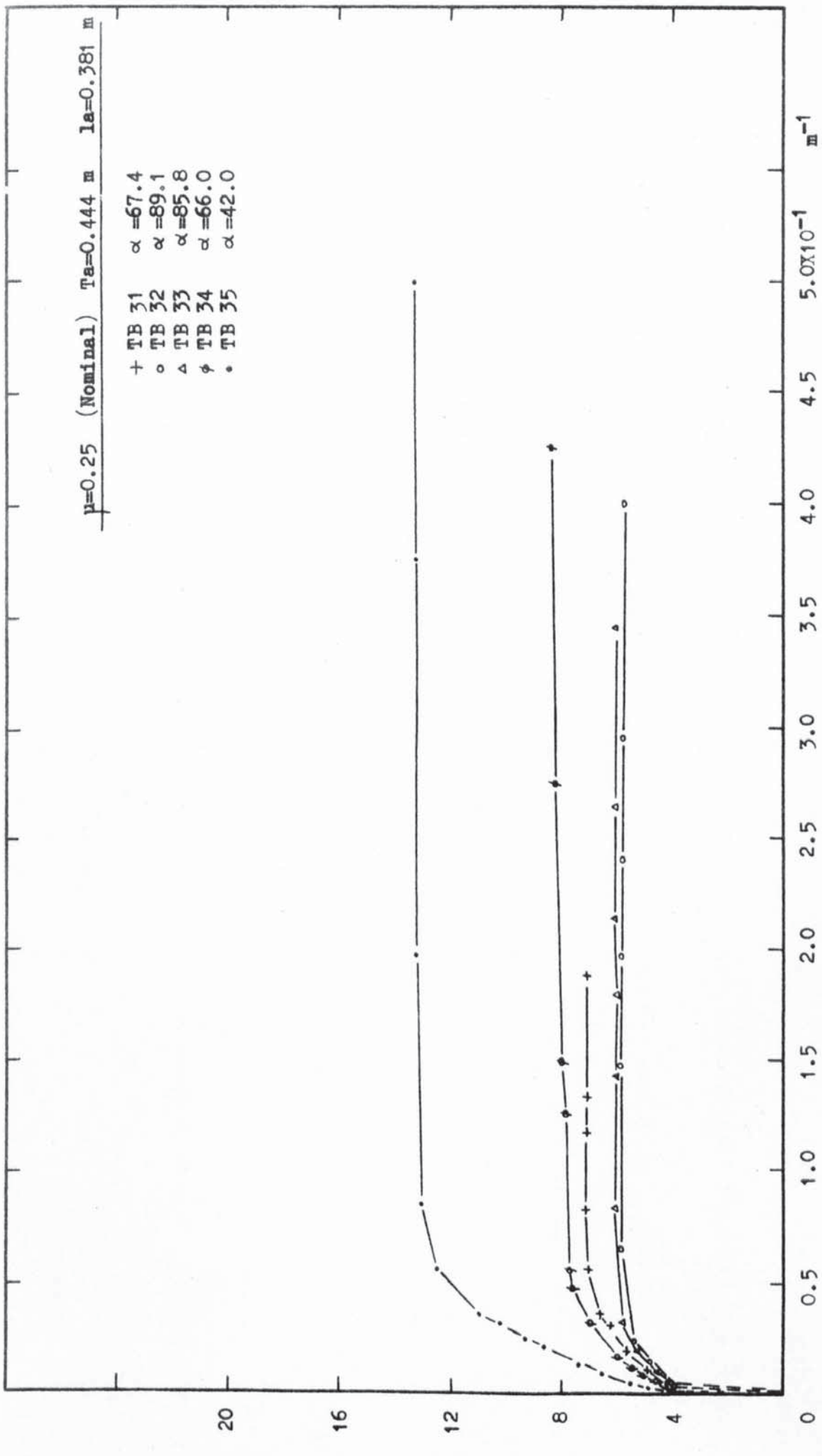

Figure 6.14 PLOT OF MAXIMUM PRINCIPAL CURVATURE

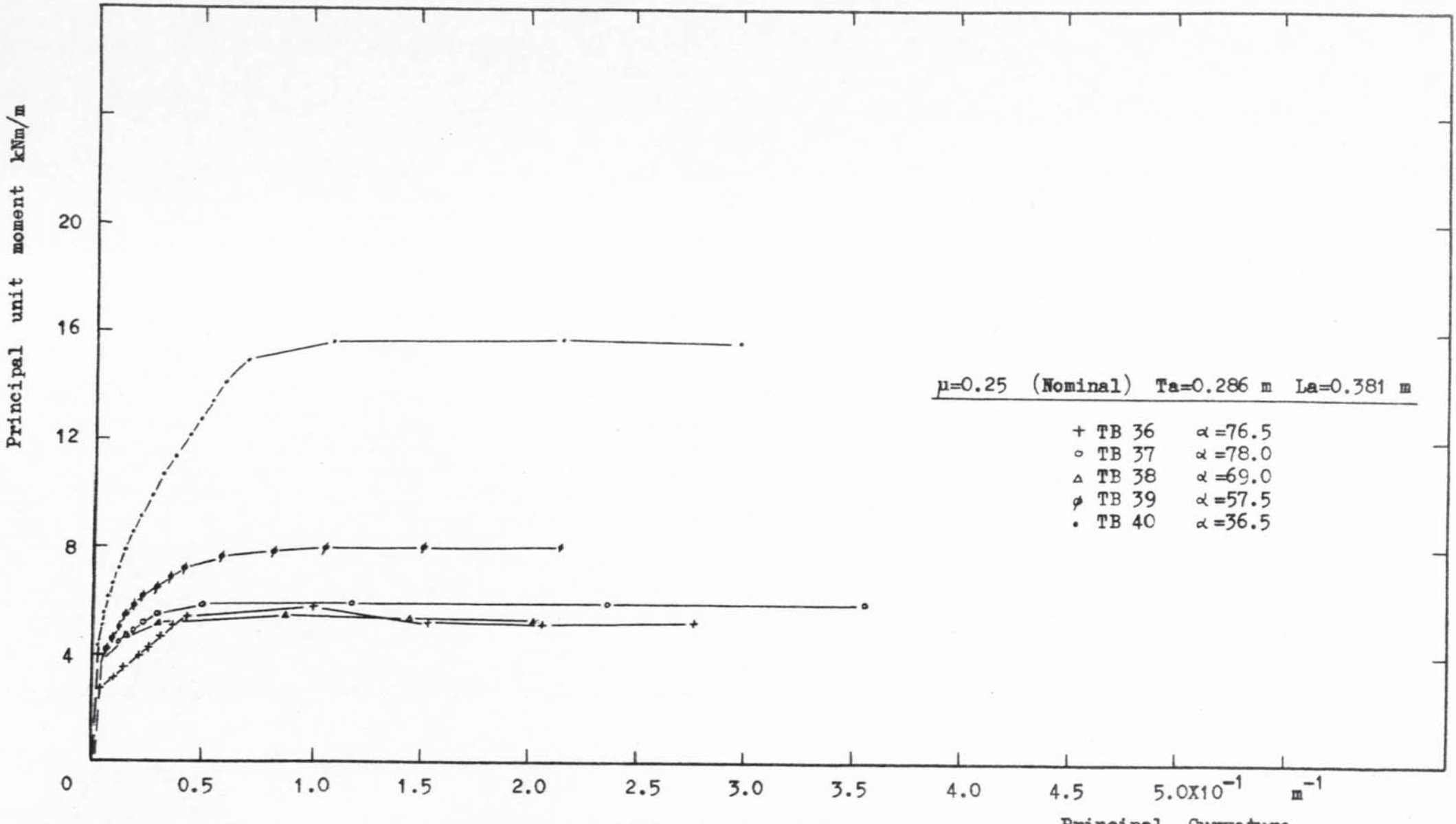

Figure 6.15 PLOT OF MAXIMUM PRINCIPAL CURVATURE

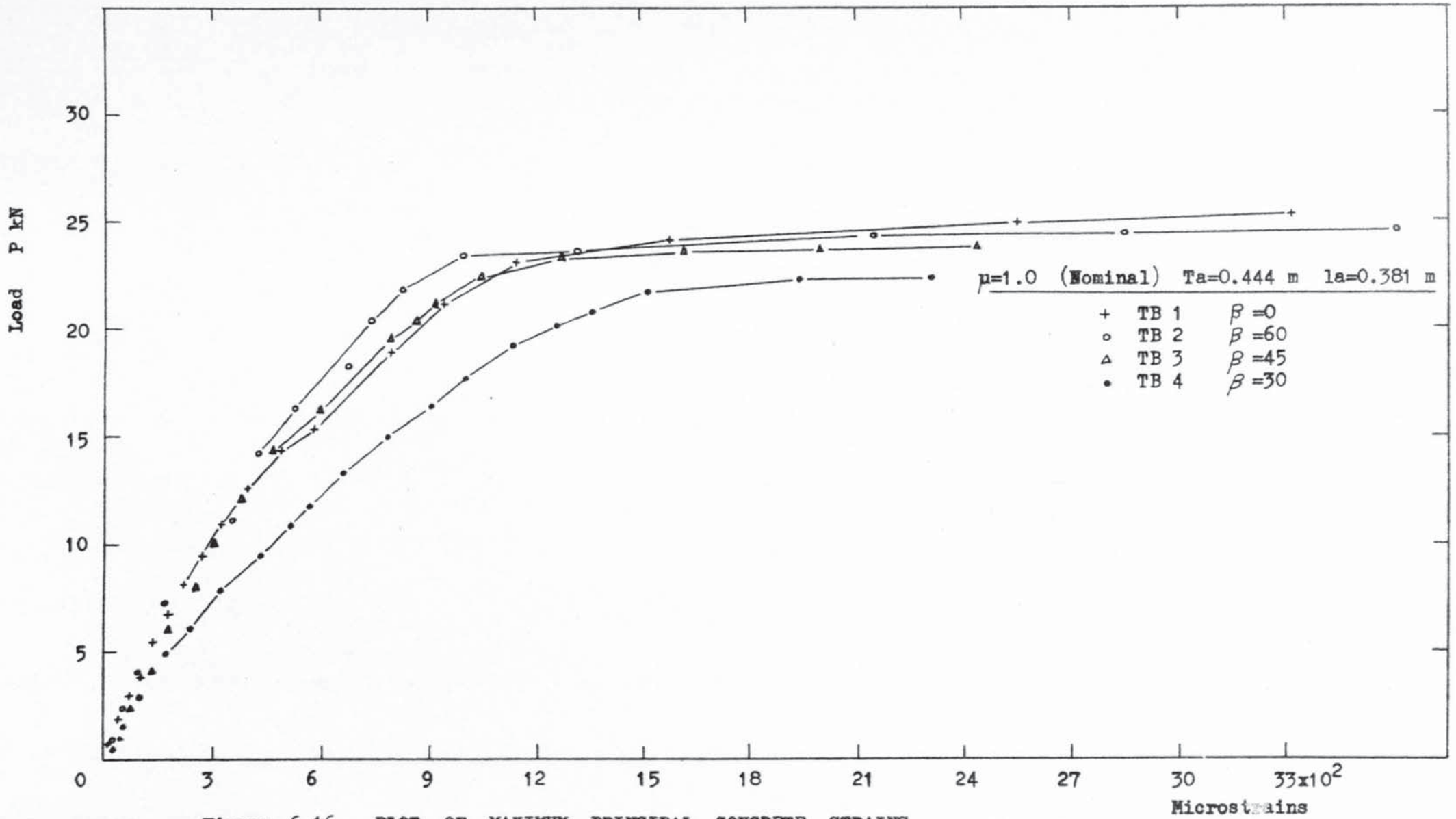

Figure 6.16 PLOT OF MAXIMUM PRINCIPAL CONCRETE STRAINS

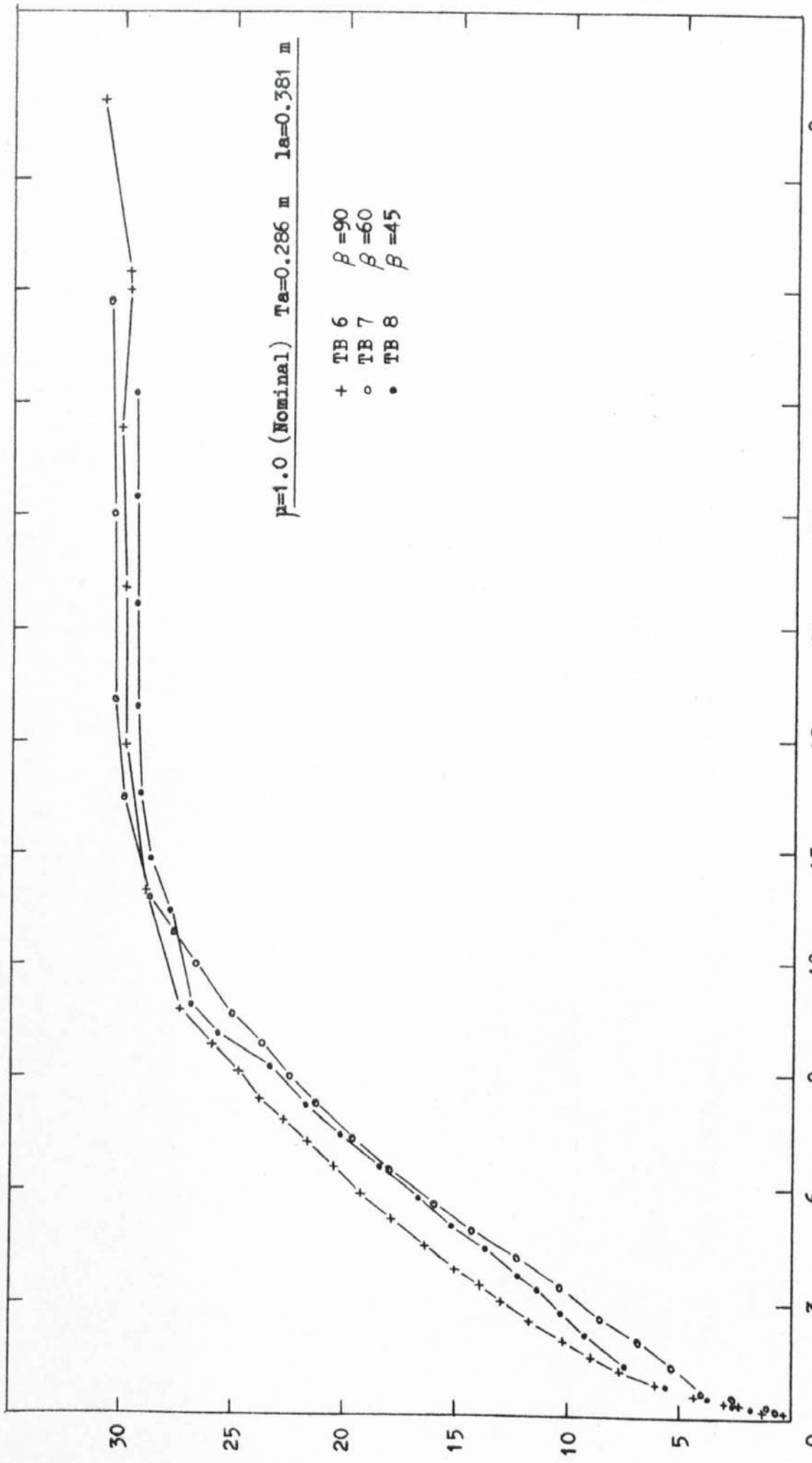

Figure 6.17 PLOT OF MAXIMUM PRINCIPAL CONCRETE STRAINS

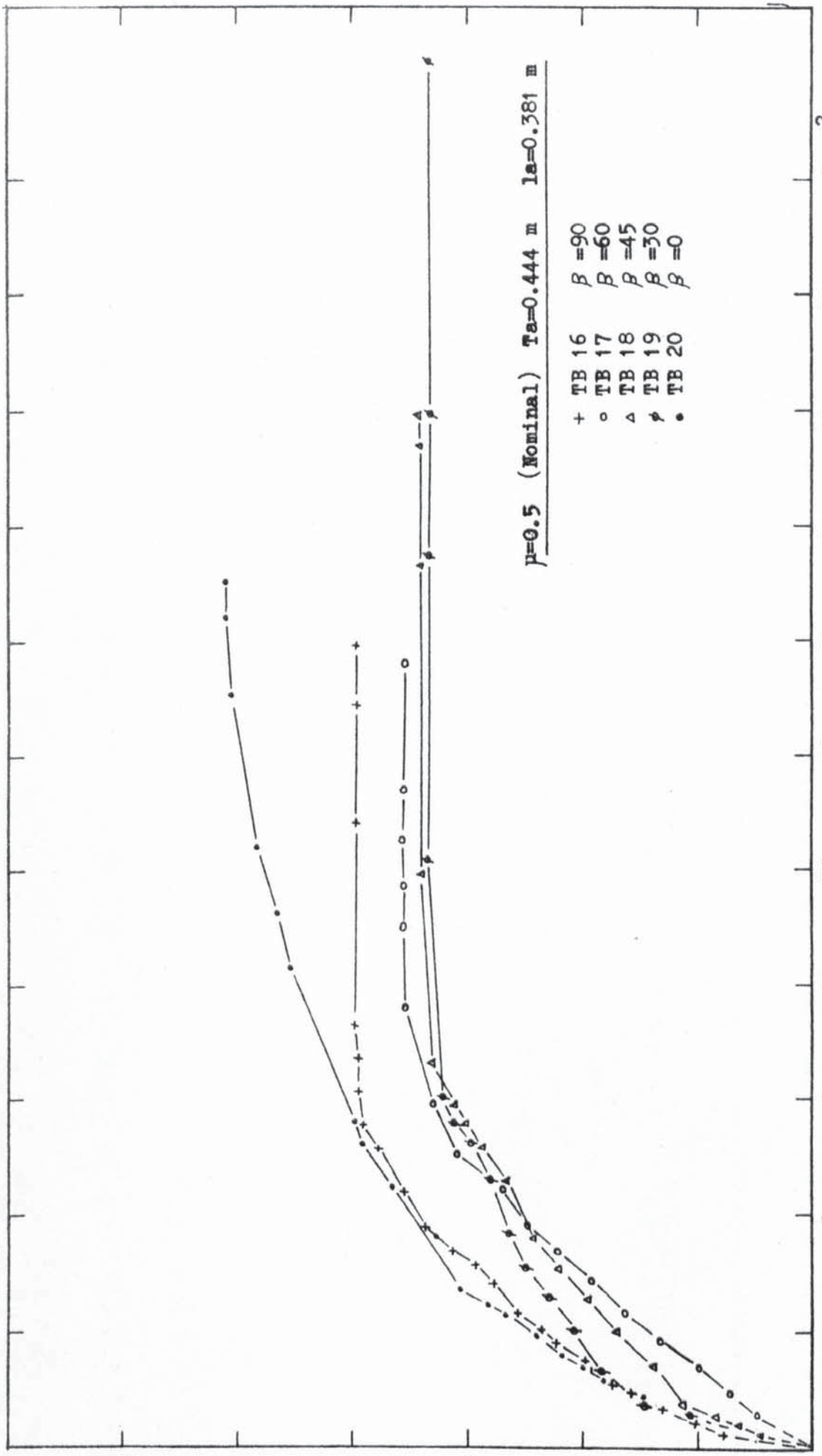

Figure 6.18 PLOT OF MAXIMUM PRINCIPAL CONCRETE STRAINS

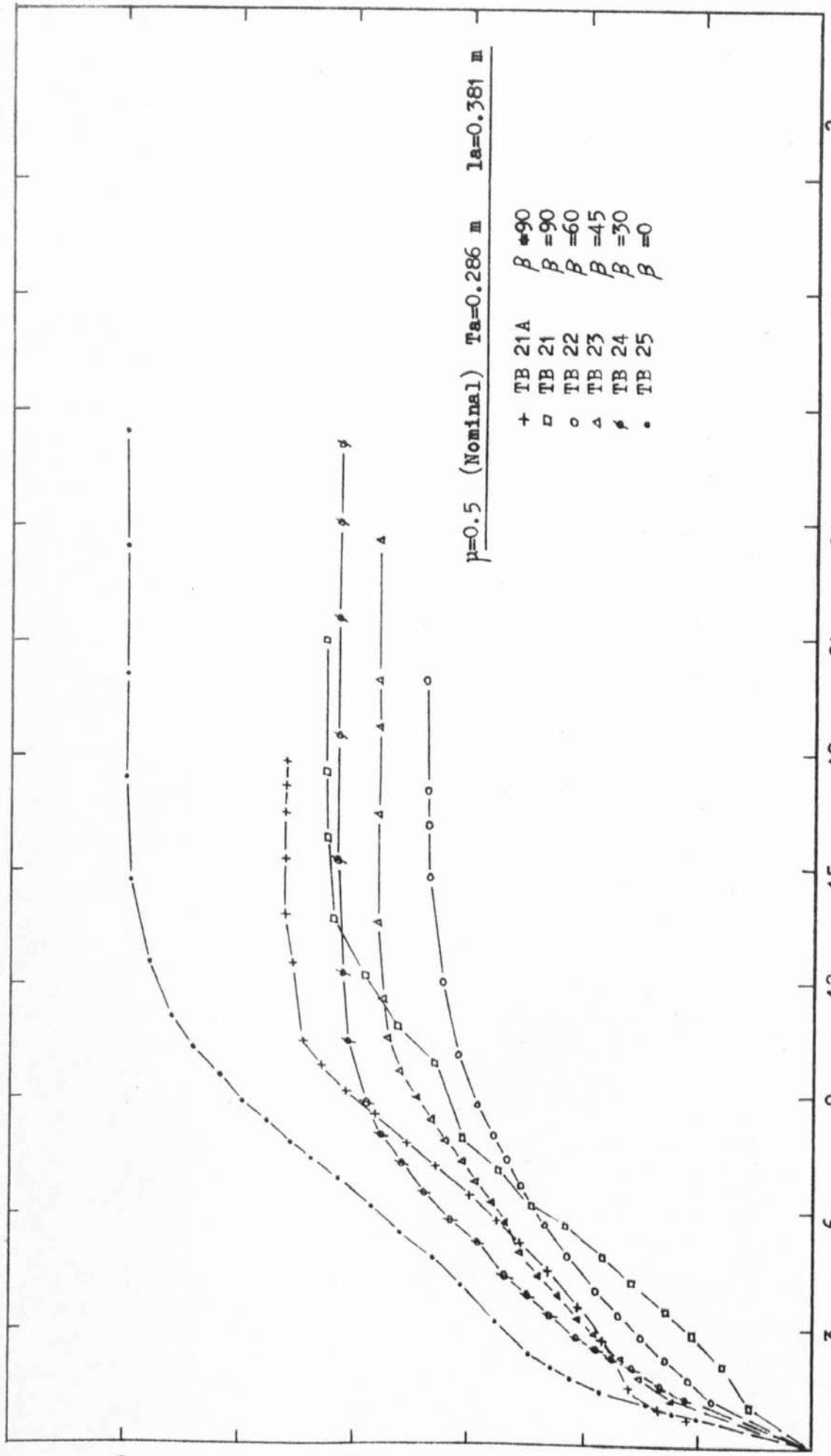

Figure 6.19 PLOT OF MAXIMUM PRINCIPAL CONCRETE STRAINS

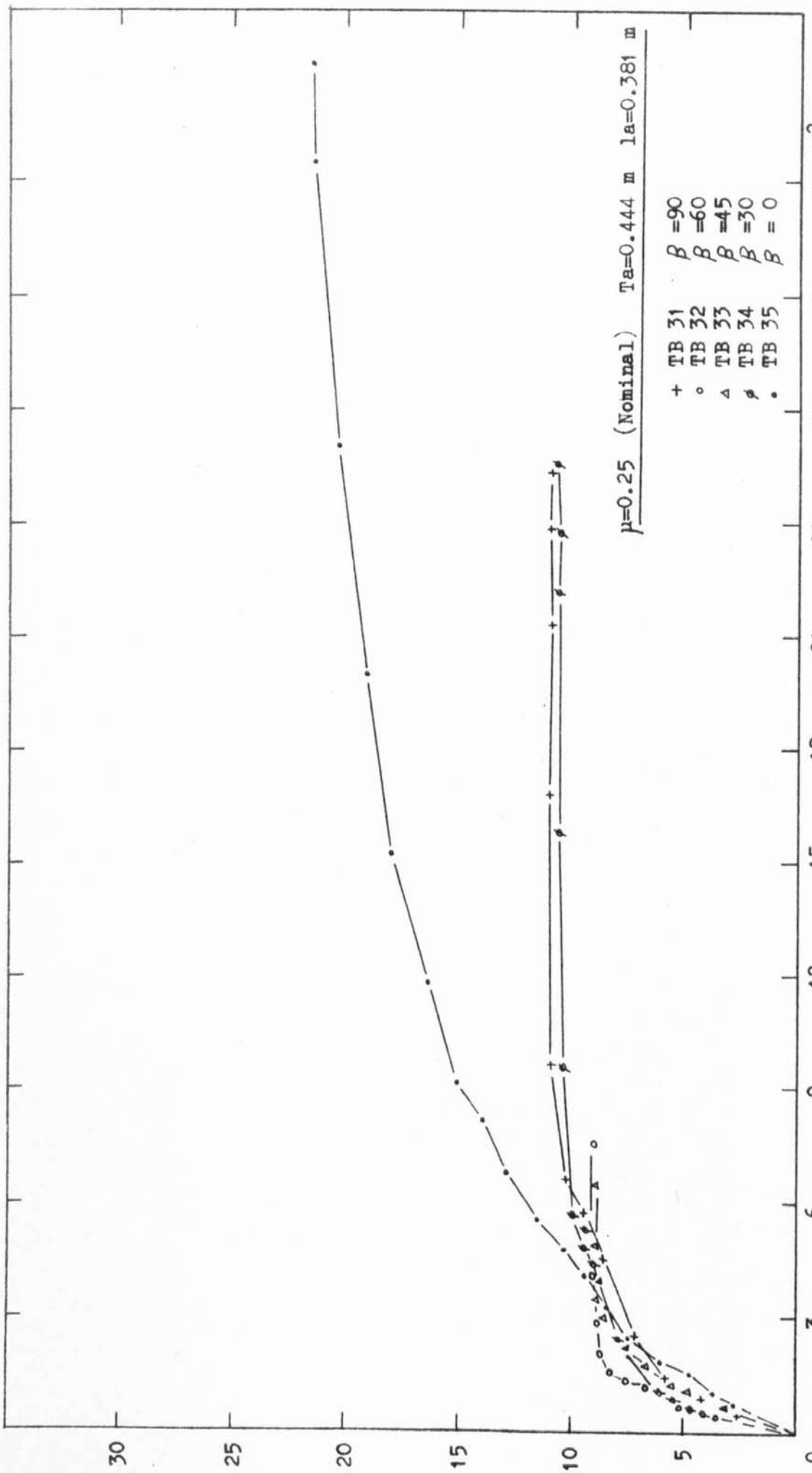

Figure 6.20 PLOT OF MAXIMUM PRINCIPAL CONCRETE STRAINS

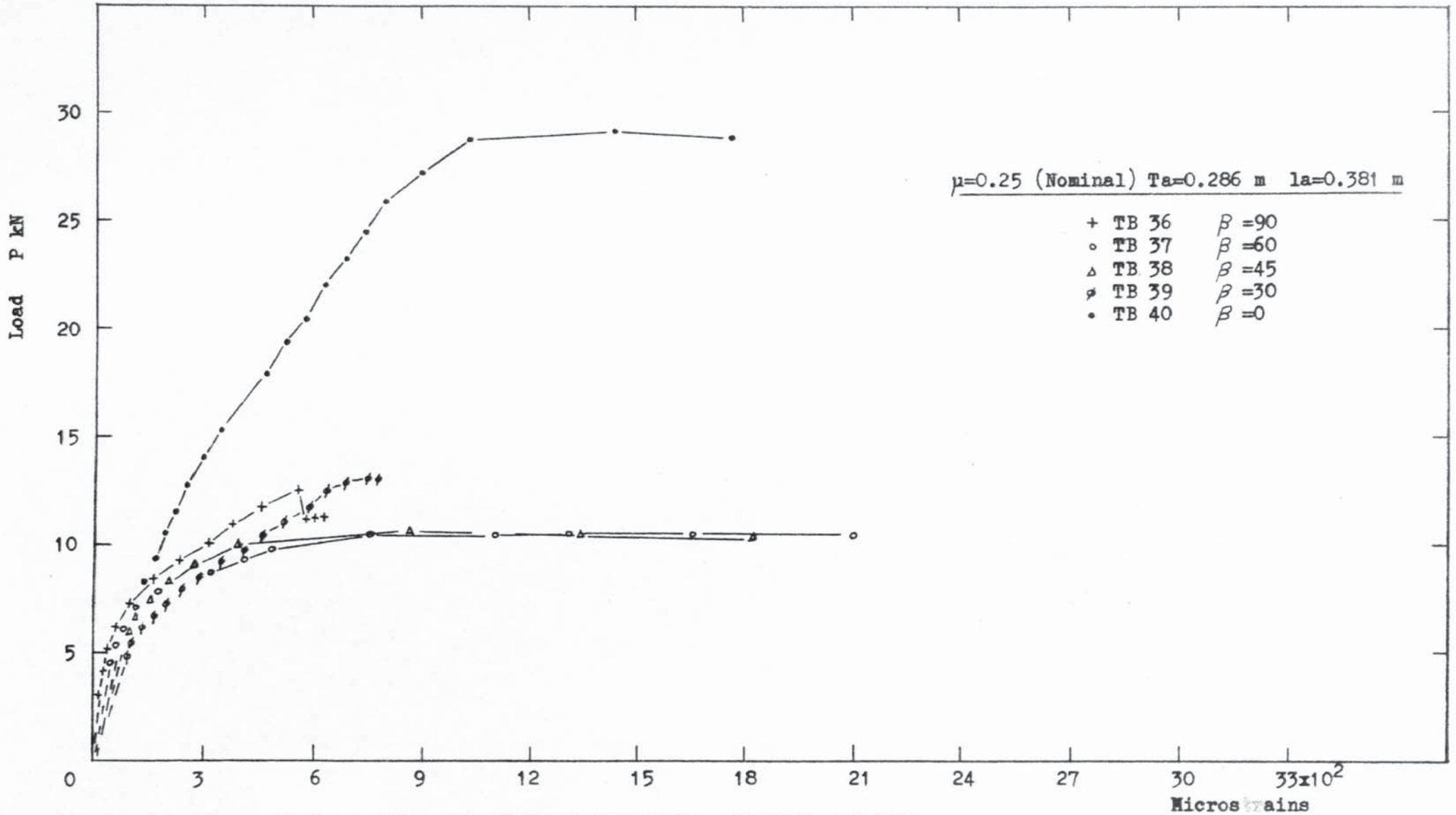

Figure 6.21 PLOT OF MAXIMUM PRINCIPAL CONCRETE STRAINS

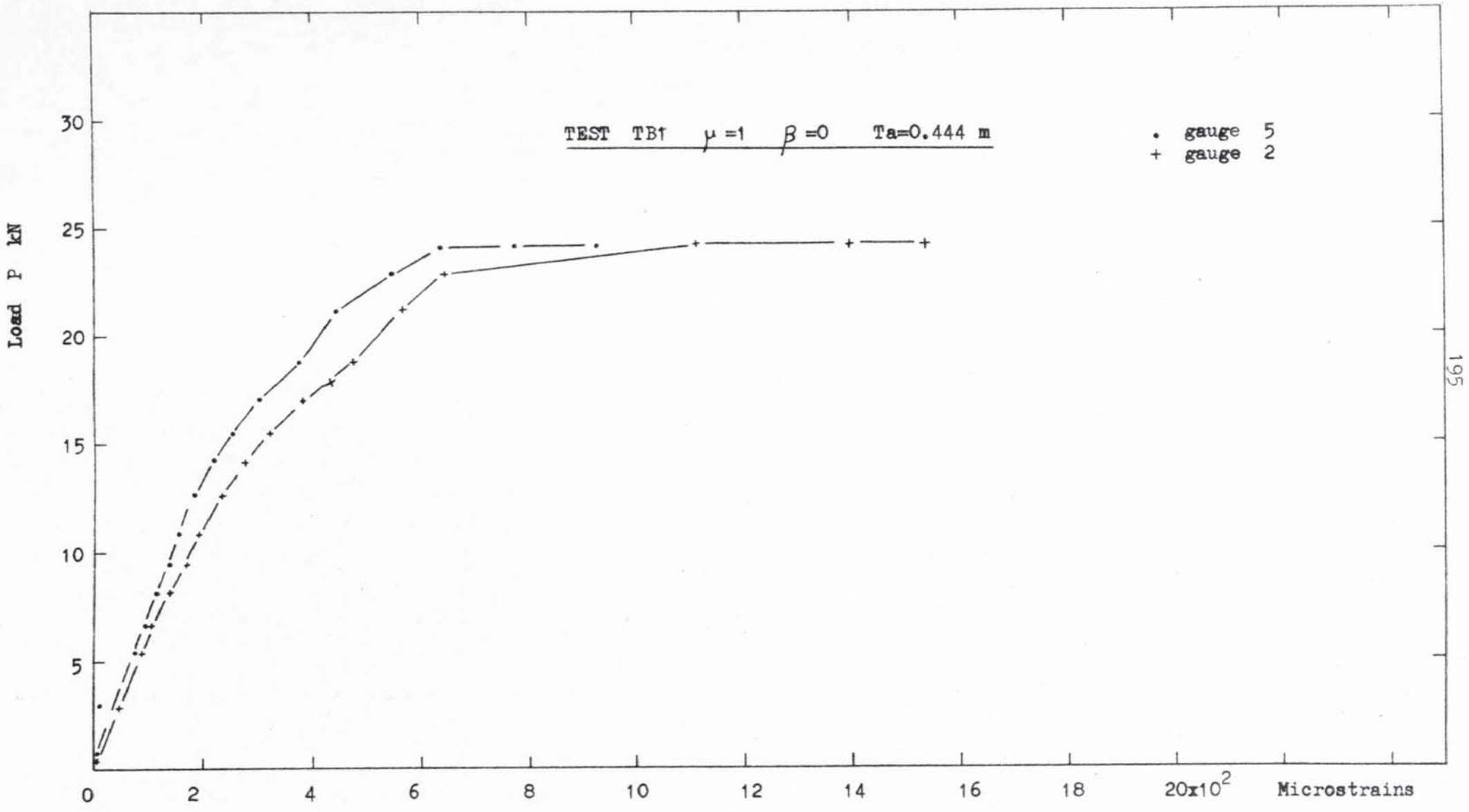

Figure 6.22 PLOT OF STEEL STRAIN

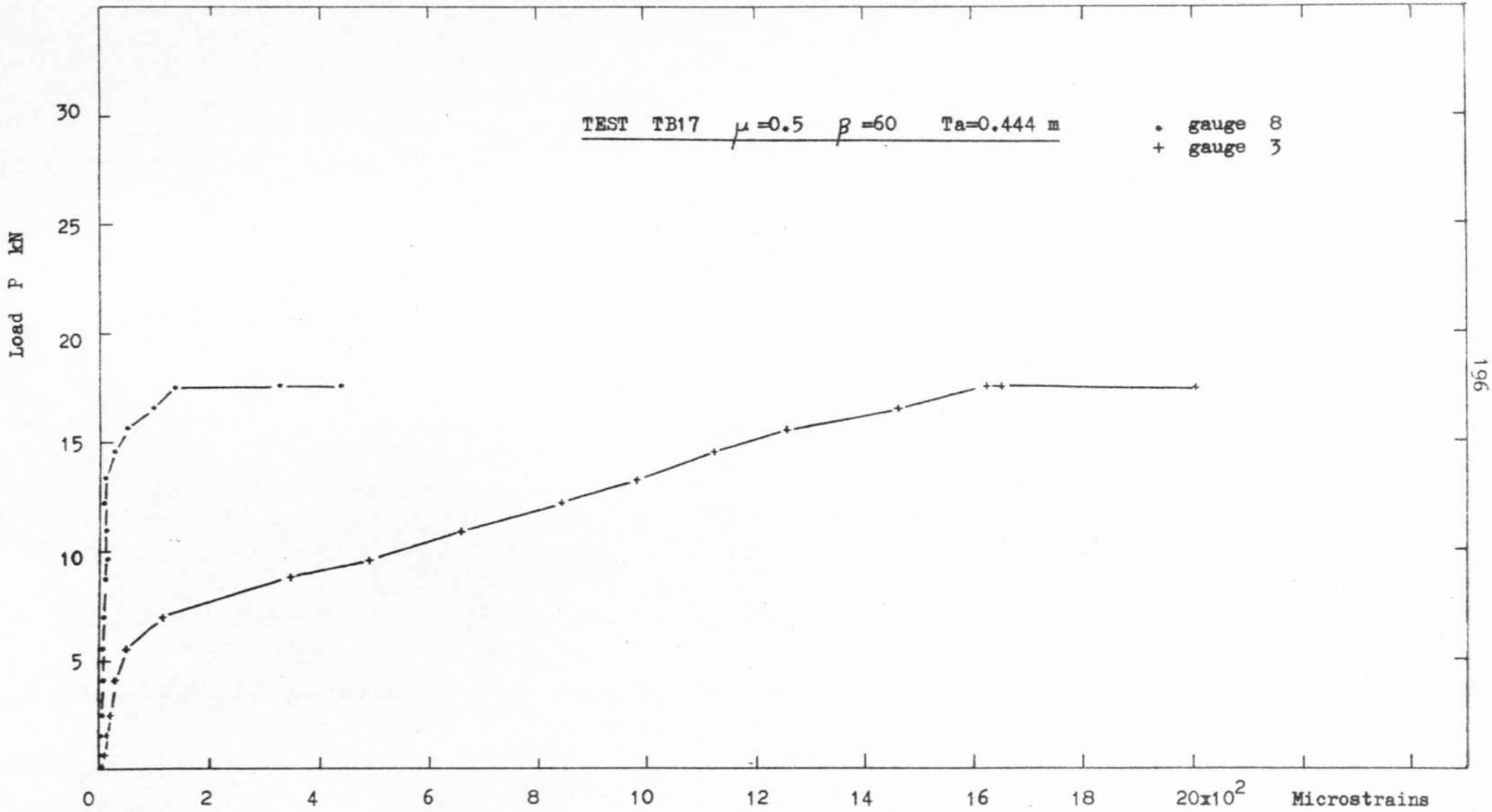

Figure 6.23 PLOT OF STEEL STRAIN

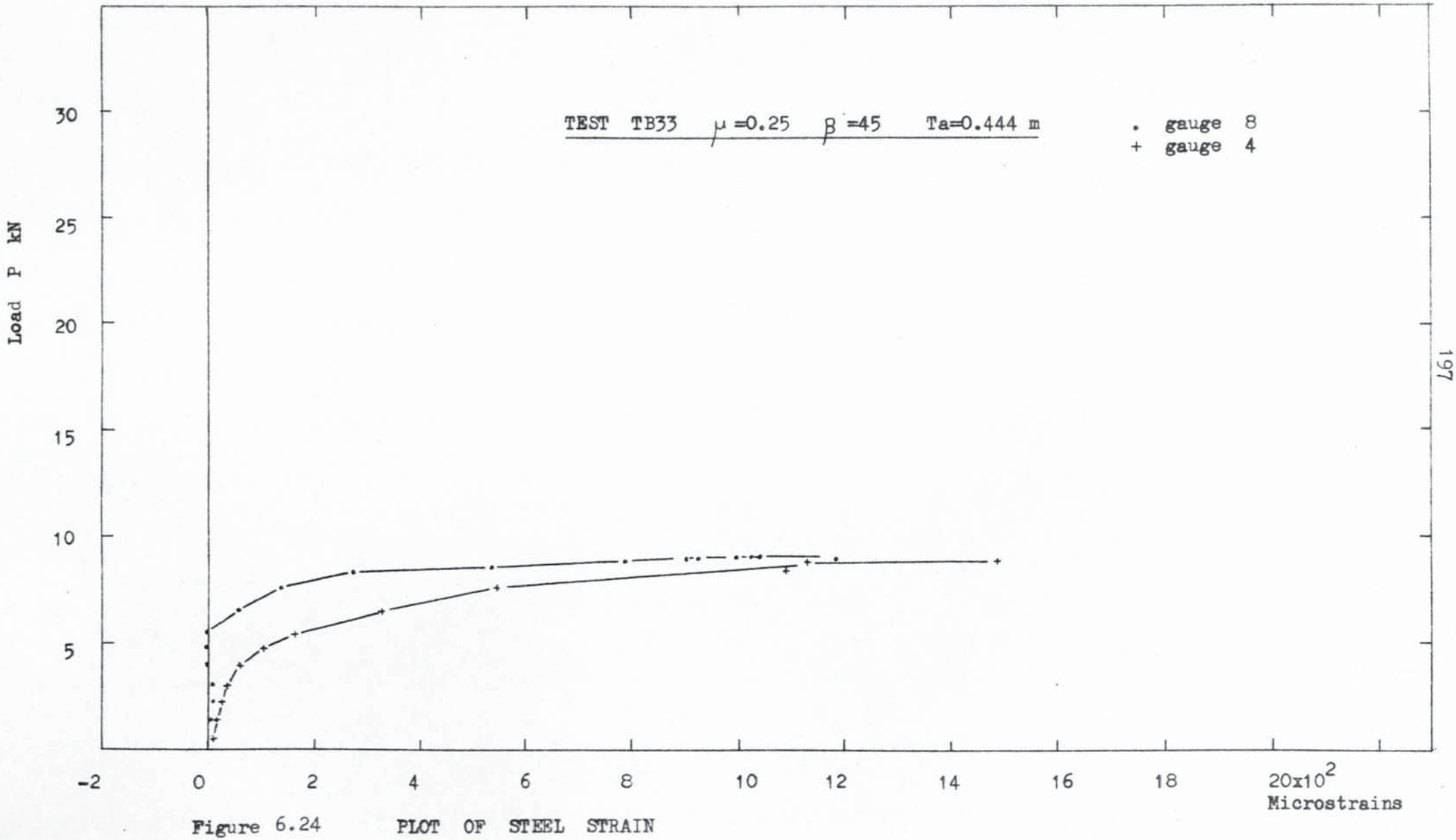

Figure 6.24 PLOT OF STEEL STRAIN

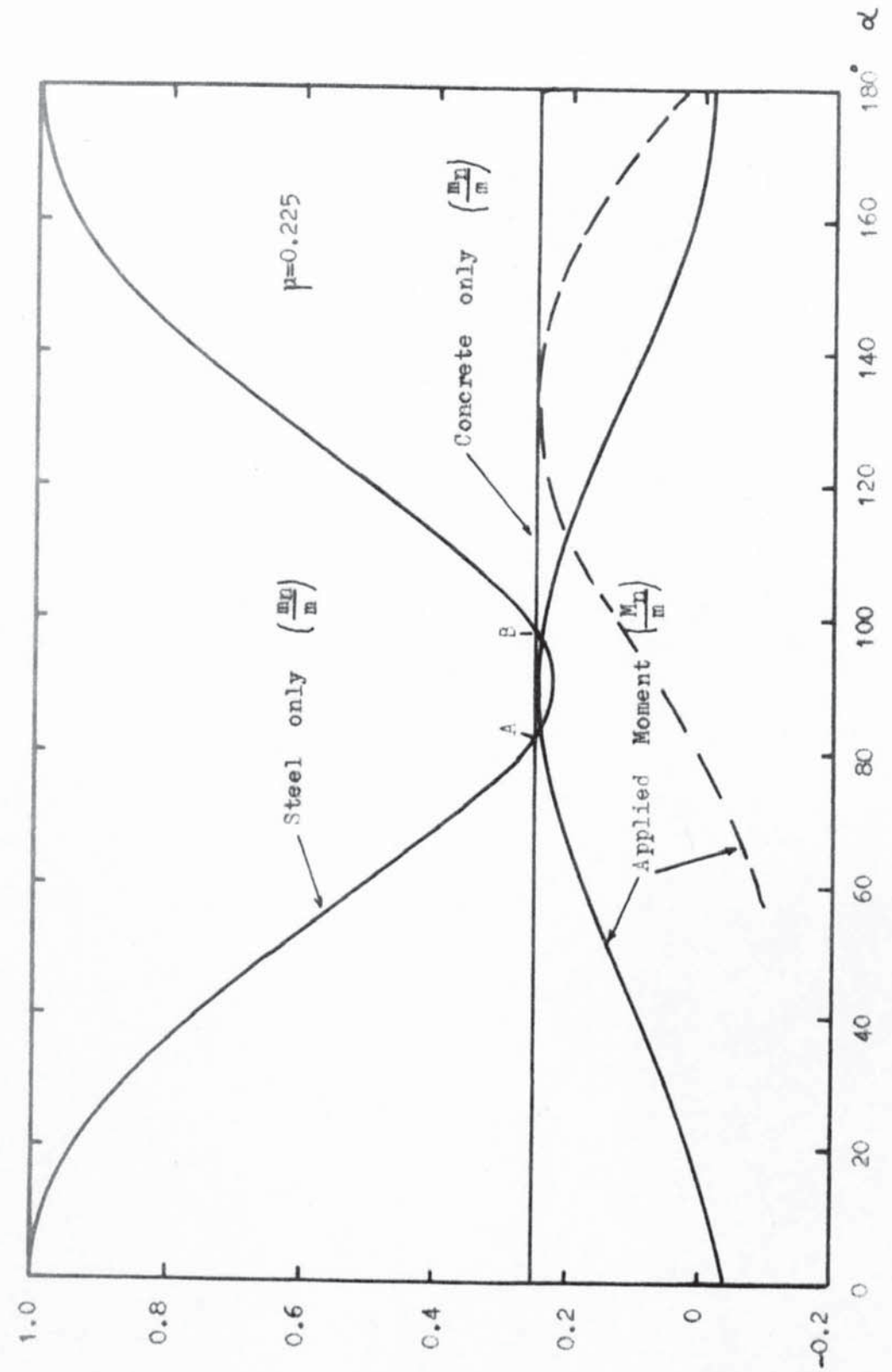

Figure 6.25 FAILURE IN SLAB

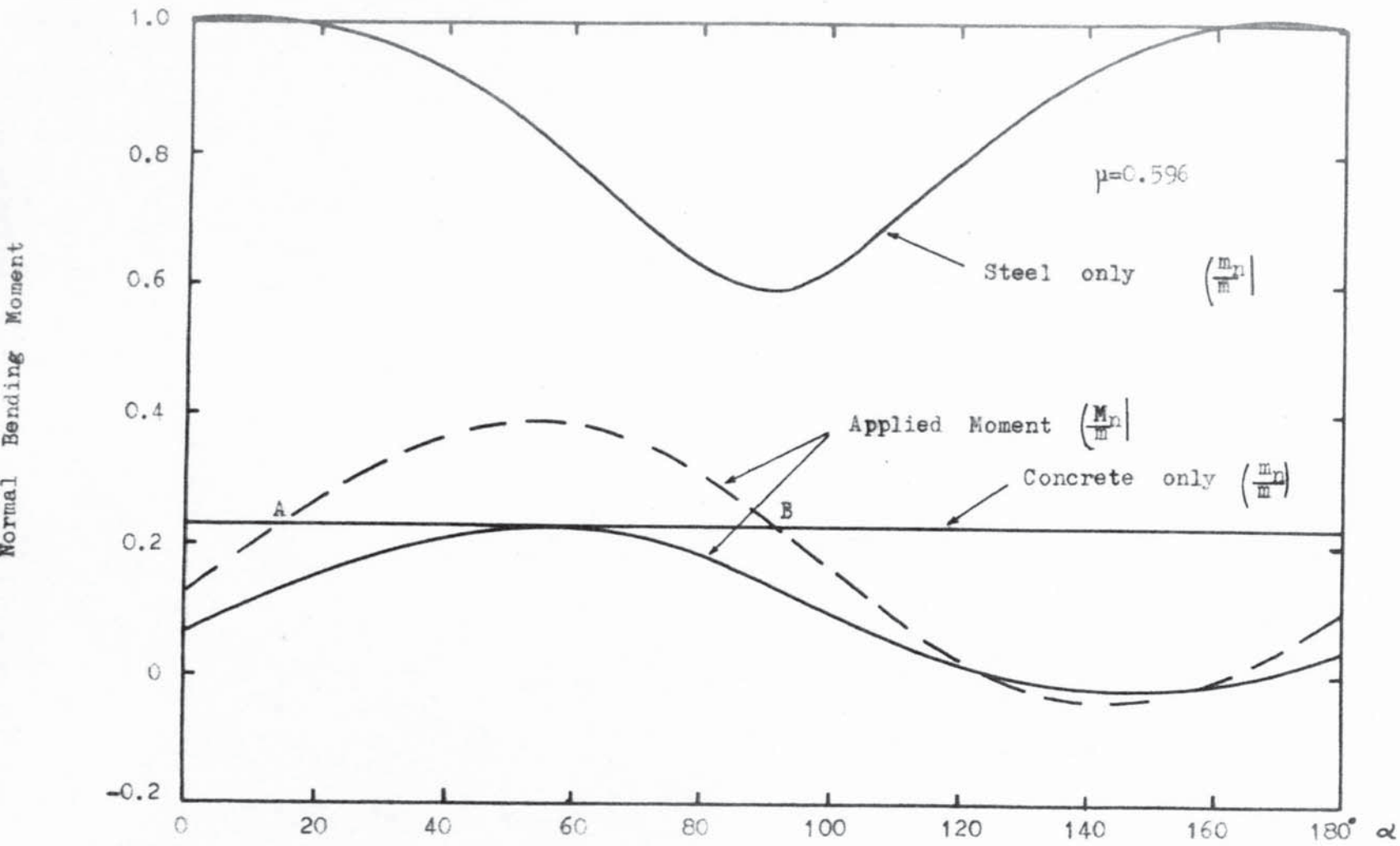

Figure 6.26 FAILURE IN SLAB

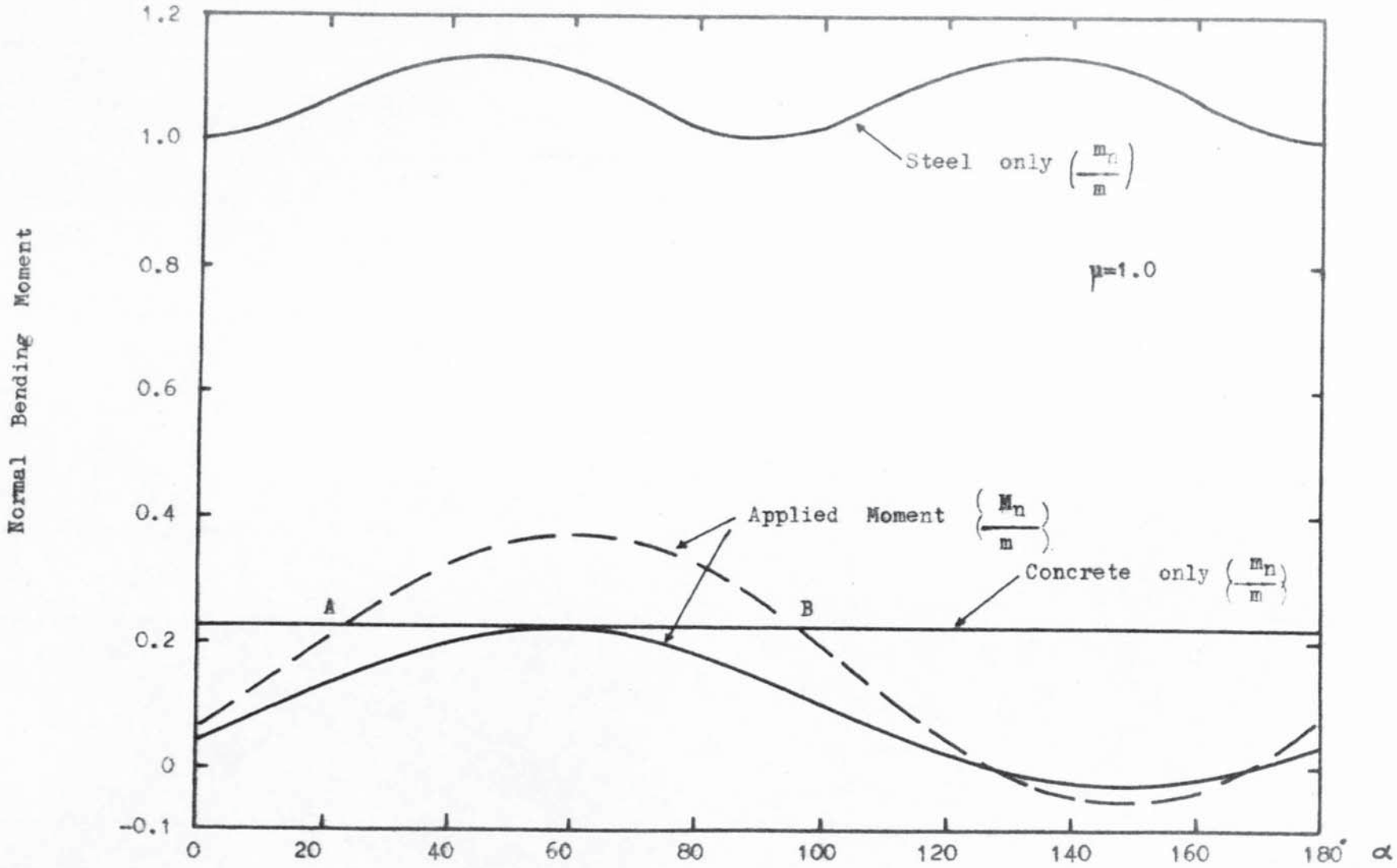

Figure 6.27 FAILURE IN SLAB

KEY TO PRINCIPAL DIRECTION GRAPHS

+	γ	Principal concrete strain direction
•	ω	Principal curvature direction
▬	η	Average measured yield line orientation
—	η_1	Principal Applied Moment direction

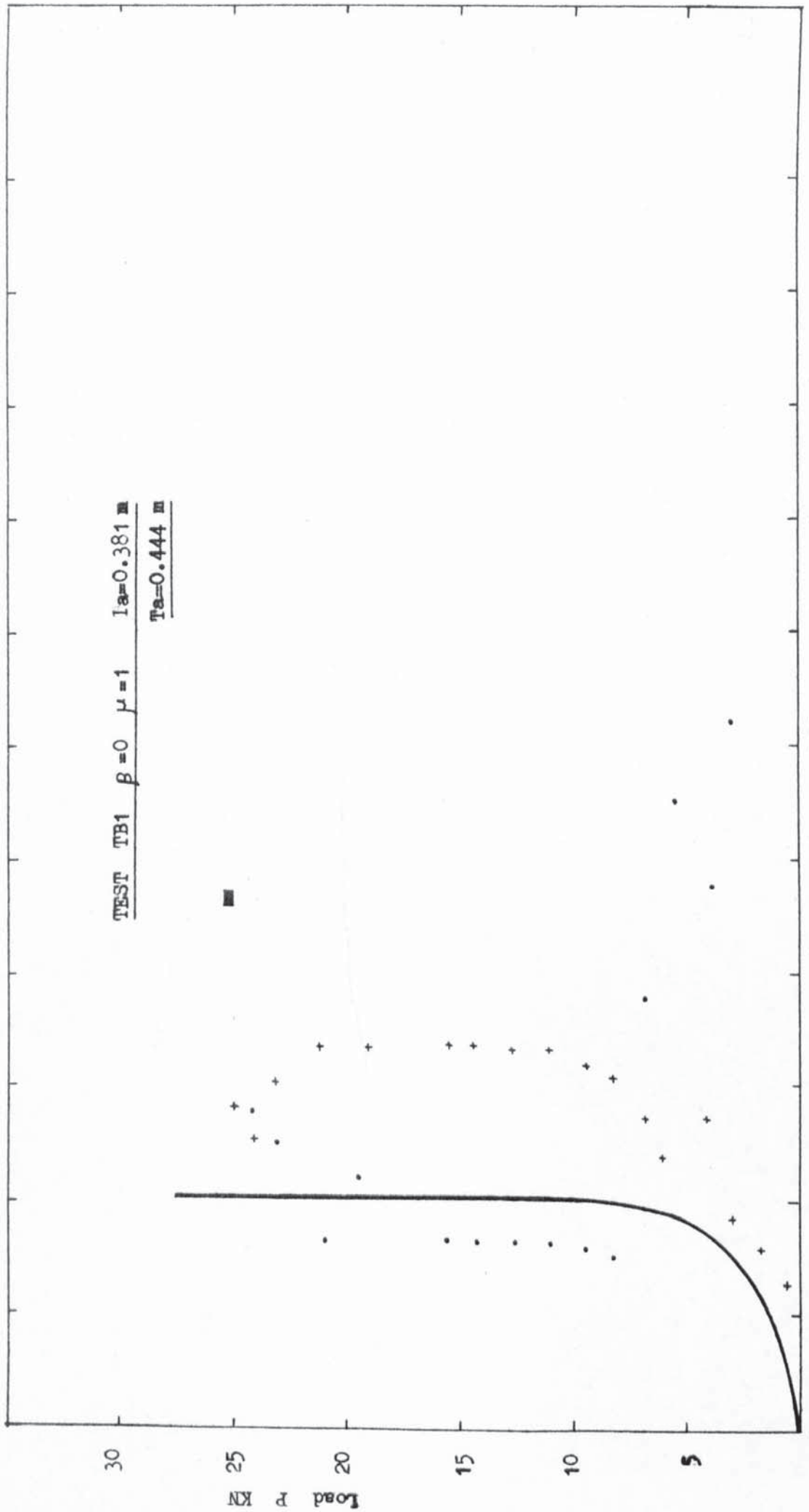

Figure 6.28 PLOT OF PRINCIPAL DIRECTIONS

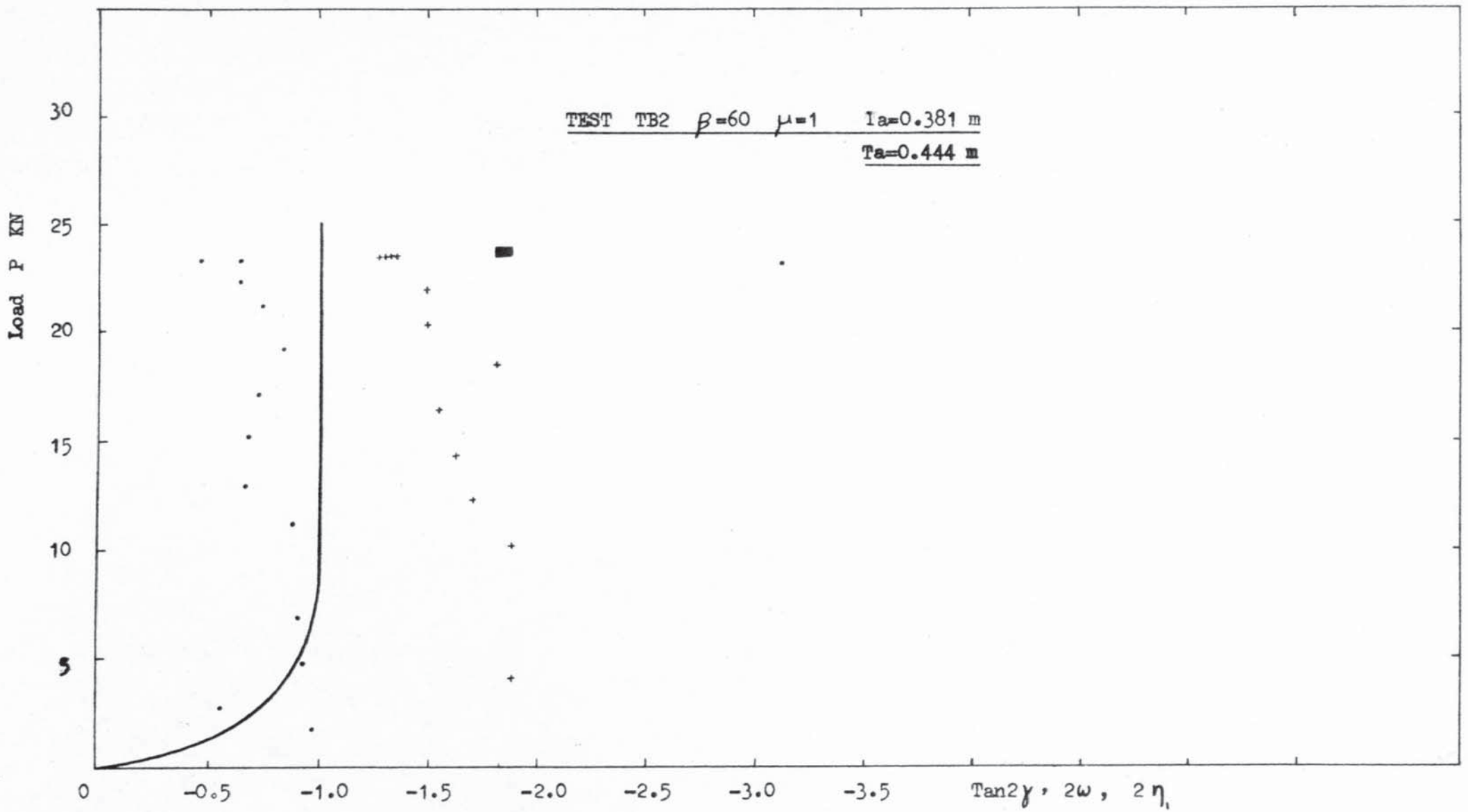

Figure 6.29 PLOT OF PRINCIPAL DIRECTIONS

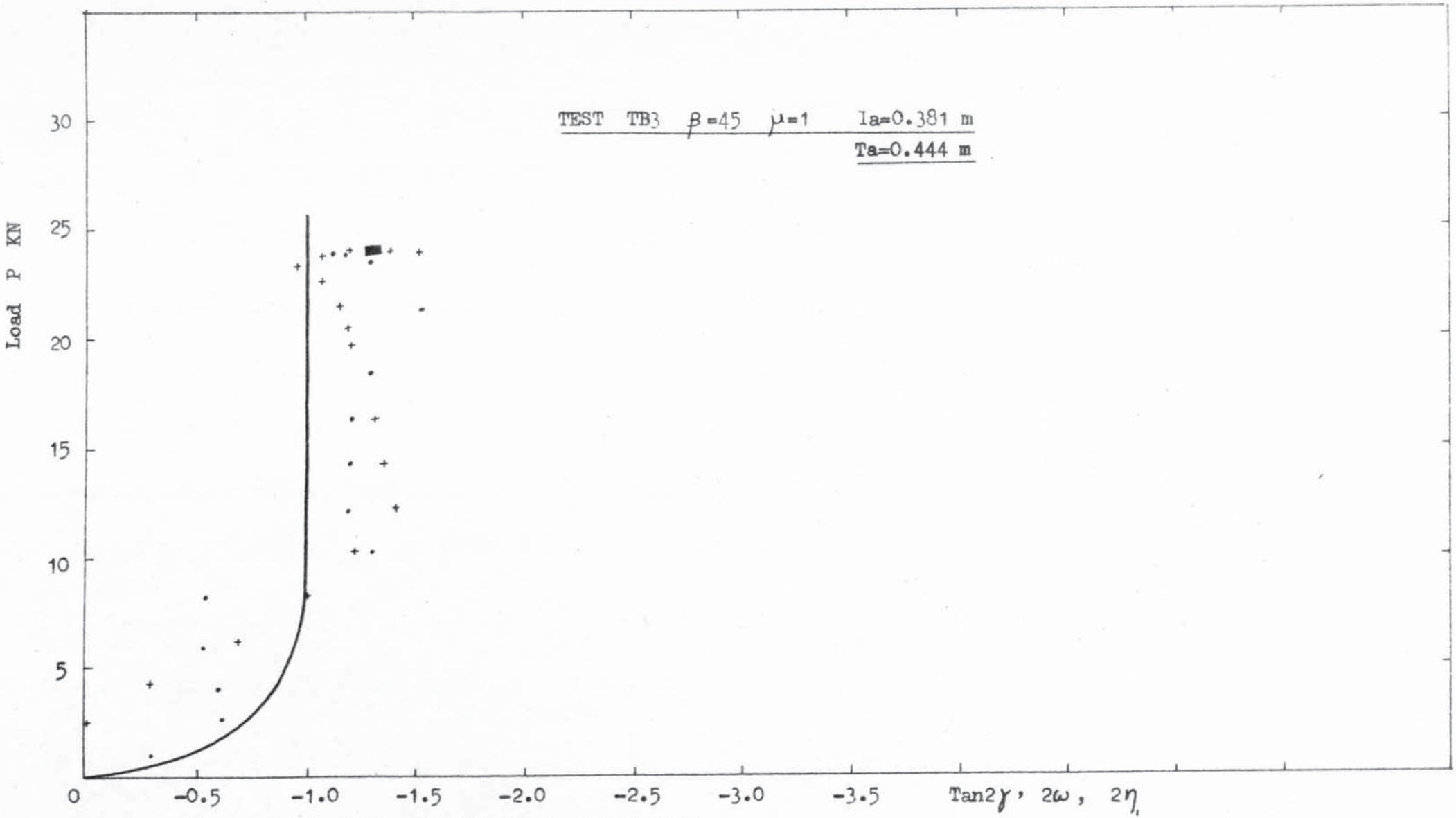

Figure 6.30 PLOT OF PRINCIPAL DIRECTIONS

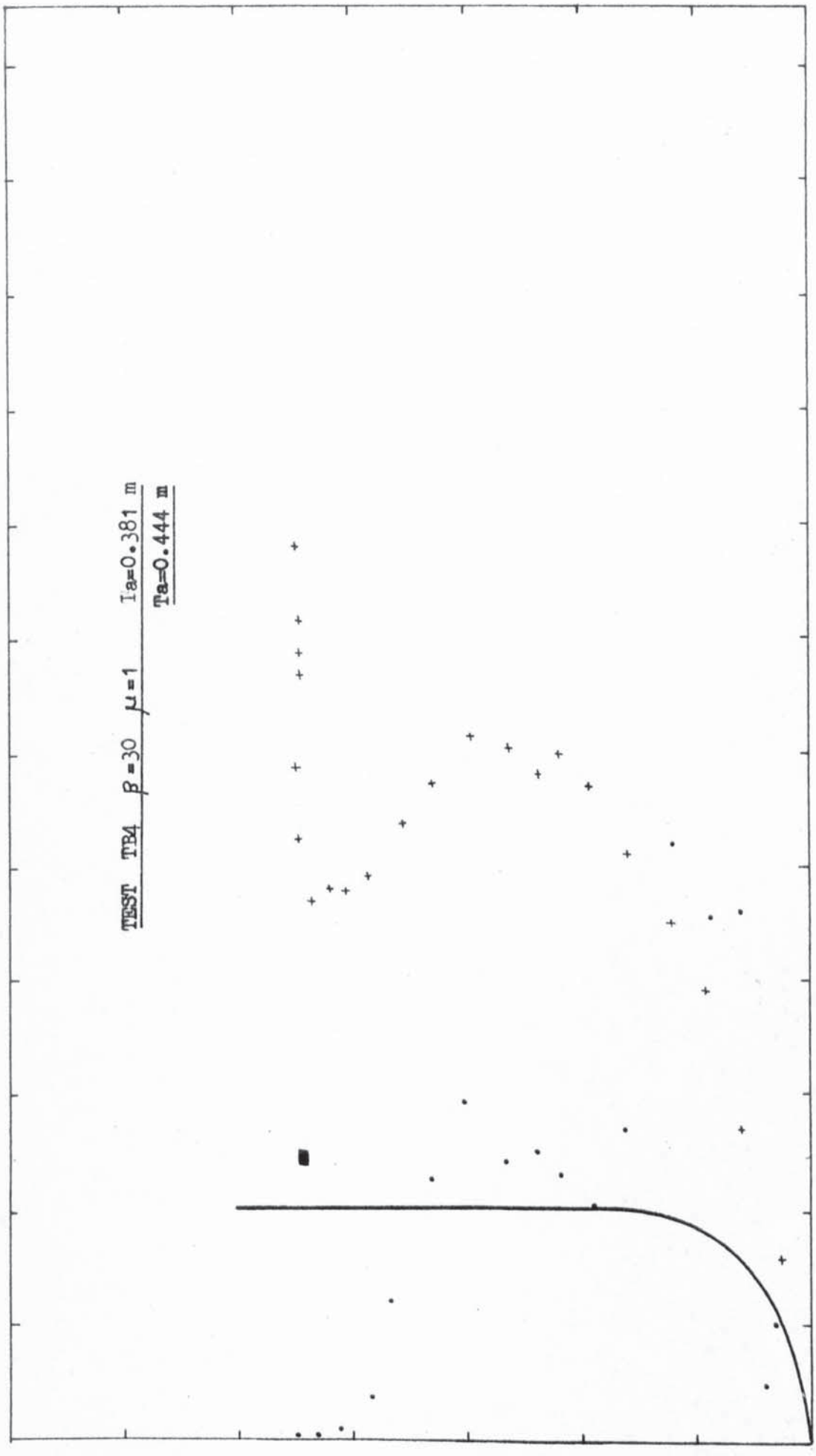

Figure6.31 PLOT OF PRINCIPAL DIRECTIONS

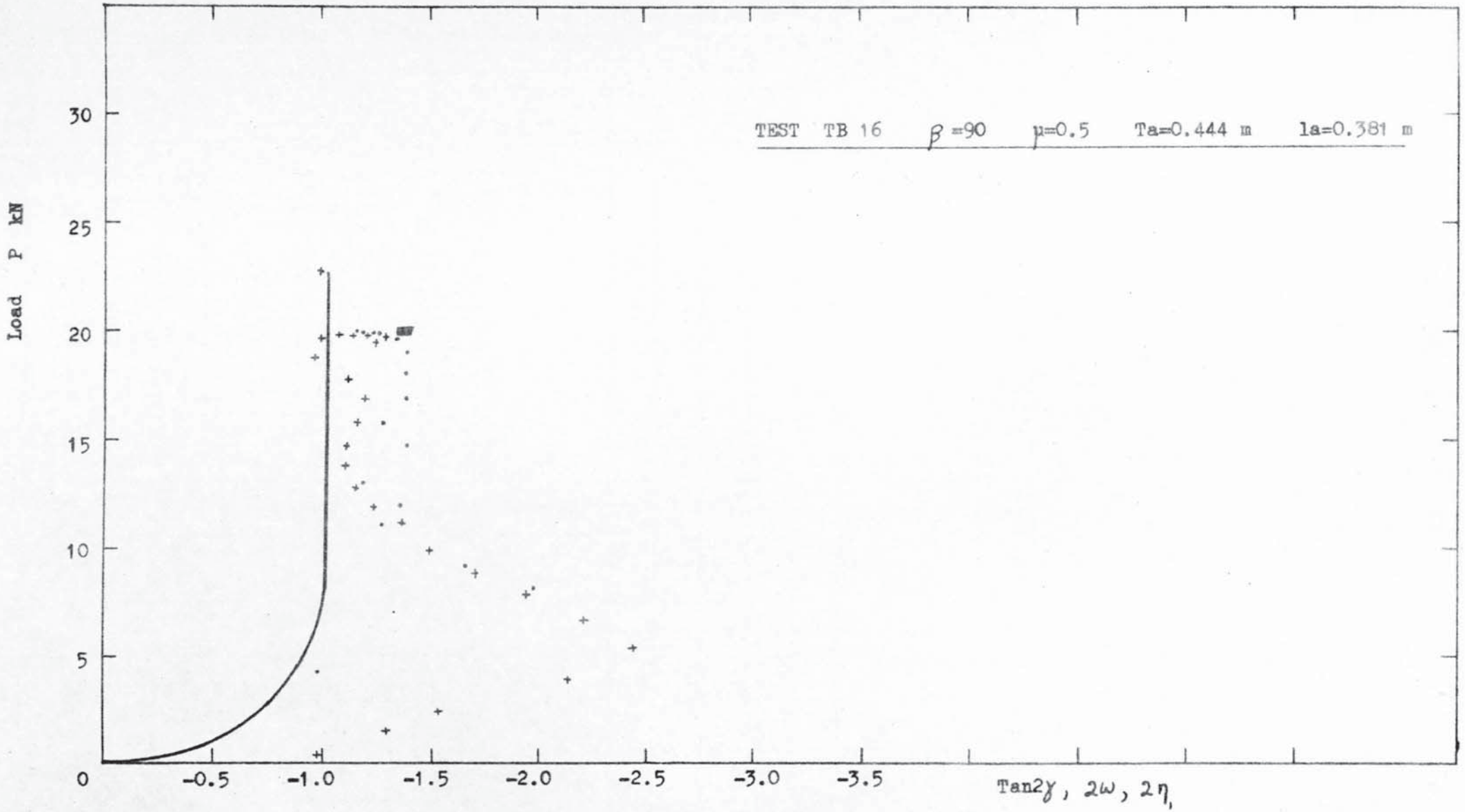

Figure 6.32 PLOT OF PRINCIPAL DIRECTIONS

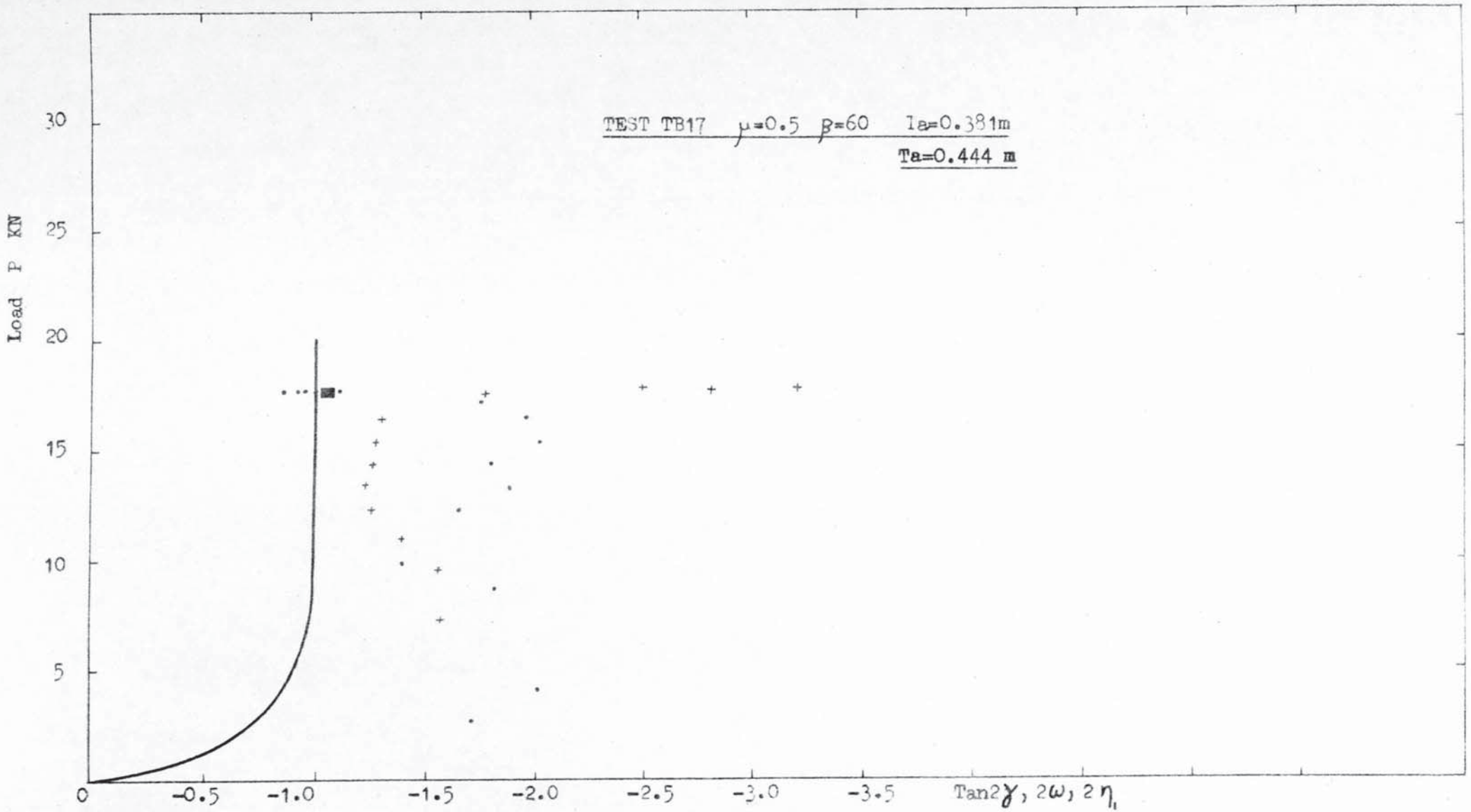

Figure 6.33 PLOT OF PRINCIPAL DIRECTIONS TB17

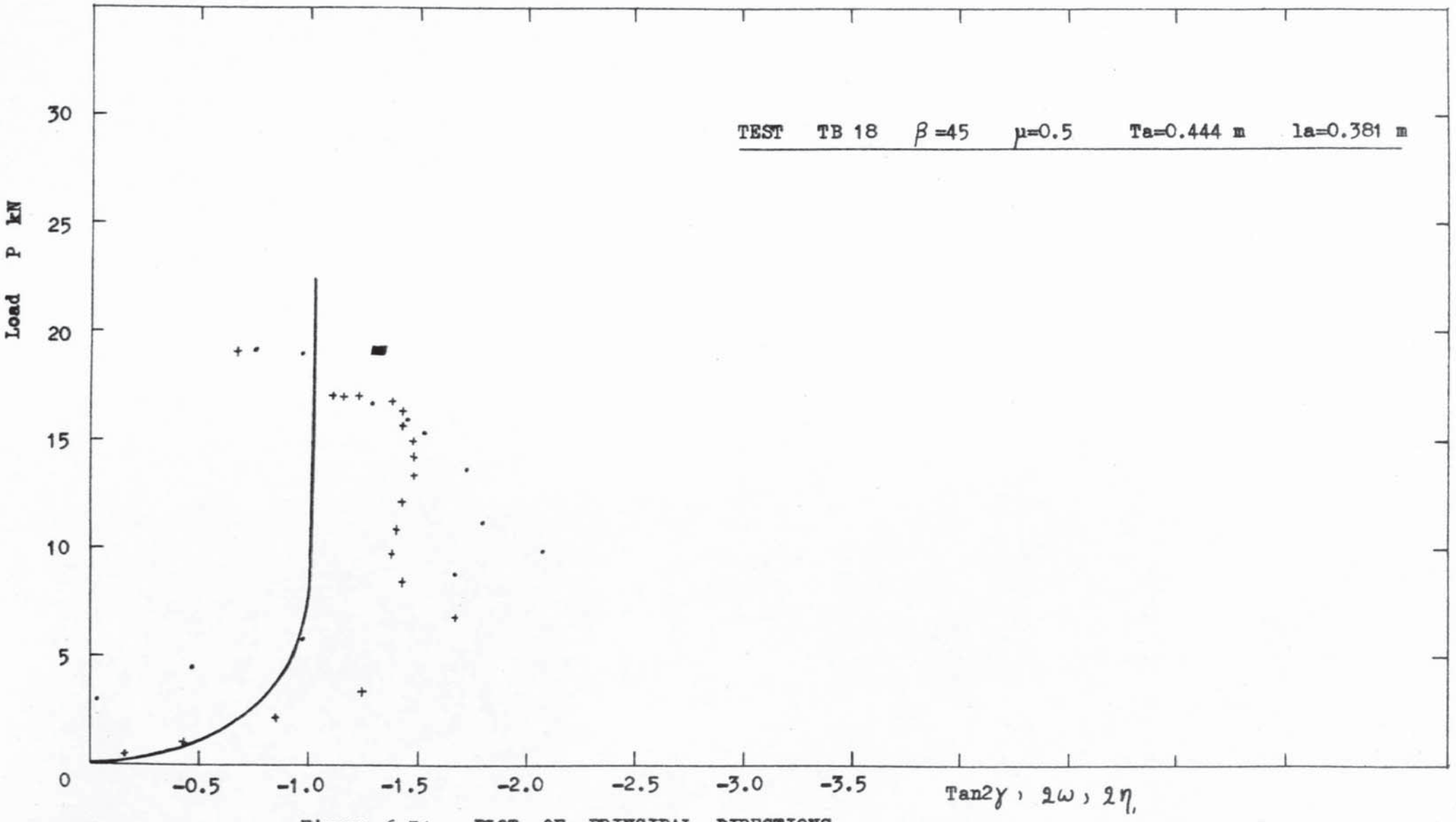

Figure 6.34 PLOT OF PRINCIPAL DIRECTIONS

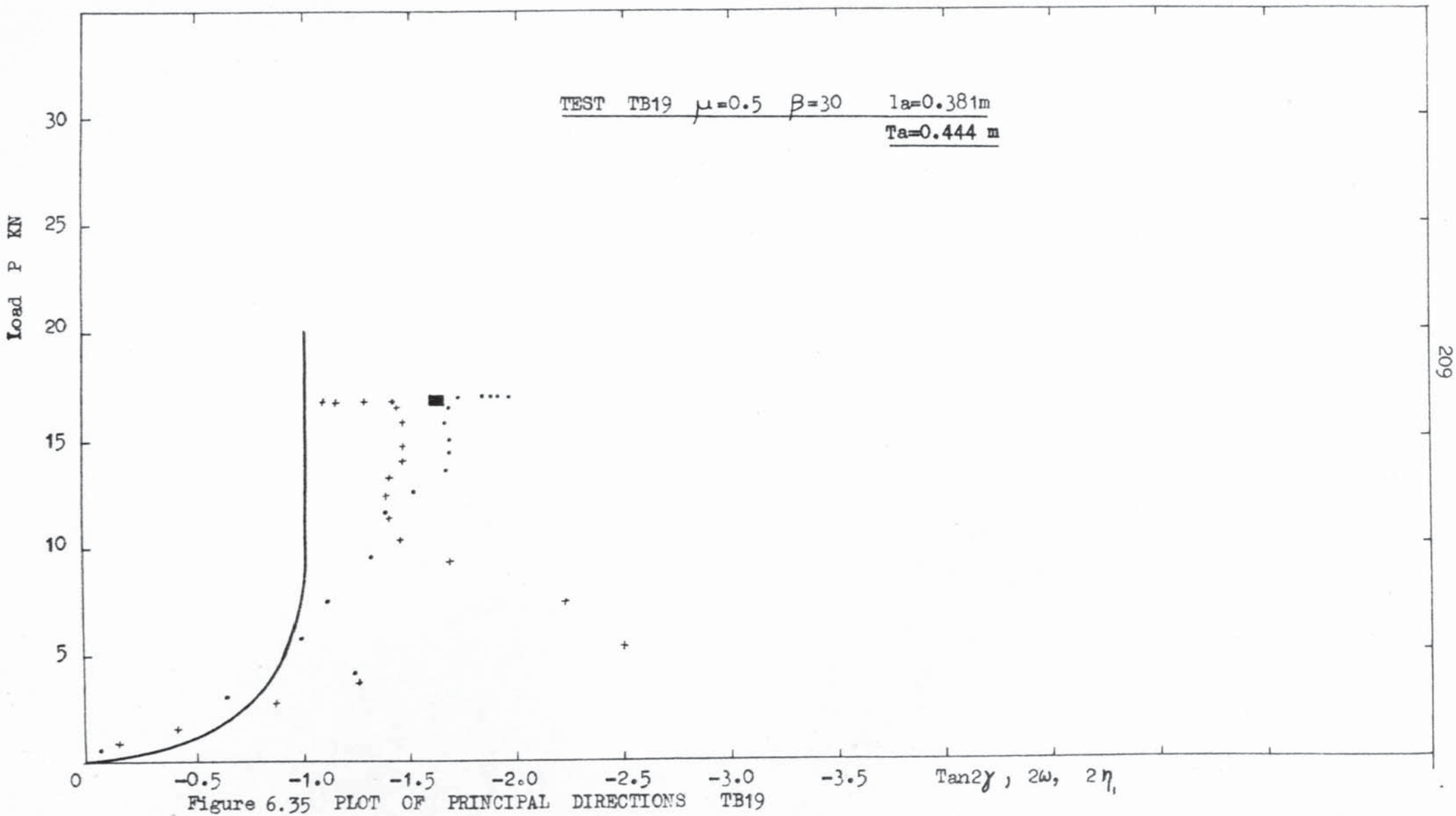

Figure 6.35 PLOT OF PRINCIPAL DIRECTIONS TB19

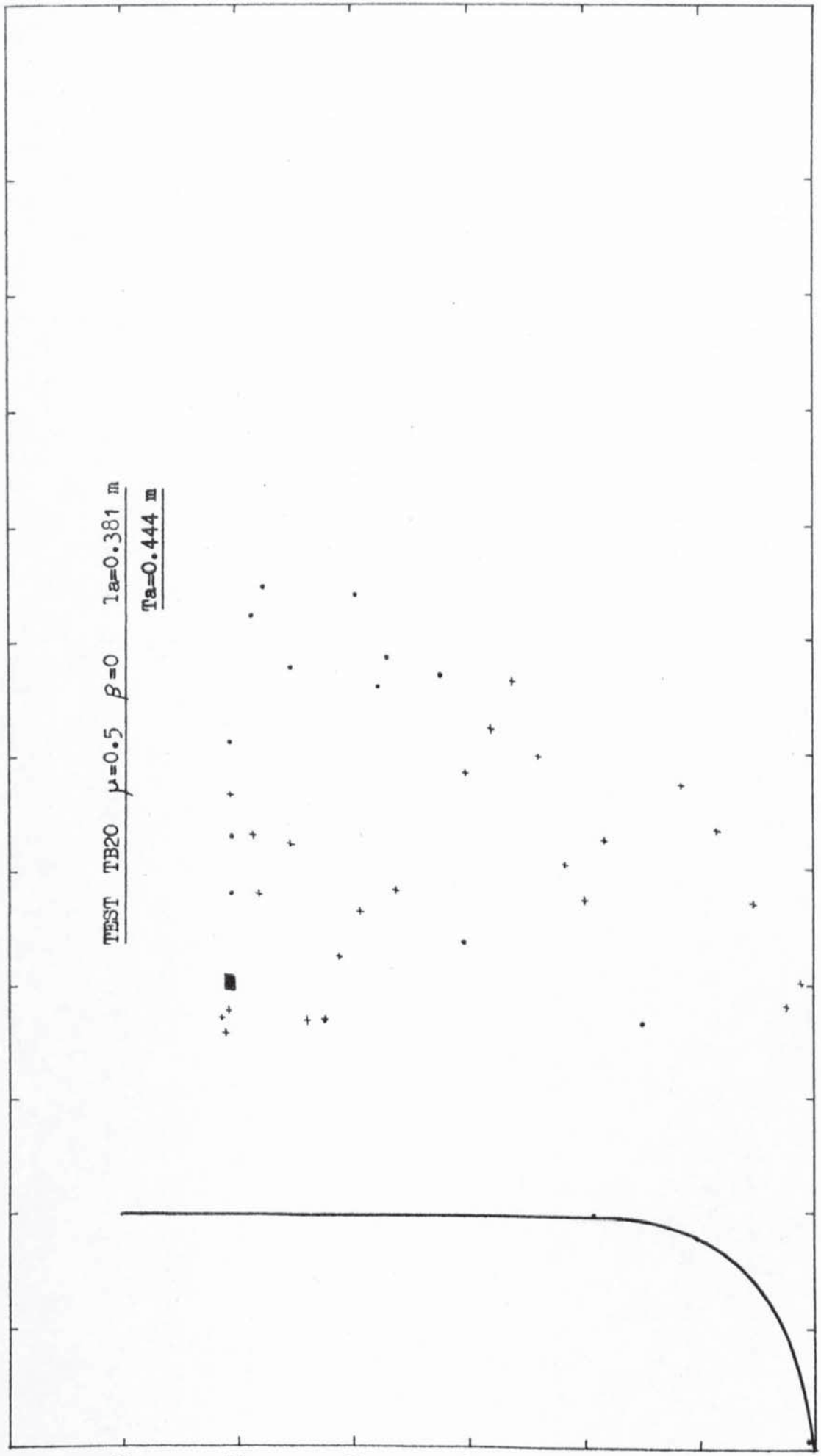

Figure 6.36 PLOT OF PRINCIPAL DIRECTIONS TB20

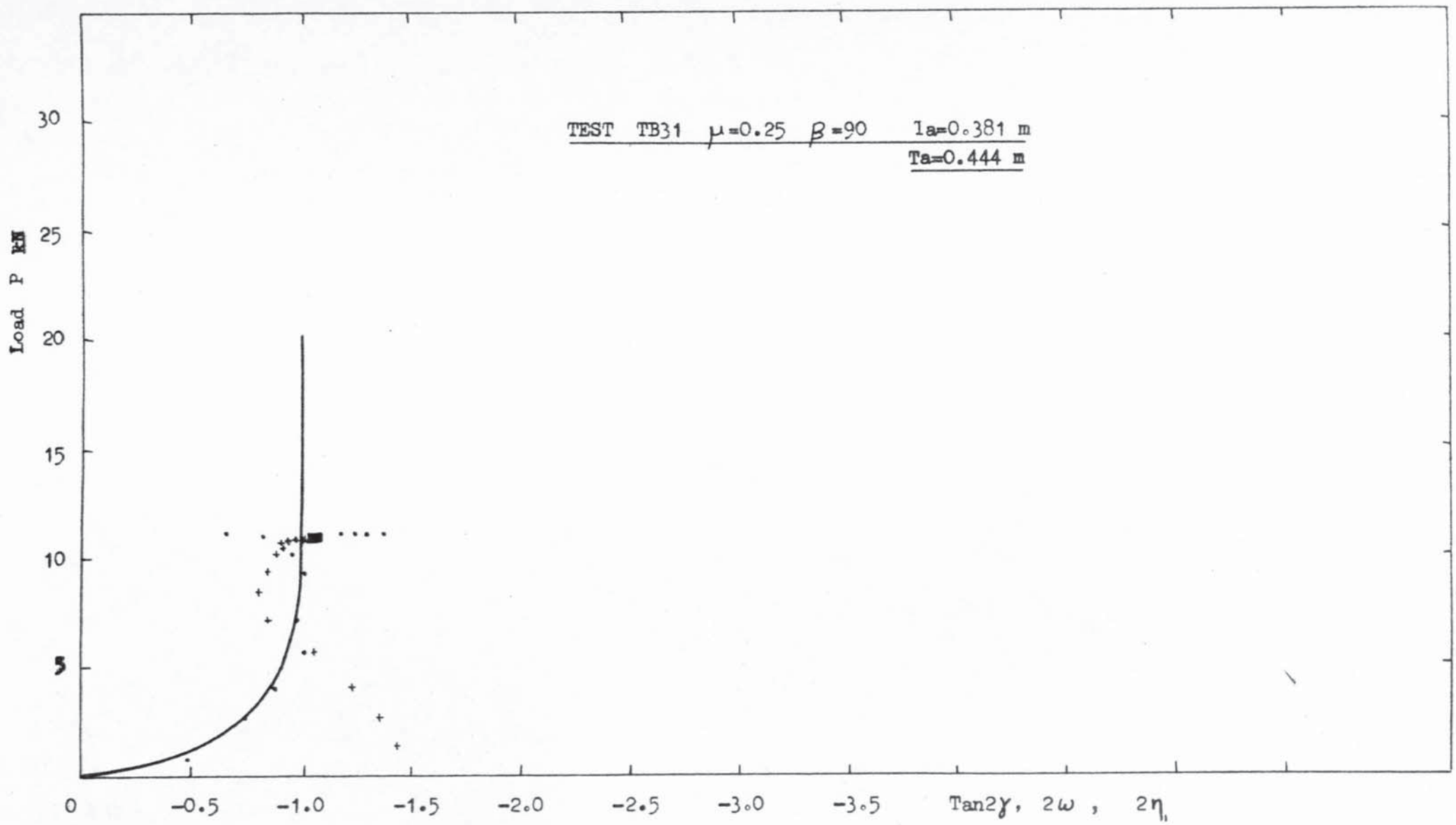

Figure 6.37 PLOT OF PRINCIPAL DIRECTIONS

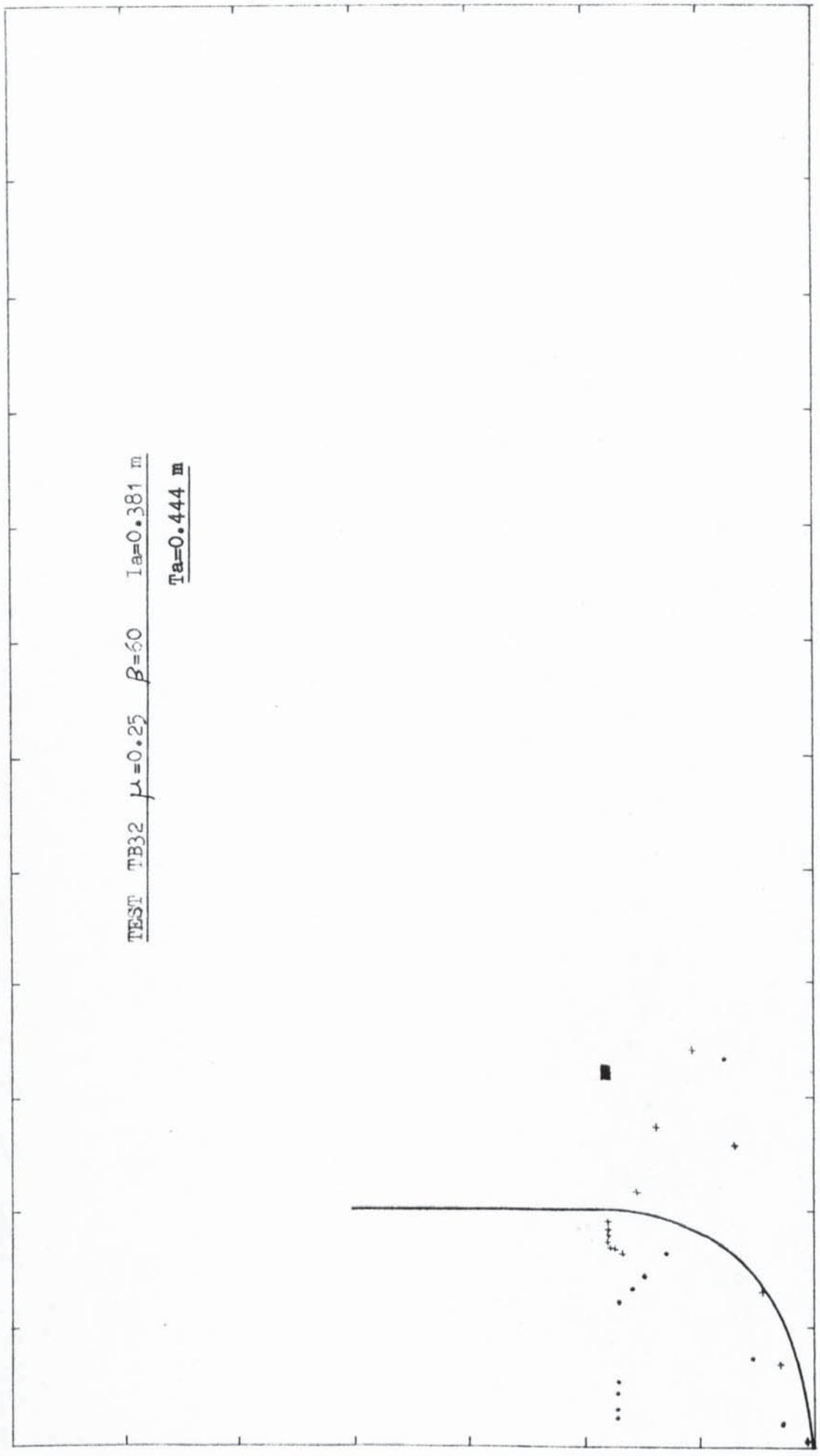

Figure 6.38 PLOT OF PRINCIPAL DIRECTIONS

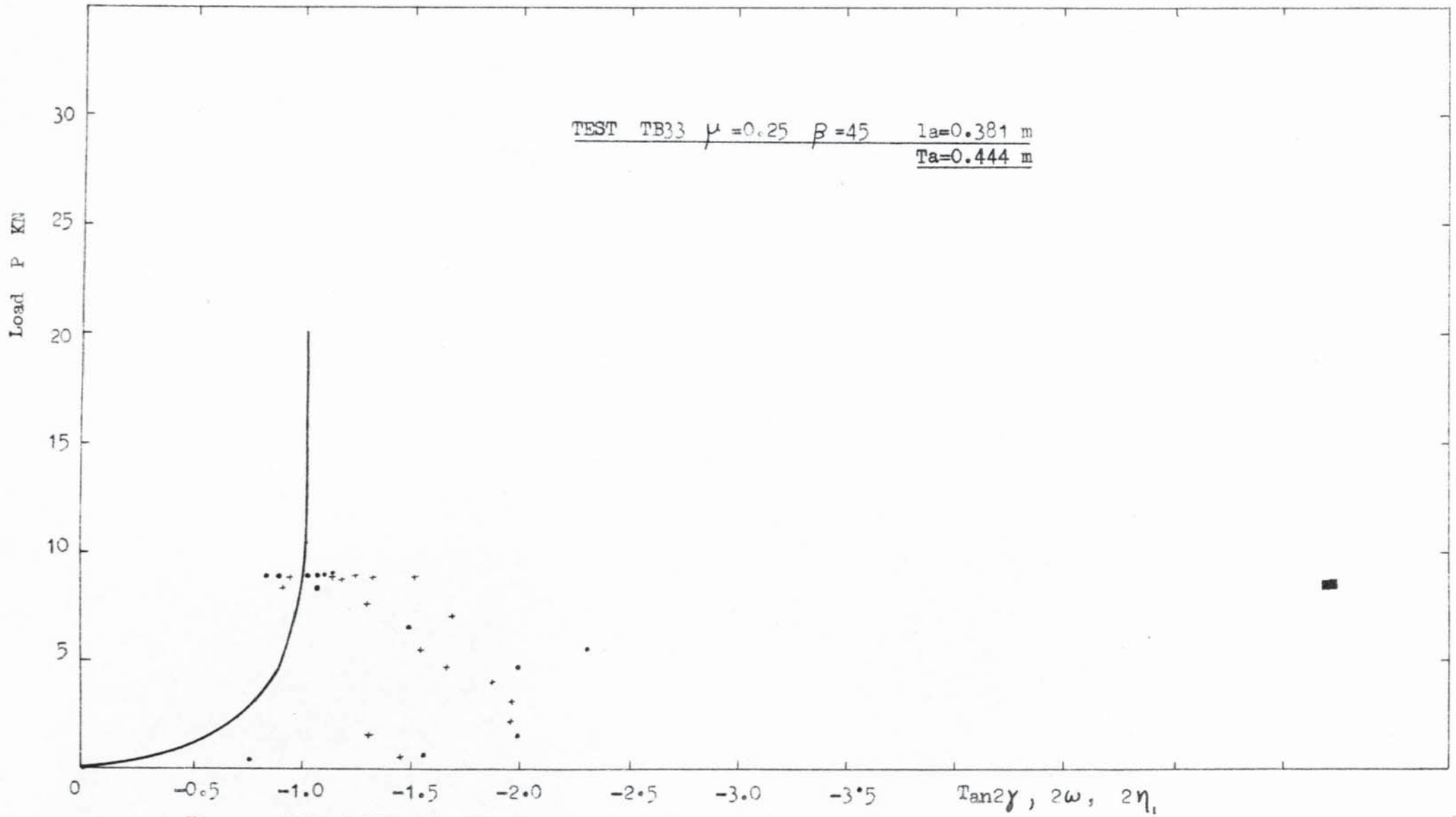

Figure 6.39 PLOT OF PRINCIPAL DIRECTIONS

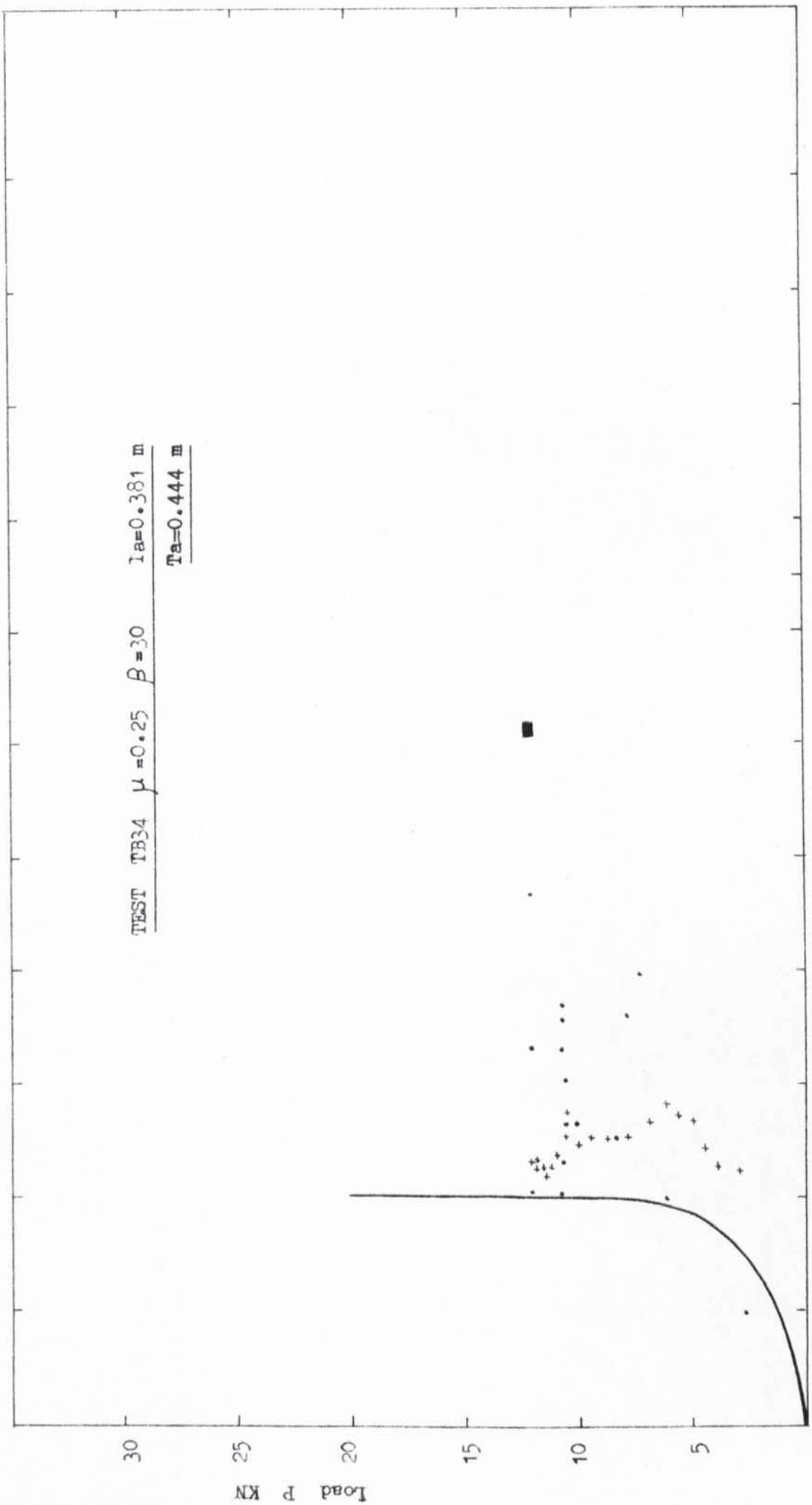

Figure 6.40 PLOT OF PRINCIPAL DIRECTIONS

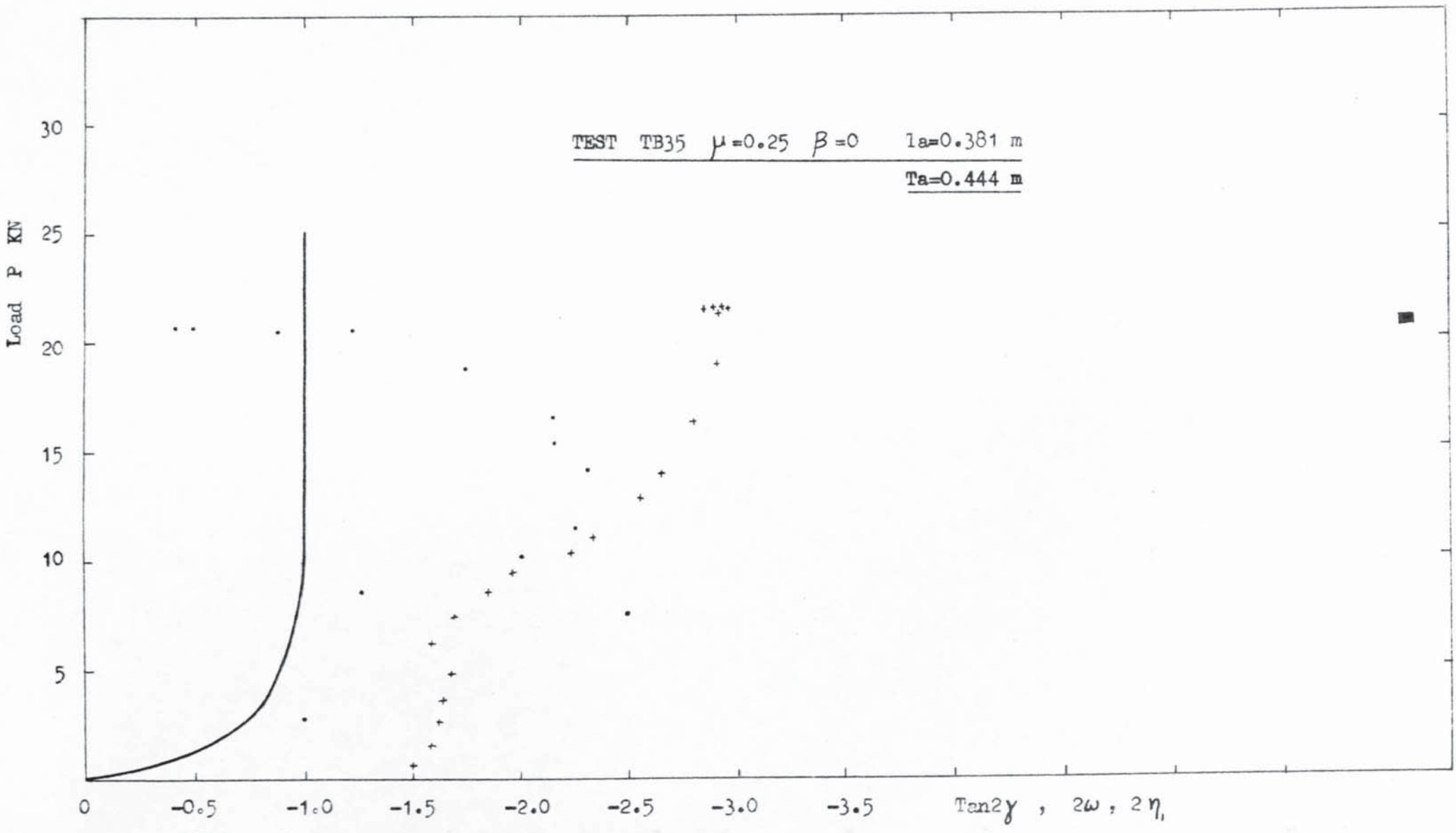

Figure 6.41 PLOT OF PRINCIPAL DIRECTIONS

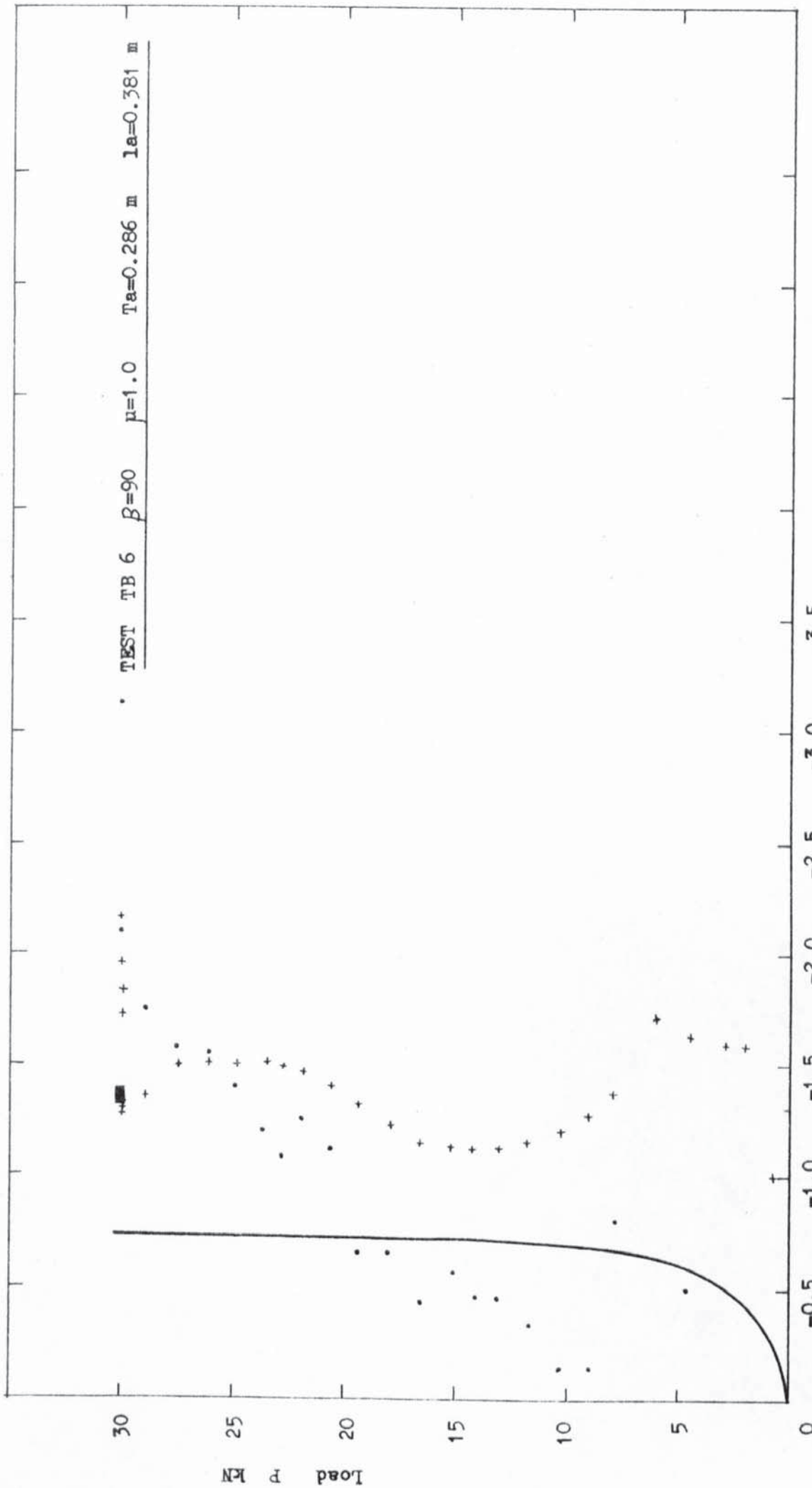

Figure 6.42 PLOT OF PRINCIPAL DIRECTIONS

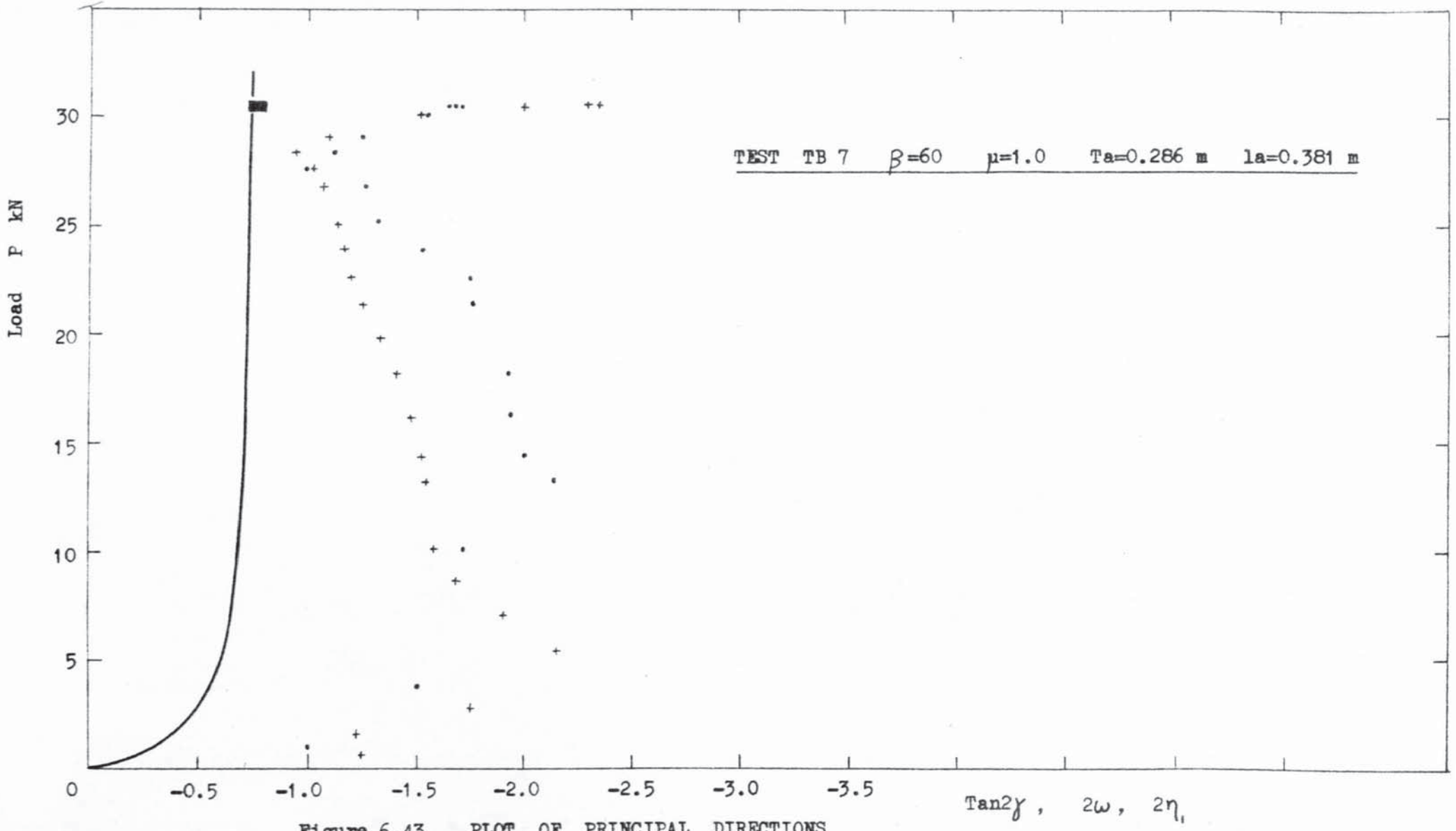

Figure 6.43 PLOT OF PRINCIPAL DIRECTIONS

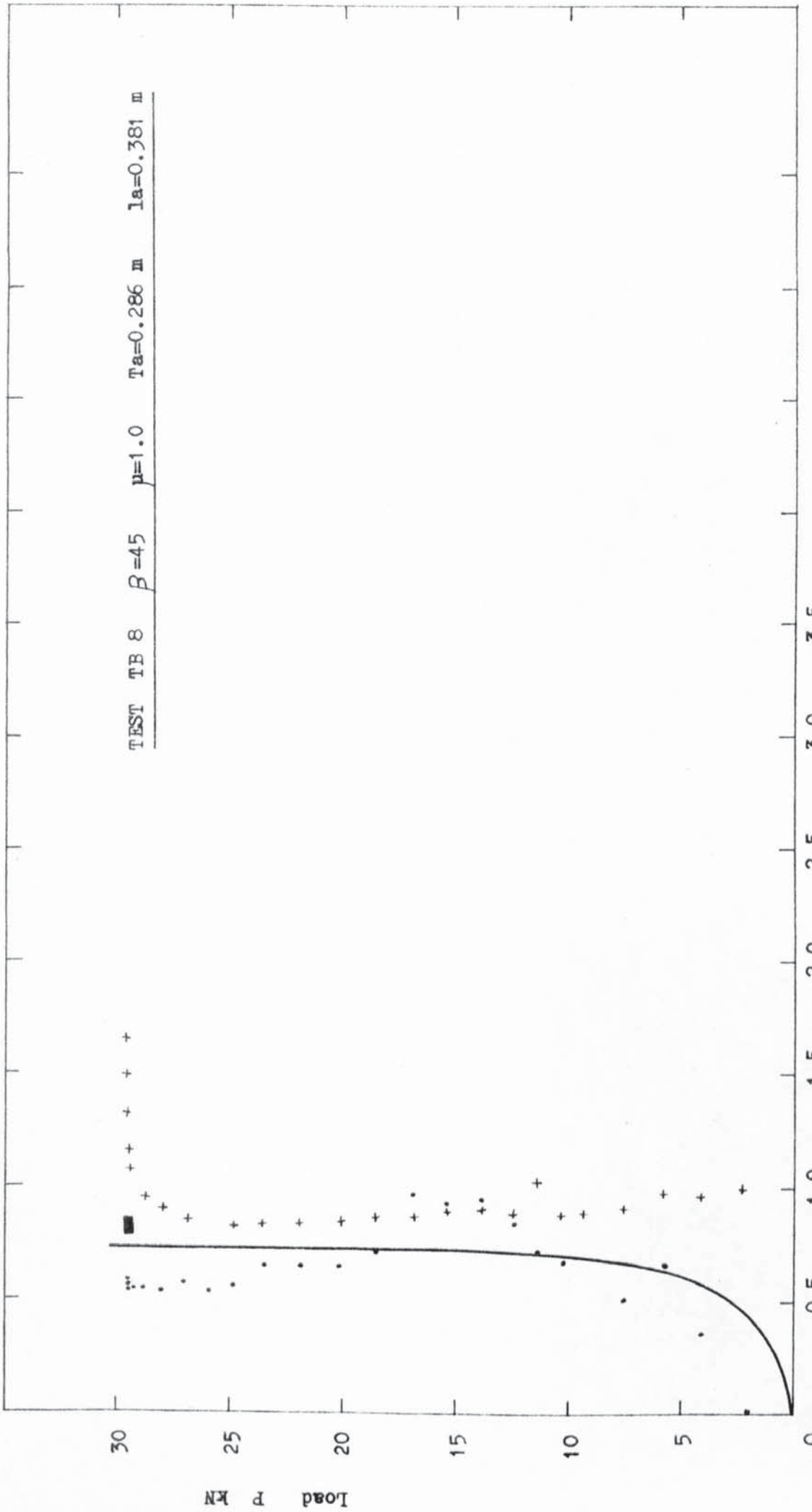

Figure 6.44 PLOT OF PRIMCIPAL DIRECTIONS

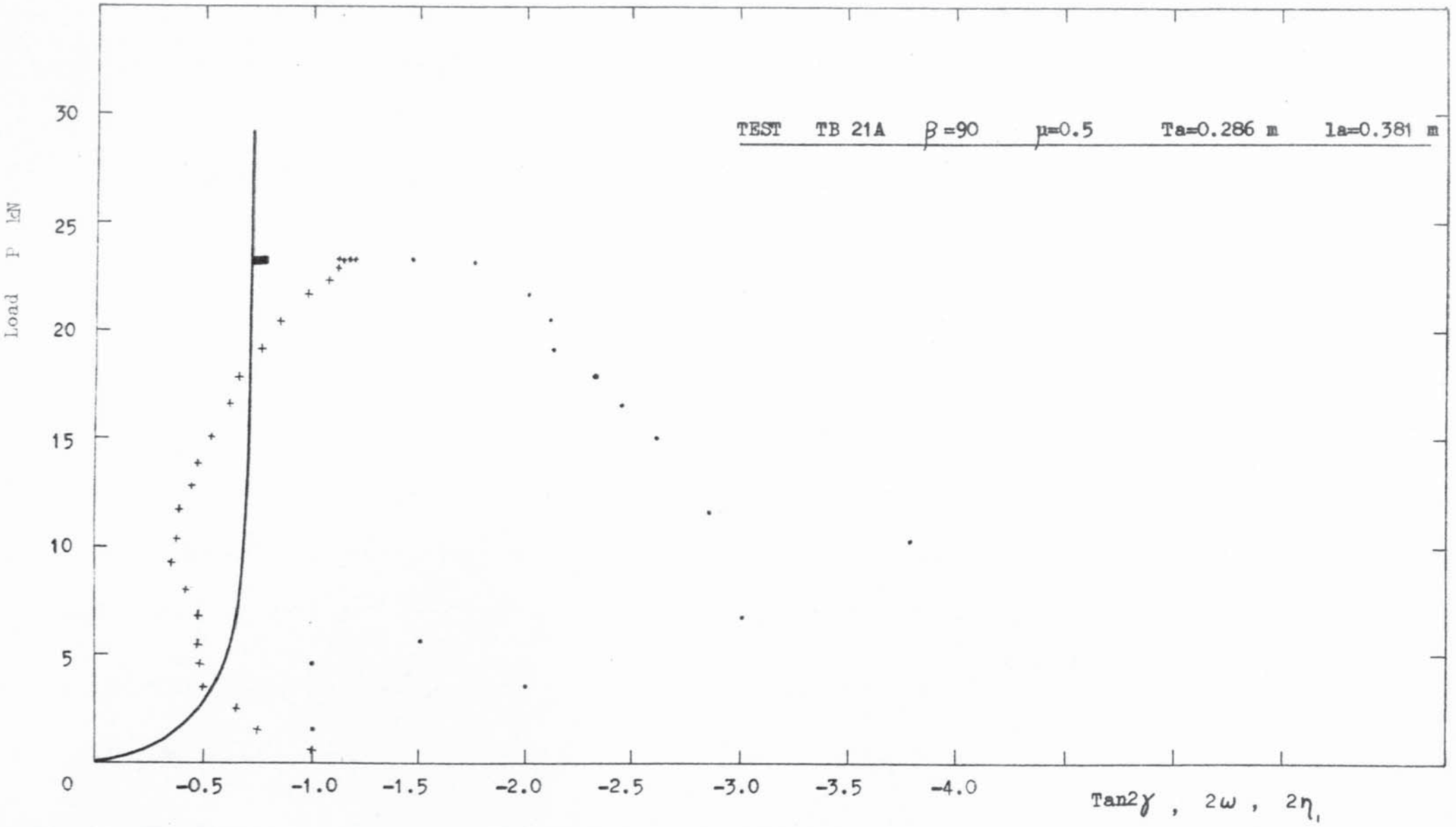

Figure 6.45 PLOT OF PRINCIPAL DIRECTIONS

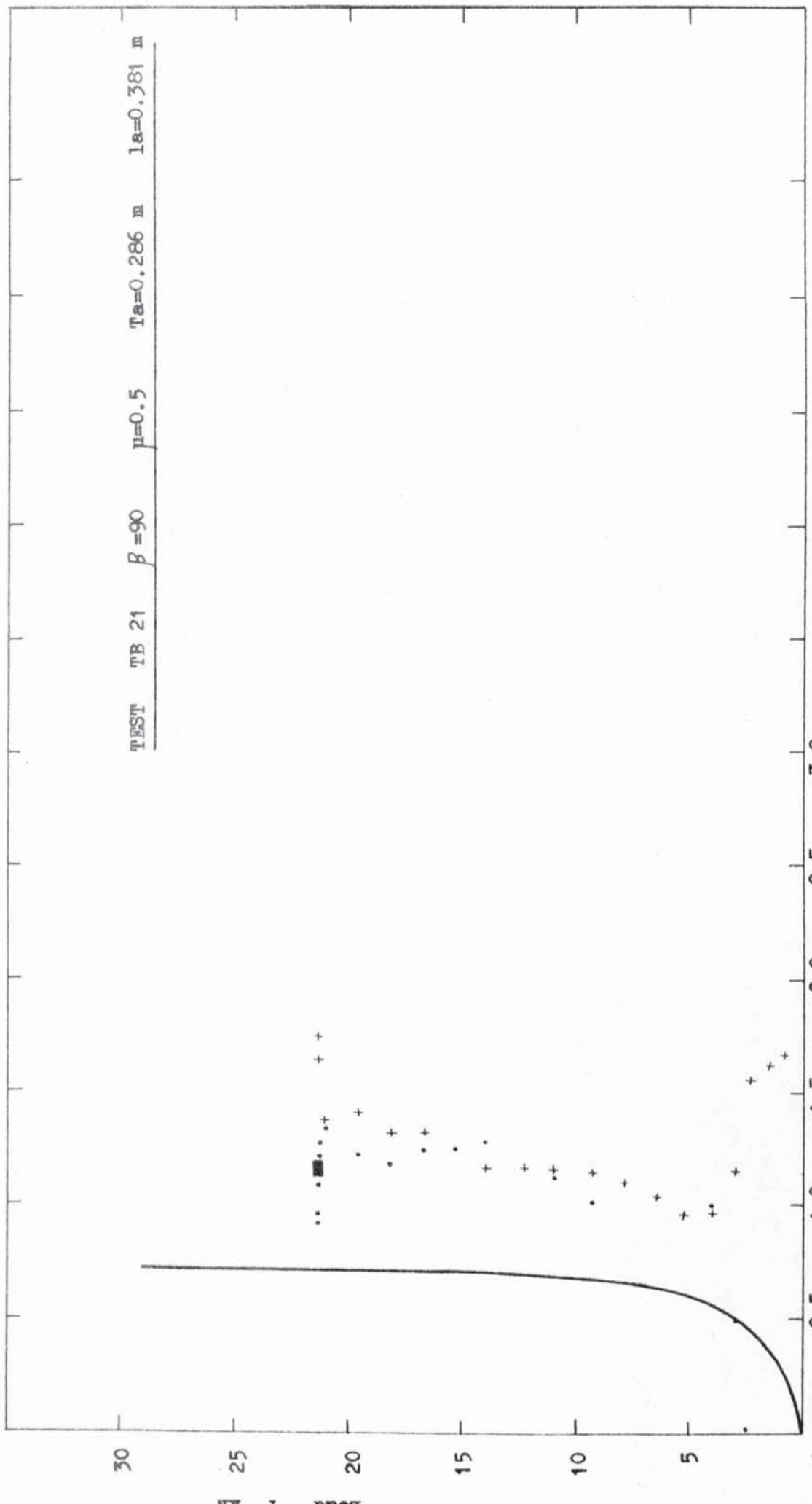

Figure 6.46 PLOT OF PRINCIPAL DIRECTIONS

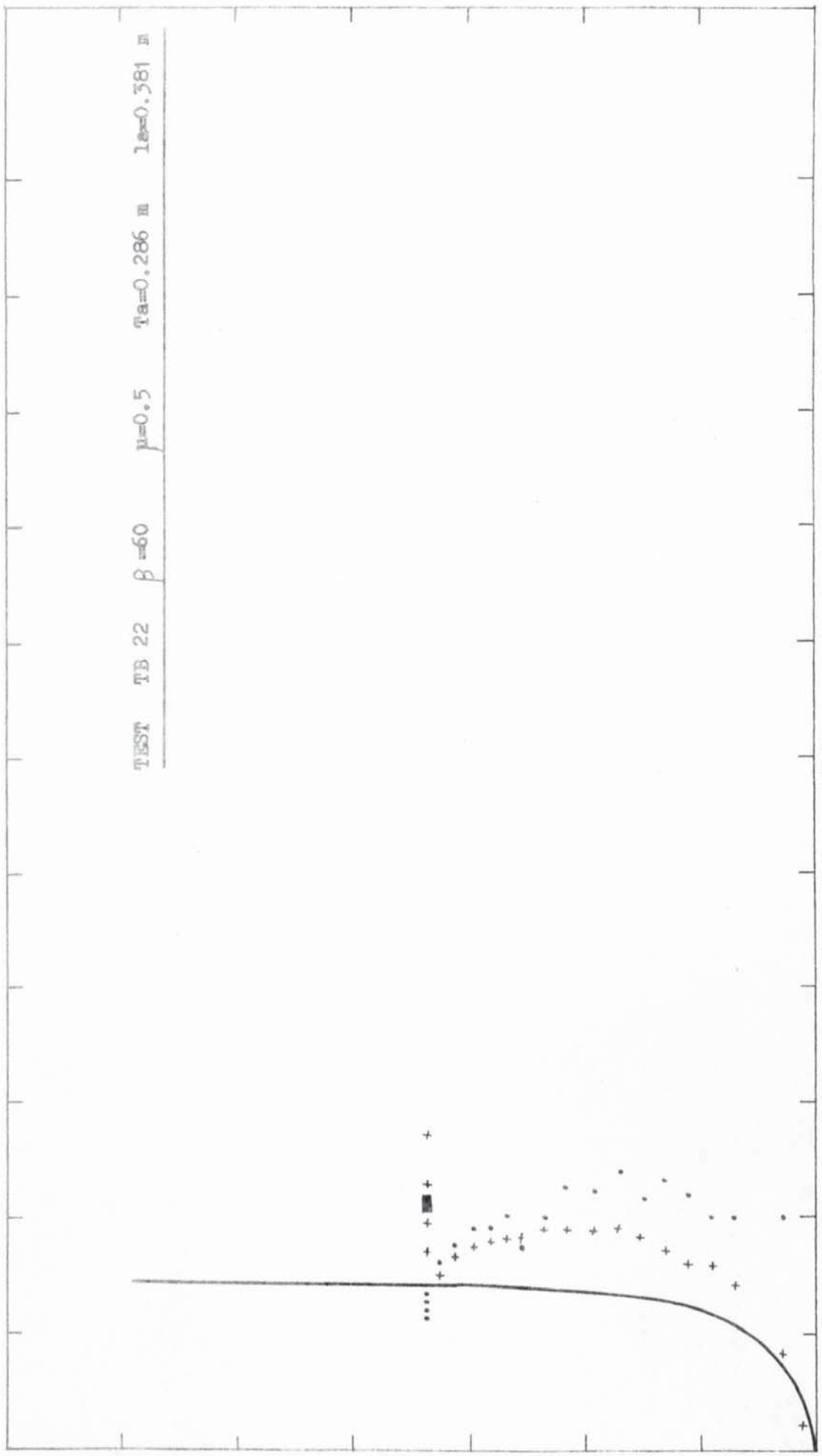

Figure 6.47 PLOT OF PRINCIPAL DIRECTIONS

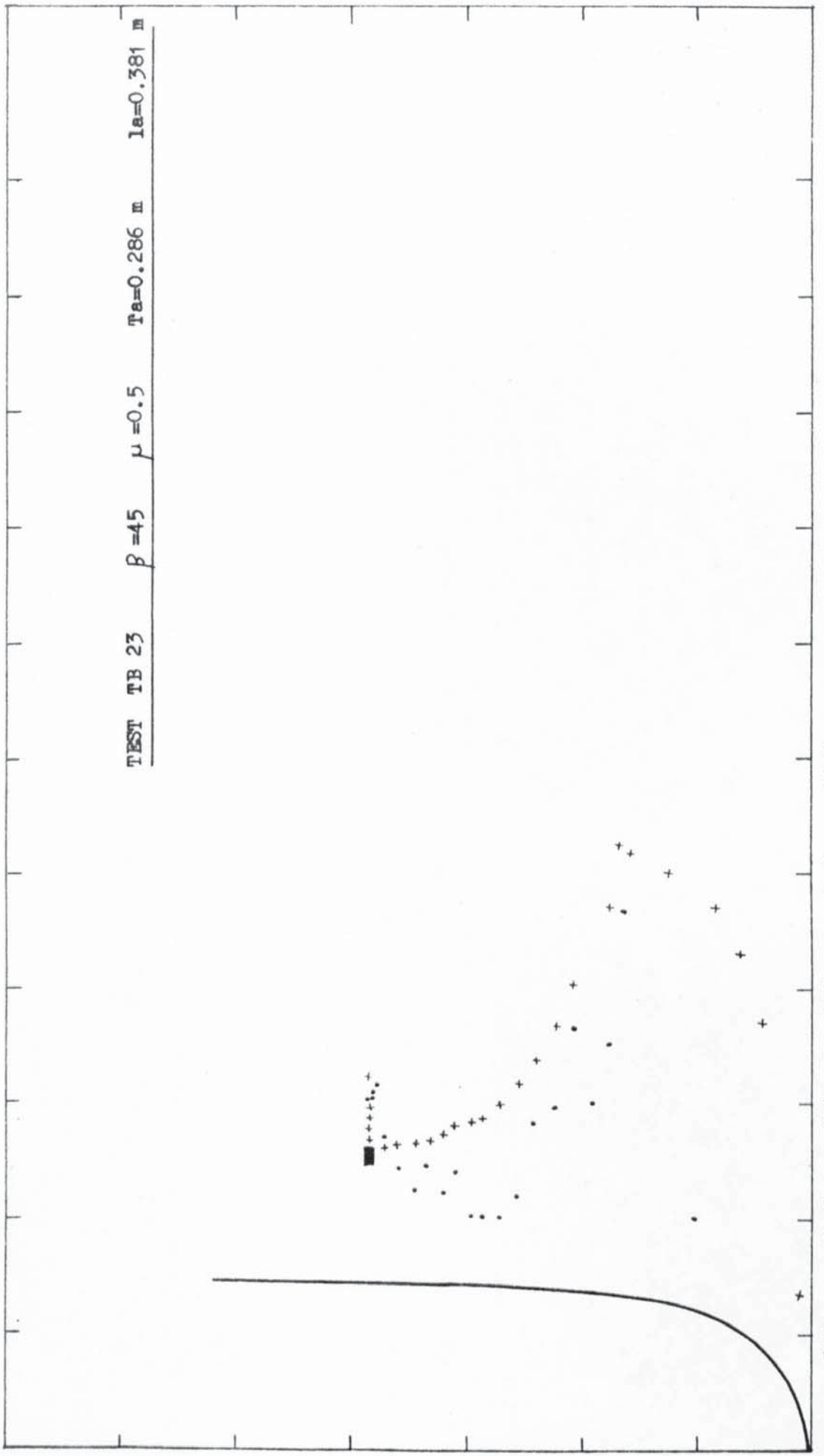

Figure 6.48 PLOT OF PRINCIPAL DIRECTIONS

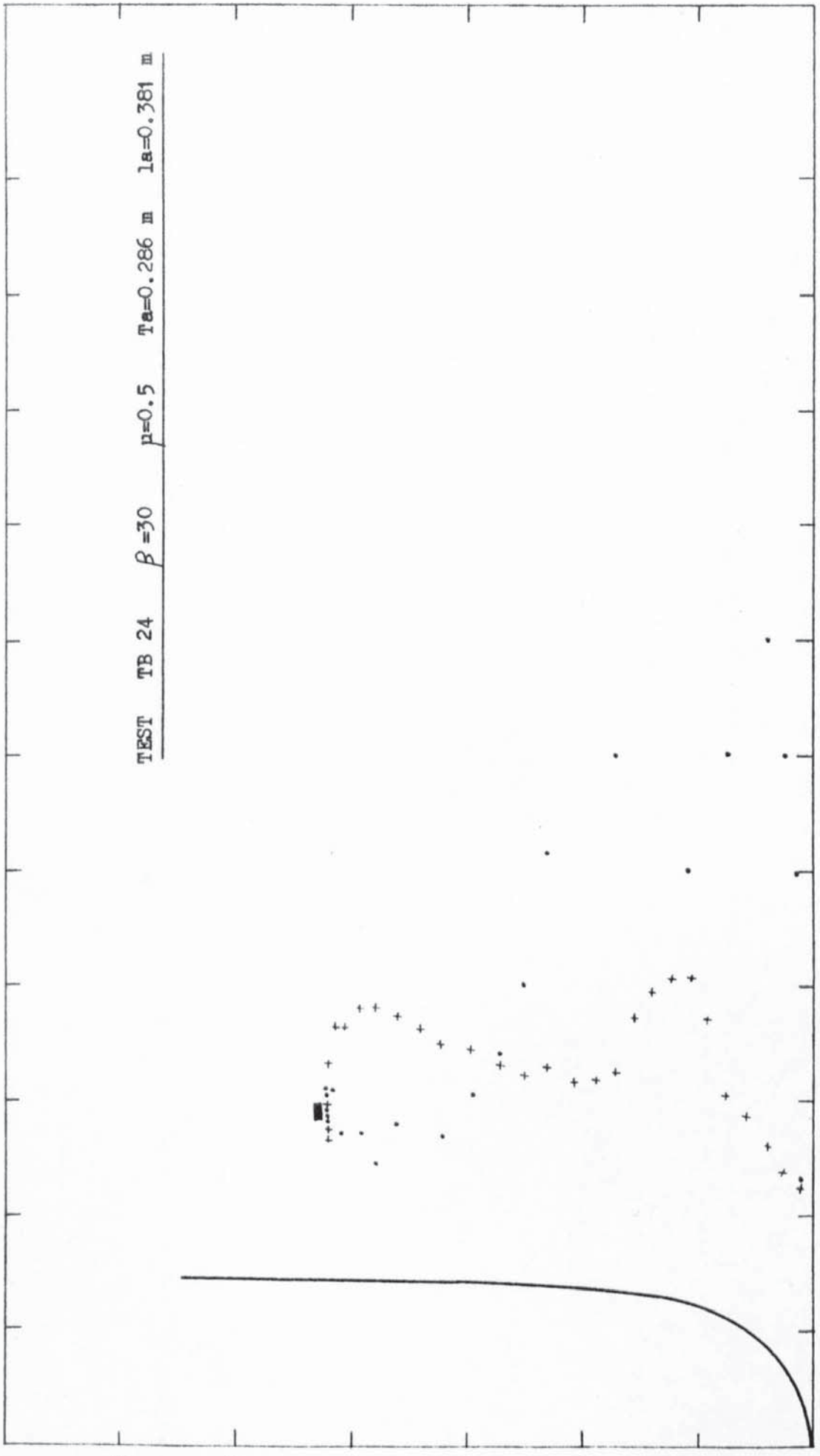

Figure 6.49 PLOT OF PRINCIPAL DIRECTIONS

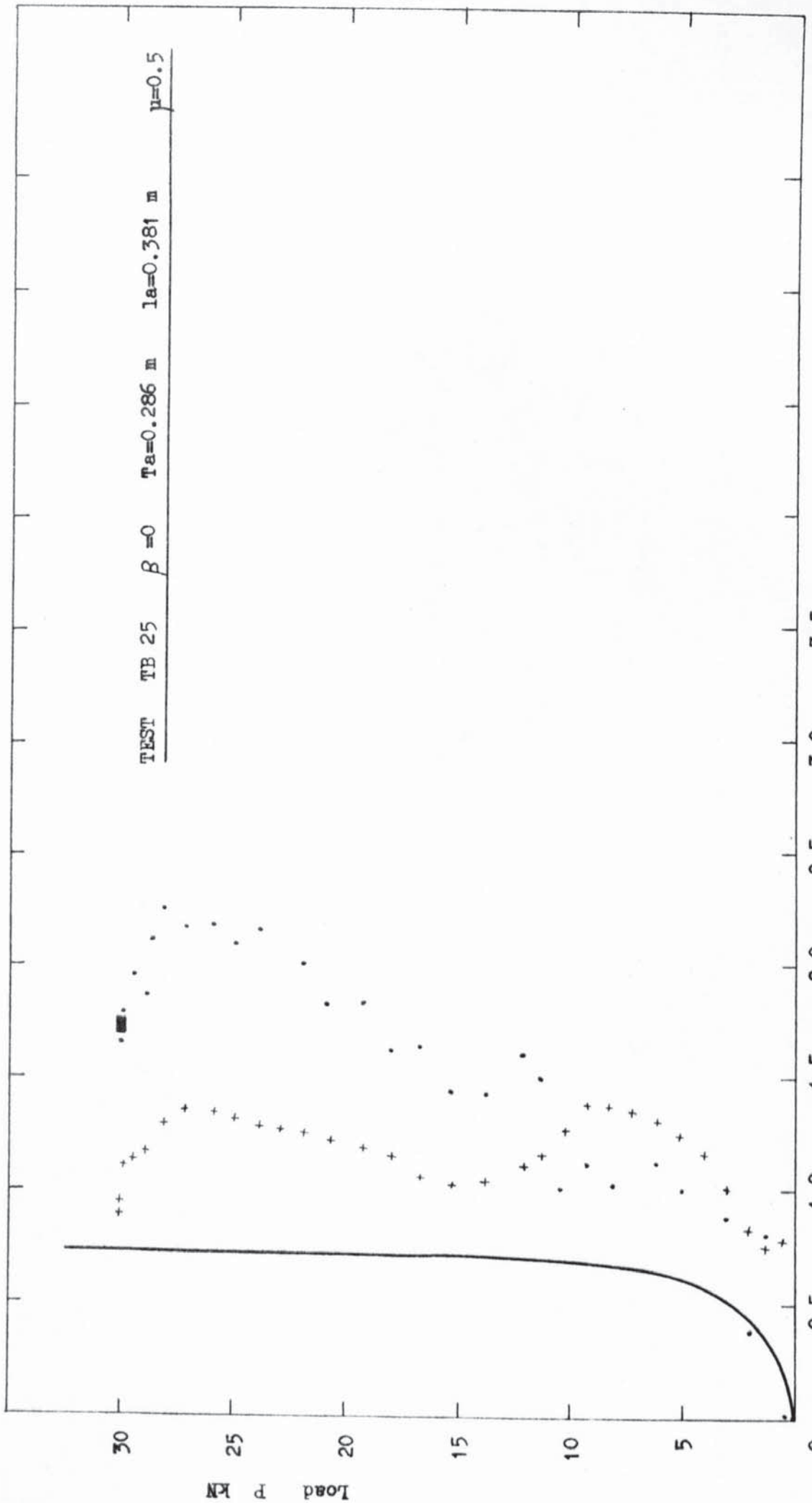

Figure 6.50 PLOT OF PRINCIPAL DIRECTIONS

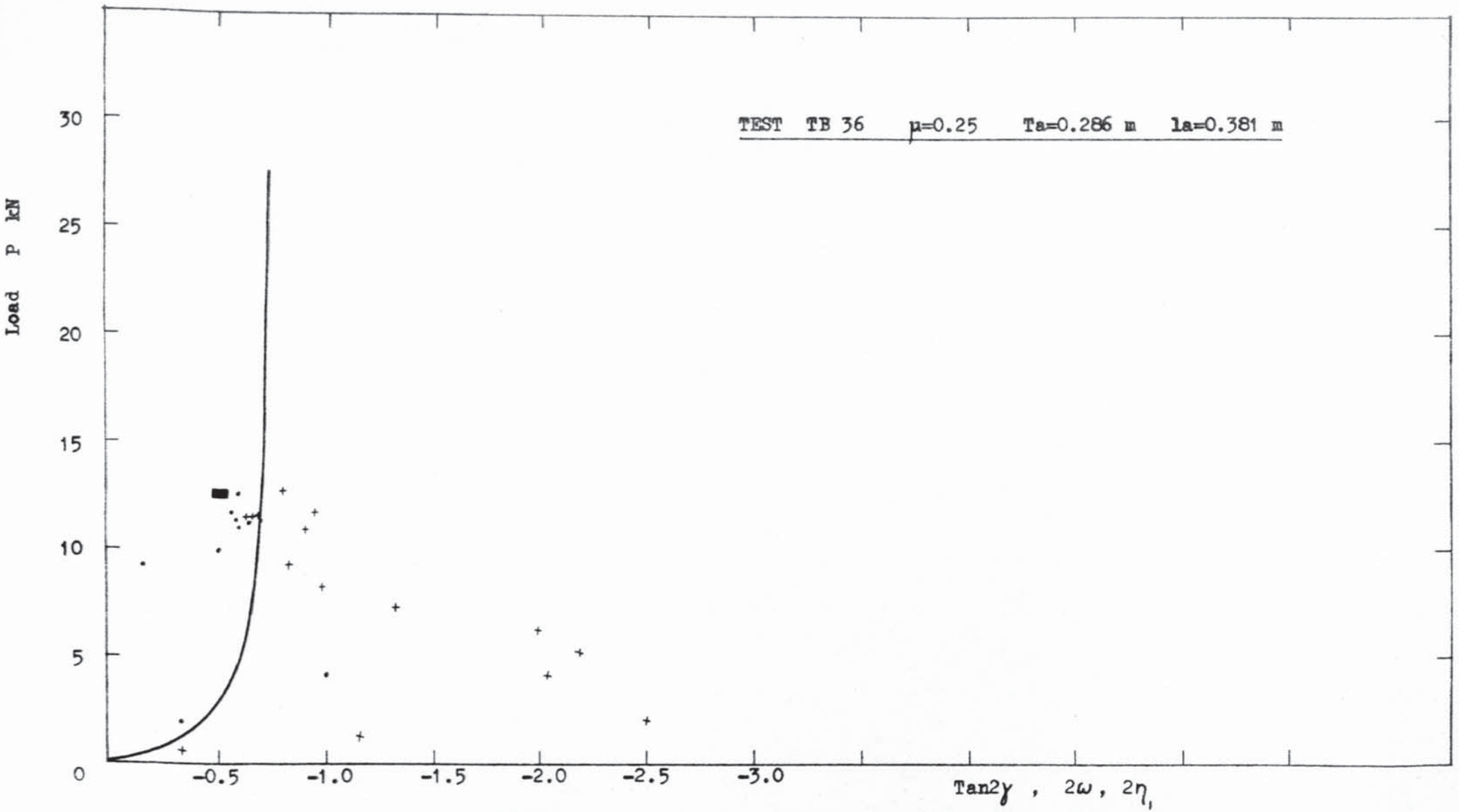

Figure 6.51 PLOT OF PRINCIPAL DIRECTIONS

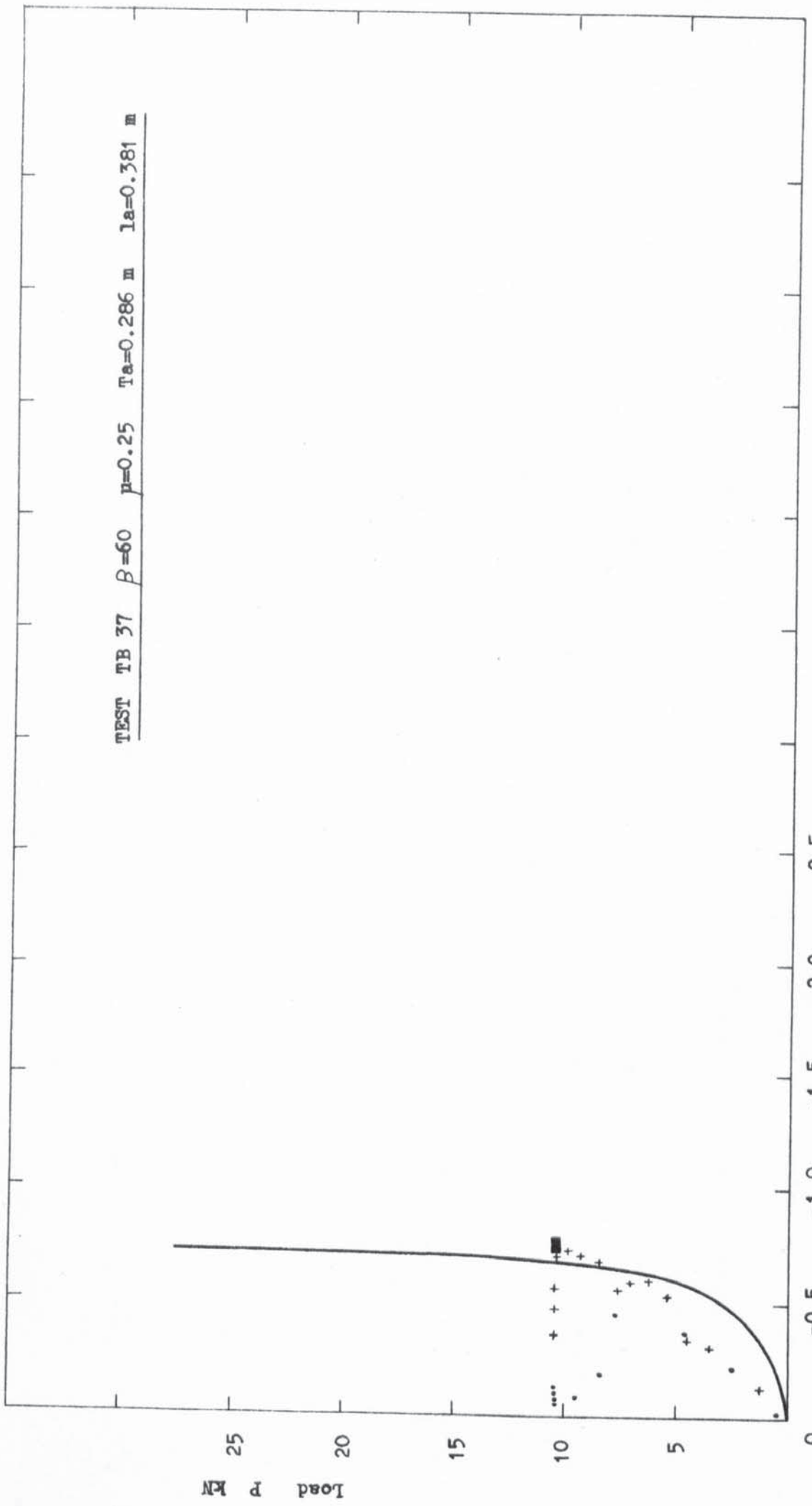

Figure 6.52 PLOT OF PRINCIPAL DIRECTIONS

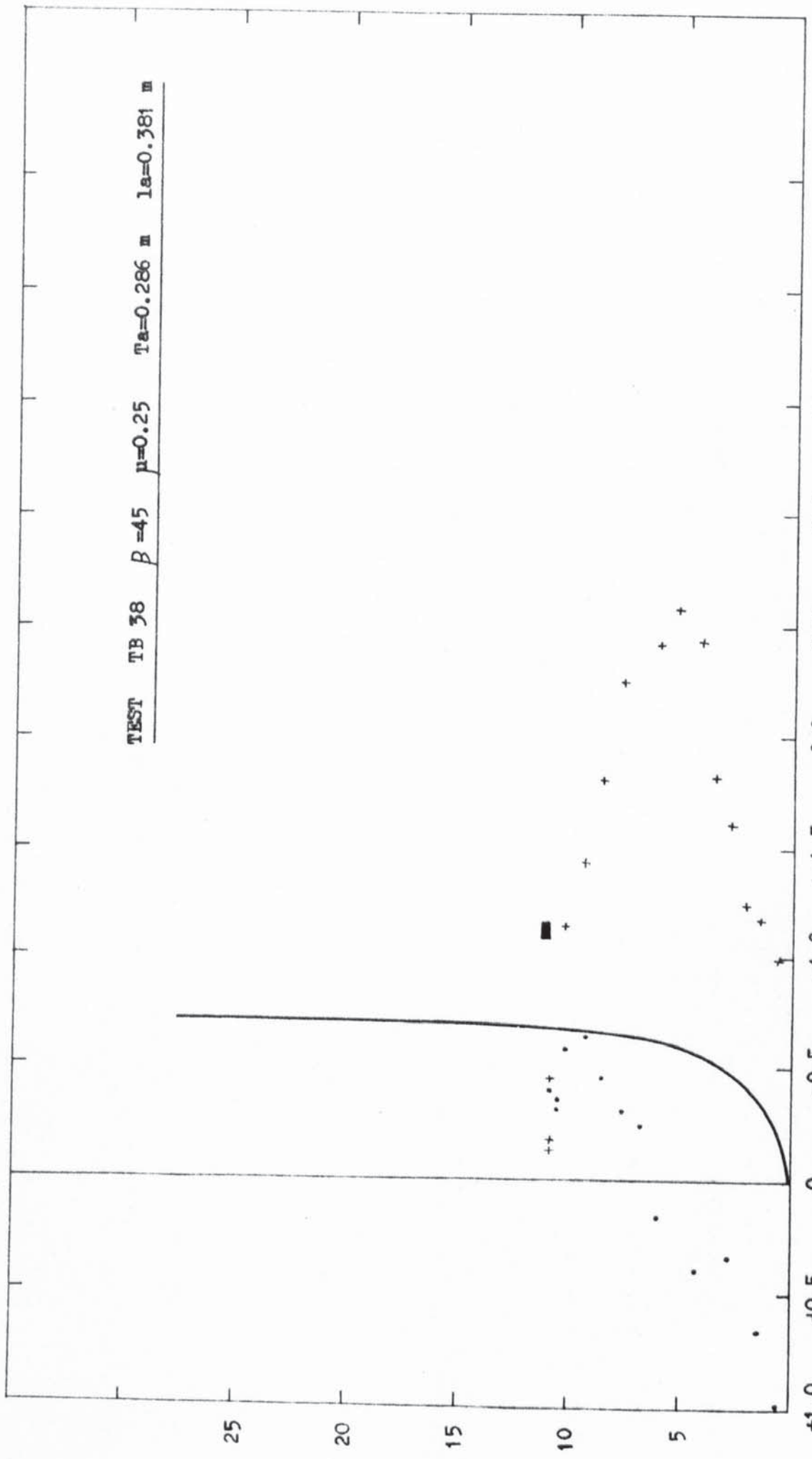

Figure 6.53 PLOT OF PRINCIPAL DIRECTIONS

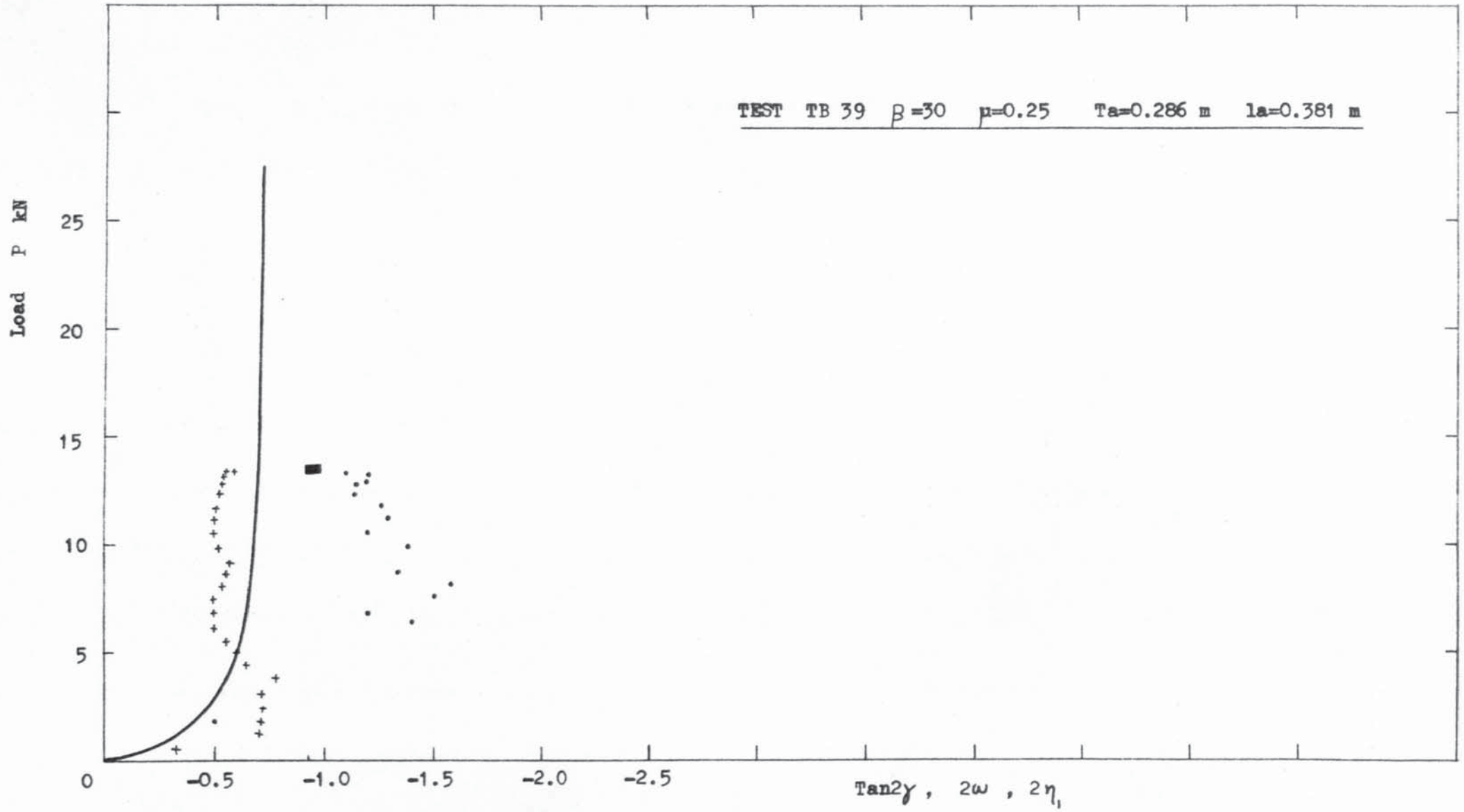

Figure 6.54 PLOT OF PRINCIPAL DIRECTIONS

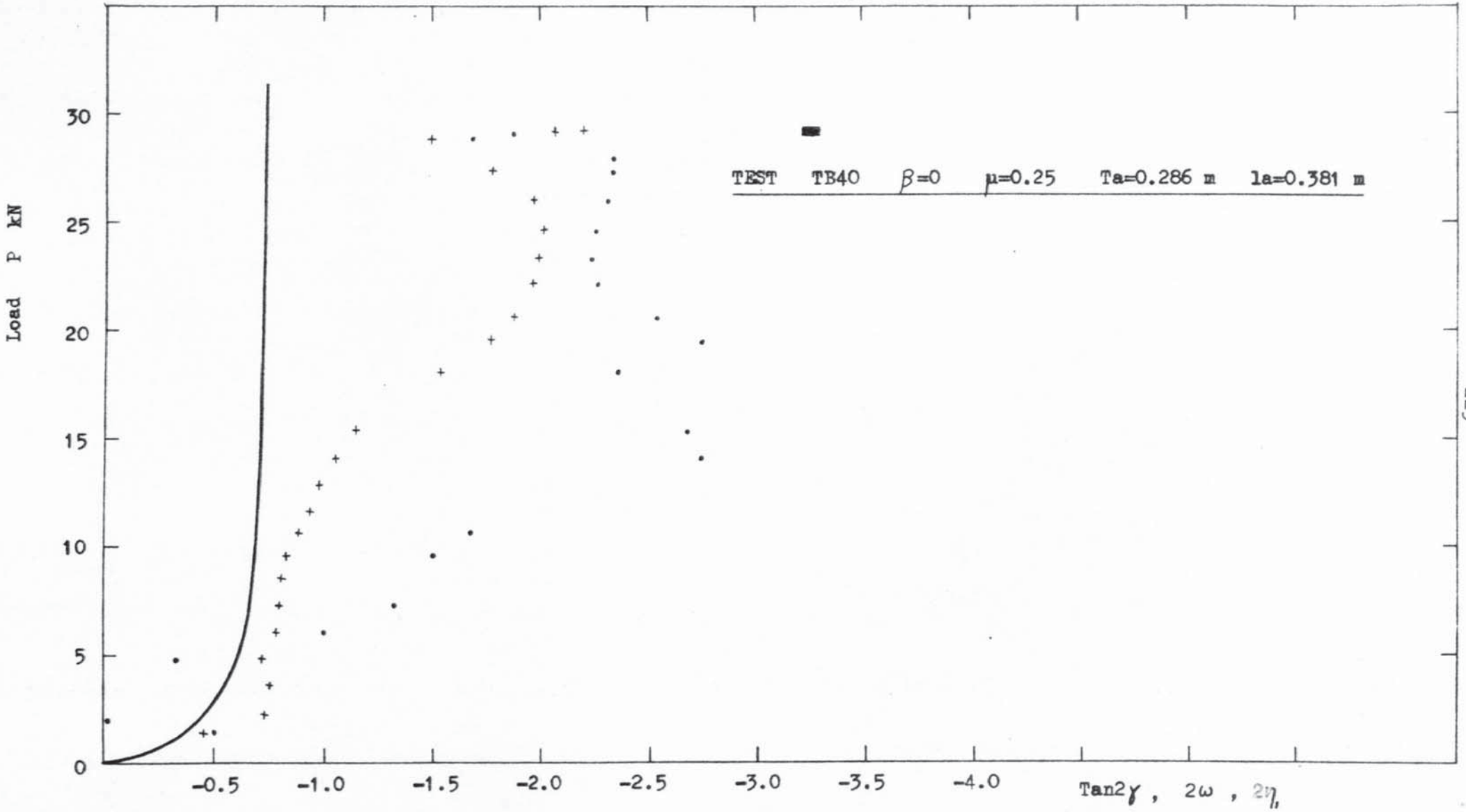

Figure 6.55 PLOT OF PRINCIPAL DIRECTIONS

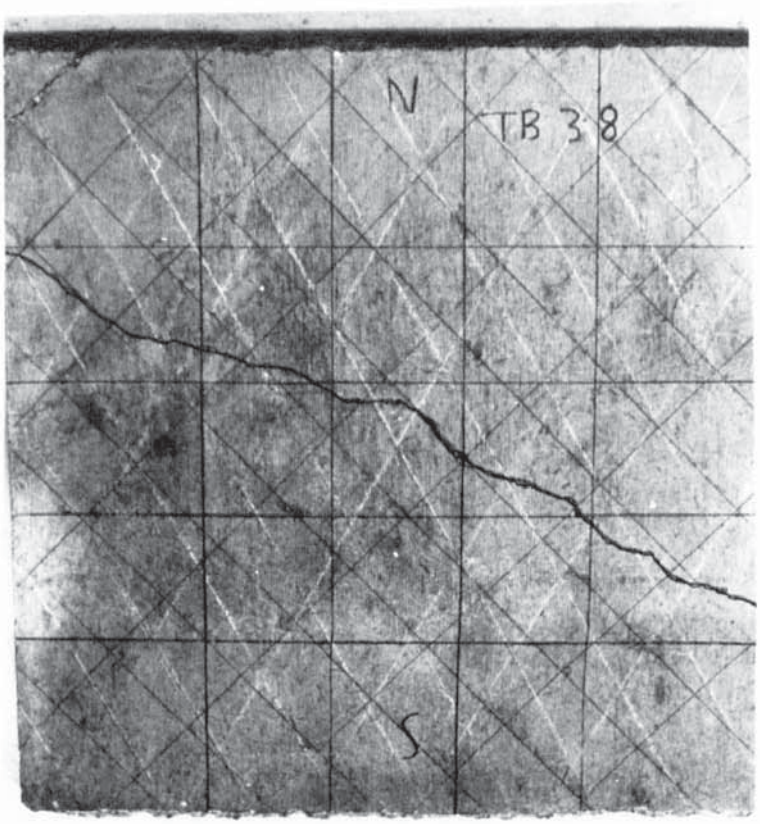

PLATE 6.1 SINGLE CRACK FAILURE (SPECIMEN TB 38)

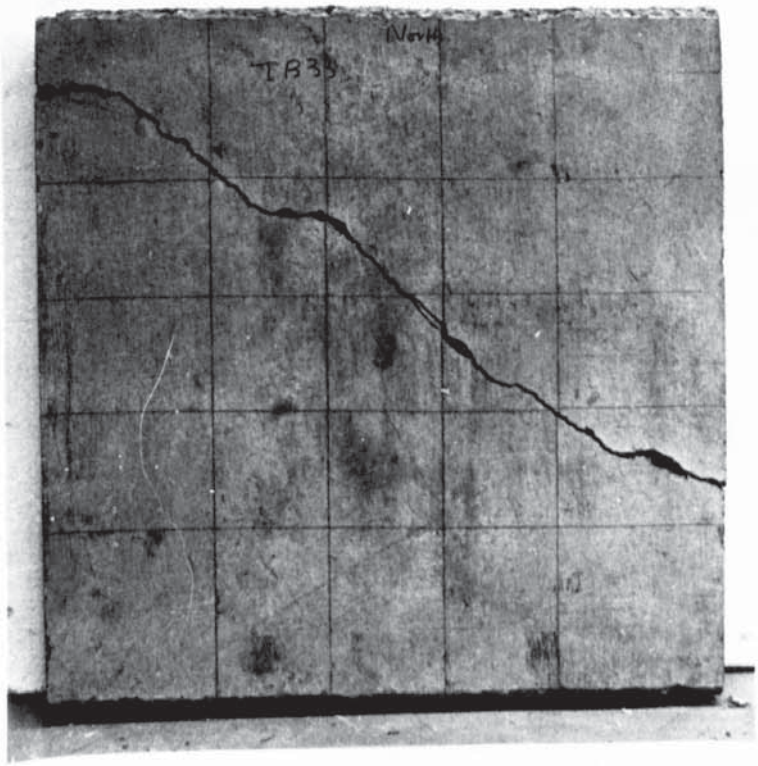

PLATE 6.2 SINGLE CRACK FAILURE (SPECIMEN TB 33)

PLATE 6.3 MULTIPLE CRACK FAILURE (SPECIMEN TB 4)

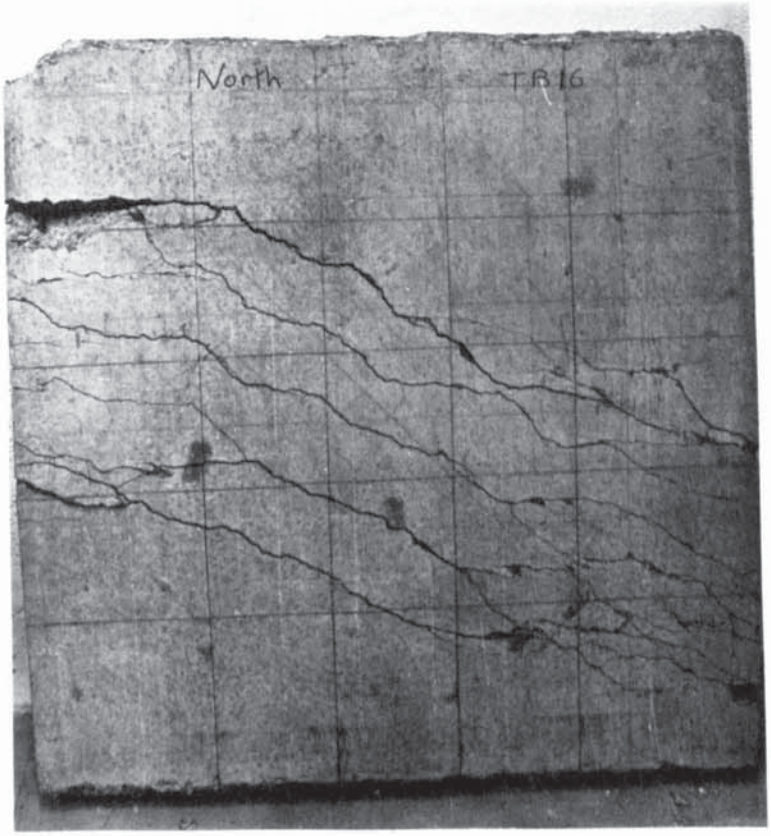

PLATE 6.4 MULTIPLE CRACK FAILURE (SPECIMEN TB 16)

CHAPTER 7.

DISCUSSIONS AND CONCLUSIONS.

7.1 Introduction.

The literature on the yield behaviour of concrete slabs is accumulating rapidly, though the picture of the slab behaviour and the behaviour of the reinforcing bars crossing a yield line at an oblique angle at ultimate loads is becoming more confused than clear. The author, having read all the available literature on this subject, embarked upon this research project with great caution. Before any attempt was made to develop a new criterion all the possible parameters controlling the slab strength at yield were collected and studied in detail. Finally, a decision was made which variables were to be incorporated in the new theory. For instance, the addition of membrane and shear effects on the slabs were not considered as this could constitute a separate research project.

The original hypothesis of Johansen [2] that collapse of a slab occurs by the formation of yield lines dividing the slab into a number of plane elements has been universally accepted. As other authors, the present author has shown that there is a difference of opinion of how the ultimate moment at yield is calculated.

The work undertaken by the author was of three phases. The first phase was the development of a theoretical yield criterion, taking into account axial and shear forces in the reinforcing bar. The second phase of this research was basically experimental. The objective of the second phase was to test certain conditions that were made in developing the new yield criterion. Steel analogue slabs were tested and the results and behaviour were compared with the results and

behaviour of Mono-steel bar concrete strips. The results obtained in this series justified the existence of the 'effective crack width' and also the crushing effect of the concrete around the bar was assessed.

The third phase of this research was to carry out a series of tests on concrete slabs and study the behaviour of these slabs in the elastic and plastic ranges, and to find the bending and twisting moments on the yield line and compare them with existing theories and the new theory developed by the author.

7.2 The Theoretical Yield Criterion.

This problem was approached on a logical basis. As mentioned in the introduction of this section, all the parameters that control the strength of the slab were selected and studied. A decision was then made regarding the parameters to be incorporated in the new criterion. The effect of membrane and shear forces on the slabs was not included, and the investigation was limited to biaxial bending effects. The parameters considered in developing an expression for the normal and twisting moments on the yield line were: the crushing strength of the concrete adjacent to the bars crossing the yield line, the 'effective crack width', and the shear and axial forces on the reinforcing bar crossing the yield line. All these effects were included in developing an expression for the normal and twisting moments on the yield line. A number of other theories for the normal and twisting moments were put forward by other researchers. The most important of these are Wood's and Johansen's. Johansen assumes that the reinforcement is stressed axially and yields because of these axial stresses. This concept results in a kinematically inadmissible mechanism of failure. Wood's theory is based on the concept that the reinforcement 'kinks'

across the crack. This concept corrects the mechanism to a kinematically admissible one, but is completely unrealistic, and is based on uniaxial stress failure.

The new theory developed in this thesis is based on the assumption that the steel fails because of a combination of shear and axial stresses, which are inter-related by the Von-Mises criterion. The shear and axial stresses on the bar were also related to each other by considering the effective crack width and the movement of the bar at yield within the effective crack width. For the first time an expression for the normal and twisting moments on the yield line has been developed that considers the bending and shear stiffness of the bar as well as the crushing strength of the concrete adjacent to the bar.

It was found that for an 'isotropic' slab, the maximum moment of resistance enhancement in relation to Johansen's theory is 13.4%. Wood's [6] theory predicts an enhancement of 41.4%. Experiments carried out at the Building Research Station under the supervision of Dr. Wood showed an enhancement of 16%.

It has been assumed that the shear and axial stresses are uniform over the cross section of the bar; this assumption is not far from reality in consideration of the small section of the bars used in reinforcing slabs.

Having developed an expression for the normal and twisting moments on the yield line, the next step was to develop the yield criterion. The development of the criterion was based on arguments put forward by Kemp [9] when he developed the yield criterion using Johansen's normal moment expression. In addition to the two conditions used by Kemp, the author thought it necessary to use another two conditions concerning the relationship of the twisting moment of resistance and

the applied twisting moment. A comparison of the new criterion and the yield criterion developed by Kemp shows a general moment enhancement.

The criterion developed in this thesis has a two-fold value:-

(a) as a criterion in its own right to be used in the design office,

(b) also as a check on other criteria.

It might be argued that the criterion is too complex to be used in design; this might be true to a certain extent if a computer is not available.

7.3 Experimental Work.

The experimental work carried out in the concrete laboratory of the University of Aston in Birmingham was of two phases. The first phase was to investigate the existence of the 'effective crack width', shear and axial stress on the reinforcing bar crossing the yield line at some oblique angle and the effects of concrete crushing adjacent to the reinforcing bar in the crack. To investigate the above parameters, two series of tests were designed and carried out. The first series was the Steel Analogue slab, and the second was the Mono-steel bar Concrete Strip slab. The results obtained in these series of tests were of great interest. The effects of shear on the reinforcing bar was demonstrated very clearly in the Steel Analogue series. It was shown that the bar at yield 'kinks' a few degrees. This kinking must be caused by the shear on the bar. By comparing the experimental normal moment strength obtained from the steel analogue slabs and the mono-steel bar slabs the effect of the crushing of concrete was assessed and found to have a detrimental effect on the slab strength. It has

also been shown that the effective crack width is larger than the physical crack width.

The second phase of tests was designed to study the general applicability of the new criterion and also study the elastic behaviour of concrete slabs. In designing this series of tests on under-reinforced concrete slabs subjected to combine bending and torsion, due regard was given to the conditions already laid down to ensure an unrestrained slab element. In fact, the only restraint was near the jaws, but it was felt that the effect of the fixity at the jaws was too far from the critical central region to cause any significant effect. The supports and loading arrangement appeared to work very satisfactorily. From this series of experiments, normal and twisting moments were obtained at yield. The normal moments at yield were compared with those predicted by the new theory. This comparison showed that these values were in good agreement. Normal moments at yield obtained by Downham [3] were also used to test the theory. Again, a close agreement between theory and experiment existed.

Apart from obtaining normal and twisting moments at yield, the following additional information was obtained.

(i) principal compression strain on the concrete and the principal strain directions,

(ii) principal bending moments and principal bending directions,

(iii) principal curvature of concrete slabs and principal curvature directions,

(iv) steel strains adjacent to the crack.

Using the information obtained from both phases of tests, the following important conclusions were made:-

1) Plastic flow does not occur in the same direction at yield.

2) The crack direction is not necessarily normal to the principal curvature direction after yield, but tends to coincide with it at failure.

3) Single crack failure, which is normal to the principal curvature direction, occurs when and where the direction of the maximum principal moment lies within the range of angles where the moment strength of a slab element, neglecting the steel reinforcement and considering the tensile strength of concrete, has a larger moment strength than a slab element, considering the tensile strength of steel and neglecting that of concrete.

4) Multiple crack failure, which is not necessarily normal to the principal curvature direction, occurs when and where the direction of the maximum principal moment lies within a range of angles where the moment strength of the slab element, considering the tensile strength of steel only, is larger than the moment strength of the slab element, considering the tensile strength of concrete only.

5) The stiffness of the slab element before any cracks develop is independent of the mesh orientation and degree of orthotropy, but depends on both after cracks develop.

6) The shear and bending stiffness of the reinforcing bars and the crushing strength of concrete adjacent to bars is a significant property in the behaviour of the slab.

7) The yield criterion does not depend only on the normal moment to the yield line but is very significantly effected by the tangential and twisting moments acting on it.

8) The shape of the yield locus does not appear to be convex, thus one of the conditions of Limit Analysis is violated; although conclusive proof of a concave yield locus was not obtained.

7.4 Conclusions.

This thesis presents the present state of knowledge in this field in a critical manner. The presentation is made in a rational manner and any inconsistencies are pointed out. Further, this thesis presents a new yield criterion derived from the origins of the problem. The new theory for yield expressly excludes slabs which are subjected to membrane forces or shear forces. In practice, the membrane effect on the moment strength of a slab could be considerable. The shear forces though on these slabs are not normally large enough to have any significant effect. The new criterion developed in this thesis is shown to lie wholly outside the criterion developed by Kemp [9] and based on the Johansen [2] expression. The experimental results obtained by the author justify the new criterion and showed that the Johansen criterion is conservative and the Wood [6] criterion overestimates the moment strength of the concrete slabs.

It is hoped that this thesis, as presented, will assist in clarifying the overall behaviour of underreinforced concrete slabs. It is also hoped that the new criterion will form a basis for further development of the yield criterion to incorporate the effects of membrane action on concrete slabs.

7.5 Future work.

Research is still required into the experimental and theoretical aspects of the behaviour of reinforced concrete slabs.

The experimental work must be carried out on 'isotropic' slabs subjected to biaxial moments so that the shape of the yield criterion is completely investigated. A biaxial moment field can be created by a series of hydraulic jacks aligned to form a rectangle or a square frame on which the slab is supported and another series of hydraulic jacks are used to form a larger rectangle or square which act as line loads on the slab. The support and loading jacks must be interconnected so that the ratio of the applied moments is controlled at will. The main variables to control are the ratio of the applied biaxial moments and the mesh orientation.

As has been mentioned earlier, the present theory could be extended to include membrane force action. It is suggested that the membrane forces acting on the reinforcing bars should be found and superimposed on the forces acting on the reinforcing bars found by the author. The author suggests that the membrane forces can be found if the following approach is considered. When the slabs are gradually loaded, tensile cracks develop in the concrete. The tensile cracks cause a shift of the neutral axis at a given section. The depth of the cracks is a function of the deflection of the slab. By considering the uncracked concrete and the steel reinforcement, the neutral axis trajectory perpendicular to the crack directions can be found. The trajectory of the neutral axis should be treated as an arch and the membrane forces evaluated.

LIST OF REFERENCES

1 INGERSLEV, A., 1921, Om en elementär Beregningsmaade av Krydsarmerede, Ingeniøren, 27, 507 pp.
The strength of rectangular slabs, paper read before Inst. Str. Engrs., London, December 1922.

2 JOHANSEN, J., Yield Line Theory, 1962. Cement and Concrete Association, London.

3 DOWNHAM, R.J., An Investigation into the Plastic and Elastic Behaviour of Reinforced Concrete Slab Elements, 1968, Ph.D. Thesis, University of Aston in Birmingham.

4 KWIECINSKI, M.W., Some tests on the yield criterion for reinforced concrete slabs; 1965, Mag. Conc. Res., 17 No. 52, 135-138.

5 KWIECINSKI, M.W., Yield Criterion for isotropically reinforced slabs 1965, Mag. Conc. Res., 17 Nos. 51, 97-100.

6 WOOD, R. H., Plastic and Elastic design of slabs and plates, 1961, Thames and Hudson, London.

7 MORLEY, C.T., The ultimate bending strength of reinforced concrete slabs, 1965, Ph.D.Thesis, University of Cambridge.

8 PRINCE, M.R., The yield behaviour of unrestrained reinforced concrete slabs, 1967, Ph.D. Thesis, University of London.

9 KEMP, K.O., 1965, The Yield Criterion for orthotropically reinforced concrete slabs; Int. J. Mech. Sci., 7, 737-746.

10 BAUS, R, and TOLACCIA, S., Calculs à la Rupture des Dalles en Béton Armé, (English translation) Building Research Station, Library Communication No. 1210.

11 MORLEY, C.T., 1966, On the yield criterion of orthogonally reinforced concrete slabs, J. Mech. Phys. Solids, 14 33-47.

12 LENSCHOW, R.J. and SOZEN, M.A., A Yield Criterion for Reinforced Concrete under Biaxial Moments and forces, University of Illinois, Research Report No. 311, July 1966.

13 NIELSEN, M.P., "Limit Analysis of Reinforced Concrete Slabs", Acta Polytechnica Scandinavica, Civil Eng. & Building Construction Series No. 26, Copenhagen 1964.

14 KEMP. K.O., MORLEY, C.T., NIELSEN, M.P., WOOD, R.H., and JONES, L.L., Recent Development in Yield Line Theory, 1965, Mag. Conc. Res. Special Publication, Cement and Concrete Ass., London.

15 KEMP, K.O., 1962, A lower bound solution to the collapse of an orthotropically reinforced slab on simple supports; 1962, Mag. Conc. Res., vol. 14, No. 41.

16 HOLMES, M. and DOWNHAM, R.J., An Experimental Yield Criterion into the Yield Criterion for reinforced concrete slabs, International conference, Solid Mechanics and Engineering Design, University of Southampton, April 1969.

17 HOLMES, M., and DOWNHAM, R.J., Experimental Stiffness and Yield criteria for Reinforced Concrete slabs, Build. Sci. Vol 4, 31-42, Pergamon Press, 1969.

18 HOLMES, M. and STEEL, K.A., Upper and Lower bound solutions to the collapse of a continuous slab under uniform load, 1964, Mag. Conc. Res., vol. 16, No. 47.

19 MORLEY, C.T., Experiments on the distortion of steel bars across cracks in reinforced concrete slabs, 1966, Mag. Conc. Res., Vol. 18, No. 54.

20 MASSONNET, Ch., Complete solutions describing the limit state of reinforced concrete slabs, 1967, Mag. Conc. Res., vol. 19, No. 58.

21 NEVILLE, A.M., Properties of Concrete, 1963, Pitman, London.

22 PRAGER, W., and HODGE, P.G., The Theory of Perfectly Plastic Solids, 1951, J. Wiley and Sons.

23 ODEN, J., Mechanics of Elastic Structures, 196 , McGraw and Hill.

24 SAVE, M., A consistent limit analysis theory for reinforced concrete slabs, 1967, Mag. Conc. Res., vol 19, No. 58.

25 TIMOSHENKO, S., and GOODIER, J.N., Theory of Elasticity, 1934, McGraw - Hill, New York.

26 WOOD, R.H., A partial failure of limit analysis for slabs, and the consequences for future research, 1969, Mag. Conc. Res. vol. 21, No. 67.

27 WOOD, R.H., and JONES, L.L., Yield-line Analysis of slabs, 1967, Chatto-Windus and Thames and Hudson, London.